8. SITE 693[1]

Shipboard Scientific Party[2]

HOLE 693A

Date occupied: 30 January 1987, 0115 local time

Date departed: 5 February 1987, 0315 local time

Time on hole: 146 hr

Position: 70°49.892′S, 14°34.410′W

Bottom felt (m, drill pipe): 2370.5

Distance between rig floor and sea level (m): 11

Water depth (drill-pipe measurement from sea level, m): 2359

Penetration (m): 483.9

Number of cores: 51

Total length of cored section (m): 483.9

Total core recovered (m): 213.5

Core recovery (%): 44

Oldest sediment cored:
Depth sub-bottom (m): 476.2
Nature: claystone
Age: Early Cretaceous (Albian)
Measured velocity (km/s): 1.99

HOLE 693B

Date occupied: 5 February 1987, 0315 local time

Date departed: 6 February 1987, 2115 local time

Time on hole: 42 hr

Position: 70°49.888′S, 14°34.461′W

Bottom felt (m, drill pipe): 2370.5

Distance between rig floor and sea level (m): 11

Water depth (drill-pipe measurement from sea level, m): 2359

Penetration (m): 403.1

Number of cores: 19

Total length of cored section (m): 167.4

Total core recovered (m): 92.2 (exclusive of wash core)

Core recovery (%): 55

Oldest sediment cored:
Depth sub-bottom (m): 399.0
Nature: diatom-bearing clayey mudstone
Age: Early Cretaceous (Albian?)
Measured velocity (km/s): 1.67

Principal results: Site 693 lies on a midslope bench on the Weddell Sea margin of East Antarctica, 10 km southwest of the rim of Wegener Canyon and 30 km from Sites 691 and 692, in 2359 m water. Like Sites 691 and 692, it was planned to examine the Cenozoic record of Antarctic continental cooling and ice-sheet formation, and to complement studies of the development of circum-Antarctic water masses at the other Leg 113 sites.. Two holes were drilled from 30 January to 6 February 1987. Hole 693A was rotary drilled because of the possibility of widespread occurrence of the "boulder beds" encountered at Sites 691 and 692. The hole penetrated to 483.9 mbsf in 51 cores, with a recovery of 213.5 m (44%), and was terminated in Lower Cretaceous (Albian-Aptian) claystones. One logging run (gamma, resistivity, sonic) was made to 446 mbsf in Hole 693A, with the pipe at 108 mbsf. Hole 693B was washed to 233.8 mbsf, then cored continuously (16 extended core barrel (XCB) and 2 advanced piston corer (APC) cores) to 403.1 mbsf, with a recovery of 92.2 m (55%), in order to improve core recovery and core quality in crucial intervals. We stopped drilling at Hole 693B with the XCB bit broken off and left down the hole. Seven lithostratigraphic units were drilled: 0–12.2 mbsf, middle to upper Pleistocene foraminifer-bearing clayey mud; 12.2–31.4 mbsf, upper Pliocene to lower Pleistocene(?) mostly barren clayey mud; 31.4–325.8 mbsf, upper Oligocene to upper Pliocene diatom mud and silty to clayey diatom-bearing mud, with upper Miocene clayey nannofossil diatom ooze interbeds; 325.8–345.1 mbsf, upper Oligocene alternating diatom mud and silt and nannofossil-bearing clayey mud; 345.1–397.8 mbsf, middle lower Oligocene diatom mud and silt, partly slumped; 397.8–409.0 mbsf, middle Cretaceous (?) radiolarian diatomite; 409.0–483.9 mbsf, Albian-Aptian dark terrigenous claystones and organic-rich mudstones.

Approximate sedimentation rates were lower than 10 m/m.y. in the Pleistocene, 21–46 m/m.y. in the Pliocene and late Miocene, 7 m/m.y. in the early Miocene and Oligocene. Hiatuses of regional extent occur at 262 mbsf, spanning the middle Miocene (duration about 7 m.y.) possibly at 342 mbsf in the middle lower Oligocene and at 398 mbsf covering the Upper Cretaceous, Paleocene, Eocene, and lowermost Oligocene (duration about 60 m.y. minimum).

Glacial dropstones are abundant down to the middle Miocene hiatus, and present but less common (some are weathered) to 398 mbsf (i.e., through the Oligocene). Illite is the dominant clay through the Cenozoic section sampled, reflecting the physical nature of erosion. Smectite is the most abundant clay in Cretaceous sediments, probably from a volcanic source. The biogenic component is almost entirely siliceous: diatoms are common to abundant and well-preserved in the lower Pliocene and upper Miocene and in the Cretaceous, but few and poorly preserved elsewhere. Silicoflagellates and radiolarians are proportionally less abundant but show similar preservation. Foraminifers occur in upper Pleistocene sediments, are well-preserved with nannofossils in thin upper Miocene and upper Oligocene interbeds, and occur in part of the Albian-Aptian. They are absent elsewhere, including the Oligocene and lower Miocene, in contrast to Maud Rise. Magnetostratigraphy is good for the top 140 mbsf and in the Cretaceous, but needs much shore-based work elsewhere in the section. Cretaceous sediments are more oxidized, less organic-rich, than the Barremian-Valanginian(?) sediments of Site 692.

Seismic profiles confirm speculation that 90% of sediments around Site 693 are pre-Upper Cretaceous. The estimated, maximum erosion in the Oligocene–Lower Cretaceous hiatuses at Site 692 was 300 m, which implies original sedimentation rates of the sediment since eroded of 5 m/m.y. through the period of the hiatus, if erosion took place at the Eocene/Oligocene boundary. The rate is similar to rates for the lower Miocene/Oligocene at this site (although these are poorly constrained), but much less than before or since: between about 100 and 12 Ma this was a starved margin. Benthic diatoms in the lower Miocene and Oligocene indicate the presence of a shallow, partly ice-free shelf, but ice-rafted debris indicates some glaciation. We conclude that the East Antarctic ice-sheet strongly expanded or formed in the middle Miocene, increasing sediment supply to the margin and starting canyon-cutting, after an ini-

[1] Barker, P. F., Kennett, J. P., et al., 1988. *Proc. ODP, Init. Repts.* 113: College Station, TX (Ocean Drilling Program).

[2] Shipboard Scientific Party is as given in the list of Participants preceding the contents.

tial early middle Miocene cooling of circum-Antarctic water masses. Pliocene and late Miocene siliceous productivity was similar at the Maud Rise sites, and Site 693 parallels coeval high calcareous productivity in lower latitudes. There is no evidence of a major East Antarctic deglaciation since the middle Miocene, not even in the high-resolution lower Pliocene record. Lower sedimentation rates and diatom abundance, and poor preservation over the last 2.4 Ma may reflect glacial intensification, and increased sea-ice extent.

BACKGROUND AND OBJECTIVES

Site 693 lies in 2359 m of water on the midslope bench extending along the eastern continental margin of the Weddell Sea. The site was selected on board ship on the basis of drilling results from Sites 691 and 692 (located in Fig. 1), and successfully submitted for approval by the Pollution Prevention and Safety Panel.

The principal aim of drilling at Sites 691 and 692 had been to obtain information about the evolution of the Antarctic continental climate through the Cenozoic, with a secondary aim of dating the seaward-dipping basement reflectors of the "Explora Wedge." Site 691 had been located in the axis of the upper reaches of the large submarine Wegener Canyon (Fig. 1), to avoid what was thought to be a thick Neogene glacial sequence and to sample the Paleogene to late Mesozoic sediments and basement. The upper part of the succession was to have been sampled by APC and XCB at a second site high on the canyon's outer slope. At Site 691, three attempts to spud-in failed, because of the presence of a "boulder bed," an accumulation of coarse detritus in the canyon bottom. At Site 692, on the canyon shoulder, the first hole was similarly unsuccessful. However, Hole 692B sampled the "boulder bed" in the top 52 m, showing that the canyon had cut to that depth at the site by the early late Miocene or before.

Beneath the boulders, 40 m of Early Cretaceous (probably Berriasian-Valanginian(?)) organic-rich sediment (predominantly claystone and mudstone) was sampled. The base of the hole lay about 60 m above seismic reflector U6, which defines the base of seismic stratigraphic sequence WS-2 of Hinz and Krause (1982). The prime interest of drilling in this area (Cenozoic climatic evolution) could not be pursued at Site 692. For this reason, and because the coarse, unconsolidated material at the top of the hole was continually caving in, the decision was made to abandon the hole and seek a thick Cenozoic section elsewhere.

None of the sites already approved for drilling were optimal in the new circumstances; it was clear that as much section above U6 as possible should be found. Also, in case there was time available, a site should be proposed at which basement would be easily accessible. The three sites approved were:

1. B1, 70°28′S, 13°59′W, shotpoint (SP) 188 on BGR78-019.
2. C1, to basement (estimated 200 m maximum), 70°50′S, 14°35′W, common depth point (CDP) 880 on BGR86-07.
3. C3, to 600 m (assumed K/T boundary), 70°57′S, 13°38′W, SP1320 on BGR78-019.

Site 693, option C1, lies in 2359 m of water on the main, northwest-facing slope of the margin, south of the canyon (Fig. 1). At this site, there was no indication of a major unconformity associated with Neogene canyon-cutting such as was found at Site 692, and reflector U6 lies about 1000 ms (more than 900 m) below the seabed (Fig. 2), presenting the possibility of a thick Cenozoic section.

The prime aim of drilling at Site 693 remained that of examining the Cenozoic cooling and glaciation of the Antarctic continent. We could expect to see some of the following changes:

1. A difference in sedimentation between the Quaternary and the Pliocene, as on Maud Rise where a calcareous Quaternary facies overlies siliceous Pliocene sediments.
2. Terrigenous sediment with a siliceous biogenic component through the Pliocene and upper Miocene, changing to a mixed siliceous and calcareous biogenic component back to the lower Oligocene. Unlike Maud Rise, there should be a considerable admixture of ice-rafted detritus, and probably some debris flows and turbidites. On Maud Rise there were several hiatuses in deposition during the Cenozoic which, probably having been caused by bottom currents, might occur also along the continental margin. The canyon-cutting on this margin, which Site 692 drilling showed had started by the early late Miocene, may be associated with one such hiatus.
3. The presence in Cenozoic sediments of spores and pollen of terrestrial plants from East Antarctica. During the glacial late Cenozoic, these will all have been derived from older sediments by glacial erosion. Before glaciation, the dominant source would have been contemporaneous continental vegetation: the Eocene to Cretaceous forms seen rarely in modern sediments should be seen in stratigraphic sequence here.
4. In water depths of around 2500 m, a mainly calcareous biofacies would be expected in Eocene, Paleocene, and Upper Cretaceous sediments. The Lower Cretaceous organic-rich mudstones found at Site 692 should be encountered. Wind-blown terrigenous debris, clays, quartz, and mica were found in lower Tertiary and Upper Cretaceous sediments at Site 690 on Maud Rise; we thought that it might be possible to distinguish them here also.

Site 693 was intended to be rotary-drilled initially: the APC was not used on the first run, because the boulder beds at Sites 691 and 692 might have been mainly ice-rafted and thus likely to pervade the margin. If the first hole should exceed 400 m it was to be logged, and part of the section could be recored using the APC/XCB, depending on recovery, interest, and time available.

OPERATIONS

At Site 692 the presence of ice-rafted rocks concentrated by erosion in the bottom and shoulder of Wegener Canyon produced difficult drilling conditions. An additional site was needed on the main continental slope away from the canyon.

Pollution Prevention and Safety Panel approval was obtained for a site at about 70°49.89′S, 14°34.41′W which is 16.3 mi (26 km) west-southwest of Site 692. Steaming time was a little less than 7 hr and the site was reached on the morning of 30 January. A recall beacon (serial number 306) was dropped, but its signal was lost. The backup beacon was dropped and the signal acquired. Two hours later the original beacon was seen floating in front of the ship and was picked up by *Maersk Master*'s rescue boat.

Hole 693A

Because of the experience of a hard seafloor at Site 692 it was decided to rotary-core this site. An 9 7/8-in. Rock Bit International (RBI) C3 bit was selected. The bottom hole assembly (BHA) comprised the bit, hydraulic bit release, profile sub, outer core barrel, long topsub, head sub, seven 8 1/4-in. drill collars, one 7 1/4-in. drill collar, and two stands of 5 1/2-in. drill pipe.

The precision depth recorder (PDR) indicated a water depth of 2374.3 m and a soft bottom was felt at 2370.5 m (rig-floor depth). Coring continued to 128 mbsf (Table 1) in a very soft formation and recovery was high. It was necessary to core with little or no circulation. At 137 mbsf the core recovery decreased dramatically and from that depth to the total depth of 483.9 mbsf recovery was low. Just about every combination of weight, rotary revolutions per minute (RPM), and pump rate was tried in an effort to improve recovery, but for such a soft sticky formation an APC/XCB system should have been in use. A total of 483.9 m was cored and 213.5 m (or 44%) was recovered.

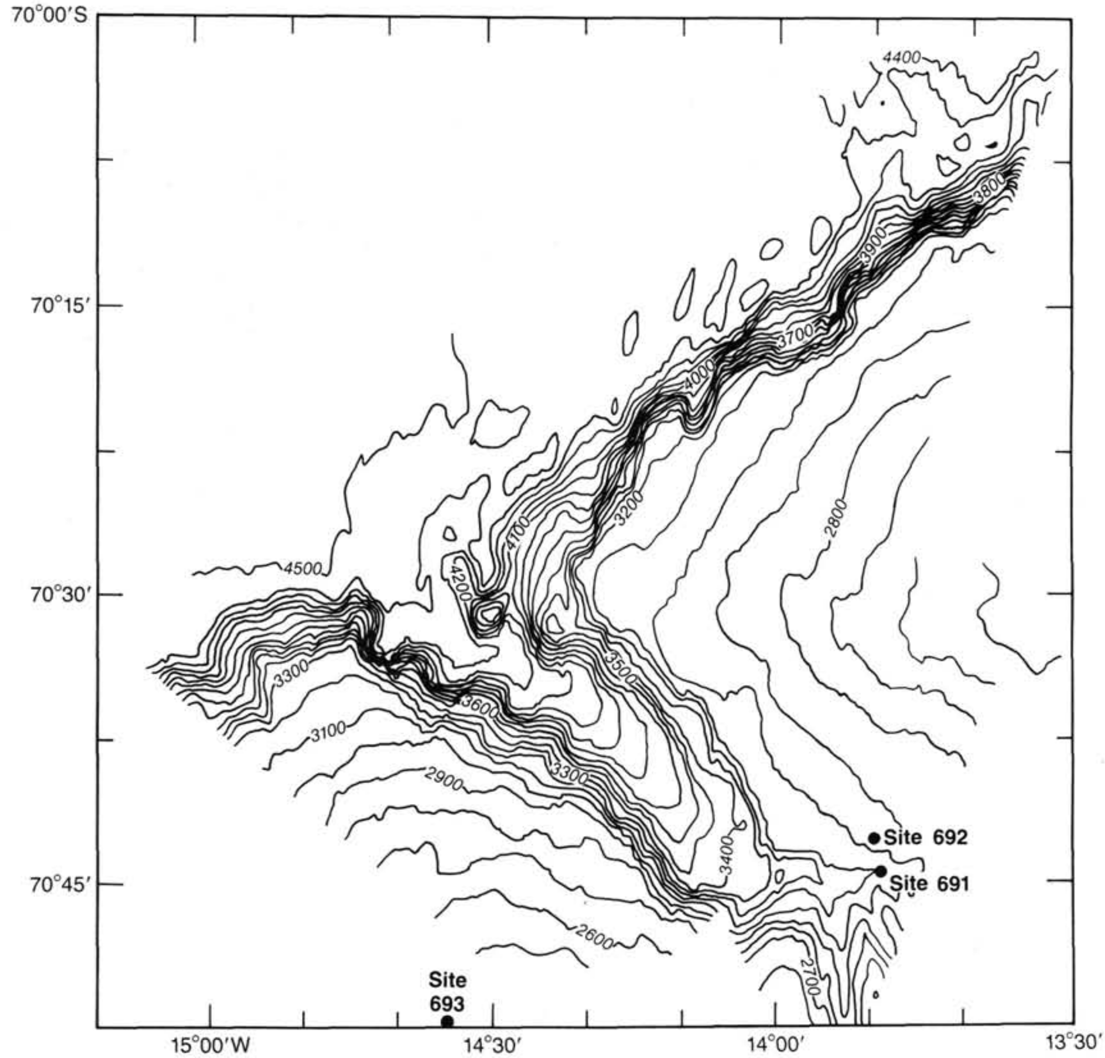

Figure 1. Sea Beam bathymetric map of Wegener Canyon on Dronning Maud Land margin, eastern Weddell Sea, showing locations of Sites 691, 692, and 693. Contours in uncorrected meters; contour interval is 100 m (map is unpublished data collected by *Polarstern* during austral seasons 1985-86 and 1986-87). SOM = South Orkney microcontinent.

On 31 January the first of two instances occurred of not being able to pull the core barrel. The overshot would latch the barrel but it could not be pulled above 9 m. On the fifth attempt an extra heavy shear pin was used and the barrel was recovered. There was nothing in the condition of the core barrel to suggest why it could not be pulled. The next morning this happened again. Six wireline runs were required to recover the barrel. It was concluded that the new double latch APC/XCB assembly which had been adapted for the rotary system was not compatible. The old single latch system was run and no further problems were encountered.

On 4 February the bit was released hydraulically in preparation for logging. The drill pipe was withdrawn to 108 mbsf and the side-wall entry sub was installed. It took 8 hr to rig up the sub although in the future the procedure can probably be reduced to 6 hr. Although the sub was installed it was decided to attempt to log without lowering the pipe to the bottom of the hole. The LSS, DIL, GR, and MCD reached a total depth of 2819 m (rig-floor depth) where bottom was reached. The hole contained only seawater. Five and one-half hours were required to run the one log from 2819 to 1360 m (rig-floor depth). A total of 17.25 rig hours were spent logging.

The weather continued to be excellent. Ice was present in the area. On 30 January the *Maersk Master* towed a 40 × 195 × 200 m = 6.24 million ton iceberg, the largest to date. A 335,000-ton tow on 2 February was also a success.

Because of the position of the site on the continental rise and the presence of organic-rich shale, it was necessary to plug the hole with cement. The pipe was run in the hole and the bottom was found to be 37 m shallower due to fill. A total of 33.4 bbl of cement was mixed and placed. The drill pipe was pulled and Hole 693A was concluded on 5 February 1987.

Hole 693B

Because of the low core recovery with the rotary system at Hole 693A, it was decided to recore the location with the APC/XCB system. An 11 7/16-in. bit was started in the hole. The bit used was an RBI C3, field-modified as on the previous leg so that the stream of fluid from the nozzles struck the trailing edge of the cones. It was believed the fluid hitting the cones reduced bit balling and produced a faster rate of penetration. The same BHA used at Hole 693A was run, with the addition of laying out the hydraulic bit release. The prototype lock-open float device was installed.

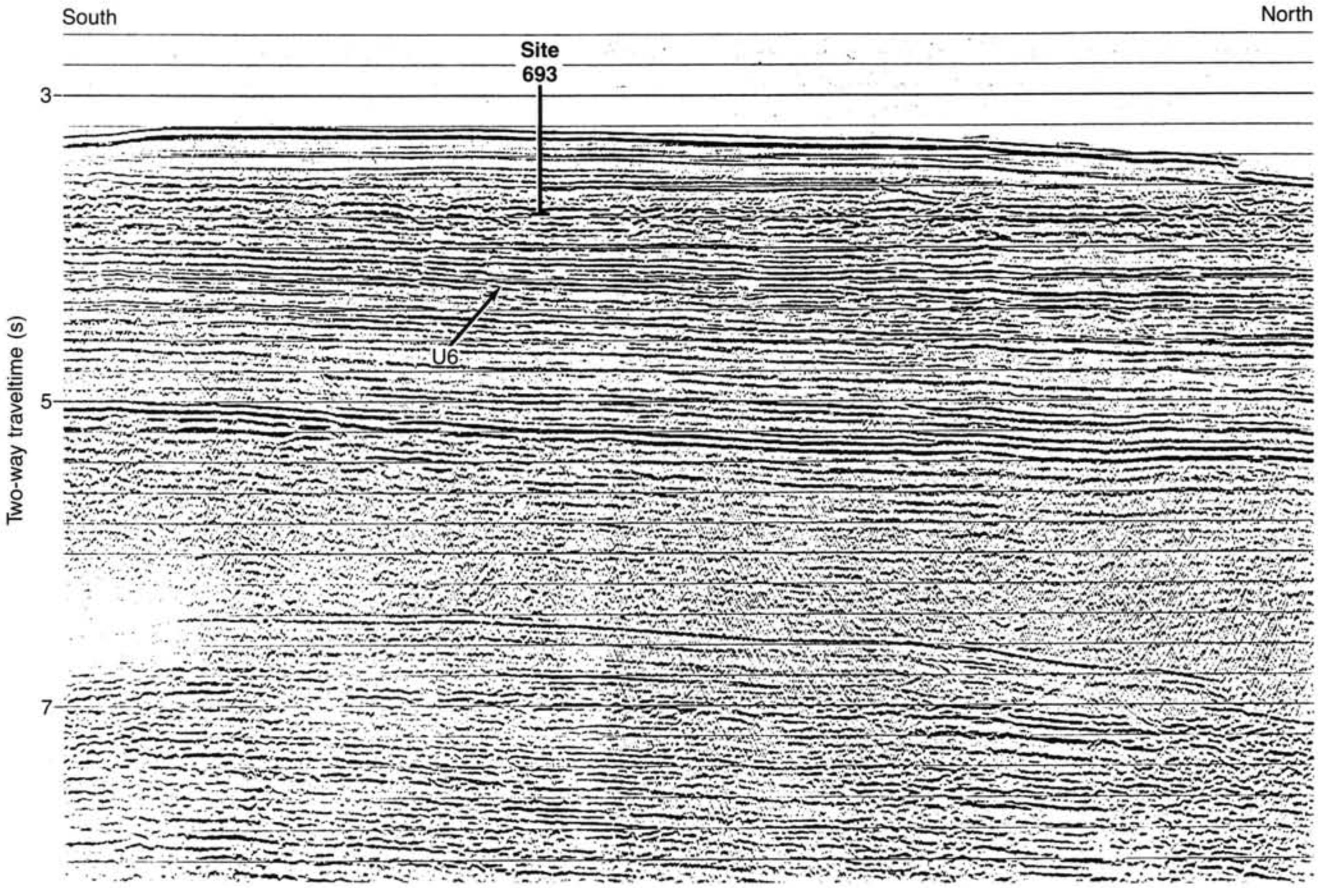

Figure 2. Multichannel seismic profile BGR86-07, showing location of Site 693.

Meanwhile the approach of an 8 × 10 mi (13 × 16 km) patch of old pack ice was closely watched. It was being driven by a 20-kt wind and its approach speed was 0.5 kt. An approaching iceberg was an added complication. When the bit was 122 m above the seafloor it became obvious that the trailing portion of the ice would pass over the site. When the ice came to within 1 mi (1.6 km) of the ship, the ship was moved to the northwest. The pipe was also brought up as a contingency. The ship moved 2.2 mi (3.5 km) from the site. Three hours after leaving the site, *JOIDES Resolution* began to move back, and *Maersk Master* began towing operations on iceberg #142. The site was only reached after 10.5 hr, because the ship moved very slowly and, without GPS, the true motion of the ship could not be judged accurately.

The first core was a wash core to 233.8 mbsf (Table 1). Total recovery on the next four cores was a disappointing 6.2 m. The recovery was so low that there was little scientific value in continuing if it could not be increased. It was decided to try a piston core, although it was understood by all that a piston core at 277 mbsf had a very high chance of not being pullable. It was shot with only two pins and the barrel was pulled free with 60,000 lb. Recovery was a beautiful 9.17 m of sticky greenish gray diatom clayey mud. Generally, a pull-out this high is reason to start using the XCB. The pump pressure bled off the next shot indicated the piston did not stroke the full 9.4 m. Only 4.51 m of core were recovered. Judgment then overcame valor and the remaining cores were obtained with the XCB. The twelve XCB cores to the total penetration of 403.1 m averaged 62.3% m recovery.

Core 113-693B-19X was to be the next to the last core. An unconformity was sampled by 113-693B-19X and it was desired to core below the transition. It took 60 min to make 5.5 m and when the barrel reached the surface it was found that about 6 in. of the XCB cutter had been worn or broken off and left in the hole. This effectively prevented attempting another core.

The bit was positioned at 2769 m (rig-floor depth) and 200 sacks of cement were mixed and placed. The ship was underway to Site 694 (W5) at 2115, 7 February 1987.

LITHOSTRATIGRAPHY

Introduction

Two holes were drilled at Site 693. Hole 693A was drilled to 483.9 mbsf and recovered 213.5 m of sediment. Hole 693B was washed to 233.8 mbsf, cored to 403.1 mbsf, and recovered 92.2 m of sediment (exclusive of wash core). The sedimentary sequence recovered at Site 693 is primarily terrigenous; the biogenic calcareous (foraminifers and nannofossils) and siliceous (diatoms, sponge spicules, and radiolarians) content averages about 30% and ranges between 0% and 74%. Seven lithostratigraphic units are recognized (Fig. 3 and Table 2), based upon visual core descriptions and smear slide analysis (Figs. 4–7). Boundary locations for the lithostratigraphic units are determined from their location in either Hole 693A or 693B, depending on where recovery was better.

Unit 1, 12.2 m thick, is a foraminifer-bearing clayey and silty mud, of middle to late Pleistocene age. Unit II, 19.2 m thick, is a clayey mud devoid of any biogenic component and is late Pliocene to early Pleistocene in age. Unit III, the longest unit, is 294.4 m thick. It is dominated by clayey mud, diatom-bearing mud, and diatom mud, with a minor component of mud-bearing nannofossil diatom ooze and diatom-nannofossil ooze in

Table 1. Coring summary, Site 693.

Core no.	Date (1987)	Time (local)	Depths (mbsf)	Cored (m)	Recovered (m)	Recovery (%)
Hole 693A						
1R	30 Jan	1615	0.0-2.5	2.5	2.48	99.2
2R	30 Jan	1730	2.5-12.2	9.7	9.61	99.1
3R	30 Jan	1845	12.2-21.9	9.7	2.95	30.4
4R	30 Jan	2020	21.9-31.4	9.5	7.02	73.9
5R	30 Jan	2150	31.4-41.1	9.7	8.55	88.1
6R	30 Jan	2359	41.1-50.8	9.7	8.35	86.1
7R	31 Jan	0125	50.8-60.4	9.6	2.78	28.9
8R	31 Jan	0245	60.4-70.1	9.7	9.76	100.0
9R	31 Jan	0415	70.1-79.7	9.6	9.67	101.0
10R	31 Jan	0600	79.7-89.3	9.6	9.67	101.0
11R	31 Jan	0745	89.3-98.9	9.6	9.59	99.9
12R	31 Jan	0945	98.9-108.6	9.7	9.64	99.4
13R	31 Jan	1130	108.6-118.2	9.6	8.40	87.5
14R	31 Jan	1330	118.2-127.8	9.6	7.14	74.4
15R	31 Jan	1800	127.8-137.5	9.7	5.22	53.8
16R	31 Jan	2015	137.5-147.2	9.7	1.48	15.2
17R	31 Jan	2215	147.2-156.9	9.7	3.64	37.5
18R	1 Feb	0015	156.9-166.6	9.7	6.31	65.0
19R	1 Feb	0830	166.6-176.3	9.7	7.70	79.4
20R	1 Feb	1015	176.3-185.9	9.6	0.11	1.1
21R	1 Feb	1205	185.9-195.6	9.7	2.58	26.6
22R	1 Feb	1640	195.6-205.3	9.7	3.93	40.5
23R	1 Feb	1800	205.3-214.9	9.6	0.00	0.0
24R	1 Feb	1945	214.9-224.6	9.7	9.34	96.3
25R	1 Feb	2120	224.6-234.3	9.7	5.95	61.3
26R	1 Feb	2330	234.3-243.9	9.6	7.08	73.7
27R	2 Feb	0130	243.9-253.6	9.7	2.19	22.6
28R	2 Feb	0315	253.6-262.9	9.3	5.77	62.0
29R	2 Feb	0500	262.9-272.5	9.6	7.60	79.1
30R	2 Feb	0700	272.5-282.2	9.7	0.00	0.0
31R	2 Feb	0845	282.2-291.9	9.7	1.33	13.7
32R	2 Feb	1030	291.9-301.5	9.6	0.00	0.0
33R	2 Feb	1230	301.5-311.2	9.7	1.28	13.2
34R	2 Feb	1450	311.2-320.9	9.7	3.78	38.9
35R	2 Feb	1700	320.9-330.5	9.6	1.93	20.1
36R	2 Feb	1815	330.5-340.2	9.7	0.80	8.3
37R	2 Feb	2100	340.2-349.9	9.7	0.70	7.2
38R	2 Feb	2300	349.9-359.6	9.7	1.65	17.0
39R	3 Feb	0100	359.6-368.9	9.3	2.65	28.5
40R	3 Feb	0245	368.9-378.6	9.7	4.14	42.7
41R	3 Feb	0415	378.6-387.5	8.9	0.00	0.0
42R	3 Feb	0600	387.5-397.1	9.6	0.20	2.1
43R	3 Feb	0845	397.1-406.7	9.6	0.67	7.0
44R	3 Feb	1230	406.7-416.5	9.8	0.76	7.8
45R	3 Feb	1500	416.5-426.1	9.6	1.29	13.4
46R	3 Feb	1615	426.1-435.7	9.6	1.44	15.0
47R	3 Feb	1800	435.7-445.4	9.7	3.15	32.5
48R	3 Feb	1915	445.4-455.0	9.6	5.67	59.0
49R	3 Feb	2130	455.0-464.8	9.8	3.10	31.6
50R	3 Feb	2300	464.8-474.3	9.5	2.52	26.5
51R	4 Feb	0045	474.3-483.9	9.6	1.91	19.9
				483.9	213.48	
Hole 693B						
1W	6 Feb	0815	0.0-233.8	N.A.	N.A.	3.7
2X	6 Feb	1015	233.8-238.8	5.0	5.71	114.0
3X	6 Feb	1145	238.8-248.4	9.6	0.50	5.2
4X	6 Feb	1330	248.4-258.1	9.7	0.00	0.0
5X	6 Feb	1445	258.1-267.8	9.7	0.00	0.0
6H	6 Feb	1630	267.8-277.5	9.7	9.17	94.5
7H	6 Feb	1715	277.5-287.1	9.6	4.51	47.0
8X	6 Feb	1930	287.1-296.8	9.7	5.00	51.5
9X	6 Feb	2100	296.8-306.5	9.7	8.22	84.7
10X	6 Feb	2230	306.5-316.1	9.6	6.29	65.5
11X	7 Feb	0000	316.1-325.8	9.7	2.43	25.0
12X	7 Feb	0145	325.8-335.5	9.7	8.29	85.4
13X	7 Feb	0300	335.5-345.1	9.6	3.35	34.9
14X	7 Feb	0430	345.1-354.7	9.6	8.05	83.8
15X	7 Feb	0600	354.7-364.4	9.7	4.69	48.3
16X	7 Feb	0745	364.4-374.0	9.6	7.92	82.5
17X	7 Feb	0915	374.0-383.7	9.7	2.62	27.0
18X	7 Feb	1100	383.7-393.4	9.7	9.82	101.0
19X	7 Feb	1315	393.4-403.1	9.7	5.59	57.6
				169.3	92.16	

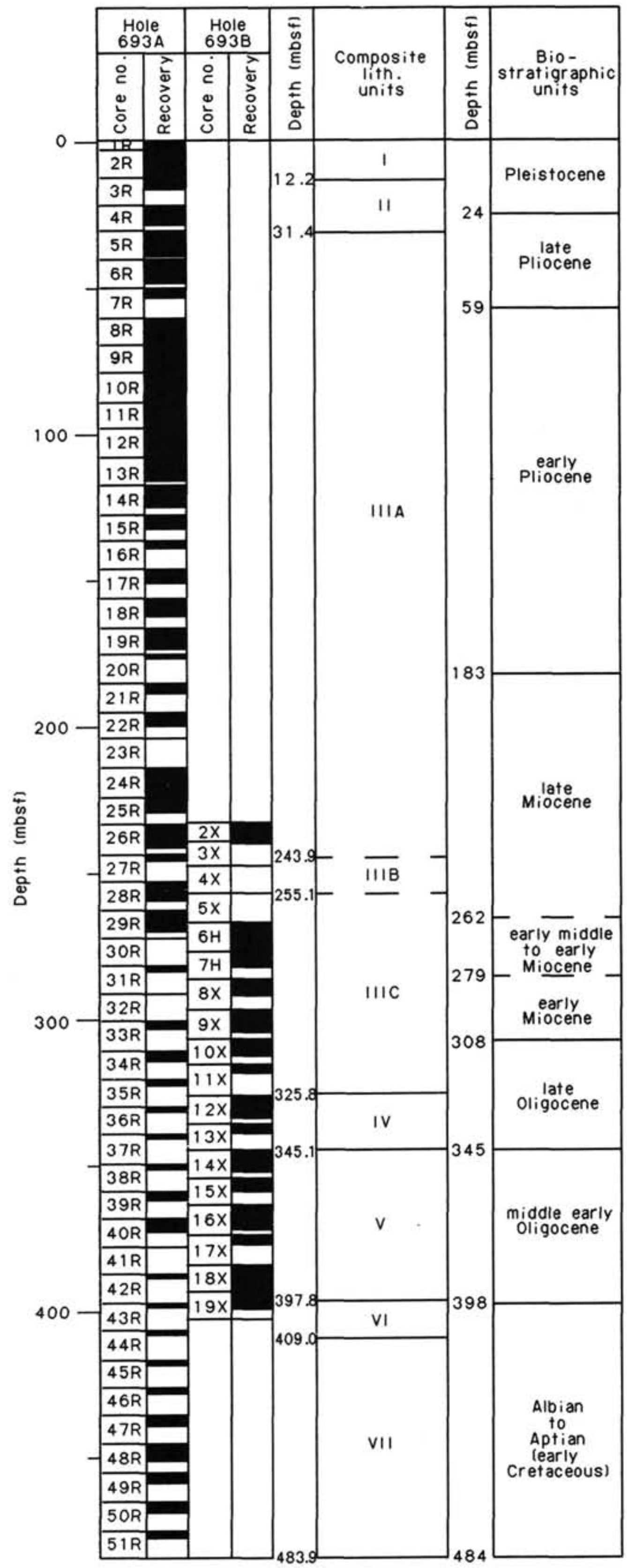

Figure 3. Lithostratigraphic unit summary for Site 693.

Table 2. Summary of dominant lithologies at Site 693.

Unit	Lithology	Depth interval (mbsf)	Thickness (m)	Age
I	Clayey mud and foraminifer-bearing clayey mud	0–12.2	12.2	middle to late Pleistocene
II	Clayey mud	12.2–31.4	19.2	late Pliocene to early Pleistocene
III	Divided into three subunits (see below)	31.4–325.8	294.4	late Oligocene to late Pliocene
IIIA	Clayey mud, diatom mud, silty and clayey diatom-bearing mud	31.4–243.9	212.5	late Miocene to late Pliocene
IIIB	Muddy diatom-nannofossil ooze and diatom clay	243.9–255.1	11.2	late Miocene
IIIC	Clayey mud, diatom mud, silty and clayey diatom-bearing mud	255.1–325.8	70.7	late Oligocene to late Miocene
IV	Muddy nannofossil ooze, nannofossil-bearing clayey mud and diatom clayey mud	325.8–345.1	19.3	late Oligocene
V	Diatom silty mud, diatom clayey mud	345.1–397.8	52.7	early Oligocene
VI	Radiolarian diatomite	397.8–409.0	11.2	Albian-Santonian
VII	Organic-rich claystone (black shales)	409.0–483.9	74.9	Albian to lower Albian? (Early Cretaceous)

Core 113-693A-27R and Section 113-693A-28R-1. The age of this unit ranges from late Oligocene to late Pliocene. Unit III is divided into three subunits based upon variations in the diatom and nannofossil content. Subunit IIIA, 212.5 m thick, is late Miocene to late Pliocene in age, and consists of clayey mud, diatom mud, and silty to clayey diatom-bearing mud. Subunit IIIB, 11.2 m thick, is late Miocene in age and is composed of muddy diatom-nannofossil ooze and diatom clay. Subunit IIIC, 70.7 m thick, is late Oligocene to late Miocene in age. The sediment facies of IIIC is similar to that of Subunit IIIA, and consists of clayey mud, diatom mud, and silty to clayey diatom-bearing mud. Unit IV, 19.3 m thick, is late Oligocene in age, and consists of muddy nannofossil ooze, nannofossil-bearing clayey mud, and diatom-bearing clayey mud. Unit V, 52.7 m thick, is early to middle Oligocene in age, and consists of diatom mud, mudstone, and diatom-bearing clayey mud, with a wide variety of sedimentary structures, including laminae, graded beds, slump folds, intraformational clasts, and tilted blocks. Unit VI, 11.2 m thick, consists of Cretaceous (Albian-Santonian) radiolarian diatomite and siliceous-bearing clayey mud. Unit VII, 74.9 m thick, is Early Cretaceous (Aptian to lower Albian?) in age and consists of organic-rich clayey mudstones and claystones (black shales).

Sediments from Hole 693A are moderately to strongly disturbed by drilling, with good core recovery and quality only obtained at the top and bottom of the hole. Core recovery and quality were extremely poor between Core 113-693A-30R (272 mbsf) and Core 113-693A-46R (435 mbsf). In comparison, sediment recovered from the adjacent Hole 693B has been only moderately to slightly disturbed by drilling, and core recovery was generally good for the same depth interval.

Poor core recovery and coring disturbance have created difficulties in defining both unit and subunit boundaries. Hence in some instances, (e.g., Unit VI), it is necessary to incorporate different lithologies, and to draw unit boundaries where only partial recovery was achieved (e.g., Unit IV).

Unit I (0–12.2 mbsf; Age middle to late Pleistocene)

Cores 113-693A-1R and 113-693A-2R; depth 0.0–12.2 mbsf; thickness 12.2 m. Age: middle to late Pleistocene.

Unit I consists of clayey mud and foraminifer-bearing clayey mud with a relatively high proportion of sand (Fig. 4). The percentage of sand increases from about 8% at the top of Core 113-693A-1R to about 20% at the base of Core 113-693A-1R (Fig. 6). It remains high (20%) at the top of Core 113-693A-2R, and drops to about 5% at the base of Core 113-693A-2R. Many of the quartz sand grains are well-rounded and partially polished, whereas the sand-size lithic grains are more angular. The terrigenous fraction consists predominantly of clay and quartz, with minor amounts of feldspars, and opaque and heavy minerals. Sediment color is almost uniform and ranges between dark grayish brown (2.5Y 4/2) and olive gray (5Y 4/2). There are faint suggestions of burrows, but extensive drilling disturbance prevents their positive identification.

Dropstones of variable sizes not exceeding a few centimeters in diameter are found throughout, with one dropstone 9 × 4 cm (Interval 113-693A-2R-5, 130–140 cm, working half). The igneous dropstones (granite) and metasediments (quartzite) are subangular to angular in shape and are manganese coated. Foraminifers occur in minor amounts and are more common in the sandier parts of the unit.

The sediment at the top of the unit has been extensively disturbed and homogenized by drilling, but is only moderately disturbed toward the base.

Unit II (12.2–31.4 mbsf; Age late Pliocene to early Pleistocene)

Cores 113-693A-3R and 113-693A-4R; depth 12.2–31.4 mbsf; thickness 19.2 m. Age: late Pliocene to early Pleistocene.

Sediment in Unit II, a clayey mud, is almost wholly terrigenous with only a trace biogenic component (Fig. 4). The sand fraction gradually decreases toward the base (Fig. 6). Quartz, feldspar, opaque and heavy minerals, volcanic glass, and mica occur in the terrigenous fraction (see "Summary Analysis of Sand Fraction" discussion below). The sediment varies between dark grayish brown (2.5Y 4/2), dark greenish gray (5GY 4/1), dark gray (5Y 4/1) to gray (5Y 5/1), olive gray (5Y 5/2), and light olive brown (2.5Y 5/3), with gray (5Y 5/1) being the dominant color. A graded very fine sand to coarse silt layer with sharp top and base occurs in Interval 113-693A-4R-5, 72–80 cm (Fig. 8).

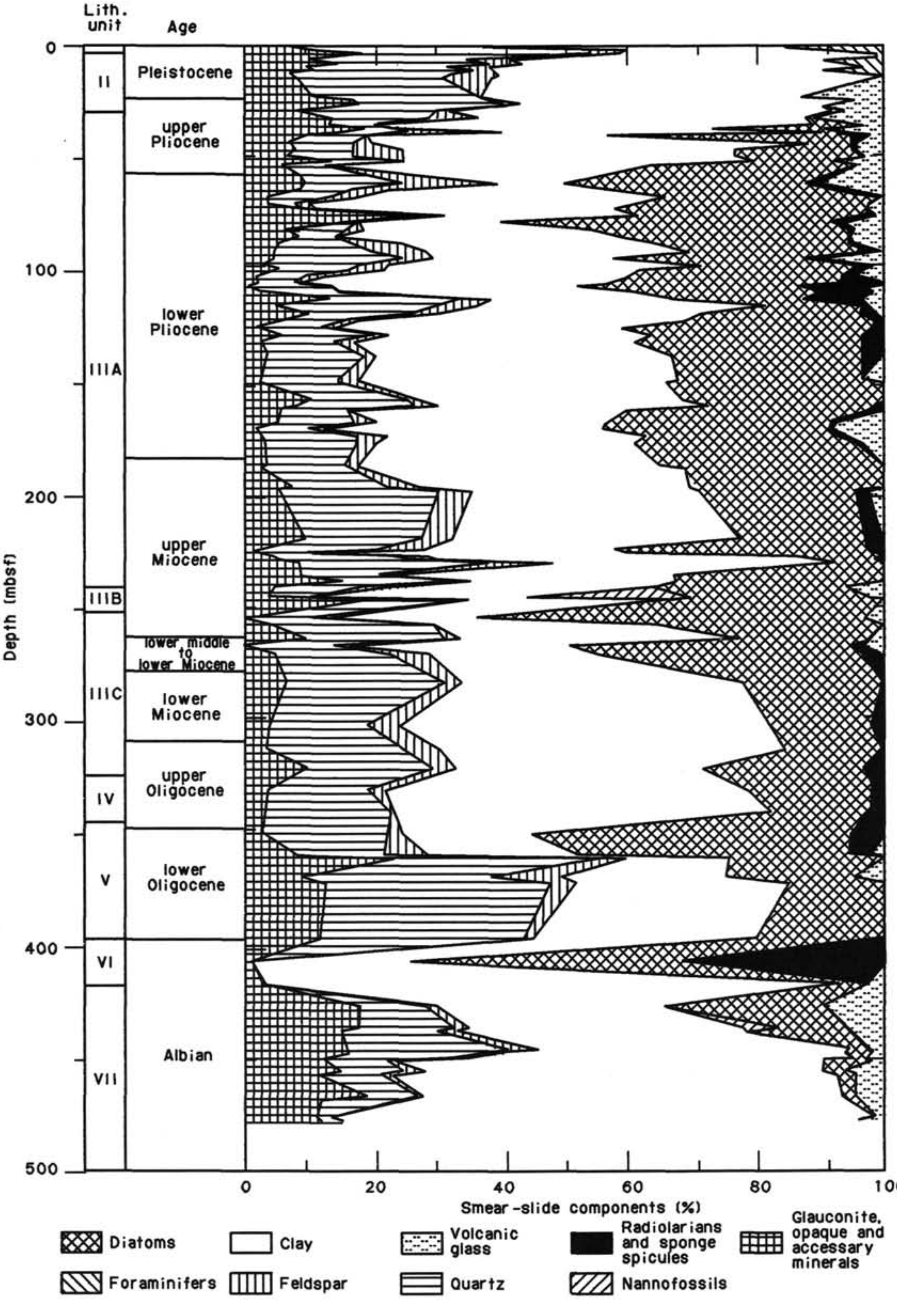

Figure 4. Sediment composition for Hole 693A from shipboard smear-slide data.

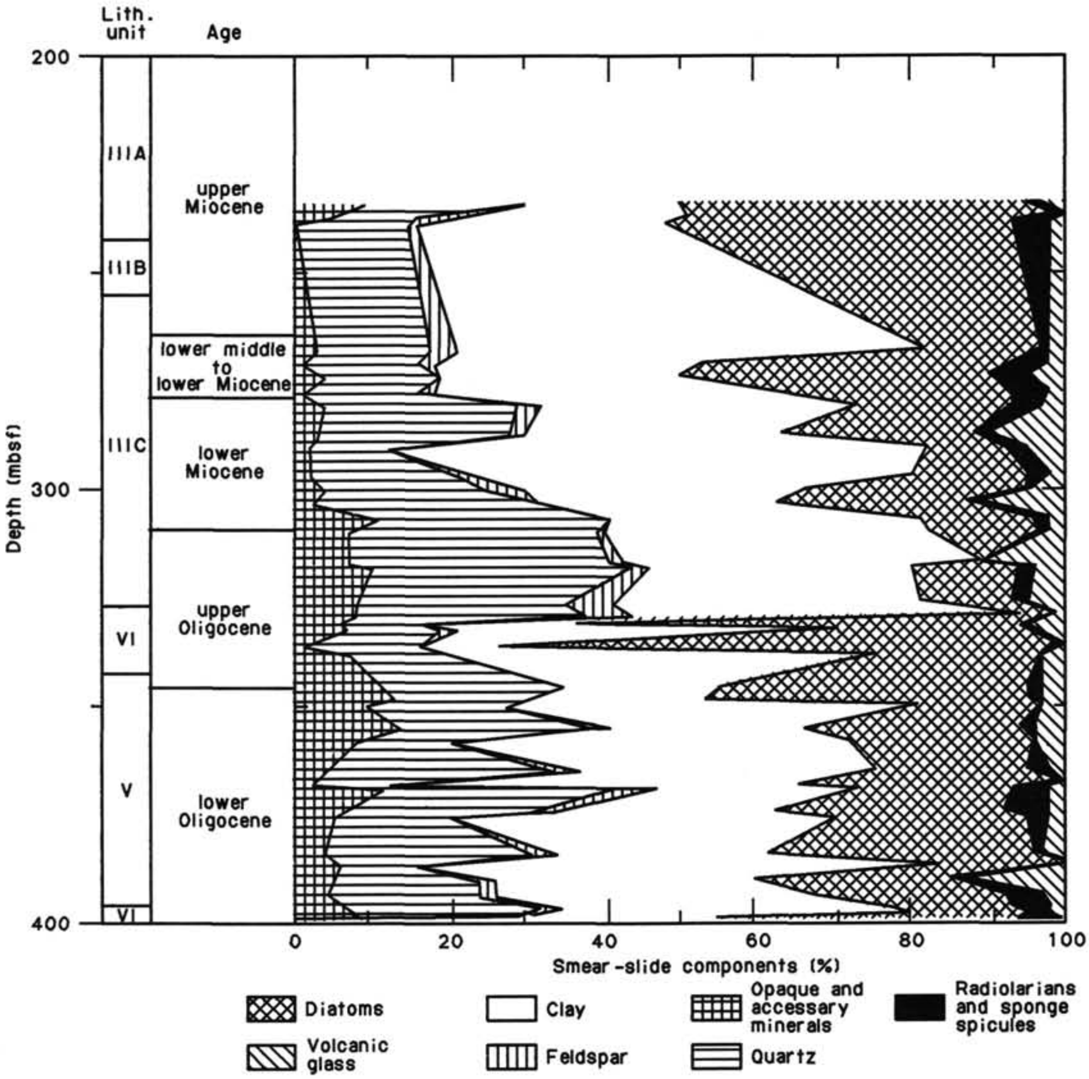

Figure 5. Sediment composition for Hole 693B from shipboard smear-slide data.

Dropstones in the millimeter-size range are common throughout the unit. A few centimeter-sized dropstones also occur. These are well-rounded, feldspathic sandstones and angular igneous rocks that have a thin coating of manganese.

Bioturbation is difficult to detect due to poor core quality. The sediment in this unit is moderately disturbed to soupy.

Unit III (31.4–325.8 mbsf; Age late Oligocene to late Pliocene)

Cores 113-693A-5R through 113-693A-35R; 31.4–330.5 mbsf; thickness 299.1 m. Cores 113-693B-2X through 113-693B-11X; depth 233.8–325.8 mbsf: thickness 92.0 m. Age: late Oligocene to late Pliocene.

Unit III is divided into three subunits on the basis of variations in the nannofossil and diatom content (Figs. 4–7). Subunit IIIA consists of clayey mud and diatom clayey mud and silty and clayey diatom-bearing mud. Subunit IIIB is characterized by muddy diatom-nannofossil ooze and diatom clay. The boundary between Subunits IIIA and IIIB shows a marked increase in the nannofossil content. Similarly, the decrease in the nannofossil content defines the boundary between Subunit IIIB and IIIC. Subunit IIIC consists of clayey mud and silty to clayey mud. Subunit IIIB also contains less quartz than the other two subunits.

Subunit IIIA (31.4–243.9 mbsf; Age late Miocene to late Pliocene)

Cores 113-693A-5R through 113-693A-26R; depth 31.4–243.9 mbsf; thickness 212.5 m. Cores 113-693B-2X through 113-693B-3X; depth 233.8–248.4 mbsf; thickness 14.6 m. Age: late Miocene to late Pliocene.

The predominant sediments of Subunit IIIA are diatom mud and diatom clay with minor occurrences of diatom ooze (Sections 113-693A-9R-6 and 113-693A-9R-7), and silicoflagellate-bearing diatom mud (Section 113-693A-12R-6). Diatoms first appear in Subunit IIIA. The terrigenous component shows a very gradual increase downcore (Figs. 4 and 5). Within the terrigenous component, silt shows a marginal increase, accompanied by a decrease in the clay content (Figs. 6 and 7). Fine sand is a background constituent within the terrigenous component, but it has two abundance peaks, one at about 120 mbsf, (a double peak, Cores 113-693A-13R and 113-693A-14R) and the other at about 200 mbsf (Core 113-693A-22R). The peaks are a result of an increase in the quartz input (Fig. 4). Sediment color varies from very dark greenish gray (5G 3/1) and dark greenish gray (5GY 4/1) to greenish gray (5G 5/1) and gray (N 5/0), although a systematic color variation is not observed. Color changes generally occur over an interval of a few millimeters to centimeters. The diatom component in the dominant lithology ranges from

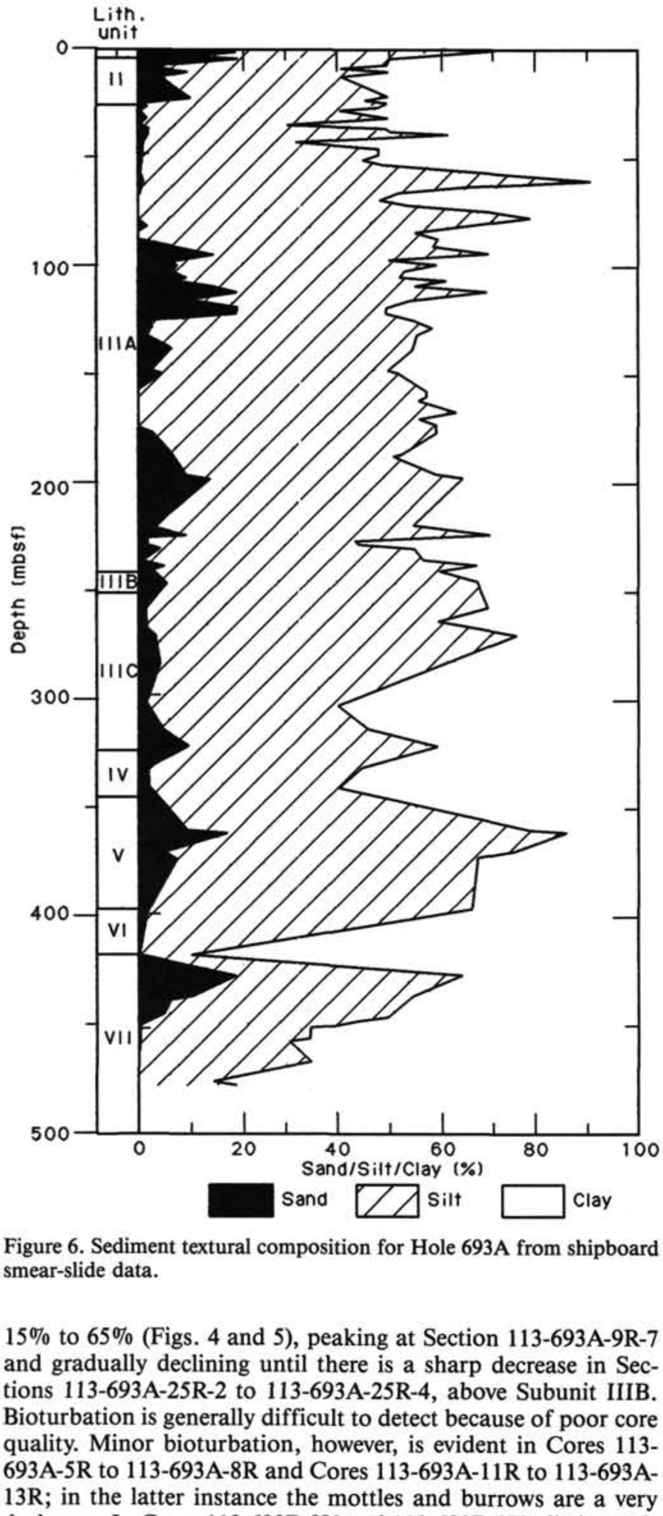

Figure 6. Sediment textural composition for Hole 693A from shipboard smear-slide data.

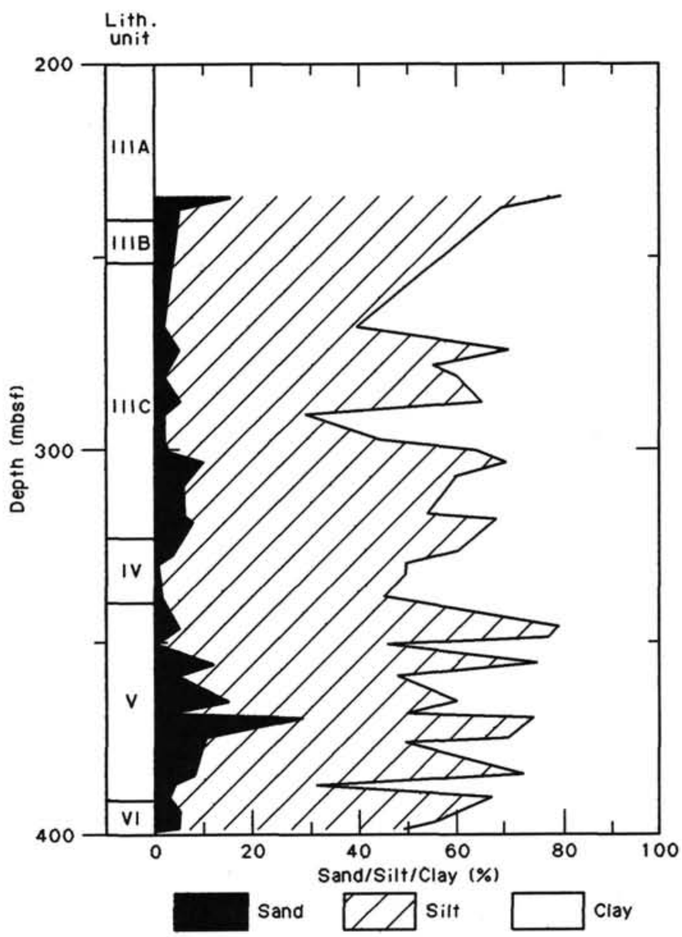

Figure 7. Sediment textural composition for Hole 693B from shipboard smear-slide data.

15% to 65% (Figs. 4 and 5), peaking at Section 113-693A-9R-7 and gradually declining until there is a sharp decrease in Sections 113-693A-25R-2 to 113-693A-25R-4, above Subunit IIIB. Bioturbation is generally difficult to detect because of poor core quality. Minor bioturbation, however, is evident in Cores 113-693A-5R to 113-693A-8R and Cores 113-693A-11R to 113-693A-13R; in the latter instance the mottles and burrows are a very dark gray. In Cores 113-693B-2X and 113-693B-3X, distinct minor bioturbation structures and small halo burrows are observed.

Primary structures (e.g., bedding and laminae) and compositional structures (e.g., shell fragments) are not commonly observed. A few sandy layers, however, are observed in Cores 113-693A-12R, 113-693A-19R, 113-693A-21R, and 113-693A-26R. In Section 113-693A-12R-7, a 5-cm thick, graded bed from silt to fine sand has a sharp base and a partially mottled gradational top. The sand grains are predominantly angular to subangular. Toward the base of the unit, well-sorted fine sand occurs in 2-3-mm "pockets" (Sections 113-693A-25R-2 and -3) which have sharp contacts with the surrounding clay. Parts of Sections 113-693B-2X-2 and 113-693B-2X-3 contain thin, fine silt and clay layers.

Millimeter-sized dropstones, including aggregates of white sand (white clasts), which disintegrate when touched, are found throughout this unit. The aggregate dropstones occur in Cores 113-693A-11R and 113-693A-13R. Dropstones greater than 5 cm in diameter occur irregularly. They are angular, subangular to subrounded, and consist of gneiss, quartzites, and metamorphic and plutonic rocks.

The entire Subunit IIIA in Hole 693A has been severely disturbed by coring, including a soupy top core and moderately to severely disturbed lower intervals. Drilling-induced structures, including grading, occur in some of the cores in Hole 693A. Preservation of primary structures in Hole 693B is considerably better.

Subunit IIIB (243.9–255.1 mbsf; late Miocene)

Core 113-693A-27R through Section 113-693A-28R-1; depth 243.9–255.1 mbsf; thickness 11.2 m. No recovery of this interval in Hole 693B. Age: late Miocene.

Subunit IIIB is distinguished by the presence of nannofossils in a relatively thin interval of 11.2 m (Figs. 3 and 4) of diatom-nannofossil ooze. Accompanying the nannofossils, there is a decrease in the terrigenous component and a minor increase in volcanic glass and opaque minerals. The sediment texture (Fig. 6) and color remains relatively uniform. Minor color variations occur between greenish gray (5G 5/1, 6/1) and dark greenish

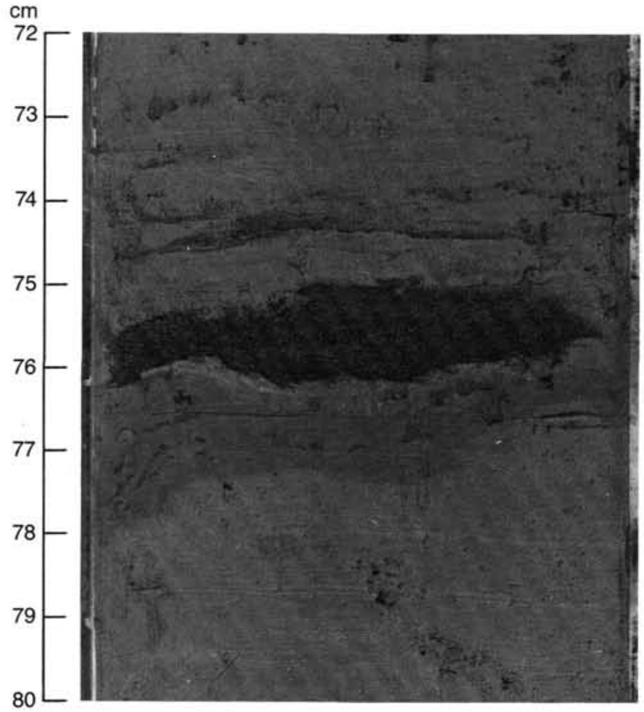

Figure 8. Very fine sand to coarse silt graded sediment layer with sharp contact boundaries to the adjacent clay (Interval 113-693A-4R-5, 72–80 cm).

gray (5G 4/1). Bioturbation is sparse in the subunit, and only Zoophycos burrows are identified.

Millimeter-sized dropstones occur throughout. Pebble-sized dropstones are only observed at the top and base of the unit and are dominantly gneiss.

Core recovery in this subunit is relatively good (Fig. 3), but the cores are moderately to very disturbed, and may have some drilling-induced sand layering.

Subunit IIIC (255.1–325.8 mbsf; Age late Oligocene to late Miocene)

Section 113-693A-28R-2 through Core 113-693A-35R; depth 255.1–330.5 mbsf; thickness 80.9 m. Cores 113-693B-5X through 113-693B-11X; depth 258.1–325.8 mbsf; thickness 67.7 m. Age: late Oligocene to late Miocene.

The recovery and quality of cores for Subunit IIIC were generally poor. Nearly all the top and middle sections of cores were soupy and the lower sections badly disturbed.

The sediments are similar to those in Subunit IIIA. Diatom mud, clay, and ooze characterize this subunit. The terrigenous components, primarily clays, increase toward the base whereas the proportion of sand remains relatively constant (Figs. 4–7). The overall color of the subunit varies between dark greenish gray (5BG 4/1, 5GY 4/1) and greenish gray (5GY 5/1). Dark laminations of dark greenish gray (5BG 4/1) and greenish gray (5G 5/1) occur at 30–40-cm intervals throughout Sections 113-693B-6H-1 to 113-693B-6H-5. Diatom content ranges from 15% to 60% of the sediment, peaking in Sections 113-693A-28R-4 and 113-693B-6H-2, and then gradually declining to just above Unit IV. Minor bioturbation is evident throughout, including halo burrows and Planolites.

Sand beds 2–6 mm thick occur in Sections 113-693B-6H-1, 113-693B-6H-6, and 113-693B-7H-2. The basal contacts are sharp, but the tops are diffuse and moderately bioturbated. Laminations and other diffuse fine sand/silt beds (Fig. 9) occur throughout this subunit.

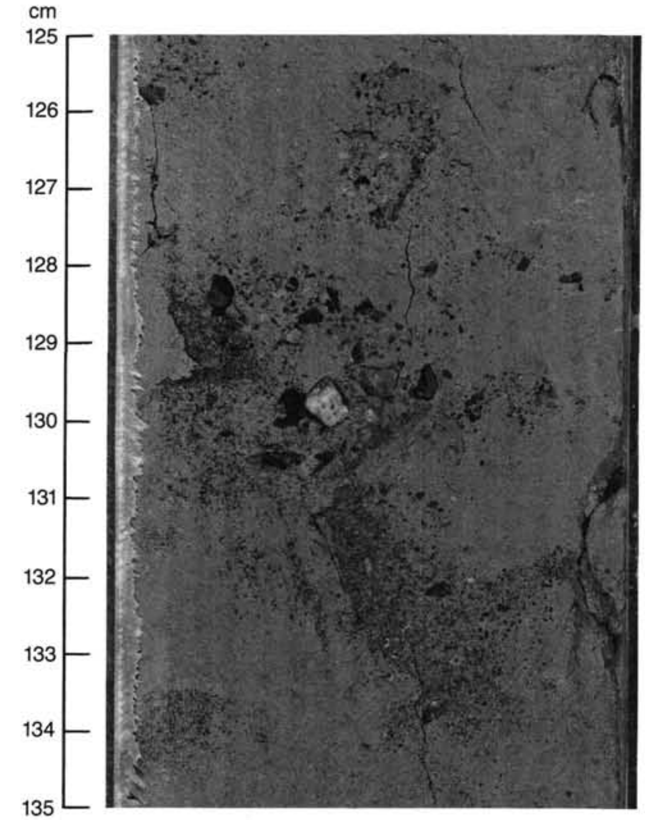

Figure 9. Diffuse coarse sand layers in lithostratigraphic Subunit IIIC (Interval 113-693B-10X-3, 125–135 cm).

Dropstones as large as 7 cm across, but in general in the millimeter size range, are found scattered throughout Subunit IIIC (Figs. 9 and 10). Some of the smaller dropstones are aggregates of white sand (white clasts) (Cores 113-693B-6H and 113-693B-7H), which disintegrate when touched. Gneiss, mica/biotite schists, and quartzite constitute the larger dropstones, which are both rounded (e.g., Section 113-693B-11X-1; Fig. 11), and angular to subrounded (e.g., Core 113-693B-8X.

Unit IV (325.8–345.1 mbsf; Age late Oligocene)

Cores 113-693A-36R and 113-693A-37R; depth 330.5–349.9 mbsf; thickness 19.4 m. Cores 113-693B-12X and 113-693B-13X; depth 325.8–345.1 mbsf; thickness 19.3 m. Age: late Oligocene.

Two biogenic sediments, one calcareous and the other siliceous, occur in Unit IV in variable length cycles (Fig. 12) interbedded with dominantly terrigenous sediments. There may be as many as four cycles in the sequence (Cores 113-693B-12X and 113-693B-13X). The two dominant biogenic lithologies are (1) muddy nannofossil ooze and nannofossil-bearing clayey or silty mud and (2) diatom-bearing silty and clayey mud. The diatomaceous sediments (5%–12% diatoms), generally dark greenish gray (5GY 4/1) and dark gray (5Y 4/1, N 4/0) in color, are darker than the nannofossil sediments which are gray (5Y 6/1, 5/1). The latter have sharp bases and gradational, bioturbated tops (Fig. 13). Terrigenous clay input increases and the sand fraction decreases downsection in this unit (Figs. 6 and 7).

Minor to moderate bioturbation occurs in the light colored nannofossil lithofacies (Figs. 12 and 13). This is seen by the extensive occurrence of Planolites, Zoophycos burrows, and Chondrites and the rare occurrence of vertical burrows. Millimeter-size dropstones are rare.

Drilling disturbance in Unit IV is minor to moderate in both Holes 693A and 693B and soupy core tops occur in Hole 693A.

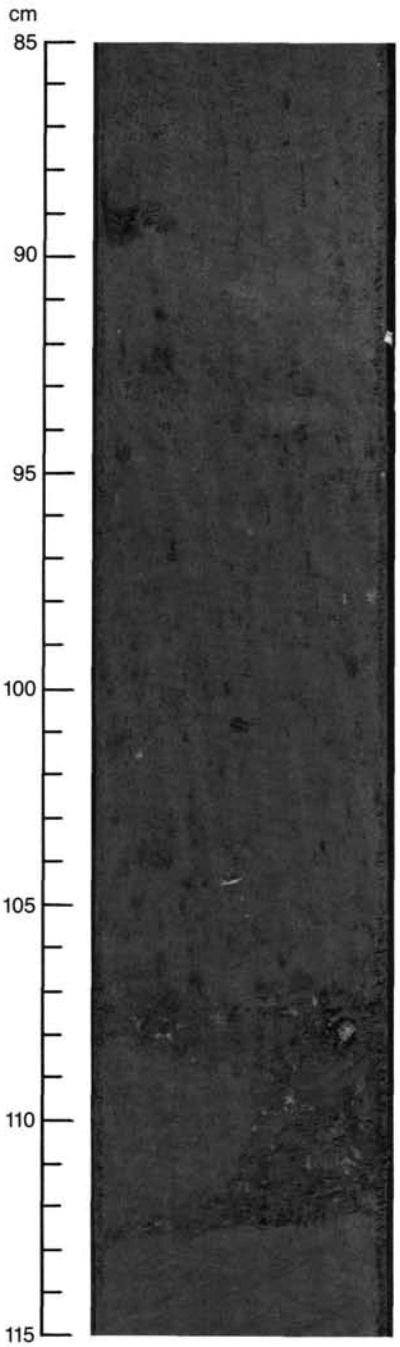

Figure 10. Dropstones, in the millimeter-size range scattered randomly throughout lithostratigraphic Subunit IIIC (Interval 113-693B-6H-5, 85–115 cm).

Unit V (345.1–397.8 mbsf; lower Oligocene)

Cores 113-693A-38R through 113-693A-42R; depth 349.9–397.1 mbsf; thickness 47.2 m. Cores 113-693B-14X through Interval 113-693B-19X-4, 68 cm; depth 345.1–397.8 mbsf; thickness 52.7 m. Age: lower Oligocene.

This unit is a sequence of deformed sediments. Fracturing of the cores during the drilling process may have rotated some of the drilling biscuits, making it difficult to estimate the percentage of deformed sediments.

Unit V includes at least three deformed sedimentary intervals. These are observed in Core 113-693B-14X, the base of Cores 113-693B-15X through 113-693B-16X, and Cores 113-693B-18X through 113-693B-19X-4, respectively. Diatom silty mud and diatom clayey mud are the dominant lithologies. The occurrence of terrigenous sediment is similar to the other units, however, there is a marginal increase in the overall quartz and opaque mineral constituents (Figs. 4 and 5). Colors, dark gray (5Y 4/1), dark greenish gray (5G 4/1), and greenish gray (5G 5/1), are fairly constant and do not reflect specific lithologies. In the deformed sediment interval in Core 113-693B-18X, both sharp and gradational color changes occur, from a dark greenish gray (5GY 4/1) to dark gray (N 4/0) to greenish gray (5G 5/1). Core 113-693B-18X has numerous colored laminae, generally a few millimeters thick, some of which exhibit coarse to fine silt grading. Others have sharp basal contacts and just discernible size grading.

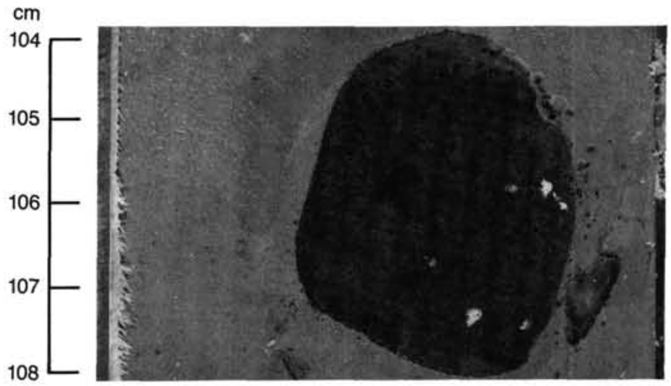

Figure 11. Large black rounded dropstone, approximately 4 cm long, 2.5 cm wide (Interval 113-693B-11X-1, 104–108 cm).

The deformed sediments in Core 113-693B-14X consist of wavy folds (Fig. 14) interbedded with coarse gravel layers (Fig. 15). Further downcore a well-preserved gastropod shell (Fig. 16), with a few shell fragments, was observed. Minor to moderate bioturbation is present in this sequence. Lower in the unit some of the laminated beds have been deformed and show slump folds and microfaulting (Fig. 17).

The textural heterogeneity of this unit makes it difficult to distinguish gravel/pebbles transported by mass wasting processes, from those derived as ice-rafted debris. The isolated occurrences of gravel/pebbles are considered to be ice rafted. Such pebbles are observed in all cores as are less-lithified mud clasts.

Unit VI (397.8–409.0 mbsf; Albian-Santonian)

Cores 113-693A-43R and 113-693A-44R; depth 397.1–409.0 mbsf; thickness 11.9 m. Interval 113-693B-19X-4, 69 cm, to bottom of Core 19X: depth 397.8–403.1 mbsf; thickness 5.3 m. Age: Albian-Santonian.

Unit VI consists of a drilling sand (Core 113-693A-43R) and radiolarian diatomite (Core 113-693A-44R). A marked increase in the radiolarian content is associated with the virtual disappearance of the terrigenous component (Fig. 4). The sediment color is very dark gray (5Y 4/1), greenish gray (5GY 5/1), and dark greenish gray (5GY 4/12).

Drilling disturbance has resulted in a highly fragmented sequence, however it appears that most of the biscuits have not been rotated. The unit is moderately bioturbated by Planolites, Zoophycos, vertical burrows, and also Chondrites (Core 113-693A-44R).

No dropstones were observed in this unit.

Core 113-693A-43R is a drilling-induced graded sedimentary sequence. However, an examination of the sand grains suggests that two modes exist, distinguished by their abrasion characteristics; a very angular, fine to medium sand probably drilling induced and a subrounded to rounded fine to coarse sand mode

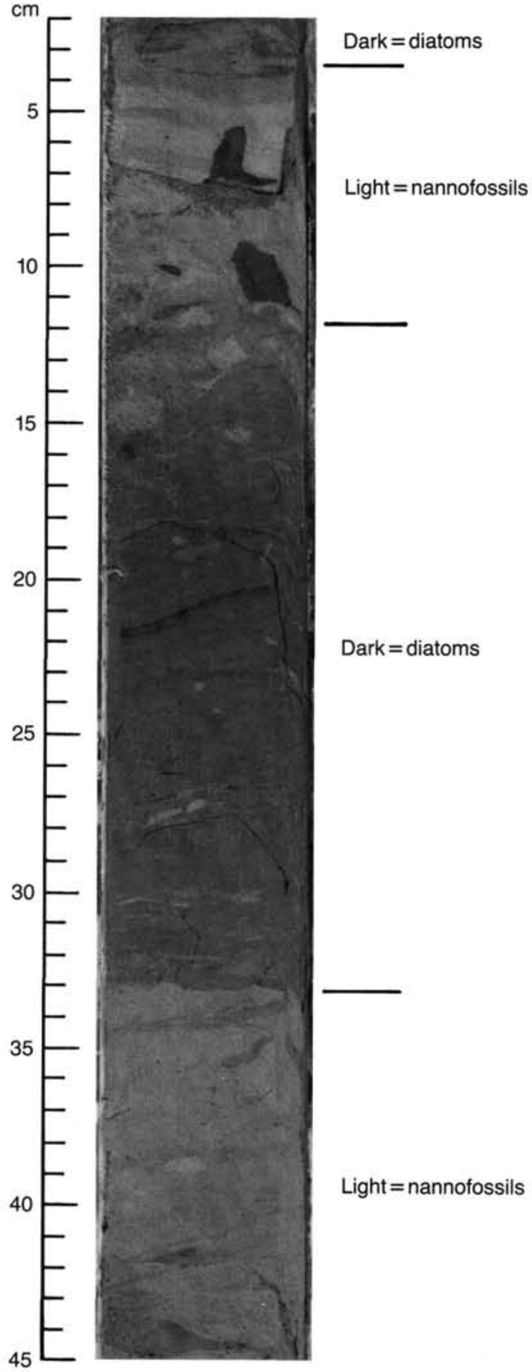

Figure 12. Example of the two biogenic lithologies, one calcareous (the lighter one) and the other siliceous (the darker one) occuring in irregular cycles (Interval 113-693B-12X-6, 2–45 cm).

probably *in situ*. The existence of a sand interval is indicated by the downhole logging results (see "Downhole Measurements" section, this chapter). The poor recovery and quality of Core 113-693A-43R, compared with the equivalent depth interval lithology of the adjacent Hole 693B and the downhole logs, give conflicting information about the composition and age of this interval. However, the base of this unit has been determined on the basis of downhole measurements and is set at 409.0 mbsf.

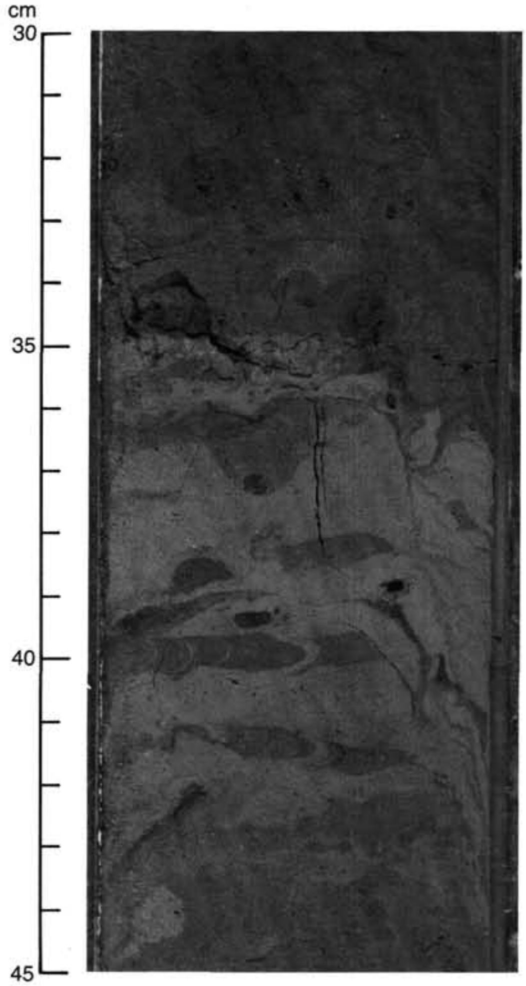

Figure 13. Upper contact of muddy nannofossil ooze (light colored sediment), moderately bioturbated, showing extensive Planolites, Zoophycos, and Chondrites (Interval 113-693B-12X-3, 30–45 cm).

Unit VII (409.0–483.9 mbsf; Aptian to lower Albian?)

Cores 113-693A-45R to 113-693A-51R; depth 409.0–483.9; thickness 74.9 m. Age: Aptian to lower Albian? (Early Cretaceous).

The sediments in Unit VII are primarily claystones with minor occurrences of clayey mudstone and silty mudstone. They differ from the sediment of Unit VI in that the biogenic component rarely exceeds a few percent (Fig. 4). Terrigenous sediments dominate with high abundances of opaque minerals, volcanic glass, and mica and glauconite in the upper part. The biogenic component is poorly preserved, rarely exceeds 3%, and consists of nannofossils and diatoms with trace amounts of foraminifers and radiolarians (Fig. 4). Sediment colors are dark and range between black claystones (5Y 2.5/1, 7.5YR 2/1), black (2.5Y 2/0) and dark gray (5Y 3/1) mudstones, and very dark gray silty mudstones (5Y 3/1), with the occasional dark gray clayey mudstone (5Y 3/1).

The unit contains both parallel laminae and inclined bedding. The beds have sharp basal contacts and are silty fining upward. Shell fragments and pyrite are common.

Core recovery from Cores 113-693A-45R through 113-693A-51R is marginally better than that for the the preceding 15 cores; however, drilling disturbance resulted in highly fractured and fragmented core recovery.

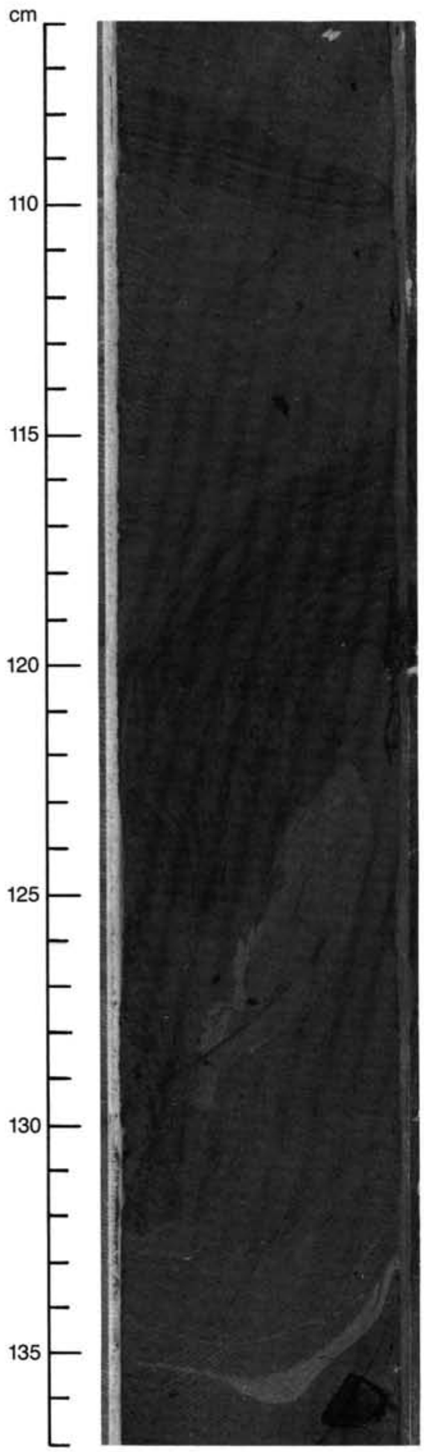

Figure 14. Deformed sediments of lithostratigraphic Unit V (Interval 113-693B-14X-4, 106–137 cm) illustrating wavy slump folds and mud clasts.

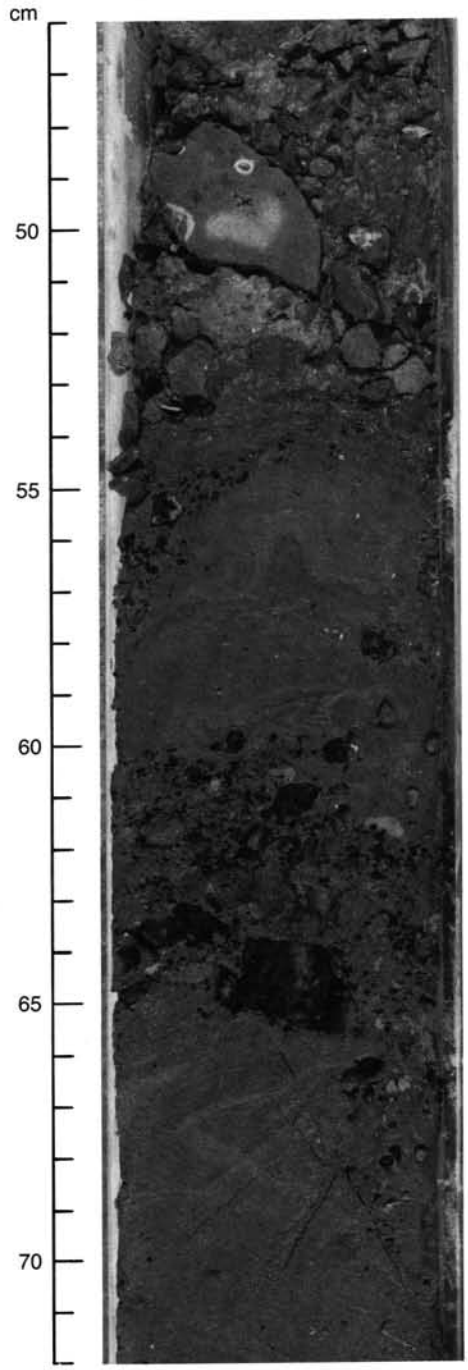

Figure 15. Coarse gravel layer interbedded with deformed sediments of lithostratigraphic Unit V (Interval 113-693B-14X-5, 46–72 cm).

Summary Analysis of Sand Fraction

Grain Size and Composition

Twenty-two samples representing sediments from Pleistocene to early Oligocene age were wet-sieved at 63 μm and the residue examined. The samples (10 cm^3) were disaggregated by magnetic stirring for 2 hr in a 1% Calgon solution, followed by 10 min in an ultrasonic bath where necessary. Sample depths and approximate ages are listed in Table 3.

The sand fractions fall into three groups:

1. Pleistocene to upper Miocene sediments contain an unsorted sand fraction (Fig. 18A) with the largest grains commonly 2–3 mm in diameter.
2. Upper Miocene to upper Oligocene sediments contain a well-sorted very fine sand mode with a small coarse tail (Fig. 18B). The transition between (1) and (2) appears to be gradual and occurs from about 150 to 250 mbsf. Cores from this interval are badly disturbed by drilling, and core recovery

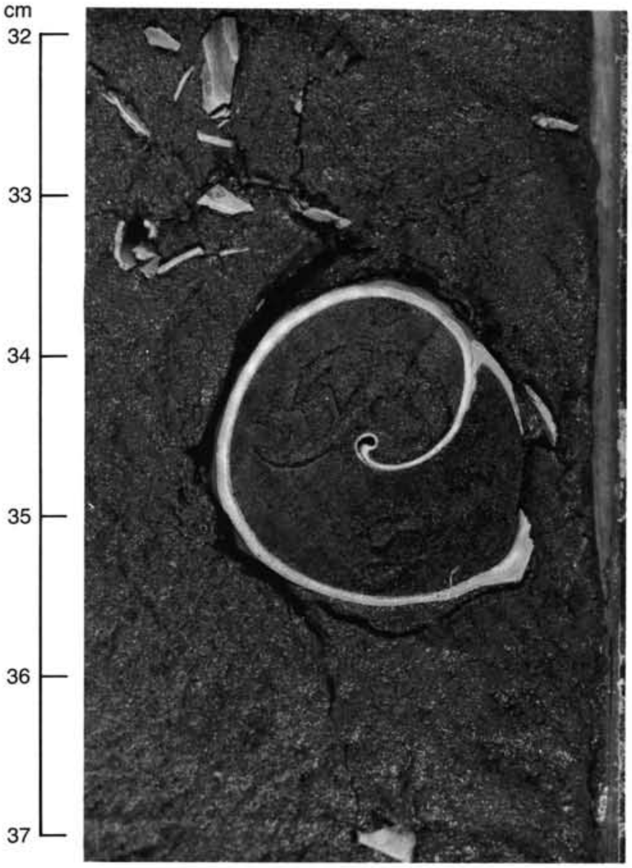

Figure 16. Well-preserved gastropod shell and shell fragments in a muddy diatom ooze (Interval 113-693B-14X-6, 32–37 cm).

was exceedingly poor, hence we do not know whether the transition is smooth or if there are oscillations between the two types of grain-size distribution.

3. Lower Oligocene sediments contain a well-sorted very fine sand fraction with a few much larger grains (1–5 mm; Fig. 18C). In one sample (113-693B-16X-3, 104–106 cm) some of the larger grains may be drill cuttings. The transition between (2) and (3) is sharp and occurs between Cores 113-693B-13X and 113-693B-14X.

Grain shape is angular to subangular, and no variation was noted downhole. A minor exception is glauconite which occurs as rounded grains. One or two quartz grains per sample in the top 40 m are rounded and polished.

There are wide compositional variations in the proportion of biogenic to terrigenous sand. Planktonic foraminifers dominate the sand fraction in the uppermost two samples and quartz forms only 50%–60% of the terrigenous fraction, the rest being mainly altered volcanic glass and feldspar, with hornblende also common. Radiolarians and large diatoms are present to abundant in Pliocene to Oligocene sediments (Table 3). Terrigenous components are relatively constant downcore, with quartz the most abundant (over 80%) followed by feldspar. Amphiboles and pyroxenes, epidote, garnet, opaque minerals, biotite, and glauconite are present in most samples. Among the larger sand grains are vein quartz, feldspar, and metasediments (quartzites, pelites, and schists). Much of the feldspar is altered and appears cloudy. Lower Oligocene samples form a separate compositional group with slightly more common glauconite and a distinctive pale brown mica.

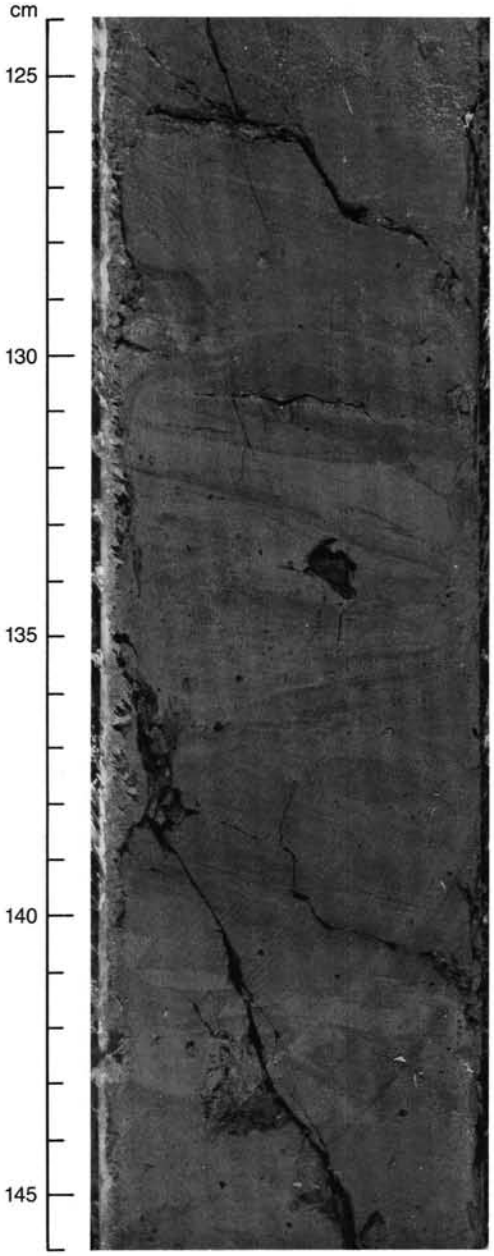

Figure 17. Deformed sediments in Interval 113-693B-18X-3, 124–146 cm (Unit V), showing laminated beds and a variety of small-scale structures including slump folds, microfaulting, and ice-rafted detritus.

Clay Mineralogy

X-ray diffraction analyses were completed on 56 samples from Holes 693A and 693B (Fig. 19). The sampling interval used was generally one per core. The objectives of clay mineral studies at Site 693 are (1) to identify major paleoenvironmental changes as expressed by clay mineral associations and (2) to compare the clay mineral associations at Site 693 with those observed on Maud Rise (Sites 689 and 690), on the Falkland Plateau, and in the Cape Basin during the same geological intervals.

Results

The clay minerals identified include chlorite, illite, kaolinite, and smectite (Fig. 19). Based on the relative abundances of the

Table 3. Samples for sand fraction analysis. Ages are core-catcher ages (see "Biostratigraphy" section, this chapter).

Sample (cm)	Depth (mbsf)	Litho-stratigraphic unit	Age	Terrigenous	Siliceous biogenic	Calcareous biogenic
693A-1R-2, 145-150	2.0		Pleistocene	--		---
693A-2R-2, 45-50	4.5	I	Pleistocene	--		---
693A-2R-7, 20-25	11.7		Pleistocene	----		
693A-3R, CC (0-5)	21.7		early Pleistocene	----		
693A-4R, CC	31.2	II	late Pliocene	----		
693A-8R, CC	69.9		early Pliocene	----		
693A-12R-3, 87-90	102.8		early Pliocene	---	--	
693A-16R-1, 16-20	137.6	IIIA	early Pliocene	----		
693A-21R-2, 113-116	188.2		late Miocene	---	-	
693B-2X-4, 118-120	239.5		late Miocene	---	-	
693B-6H-6, 13-15	275.4		early middle to Miocene	---	-	
693B-7H, CC (2-4)	281.8		early Miocene	---	--	
693B-8X-4, 35-37	292.0		early Miocene	---	-	
693B-9X, CC (21-23)	304.9	IIIC	early Miocene	---	-	
693B-10X, CC (27-29)	312.8		late Oligocene	---	--	
693B-11X, CC (27-29)	318.4		late Oligocene	---	--	
693B-12X, CC (26-28)	334.0	IV	late Oligocene	---	--	
693B-13X-2, 138-140	338.4		late Oligocene	----		
693B-14X-6, 46-48	353.1		early Oligocene	---	--	
693B-15X-3, 147-149	359.2	V	early Oligocene	---	--	
693B-16X-3, 104-106	368.4		early Oligocene	----		
693B-17X, CC (42-44)	376.6		early Oligocene	---	-	

Key:
- ---- Exclusive
- --- Abundant
- -- Common
- \- Present

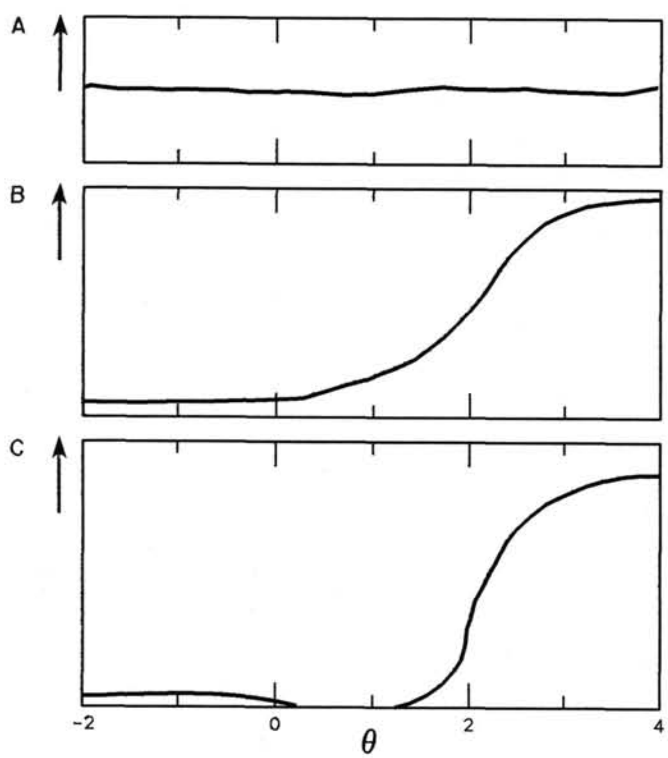

Figure 18. Schematic grain-size frequency curves for sand fractions, Site 693. A. 0–190 mbsf, i.e., Pleistocene to upper Miocene: unsorted sand. B. 230–340 mbsf, i.e., upper Miocene to upper Oligocene: well-sorted very fine sand with a coarse tail. C. 350–380 mbsf, i.e. lower Oligocene: well-sorted very fine sand, with a separate small group of coarser grains. (No vertical scale implied: total sand percent in each sample has not been determined quantitatively).

clay species, four clay units were recognized at Site 693. Units C3 and C4 are each divided into two subunits.

Unit C1 extends from the seafloor to 165 mbsf and consists of illite (common to very abundant), smectite (rare to very abundant), kaolinite (rare to common), and chlorite (rare to common, sometimes absent). The stratigraphic range of this unit is from the lower Pliocene to the Pleistocene.

Unit C2 extends from 165 to 260 mbsf and has a clay association of abundant to very abundant illite and rare to abundant chlorite, associated with rare to common kaolinite and sometimes smectite. The stratigraphic range of this unit is from the upper Miocene to the lower Pliocene.

Unit C3 extends from 260 to 398 mbsf, and the clay fraction consists mainly of illite. This unit ranges from the upper Oligocene to the lower Miocene, and is divided into two subunits. Subunit C3A extends from 260 to 340 mbsf (upper Oligocene to lower Miocene). The clay association consists of very abundant to exclusive illite, rare to common kaolinite, and sporadic rare to common smectite and rare chlorite. Subunit C3B extends from 340 to 398 mbsf (lower to upper Oligocene and one Cretaceous sample). The clay association consists of very abundant illite, common kaolinite, and sporadic rare to common smectite and rare chlorite.

Unit C4 extends from 398 mbsf to the bottom of Hole 693A at 484 mbsf, and the clay fraction consists mainly of smectite. This unit is Aptian to Albian-Santonian in age, and is divided into two subunits. Subunit C4A extends from 398 to 455 mbsf and consists of exclusive smectite, sporadically associated with rare illite. Subunit C4B extends from 455 to 484 mbsf. The clay association consists of very abundant smectite, rare illite and kaolinite, and sporadic rare chlorite.

Paleoenvironmental History

Very abundant and exclusive smectite in Unit C4 (Albian) suggests the presence of a warm continental climate with alter-

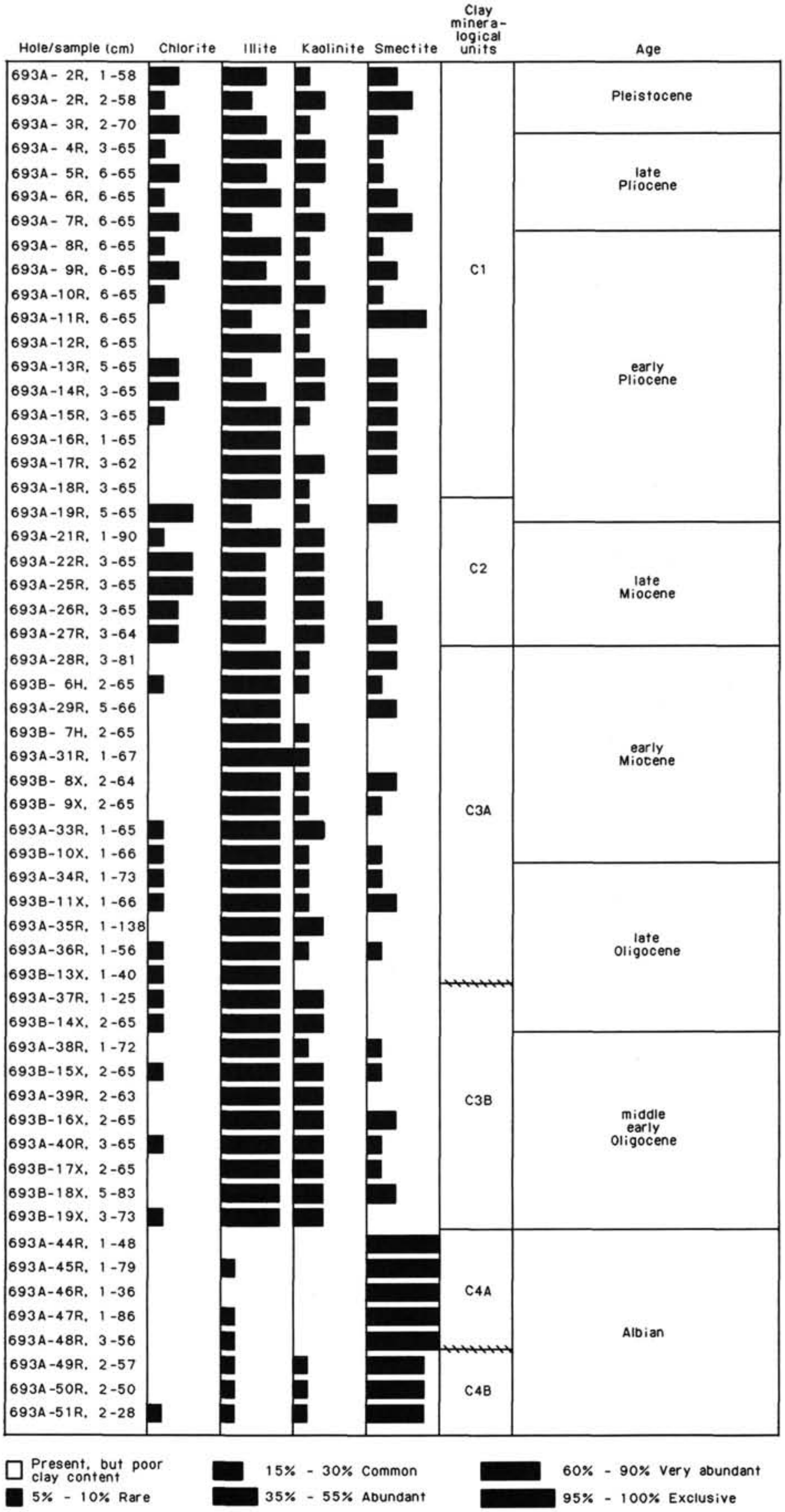

Figure 19. Clay mineralogy, Site 693.

nating wet and arid conditions on Antarctica. Similar climatic conditions prevailed during the same time interval in most Atlantic regions (Chamley, 1979; Robert, 1987). Very abundant and exclusive smectite also suggests that erosional processes were weak on a low-relief Antarctic margin. However, rare chlorite, illite, and kaolinite observed in Subunit C4B were probably derived from erosion of rugged terrain in tectonically active regions. The clay association of Subunit C4B is very similar to that seen during the Lower Cretaceous (Valanginian?) at Site 692, and on the Falkland Plateau at DSDP Sites 330 and 511 during the Aptian to Albian (Robert and Maillot, 1983). During the Aptian-Albian time interval, chlorite, illite, and kaolinite were abundant in the Cape Basin at DSDP Site 361. This clay assemblage is related to an extensional phase in the Cape Basin, associated with the shearing of the Falkland Plateau and South Africa. Detrital supply of chlorite, illite and kaolinite ceased in the Cape Basin and on the Falkland Plateau when the separation was completed (Robert, 1987). The eastern tip of the Falkland Plateau cleared the South African margin during the Albian, around 98 m.y. ago (Martin et al., 1982).

Very abundant and exclusive illite in Unit C3 (lower Oligocene to lower Miocene) reflects the paucity of chemical weathering and the predominance of physical erosion on Antarctica. It corroborates the clay mineral data from Maud Rise (Sites 689 and 690) where abundant illite is present during the same time interval. However, the occurrence of more abundant illite at Site 693, located on the Antarctic margin, is probably due to a more important detrital supply from crystalline and crystallophyllian terrain in the adjacent Dronning Maud Land where schists, greywackes, and predominantly intrusive rocks of Archean age outcrop (Bredell, 1982; Grikurov, 1982). Common kaolinite in Subunit C3B (lower to upper Oligocene) probably originates from relict deep-weathered soils which previously developed on the adjacent continent. These soils could have been formed during the Paleocene and the Eocene, as suggested by rare to abundant kaolinite (and associated chlorite) on Maud Rise (Sites 689 and 690) and by the appearance of kaolinite (in trace amounts to 5%) on the Falkland Plateau at DSDP Sites 327 and 511 (Robert and Maillot, 1983) during the same time. The appearance or increased abundance of kaolinite (even in small amounts) in Cenozoic sediments generally reflects increased humidity on adjacent land-masses, as suggested by the distribution of this mineral along the East Atlantic margins (Robert and Chamley, 1986).

A decrease of the illite content in Unit C2 (upper Miocene) is associated with increased abundances of kaolinite and principally of chlorite. This variation has not been recorded on Maud Rise where only a very brief increase of chlorite and kaolinite occurred during the upper Miocene at Site 689. Increased chlorite contents occurred at DSDP Sites 329 and 513 in the Falkland Plateau area during the late Miocene (Robert and Maillot, 1983), but chlorite abundances (5%–15%) remained generally lower than those recorded at Site 693. This event probably reflects an increased removal of chlorite from Antarctica. Present climatic conditions on Antarctica favour the formation of chlorite (and illite) in poorly developed soils of deglaciated areas (Ugolini and Jackson, 1982). Increased abundances of chlorite at Site 693 during the upper Miocene could result from erosion of poorly developed soils during a slight deglaciation in the hinterland of Dronning Maud Land. This mineralogical change probably occurred during the relatively warm period which partly characterized the upper Miocene (Kennett and Von der Borch, 1986).

Unit C1 (lower Pliocene to Pleistocene) is mainly characterized by increased contents of smectite and also by fluctuations in the abundances of the clay minerals. However, sediments at Site 693 have lower smectite contents than contemporaneous sediments on Maud Rise (Sites 689 and 690) and in the Ross Sea (Robert, Caulet, and Maillot, in press). As in these regions, smectite at Site 693 probably results from the removal of ancient smectite-rich sediments cropping out on or around Antarctica. This unit started to form during the lower Pliocene, when the Antarctic ice-sheet began to further expand to a late Neogene maximum (Mercer, 1978).

In this unit, alternating olive gray and dark grayish brown sediments were studied in Sections 113-693A-2R-1 and 113-693A-2R-2. Olive gray deposits contain abundant illite, common smectite and chlorite, and rare kaolinite. Dark grayish brown sediments are characterized by abundant smectite, common kaolinite and illite, and rare chlorite. Similar cyclic variations were described in late Pleistocene sediments off Kapp Norvegia where smectite-rich sediments were deposited during colder periods, and smectite-poor sediments during warmer periods (Grobe, 1986). At Site 693, increased abundances of smectite and kaolinite are associated in darker sediments, suggesting a more important removal of ancient sediments from the Antarctic margin during colder periods.

Smectite content is generally lower in the Cenozoic sedimentary sequence at Site 693 than on Maud Rise (Sites 689 and 690) and in the Ross Sea area at DSDP Site 274 (Robert, Caulet, and Maillot, in press). At Site 693, an important proximal detrital supply influences the record of climatic events and provides information about the hinterland of Dronning Maud Land. The proximity of the Antarctic shield favors the supply of illite throughout the Cenozoic.

More abundant smectite on Maud Rise (Sites 689 and 690) is probably derived mainly from removal processes on the Antarctic margins, where important hiatuses were recognized at Sites 692 and 693. Sediments removed extend from the middle Cretaceous to the Paleogene, a time interval characterized by dominant smectite (75%–100%) on the conjugate margin of the Falkland Plateau and in the Cape Basin (Robert, 1987).

Clay associations at Site 693 become more similar to those of Maud Rise (Sites 689 and 690) during the early Pliocene when extensive glaciation, possibly associated with increased circulation, favored the homogenization of the detrital supply in the eastern Weddell Sea.

Lithostratigraphic Appendix: Ice-Rafted Dropstones, Site 693

From a total of 50 dropstones, 30 representative specimens were selected for petrographic analysis from Holes 693A and 693B. Only those dropstones 1 cm diameter or larger were included in the sample suite.

The age of sediments containing the dropstones ranges from Pleistocene to Oligocene. Lithologically they are divided into five categories: (1) volcanic, (2) sedimentary, (3) felsic plutonic, (4) basic plutonic, and (5) metamorphic rocks. Petrogenetically, the volcanic rocks are basalt and andesite; the sedimentary rocks are sandstone; the metamorphic rocks include hornfels, gneiss, schist, and quartzite; the felsic plutonic rocks are granite; and the mafic plutonic rocks are diorite and diabase.

In hand specimen, the pebbles range in size from 1 to 9 cm; they are subangular to subrounded, some are slightly weathered and some are well polished. A detailed description of each specimen is given in Table 4.

Figure 20 shows the location of each dropstone within the lithostratigraphic column. Groups of dropstones with similar lithology occur together (Fig. 20). The pebbles can be grouped into "sets" occurring at various depths (mbsf):

Table 4. Petrographic description of selected ice-rafted dropstones from Site 693. Downcore location of dropstones is given in Figure 20.[a]

Rock number: 113-693A-2R-1; 109–111 cm
Name: garnet-hypersthene hornfels
Size: 3 × 2 cm
Shape: angular
Weathering: weakly weathered

Major minerals	%	Accessory minerals	Comments
Quartz	80	Biotite	Granoblastic texture, slight sericitization is the only alteration present
Garnet	10	Sericite	
Orthoclase	5	Ilmenite	
Perthite	3	Hypersthene	

Rock number: 113-693A-2R-5; 128–135 cm
Name: basaltic andesite
Size: 3 × 9 cm
Depth: 9.78 mbsf
Shape: subangular
Weathering: none

Major minerals	%	Accessory minerals	Comments
Plagioclase	65	Chlorite	Extensive sericitization of plagioclase, and chloritization of shards. A porphyritic rock.
Pigeonite augite	20	Sericite	
		Sphene	
Almenite	10	Epidote	
		Zircon	

Rock number: 113-693A-2R-5; 144–145 cm
Name: arkosic sandstone
Size: 1 × 1 cm
Depth: 9.94 mbsf
Shape: angular
Weathering: none

Major minerals	%	Accessory minerals	Comments
Plagioclase	75	Amphibole	Sedimentary rock with quartz interstitial to plagioclase; slight sericitization.
Quartz	20	Biotite	
		Sericite	

Rock number: 113-693A-5R-2; 89–91 cm
Name: granite
Size: 2 × 2 cm
Depth: 33.79 mbsf
Shape: angular
Weathering: some

Major minerals	%	Accessory minerals	Comments
Microcline	60	Perthite	Extensive sericitization of feldspars, and biotite replacing amphibole. Perthite and myrmekite are poikilitically enclosed by orthoclase.
Quartz	15	Amphibole	
Plagioclase	10	Sericite	
Orthoclase	5	Biotite	
		Pyrrotite	
		Pentlandite	

Rock number: 113-693A-6R-5; 23–27 cm
Name: granite
Size: 4 × 4 cm
Depth: 47.33 mbsf
Shape: subangular
Weathering: some

Major minerals	%	Accessory minerals	Comments
Quartz	40	Sericite	Evidence of extensive hydrothermal alteration in a coarse, equigranular rock. Chlorite alters amphibole (sphene is in fractures), and sericite alters feldspars.
Plagioclase	30	Sphene	
Microcline	10	Chlorite	
Amphibole	15	Carbonate	

Rock number: 113-693A-11R-4; 135–137 cm
Name: granite
Size: 3 × 2 cm
Depth: 95.15 mbsf
Shape: subangular
Weathering: none

Major minerals	%	Accessory minerals	Comments
Quartz	40	Sericite	Graphic granite, extensively sericitized and amphibolized. Pentlandite-pyrrhotite are associated with amphibole.
Plagioclase	25	Amphibole	
Graphic intergrowth	15	Biotite	
Orthoclase	10	Pentlandite	
		Pyrrhotite	

Table 4 (continued).

Rock number: 113-693A-11R-5; 136–138 cm
Name: quartz diorite
Size: 1.5 × 1.5 cm
Depth: 96.66 mbsf
Shape: subangular
Weathering: none

Major minerals	%	Accessory minerals	Comments
Plagioclase	40	Chlorite	Relatively fresh, slight chlorite alteration of biotite and amphibole, sericitization of poikilitic texture in magnetite.
Amphibole	30	Sphene	
Biotite	10	Sericite	
K-feldspar	10	Magnetite	
		Ilmenite	
		Quartz	

Rock number: 113-693A-14R-5; 87–90 cm
Name: tremolite hornfels
Size: 4 × 4 cm
Depth: 125.07 mbsf
Shape: subangular
Weathering: none

Major minerals	%	Accessory minerals	Comments
Tremolite	85	Pyrite	Probably a fragment from a contact aureole. Epidote is interstitial to tremolite, sphene is an alteration product of ilmenite, and pyroxene vein crosscuts tremolite.
Epidote	10	Clinopyroxene	
Sphene	5	Ilmenite	

Rock number: 113-693A-14R-5; 93–95 cm
Name: basalt
Size: 3 × 3 cm
Depth: 125.13 mbsf
Shape: subrounded
Weathering: none

Major minerals	%	Accessory minerals	Comments
Plagioclase	75	Epidote	Equigranular, relatively fresh basalt. Interstitial shards are chloritized, and some labradorites are sericitized.
Augite	12	Ilmenite	
Glass shards	10	Sphene	
		Sericite	

Rock number: 113-693A-18R-1, 10–15 cm
Name: diabase (miarolitic)
Size: 1 × 1 cm
Depth: 157.0 mbsf
Shape: subangular
Weathering: none

Major minerals	%	Accessory minerals	Comments
Plagioclase	75	Chlorite	High-level intrusive rock with interstitial glass devitrifying to spherulites, and it is partially chloritized. Extensive hydrothermal alteration is apparent.
Magnetite	7	Epidote	
Clinopyroxene	5	Spherulites	
Quartz	5	K-feldspar	

Rock number: 113-693A-20R, CC (4–6 cm)
Name: amphibole-biotite gneiss
Size: 4 × 3 cm
Depth: 176.34 mbsf
Shape: subrounded
Weathering: some clay minerals after feldspar

Major minerals	%	Accessory minerals	Comments
Plagioclase	30	Carbonate	Schistosity is only moderate, the rock is relatively free of alteration. Hornblende poikiloblasts enclose quartz grains.
Hornblende	20	Sericite	
Biotite	10	Magnetite	
K-feldspar	15		
Quartz	25		

Rock number: 113-693A-21R-2, 114–117 cm
Name: amphibole-biotite gneiss
Size: 4 × 4 cm
Depth: 188.29 mbsf
Shape: subrounded
Weathering: some clay minerals after feldspars

Major minerals	%	Accessory minerals	Comments
Quartz	20	Carbonate	Incompletely recrystallized gneiss. Relict pyroxene is altering to amphibole on the rim and amphibole alters to chlorite.
Plagioclase	20	Sericite	
Augite	20	Chlorite	
Amphibole	20	Sphene	
Microcline	12	Magnetite	
Biotite	6		

Table 4 (continued).

Rock number: 113-693A-22R-2, 2–4 cm
Name: amphibole-biotite gneiss
Size: 2 × 2 cm
Depth: 205.30 mbsf
Shape: subrounded
Weathering: some clay minerals after feldspars

Major minerals	%	Accessory minerals	Comments
Orthoclase	20	Sphene	Incompletely recrystallized gneiss. Granulation and elongation of grains are characteristic features. Secondary magnetite overgrows quartz.
Plagioclase	25	Magnetite	
Quartz	20	Sericite	
Amphibole	15		
Biotite	8		

Rock number: 113-693A-25R-1, 5–6 cm
Name: gneissose sandstone
size: 3 × 3 cm
Depth: 224.65 mbsf
Shape: subrounded
Weathering: some clay minerals after feldspars

Major minerals	%	Accessory minerals	Comments
Quartz	60	Magnetite	Slightly gneissose texture, quartz is anomalous blue due to strain.
Plagioclase	18	Biotite	
Orthoclase	20	Sericite	

Rock number: 113-693A-25R-1, 30–31 cm
Name: pyroxene-amphibole hornfels
Size: 2 × 1 cm
Depth: 224.90 mbsf
Shape: subrounded
Weathering: none

Major minerals	%	Accessory minerals	Comments
Quartz	30	Chlorite	Granoblastic texture, hypersthene is poikilitically enclosed by amphibole. Relatively fresh rock.
Amphibole	25	Sericite	
Plagioclase	25	Biotite	
Hypersthene	8		
Magnetite	8		

Rock number: 113-693A-27X-1; 12–17 cm
Name: gneiss
Size: 6 × 6 cm
Depth: 244.02 mbsf
Shape: subangular
Weathering: some

Major minerals	%	Accessory minerals	Comments
Quartz	60	Sericite	Gneissose texture; K-feldspar(s) segregation of quartz and biotite in alternating hands. Sericite alteration of plagioclase and orthoclase is common. Recrystallization of quartz is apparent from 120° triple junctions between adjacent grains.
K-feldspar(s)	15	Zoisite	
Plagioclase	10	Sphene	
Biotite	8	Muscovite	
		Apatite	

Rock number: 113-693A-38R-1, 24–26 cm
Name: hornblende-biotite andesite
Size: 2 × 2 cm
Depth: 350.14 mbsf
Shape: angular
Weathering: none

Major minerals	%	Accessory minerals	Comments
Plagioclase	40	Carbonate	Extensively altered rock, phenocrysts are fragmented. Matrix is recrystallized, magnetite is associated with biotite and amphibole. Plagioclase is altered to An_{10}.
Orthoclase	40	Chlorite	
Quartz	15	Sericite	
Magnetite	5	Biotite	
		Amphibole	

Table 4 (continued).

Rock number: 113-693A-39R-1, 1–8 cm
Name: pyroxene tholeiite
Size: 2 × 2 cm
Depth: 359.61 mbsf
Shape: subangular
Weathering: none

Major minerals	%	Accessory minerals	Comments
Palagonite	40	Zeolite	Glassy basalt, glass is altered to palagonite. Amygdules are empty except for minor zeolite and chlorite. Clinopyroxenes are fresh. Crystallines make up part of the matrix.
Crystallites	30	Plagioclase	
Clinopyroxene	15	Orthopyroxene	
		Chlorite	

Rock number: 113-693B-3X-1, 4–6 cm
Name: biotite-pyroxene-amphibole hornfels
Size: 1 × 1 cm
Depth: 238.84 mbsf
Shape: subangular
Weathering: none

Major minerals	%	Accessory minerals	Comments
Horneblende	50	Albite	Granoblastic texture, grain boundaries at 120 degrees indicates an equilibrium assemblage. Clear, untwinned albite. Slightly sericitized.
Hypersthene	25	Sericite	
Biotite	15	Magnetite	
Quartz	10		

Rock number: 113-693B-3X-1, 8–10 cm
Name: quartzofeldspathic sandstone
Size: 2 × 2 cm
Depth: 238.88 mbsf
Shape: angular
Weathering: clay minerals from feldspars

Major minerals	%	Accessory minerals	Comments
Quartz	50	Sericite	Granular, slightly recrystallized. Relict perthite and microcline are breaking down. Iron-rich biotite poikilitically encloses quartz.
Plagioclase	40	Microcline	
Orthoclase	5		
Biotite	5		

Rock number: 113-693B-3X-1, 4–6 cm
Name: arkosic sandstone
Size: 2 × 1.5 cm
Depth: 238.84 mbsf
Shape: subangular
Weathering: clay minerals from feldspars

Major minerals	%	Accessory minerals	Comments
Quartz	85	Apatite	Relatively fresh rock. Some sericitization, stilpnomelane overgrows quartz.
Plagioclase	10	Microcline	
Stilpnomelane	3	Muscovite	
		Sericite	

Rock number: 113-693B-3X, CC (11–14 cm)
Name: biotite-muscovite-garnet schist
Size: 3 × 3 cm
Depth: 239.26 mbsf
Shape: angular
Weathering: clay minerals from feldspars

Major minerals	%	Accessory minerals	Comments
Quartz	60	Chlorite	Slightly schistose rock, garnets are elongate, appearing as augens, and are poikilitically enclosed by biotite.
Biotite	20	Apatite	
Muscovite	10	Sphene	
Garnet	5	Sericite	
Scapolite	5	Zircon	

0–20 mbsf (Pleistocene)—hornfels, andesite, sandstone
20–100 mbsf (late Pliocene)—granite, diorite
100–170 mbsf (early Pliocene)—sandstone, tremolite aggregate, basalt, diabase
170–198 mbsf (near the Pliocene/Miocene boundary)—gneiss
198–360 mbsf, including Holes 693A and 693B (lower Miocene through lower Oligocene)—mostly sandstone, schist, and basalt; only two granites and one gabbro.

The basalts are relatively fresh except for palagonitization of the glass and alteration of shards to chlorite. Pyroxenes are un-

Table 4 (continued).

Rock number: 113-963B-6X-5; 149–150 cm
Name: hornfels
Size: 3 × 2 cm
Depth: 275.29 mbsf
Shape: subrounded
Weathering: none

Major minerals	%	Accessory minerals	Comments
Plagioclase	65	Sericite	Equigranular rock consisting mostly of plagioclase-biotite-quartz. Granoblastic texture. Carbonate and sphene are associated with alteration of biotite to amphibole.
Quartz	10	Carbonate	
Biotite	22	Sphene	
Amphibole	3	Pyrite	
		Zircon	

Rock number: 113-693B-6X-6; 1–2 cm
Name: garnet-biotite schist
Size: 2 × 1 cm
Depth: 275.31 mbsf
Shape: subangular
Weathering: some

Major minerals	%	Accessory minerals	Comments
Quartz	60	Sericite	Grains except garnets show extensive elongation. They have wrap-around biotite on the grain boundaries, and are lack inclusions. Deformation was coeval or postdates the growth of garnets.
Plagioclase	15	Magnetite	
K-feldspars	2	Muscovite	
Garnet	5		
Biotite	5		

Rock number: 113-963B-6X-6; 5–7 cm
Name: granite
Size: 3 × 2 cm
Depth: 275.35 mbsf
Shape: subangular
Weathering: slightly

Major minerals	%	Accessory minerals	Comments
Microcline	50	Sericite	Medium-grained rock. Coarse cross-hatched microcline dominates. Relatively equigranular with fine-grained interstitial biotite.
Quartz	25	Apatite	
Plagioclase	15		
Biotite	5		

Rock number: 113-693B-8X-1; 41–43 cm
Name: basalt (vesicular)
Size: 4 × 3 cm
Depth: 287.51 mbsf
Shape: subangular
Weathering: none

Major minerals	%	Accessory minerals	Comments
Plagioclase	40	Quartz	Fine-grained basalt. Glass matrix is devitrifying to plagioclase and magnetite laths. Pyroxene is interstitial to plagioclase. Vesicles are filled by quartz.
Glass	25	Chlorite	
Pyroxene	10	Biotite	
Magnetite	10	Apatite	
		Zoisite	
		Sericite	

Rock number: 113-693B-9X-1; 3–5 cm
Name: amygdaloidal basalt
Size: 7 × 4 cm
Depth: 296.83 mbsf
Shape: subrounded
Weathering: none

Major minerals	%	Accessory minerals	Comments
Glass	40	Quartz	Very fine grained basalt; vesicles are filled with chlorite, zeolite minerals and quartz. The glass devitrifies to plagioclase and needle-shaped magnetite.
Magnetite	10	Sericite	
Plagioclase	15	Apatite	
Pyroxene	5		
Zeolite	10		
Chlorite	10		

Table 4 (continued).

Rock number: 113-693B-9X-1; 1–3 cm
Name: cataclastite (basalt?)
Size: 3 × 3 cm
Depth: 296.81 mbsf
Shape: angular
Weathering: none

Major minerals	%	Accessory minerals	Comments
Carbonate	80	Pyrite	Cataclastic rock with anastomosing veins. Extensive carbonate alteration. Possible amygdules are filled by quartz aggregates and pyrite.
Quartz	10		

Rock number: 113-963B-10X-2; 64–65 cm
Name: granite
Size: 2 × 2 cm
Depth: 308.64 mbsf
Shape: subangular
Weathering: none

Major minerals	%	Accessory minerals	Comments
Microcline	50	Sericite	Identical to 693B-6X-6, 5–7 cm. Microcline-rich granite with abundant perthite. Medium-grained rock with fine-grained interstitial biotite.
Quartz	25	Apatite	
Plagioclase	15		
Biotite	5		

Rock number: 113-693B-11X-CC; 0–1 cm
Name: garnetiferous hornfels
Size: 2 × 2 cm
Depth: 318.17 mbsf
Shape: subrounded
Weathering: none

Major minerals	%	Accessory minerals	Comments
Horneblende	60	Magnetite	Granoblastic equigranular rock. Garnet is poikiliticaly enclosed by horneblende. Magnetite shows myrmekitic texture. Horneblende poikiloblasts constitute a large part of the rock.
Plagioclase	20	Sericite	
Garnet	10	Biotite	
Quartz	8		

Rock number: 113-693B-11X-1; 10–15 cm
Name: diabase
Size: 5 × 5 cm
Depth: 316.20 mbsf
Shape: subrounded
Weathering: iron staining (slightly on thin section only)

Major minerals	%	Accessory minerals	Comments
Plagioclase	60	Sericite	Equigranular, fine-grained diabase. Magnetite is slightly oxidized, iron staining is due to weathering.
Pyroxene	25	Chlorite	
Magnetite	10	Apatite	

Rock number: 113-693B-15X-2; 1–3 cm
Name: gabbro
Size: 2 × 2 cm
Depth: 356.21 mbsf
Shape: subangular
Weathering: none

Major minerals	%	Accessory minerals	Comments
Orthopyroxene	30	Quartz	Coarse-grained rock. Large orthopyroxene poikilitically encloses plagioclase. Quartz is interstitial to large pyroxene. Magnetite is often rimmed by biotite and biotite is secondary mineral. Sericitic alteration is quite extensive.
Clinopyroxene	20	Biotite	
Plagioclase	40	Magnetite	
		Sericite	
		Apatite	

altered in both the phenocrysts and in the matrix. The texture of the basalts ranges between porphyrytic and aphyric. Vesicles are common in the porphyrytic basalt and are filled with zeolite and carbonate minerals.

Andesite and basaltic andesite show evidence of extensive hydrothermal alteration. Plagioclases are extensively saussuritized, and all of the interstitial glass has been altered to chlorite.

The metamorphosed pelitic rocks are of two types; hornfels and schist. The hornfels have typical equigranular, granoblastic texture; the dark minerals are amphibole, biotite, and garnet. Most hornfels show very little hydrothermal alteration, the feldspars are clear, and untwinned albite and garnets have not been altered by chlorite. The dark minerals in the schists are predom-

Table 4 (continued).

Rock number: 113-693B-15X-1; 13–15 cm
Name: hornfels-schist
Size: 2 × 2 cm
Depth: 354.83 mbsf
Shape: subangular
Weathering: none

Major minerals	%	Accessory minerals	Comments
Plagioclase	40	Sericite	Slightly granoblastic texture; mild schistosity along biotite aggregates. Relatively fresh rock, uneven grain boundaries indicate lack of textural equilibrium.
Quartz	40	Magnetite	
Biotite	15		

Rock number: 113-693b-15x-3; 89–92
Name: sandstone
Size: 3 × 3 cm
Depth: 358.59 mbsf
Shape: subangular
Weathering: none

Major minerals	%	Accessory minerals	Comments
Quartz	70	Muscovite	Equigranular rock with interlocking grains. Cemented by epidotized feldspar(?). Grain boundaries are jagged and uneven, and grains are angular.
Epidote	10	Microcline	
Plagioclase	5	Chlorite	
Magnetite	15	Chromite	

[a] The major mineral component commonly does not equal 100%. The missing component consists of accessory minerals.

inantly amphibole and biotite. Biotite shows alteration to chlorite. Unlike the hornfels, where grain boundaries have the characteristic 120° triple junction (common to equilibrium assemblages), grain boundaries are embayed and uneven in the schists.

The texture of the gneisses shows incomplete to complete recrystallization. The incompletely recrystallized rocks contain relict clinopyroxene, and the grain boundaries are irregular. The dark minerals such as amphibole and biotite segregate into gneissic bands, and amphibole poikiloblasts enclose some quartz grains. The completely recrystallized rocks show granulation between the alternating light (feldspar and quartz) and dark layers.

The sandstones range from arkosic to quartzofeldspathic in composition. In the arkose, granular quartz acts as a cementing agent. The slightly gneissose texture in some sandstones indicate an episode of deformation, possibly related to contact metamorphism.

Granites contain quartz and feldspars in various proportions. Quartz content ranges from 15% to 30%, and K-feldspars may be as high as 65% in some specimens. The dividing line in textural characteristics between granite and a slightly recrystallized feldspathic sandstone is not always clear-cut, and some of the so-called granites may be just recrystallized sandstones. Common to all granites, however, is that they all show extensive hydrothermal alteration; saussuritization of the feldspars and chloritization of amphibole. They appear to have been derived from a similar environment.

Diorites may be distinguished from diabase by the absence of pyroxene in the former. The diorites are relatively fresh with only minor sericitic alteration. As plagioclases in the diabase are extensively saussuritized, An content of both types of rocks is similar (An_{30}). One diabase is a high-level intrusive rock with small amount of interstitial glass. The glass is devitrifying to spherulite, and oxidized magnetite stains the cuspate-shaped glass and the spherulite.

The suite of dropstones from Site 693 contains angular to subrounded shapes and from highly metasomatised to relatively unaltered specimens. The gneissic rocks could have been derived from East Antarctica, and basaltic rocks from West Antarctica. The hornfels, schist, sedimentary rocks, and intrusives may have their provenance in either East and/or West Antarctica. To solve the problem of provenance for the dropstones, two opposing factors must must be considered: (1) there is evidence that glaciation of the Antarctic Peninsula did not start until middle to late Miocene, and (2) basalt and andesite dropstones occur in sediments of early and late Oligocene age (Fig. 20). The latter suggests that the basalt and andesite must have been derived from the East Antarctic region. Although volcanic rocks commonly outcrop on the Antarctic Peninsula (Dalziel and Elliot, 1973), they are less common on the Antarctic continent. Dropstones occurring above the middle Miocene could have been derived from either the east or west, although the general flow of the Weddell Sea surface current (from east to west) would favor an eastern source.

PHYSICAL PROPERTIES

Introduction

The objectives of the physical-properties program at Holes 693A and 693B were to help characterize the physical properties of high-latitude continental margin marine sediments and provide an important link between geophysical data and the geological realities of the materials that constitute the sedimentary section described by shipboard stratigraphers and sedimentologists.

The physical properties program consisted of obtaining the following measurements: (1) Index properties—gravimetric determinations of bulk density, porosity, water content, and grain density; (2) Vane Shear Strength—a relative measure of the resistance of the sediment to loads and a measure of its cohesiveness; (3) Compressional Wave Velocity—the speed of sound in the sediments; and (4) Thermal Conductivity—the ability of the sediment to transport heat.

Index Properties

Two methods of determining the bulk densities and porosities of the sediments were used for Holes 693A and 693B. Bulk density, porosity, and water content were determined at discrete points within the cores by gravimetric determination in addition to the bulk density and porosity obtained from GRAPE (gamma ray attenuation porosity evaluation) scanning of whole-round core sections. All core sections from Site 693 were logged on the GRAPE unit, from which bulk density and porosities were computed assuming a grain density of 2.75 g/cm^3. In view of the low grain densities encountered at Hole 693A, a systematic error was introduced into the bulk density data.

Index properties measured on samples are listed in Table 5. Profiles of bulk density, water content (dry basis), and grain density are illustrated in Figure 21. A profile of porosity is shown in Figure 22.

The highly disturbed nature of the cores recovered by rotary drilling at this site precludes any meaningful measurement of the physical properties of lithified or semilithified clayey sediments. The porosity and water content profiles (Figs. 21 and 22) illustrate the high degree of disturbance of sediments recovered at Hole 693A. In most thick sediment deposits, the porosity and water content of clayey silts and silty clays decreases with depth in a more or less constant fashion due to the compaction (consolidation) process where water is driven out of the sediment pores by overburden stresses, and individual sediment particles are realigned to form a denser fabric.

Rotary drilling of unlithified sediments, and in particular the diatom-rich silty clays of Hole 693A, resulted in the almost complete remolding of the original sediment structure and the injection of additional water into the sediment. In some cases the sediment is reconstituted into a totally new sediment where

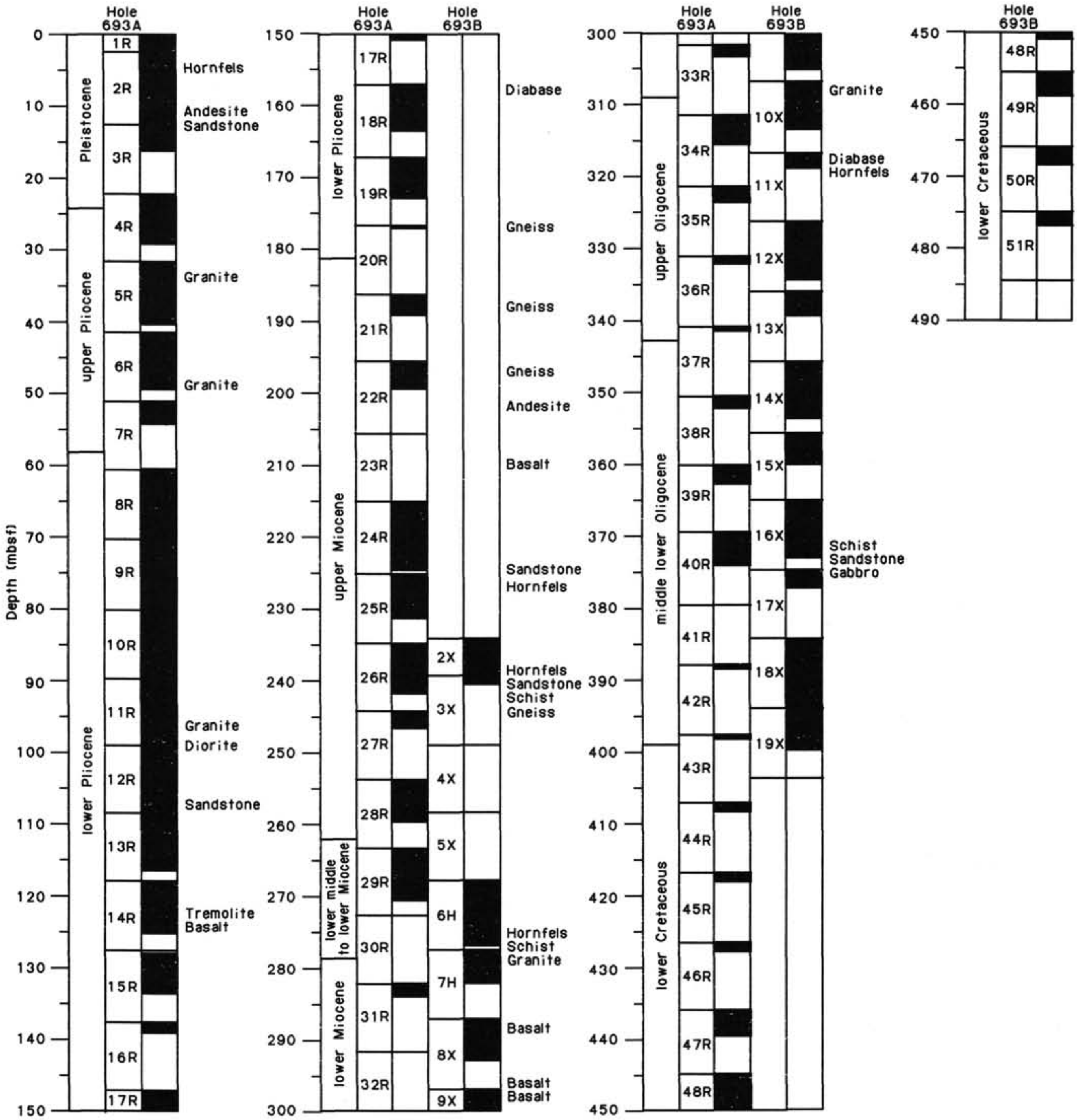

Figure 20. Plot of dropstones vs. depth of recovered cores, Site 693.

the physical properties have little resemblance to the *in-situ* conditions. The laboratory measured porosity and water content at Hole 693A do not decrease with depth until 180 mbsf. Below that level the sediments are sufficiently compacted to resist the disturbing effects of the bit and to form "biscuits" or small segments of sediment that retain some original intact fabric. When "biscuits" are present, physical property measurements are restricted to them. The totally remolded clay matrix was not measured. In general, most of the sediments recovered from Hole 693A were disturbed except for certain intervals of Cores 113-693A-44R through 113-693B-51R (407–476 mbsf). The sediment recovered from Hole 693B is less disturbed and reflects the *in-situ* conditions.

The relationship between the porosity measured in the laboratory on discrete sediment samples and the porosity determined from resistivity is also illustrated in Figure 22. The laboratory measured porosity, between the interval 100 and 150 mbsf, is 8%–25% higher than the logging porosity. This discrepancy reflects the degree of core disturbance, the amount of mixing, and the addition of water into the cored sediment. The agreement between the porosity measurements below 150 mbsf is good. In particular, the laboratory measured porosity of XCB cores from

Table 5. Index properties, water content, porosity, bulk density, and grain density measured on samples from Site 693.

Core, section top (cm)	Depth (mbsf)	Water content (% dry weight)	Porosity (%)	Bulk density (g/cm^3)	Grain density (g/cm^3)
113-693A-					
2R-1, 97	3.5	71.54	74.26	1.82	3.54
2R-3, 85	6.4	57.89	65.33	1.83	3.21
2R-5, 85	9.4	74.14	69.26	1.67	2.78
3R-2, 29	14.0	58.44	66.23	1.84	3.33
4R-1, 90	22.8	74.35	68.66	1.65	2.76
4R-2, 90	24.3	65.01	68.04	1.77	3.14
4R-3, 90	25.8	72.20	69.16	1.69	2.87
4R-4, 54	26.9	59.40	62.44	1.72	2.80
4R-5, 90	28.8	67.66	65.52	1.66	2.85
5R-3, 135	37.3	72.04	69.58	1.70	2.95
5R-4, 85	38.3	71.61	67.48	1.66	2.73
5R-5, 80	39.7	62.65	65.71	1.75	2.83
6R-3, 90	45.0	78.58	68.84	1.60	2.67
6R-6, 41	49.0	74.90	68.62	1.64	2.77
7R-1, 93	51.8	64.92	65.62	1.71	2.79
7R-2, 113	53.5	65.51	65.41	1.69	2.68
8R-1, 90	61.3	66.81	67.39	1.72	2.87
8R-4, 90	65.8	70.32	67.49	1.67	2.75
10R-6, 108	88.3	68.71	67.07	1.69	2.93
10R-7, 37	89.1	65.10	65.33	1.70	2.86
11R-3, 90	93.2	81.32	70.00	1.60	2.68
11R-4, 90	94.7	68.65	70.88	1.78	3.01
11R-6, 90	97.7	79.46	72.91	1.69	2.78
12R-1, 90	99.8	68.80	69.15	1.74	3.07
12R-3, 90	102.8	79.04	74.19	1.72	2.99
12R-5, 90	105.8	83.72	71.85	1.62	2.72
13R-1, 90	109.5	76.42	68.39	1.62	2.67
13R-3, 90	112.5	63.42	66.09	1.74	2.77
13R-5, 90	115.5	61.00	66.37	1.79	3.14
14R-1, 90	119.1	77.26	69.98	1.64	2.80
14R-3, 90	122.1	73.95	70.52	1.70	2.89
14R-5, 83	125.0	73.72	68.84	1.66	2.79
15R-2, 90	130.2	69.18	70.02	1.75	2.79
15R-4, 12	132.4	62.01	66.85	1.79	2.92
16R-1, 102	138.5	73.65	66.43	1.60	2.61
17R-2, 84	149.6	74.70	70.18	1.68	2.85
18R-3, 90	160.8	69.31	62.81	1.57	2.52
18R-4, 68	162.1	68.81	63.46	1.59	2.51
19R-1, 90	167.5	65.33	63.18	1.64	2.61
19R-3, 90	169.0	73.54	65.31	1.58	2.60
19R-4, 80	170.4	65.37	63.69	1.65	2.69
19R-5, 90	172.0	67.92	63.72	1.61	2.49
21R-2, 70	188.1	55.35	63.23	1.82	2.94
21R-3, 73	189.6	53.70	63.22	1.85	2.95
25R-2, 90	227.0	51.24	60.05	1.82	2.65
25R-4, 90	230.0	42.17	55.83	1.93	2.82
26R-4, 91	239.7	72.45	62.97	1.54	2.37
26R-4, 143	240.1	71.80	66.83	1.64	2.67
26R-5, 84	241.1	55.85	61.74	1.77	2.79
27R-1, 28	244.2	79.83	65.97	1.52	2.46
28R-1, 62	253.9	79.43	68.85	1.59	2.74
28R-1, 90	254.2	71.59	65.42	1.61	2.52
29R-6, 10	270.5	68.19	65.77	1.66	2.75
31R-1, 90	283.1	58.19	61.05	1.70	2.72
33R-1, 55	302.1	51.08	60.34	1.83	2.88
35R-2, 25	322.7	77.10	70.94	1.67	2.64
35R-2, 39	322.9	48.26	60.47	1.90	2.99
36R-1, 37	330.8	52.88	63.32	1.88	2.95
37R-1, 64	340.9	59.30	65.49	1.80	2.64
38R-1, 111	351.0	42.76	58.35	2.00	3.01
38R-1, 112	351.0	43.07	56.58	1.93	2.71
39R-2, 96	362.1	44.72	54.27	1.80	2.58
44R-1, 25	407.0	146.12	82.21	1.42	2.31
45R-7, 2	417.7	25.33	38.93	1.97	2.34
46R-1, 93	427.0	11.56	23.87	2.36	2.70
47R-1, 117	436.9	48.53	61.18	1.92	3.02
47R-1, 118	436.9	50.18	62.51	1.92	2.78
48R-1, 24	445.6	2.41	6.34	2.76	2.80
48R-1, 81	446.2	48.42	58.75	1.85	2.69
48R-4, 104	450.9	54.24	62.84	1.83	2.75
49R-2, 19	456.7	30.09	43.36	1.92	2.60
50R-1, 106	465.9	37.69	51.28	1.92	2.63
51R-1, 75	475.1	31.56	43.24	1.85	2.32
51R-2, 60	476.4	30.13	44.37	1.96	2.49

Table 5 (continued).

Core, section top (cm)	Depth (mbsf)	Water content (% dry weight)	Porosity (%)	Bulk density (g/cm^3)	Grain density (g/cm^3)
113-693B-					
2X-4, 37	238.7	59.69	66.84	1.83	2.98
6H-2, 92	270.2	58.01	64.63	1.80	2.83
6H-4, 40	273.6	58.11	62.71	1.75	2.60
6H-6, 56	275.9	57.13	62.04	1.75	2.61
7H-1, 84	278.3	59.71	65.08	1.78	2.75
7H-3, 85	281.4	48.96	62.64	1.95	3.05
8X-2, 67	289.3	49.48	58.26	1.80	2.42
8X-3, 113	291.2	55.51	66.17	1.90	2.83
8X-5, 4	292.1	48.96	59.66	1.86	2.82
9X-2, 65	299.0	42.68	57.68	1.98	2.86
9X-3, 56	300.4	48.28	59.10	1.86	2.87
10X-2, 100	309.0	55.08	62.39	1.80	2.80
10X-4, 55	311.6	57.09	61.48	1.73	2.76
11X-3, 5	319.2	55.77	64.00	1.83	2.98
12X-1, 107	326.9	42.39	56.11	1.93	2.80
12X-2, 97	328.3	56.21	61.56	1.75	2.67
12X-3, 48	329.3	63.46	64.73	1.71	2.68
12X-4, 126	331.6	53.52	58.91	1.73	2.55
12X-7, 20	335.3	56.34	60.82	1.73	2.66
13X-1, 123	336.7	59.73	63.90	1.75	2.66
14X-1, 51	345.6	55.64	60.96	1.75	2.72
14X-3, 34	348.4	38.88	54.09	1.98	2.62
14X-4, 145	351.1	37.54	51.69	1.94	2.90
14X-5, 1	351.1	36.41	50.63	1.94	2.84
15X-1, 68	355.4	38.80	52.65	1.93	2.59
17X-1, 135	375.4	35.03	53.03	2.09	2.83
17X-3, 16	376.6	33.77	48.07	1.95	2.73
18X-1, 46	384.2	35.63	51.97	2.03	2.83
18X-5, 40	390.1	47.15	57.53	1.84	2.63
18X-7, 34	393.2	46.56	56.91	1.84	2.79
19X-2, 83	395.7	36.39	53.36	2.05	3.01
19X-3, 119	397.6	40.58	55.50	1.97	3.11

Hole 693B correlates well with the logging porosity, except for an anomaly at 407 mbsf.

The only consistently valid measurement is grain density, but it may also be influenced, to an unknown degree, by the vertical mixing of a completely remolded sediment. The high values of grain density, shown in Figure 21 and listed in Table 5, reflect the presence of heavy minerals. The low values of bulk density reflect the presence of diatoms.

Compressional Wave Velocity

Sonic velocities (V_p) in sediment are measured using two methods. First, a continuous measurement of V_p was made through the unsplit core using a *P*-wave logger (PWL) installed next to the GRAPE source and detector. Second, measurements were made on individual samples removed from the core with one measurement from three different sections. V_p was measured in only one direction.

The laboratory-measured compressional wave velocity (Hamilton Frame) did not exceed the velocity in water (1500 m/s) until Core 113-693A-21R, 188 mbsf (Fig. 23 and Table 6). This is attributed to the disturbed nature of the core as discussed above. Figure 23 also illustrates the laboratory-measured compressional wave velocity as a function of downhole depth compared to the velocity determined by downhole logging. Between 350 and 416 mbsf, the laboratory measured velocities correlate reasonably well with the downhole logging results. Some of the logging velocities higher than 2300 m/s probably reflect dropstones. The velocities determined by the PWL are similar to those determined using the Hamilton Frame.

Shear Strength

The undrained shear strength of the sediment was determined with a Wykeham-Farrance motorized vane shear device

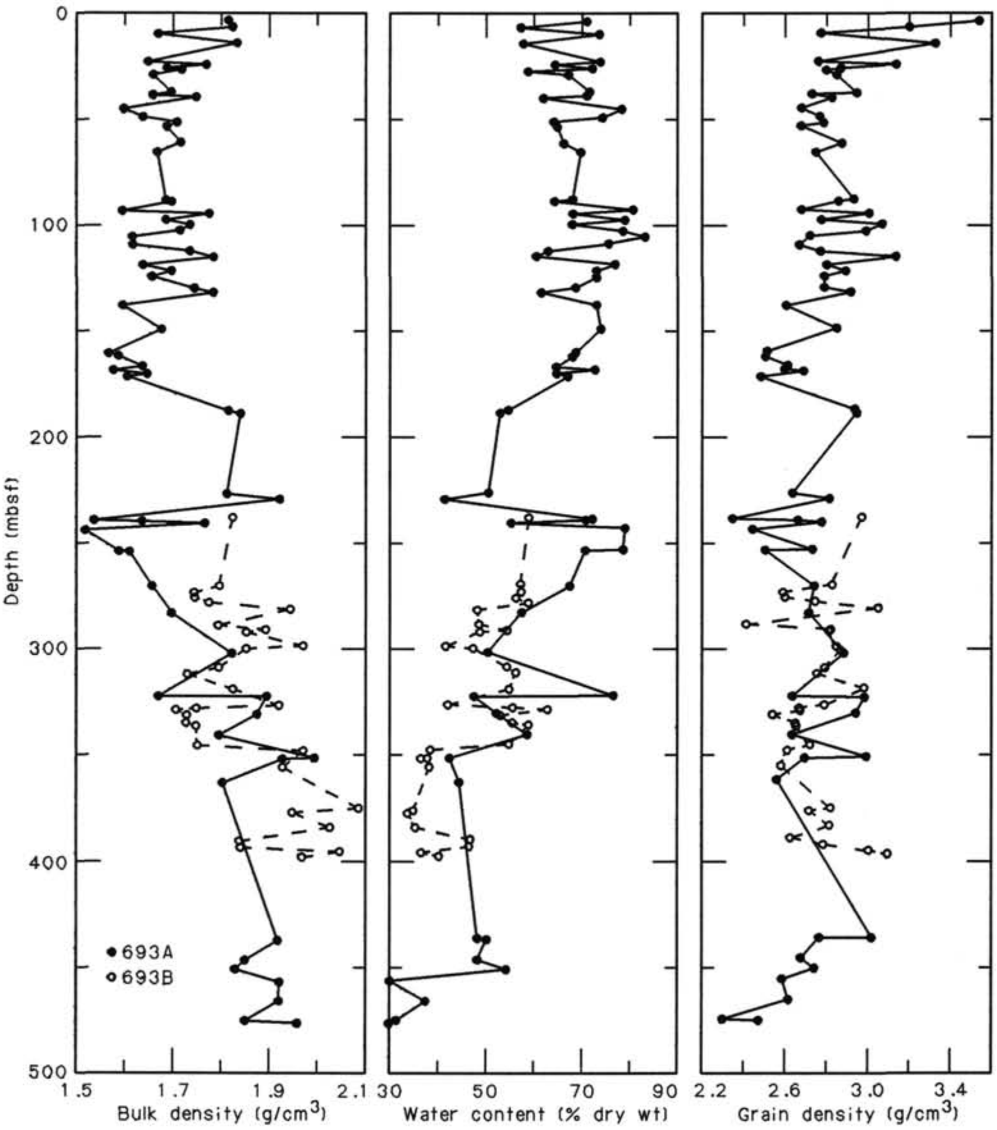

Figure 21. Profile of bulk density, water content, and grain density, Site 693.

using standard 1.2-cm equidimensional miniature vanes. Its operation and calculations follow procedures outlined by Boyce (1976). Several strength determinations were made with the ODP motorized vane shear device.

The shear strengths determined for Holes 693A and 693B are listed in Table 7 and illustrated in Figure 24. The core disturbance that affected the index properties also affected the measured shear strength. The majority of strength measurements were made on remolded sediments. Shear strength fluctuated between 5 and 50 kPa for the upper 240 m of the section. These low strength values reflect the high water-content and high porosity of the reworked sediments. Below 240 mbsf (Core 113-693B-3X) the strength increased drastically in the cores recovered by the XCB at Hole 693B (Fig. 24). Measurements on similar sediment recovered by rotary techniques increased only slightly over seafloor or upper-level sediments.

Thermal Conductivity

The thermal conductivity of the sediments sampled at Site 693A was measured following the methods of Von Herzen and Maxwell (1959) using the needle-probe technique. The needle-probe was inserted through a drilled hole in the core liner so that the probes were orientated perpendicular to the core axis.

Thermal conductivity ranged from 0.958 to 1.261 W/m-k. Table 8 lists the values of thermal conductivity, and Figure 25 is a profile generated from those values. Thermal conductivity is positively correlated with bulk density and inversely related to water content. Because of the disturbed sediments, the thermal conductivity measurements have little relationship to *in-situ* conditions.

Summary

Due to the highly disturbed nature of the sediments cored by rotary drilling at Holes 693A and 693B, the physical properties measured are of limited value. Only grain density and the properties measured on the deeply buried mudstones represent fair estimates of *in-situ* conditions. The grain density ranged from 2.37 to 3.54 g/cm^3. The low grain density reflects the diatom content and the high grain density reflects the amount of heavy minerals present. The laboratory-measured porosity in the interval between 100 and 150 mbsf is 8%–25% higher than the logging determined porosity. The correlation between the laboratory and logging porosity is in good agreement for sediments recovered in Hole 693B by the XCB. The porosity of the sediment between 250 and 350 mbsf (Core 113-693B-4X through Section 113-693B-14X-3) is 55%–65%. Below 350 mbsf it is 47%–57%.

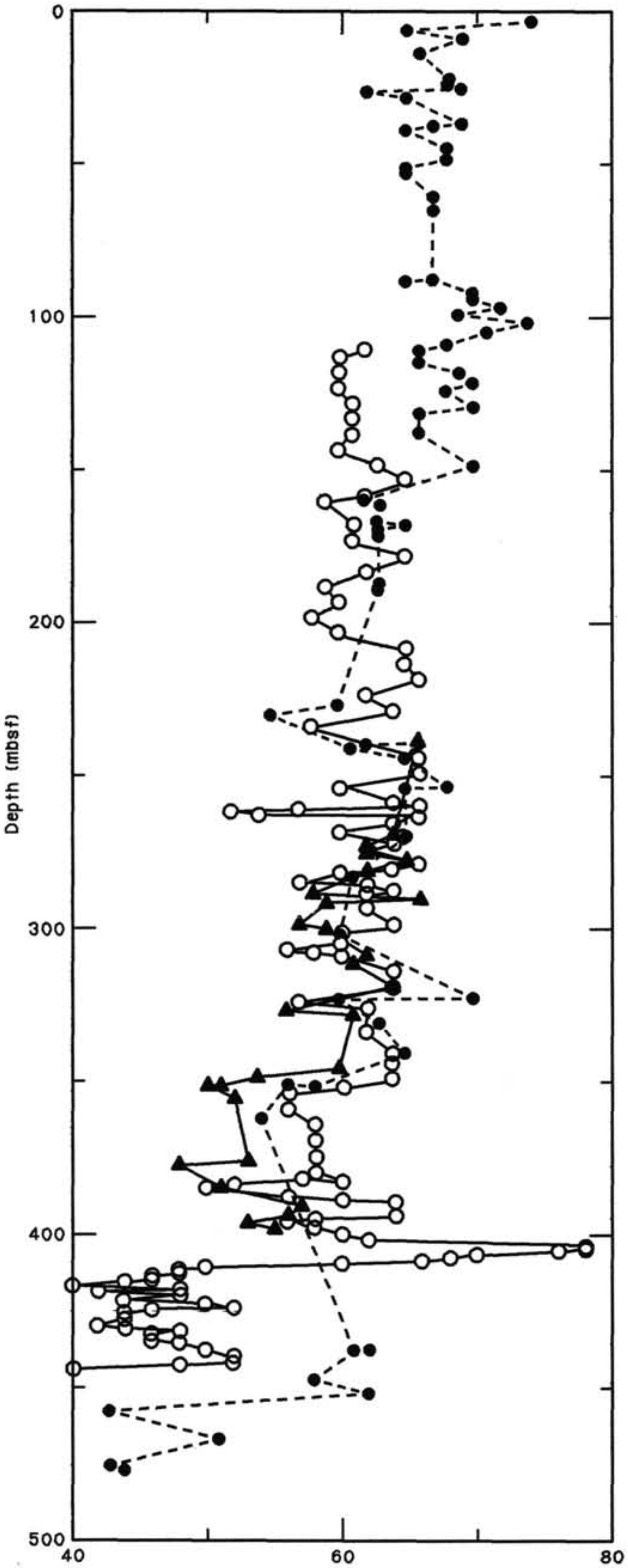

Figure 22. Profile of laboratory-measured porosity (dots = Hole 693A; triangles = Hole 693B) and logging-determined porosity calculated from resistivity logs (circles) for Site 693.

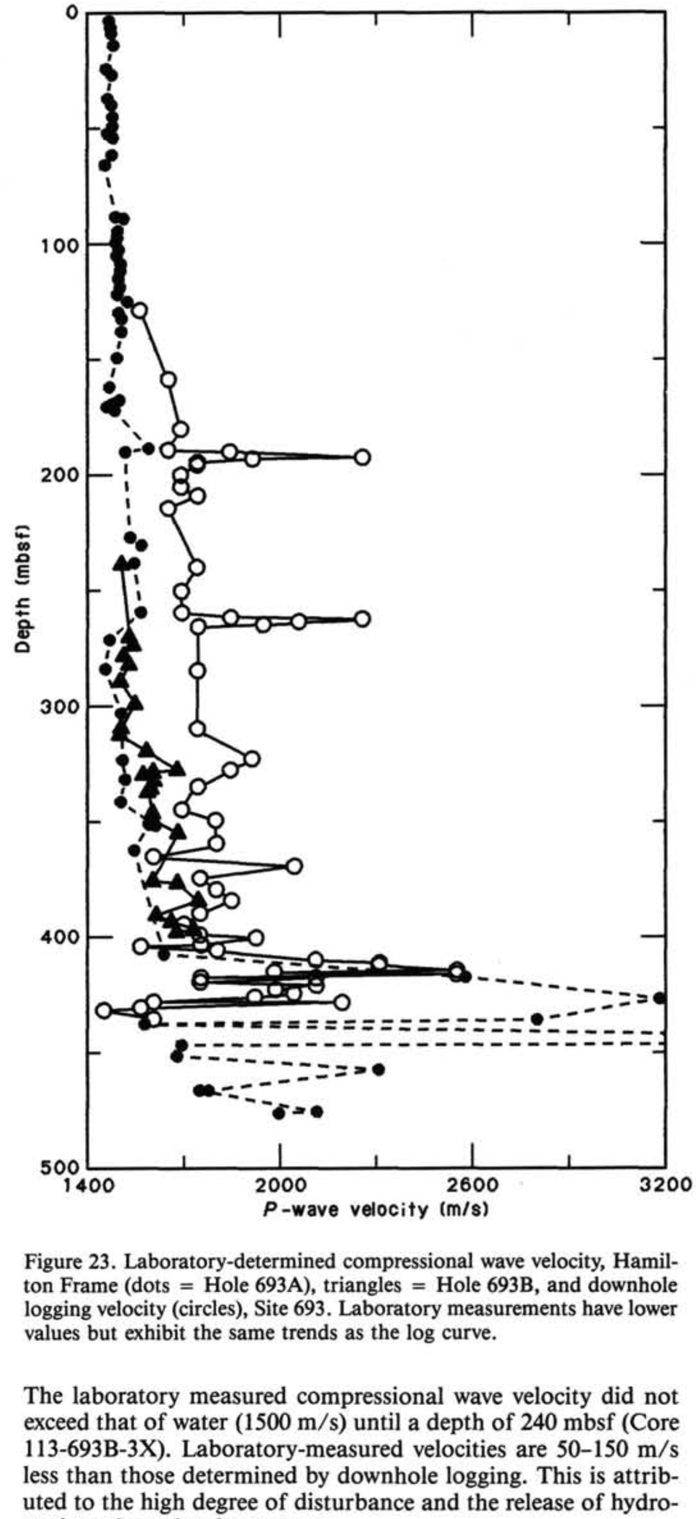

Figure 23. Laboratory-determined compressional wave velocity, Hamilton Frame (dots = Hole 693A), triangles = Hole 693B, and downhole logging velocity (circles), Site 693. Laboratory measurements have lower values but exhibit the same trends as the log curve.

The laboratory measured compressional wave velocity did not exceed that of water (1500 m/s) until a depth of 240 mbsf (Core 113-693B-3X). Laboratory-measured velocities are 50–150 m/s less than those determined by downhole logging. This is attributed to the high degree of disturbance and the release of hydrostatic and overburden stresses.

SEISMIC STRATIGRAPHY

The location of Site 693 was chosen aboard *JOIDES Resolution* during Leg 113, when it became clear that continued drilling at Site 692 would not be addressing the major problem of Cenozoic climatic deterioration. Site 693 was chosen on the basis of correlations made originally by K. Hinz (pers. comm., 1986) between existing multichannel seismic lines to provide the thickest section possible *above* his sequence boundary U6 (see

Table 6. Compressional wave velocities (Hamilton Frame) measured on samples from Site 693.

Core, section top (cm)	Depth (mbsf)	Velocity (m/s)	Remarks
113-693A-			
2R-1, 97	3.5	1467	
2R-3, 85	6.4	1471	
2R-5, 85	9.4	1474	
3R-2, 29	14.0	1477	
4R-2, 90	24.3	1459	
4R-4, 54	26.9	1474	
5R-3, 135	37.3	1465	
5R-4, 85	38.3	1469	
5R-5, 80	39.7	1475	
6R-3, 90	45.0	1478	
6R-6, 41	49.0	1480	
7R-1, 93	51.8	1463	
7R-2, 113	53.5	1476	
8R-1, 90	61.3	1475	
8R-4, 90	65.8	1453	
10R-6, 108	88.3	1488	
10R-7, 37	89.1	1511	
11R-4, 90	94.7	1492	
11R-6, 90	97.7	1492	
12R-1, 90	99.8	1487	
12R-3, 90	102.8	1494	
12R-5, 90	105.8	1491	
13R-1, 90	109.5	1503	
13R-3, 90	112.5	1502	
13R-5, 90	115.5	1496	
14R-1, 90	119.1	1499	
14R-3, 90	122.1	1493	
14R-5, 83	125.0	1520	
15R-2, 90	130.2	1497	
15R-4, 12	132.4	1505	
16R-1, 102	138.5	1506	
17R-2, 84	149.6	1491	
18R-4, 68	162.1	1470	
19R-1, 90	167.5	1498	
19R-3, 90	169.0	1481	
19R-4, 80	170.4	1463	
19R-5, 90	172.0	1486	
21R-2, 70	188.1	1591	
21R-3, 73	189.6	1517	
25R-2, 90	227.0	1533	
25R-4, 90	230.0	1565	
26R-4, 84	237.9	1544	
28R-4, 62	258.7	1566	
29R-6, 10	270.4	1470	
31R-1, 90	283.1	1458	
33R-1, 55	302.1	1505	
35R-2, 25	322.7	1509	
36R-1, 37	330.8	1516	
37R-1, 67	340.9	1500	
37R-1, 67	340.9	1503	
38R-1, 111	351.0	1602	
38R-1, 111	351.0	1585	
39R-1, 96	362.1	1540	
44R-1, 25	407.0	1630	
45R-7, 2	417.7	2570	
46R-1, 93	427.0	3182	
47R-1, 3	435.8	2793	Siltstone
47R-1, 113	436.9	1570	
48R-1, 24	445.6	4598	Limestone
48R-1, 81	446.2	1686	
48R-4, 104	450.9	1670	
49R-2, 19	456.7	2298	Mudstone
50R-1, 106	465.9	1765	Mudstone
50R-1, 107	465.9	1741	Mudstone
51R-1, 75	475.1	2108	Mudstone
51R-2, 64	476.4	1990	Mudstone
113-693B-			
2X-4, 37	238.7	1512	
6H-2, 92	270.2	1533	
6H-4, 40	273.6	1547	

Table 6 (continued).

Core, section top (cm)	Depth (mbsf)	Velocity (m/s)	Remarks
113-693B-			
7H-1, 84	278.3	1519	
7H-3, 85	281.4	1532	
8X-2, 67	289.3	1507	
9X-2, 65	299.0	1548	
10X-2, 100	309.0	1510	
10X-4, 55	311.6	1503	
11X-3, 5	319.2	1584	
12X-1, 107	326.9	1679	
12X-2, 97	328.3	1602	
12X-3, 48	329.3	1572	
12X-4, 126	331.6	1608	
12X-C, 20	335.3	1598	
13X-1, 123	336.7	1589	
14X-1, 51	345.6	1603	
14X-3, 34	348.4	1597	
14X-4, 145	351.1	1587	
14X-5, 1	351.1	1593	
15X-1, 68	355.4	1676	
17X-1, 135	375.4	1597	
17X-C, 16	376.6	1676	
18X-1, 46	384.2	1739	
18X-5, 40	390.1	1606	
18X-C, 34	393.2	1653	
19X-2, 83	395.7	1726	
19X-3, 119	397.6	1670	

"Background and Objectives" section, this chapter, and "Seismic Stratigraphy" section, "Site 692" chapter, this volume). The location chosen was at CDP 880 on profile BGR86-07, displayed in Figure 2. However, line BGR86-07 was securely tied in to the remainder of the multichannel data set on this margin only for the deeper part of the section, below the level to which Wegener Canyon has been cut. For the shallower seismic reflectors, some uncertainty in their identification remained. For this reason, *JOIDES Resolution*'s track from Site 692 to Site 693 (Fig. 26) was indirect; it first crossed the canyon southward and intersected line BGR78-19 before running westward to connect with BGR86-07. The additional initial westward loop was made to avoid a small field of rotting pack ice not far to the south of Site 692.

This exercise was moderately successful. Poor acoustic penetration where our track crossed BGR78-19, and the failure at the same time of the computer controlling our digital recording of the seismic signal add some uncertainty to the identification of U6 at this crossover. However, U6 can be traced along the *JOIDES Resolution* profile to the intersection with BGR86-07 at the location of Site 693, where it has a sub-bottom two-way traveltime (twt) of 1000 ± 100 ms. This places it between 100 and 300 ms above the reflector identified as U6 by K. Hinz (pers. comm., 1986), and represents an overburden thickness of 920 ± 95 m. For the purposes of Leg 113 drilling, a reasonably thick post-U6 section exists at the site.

The cored section at Site 693 penetrated about 400 m of Neogene and Oligocene sediments and 75 m of the underlying Lower Cretaceous material. Hole 693A was logged down to about 446 mbsf, and the drilled section has been correlated with the reflection profiles by means of the sonic log. While Hole 693A was being drilled however, before logging, a running correlation was made by means of the time-depth relation of Carlson et al. (1986). This relation had been found reasonably accurate at Sites 689 and 690, and at Site 693 the PWL measurements on the rotary-drilled 693A cores were not considered reliable because of drilling disturbance. The sonic log is described in "Downhole Measurements" section, this chapter, and the *P*-wave

Table 7. Undrained shear strengths determined for Holes 693A and 693B.

Core, section top (cm)	Depth (mbsf)	Shear strength (kPa)
113-693A-		
2R-1, 95	3.5	7.0
2R-3, 85	6.4	8.2
2R-5, 85	9.4	5.8
3R-2, 82	14.5	7.0
4R-2, 90	24.3	12.8
4R-4, 65	27.1	25.7
5R-4, 128	38.7	49.0
5R-5, 65	39.6	18.7
5R-6, 36	40.8	12.8
7R-1, 107	52.0	28.0
7R-2, 107	53.4	24.5
8R-1, 85	61.3	19.8
8R-7, 33	69.9	21.0
10R-6, 115	88.4	32.7
10R-7, 30	89.1	40.8
11R-4, 85	94.7	42.0
11R-6, 85	97.7	39.6
12R-1, 85	99.8	40.8
12R-3, 85	102.8	43.1
12R-5, 93	105.8	22.2
13R-1, 85	109.5	29.2
13R-3, 85	112.5	9.3
13R-5, 85	115.5	11.7
14R-1, 85	119.1	4.7
14R-3, 82	122.1	3.5
14R-5, 80	125.0	9.3
15R-2, 85	130.2	19.8
15R-4, 10	132.4	29.2
16R-1, 95	138.5	26.8
17R-2, 81	149.5	85.1
18R-3, 90	160.8	17.5
18R-4, 68	162.1	22.2
19R-1, 90	167.5	18.7
19R-3, 90	169.0	12.8
19R-4, 80	170.4	43.1
19R-5, 90	172.0	60.6
21R-2, 79	188.2	33.8
21R-3, 73	189.6	47.8
25R-2, 85	227.0	58.3
25R-4, 85	230.0	16.3
26R-4, 144	240.2	121.3
27R-1, 47	244.4	80.5
29R-6, 10	270.4	43.1
31R-1, 90	283.1	67.6
33R-1, 52	302.0	50.1
36R-1, 34	330.8	43.1
37R-1, 67	340.9	40.8
113-693B- (old vane device)		
2X-4, 42	238.7	73.5
6H-2, 82	270.1	130.6
6H-4, 10	273.3	246.1
7H-1, 81	278.3	110.8
7H-3, 82	281.3	184.3
113-693B- (motorized vane device)		
2X-4, 33	238.6	75.6
6H-2, 65	270.0	167.8
6H-4, 36	273.6	297.9
7H-1, 90	278.4	94.5
7H-3.	91	281.4
100.1		
8X-2, 86	289.5	139.4
8X-3, 121	291.3	238.8
9X-2, 63	298.9	69.8
9X-2, 96	299.3	69.8
10X-2, 71	308.7	69.8
10X-4, 66	311.7	76.8
11X-2, 20	317.8	148.9
12X-5, 65	332.5	104.7

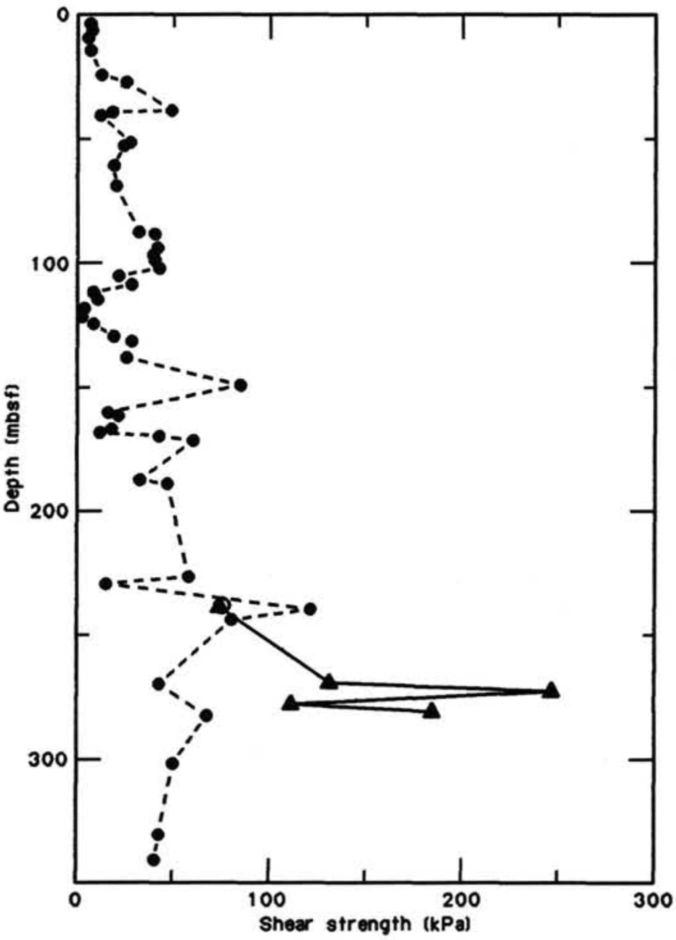

Figure 24. Undrained shear strength profile, Holes 693A (dots) and 693B (triangles).

logger data in "Physical Properties" section, this chapter. Figures 27 and 28 show the lithologic section correlated with the *JOIDES Resolution* profile and BGR86-07 respectively. The principal reflectors drilled are listed in Table 9. Compared with the time-depth relation derived from the sonic log, the relation of Carlson et al. (1986) gives depth estimates which are about 4% deeper down to 200 mbsf, and then remain about 8–11 m deeper to the base of the logged hole. This represents close agreement, and underlines the value of the Carlson et al. (1986) relation for provisional depth estimation.

The drilled section shows two major discontinuities. A hiatus at about 262 mbsf (between Sections 113-693A-28R, CC, and 113-693A-29R, CC, and above Core 113-693B-6H) cuts out most of the middle Miocene. Associated lithologic changes are minor, occurring within one main unit. Directly above the hiatus is a thin nannofossil mudstone subunit, and there is a marked downward reduction in the abundance and preservation of siliceous microfossils. Another, much longer hiatus at about 399 mbsf (within Core 113-693B-19X) separates the Lower Cretaceous (?Albian-Santonian) and lower Oligocene. Above the second hiatus, much or most of the Oligocene sediment in Hole 693B is slumped (Cores 113-693B-14X, 113-693B-18X, and part of 113-693B-19X, and possibly also Cores 113-693B-15X to 113-693B-17X). Below is a highly siliceous unit about 10 m thick (Core 113-693A-44R), underlain by more indurated claystones. These apart, the section shows no major changes except for progressive induration.

Table 8. Thermal conductivities of sediments from Hole 693B.

Core, section top (cm)	Depth (mbsf)	k (W/m-K)
113-693B-		
2X-3, 85	6.4	1.116
3X-2, 29	14.0	1.163
4X-3, 90	25.8	1.092
6H-3, 90	45.0	1.035
7H-2, 113	53.5	1.085
8X-3, 90	64.3	1.094
10X-3, 90	83.6	1.039
11X-3, 90	93.2	0.958
12X-3, 90	102.8	1.261
13X-3, 90	112.5	1.076
14X-3, 90	122.1	0.994
15X-4, 12	132.4	1.058

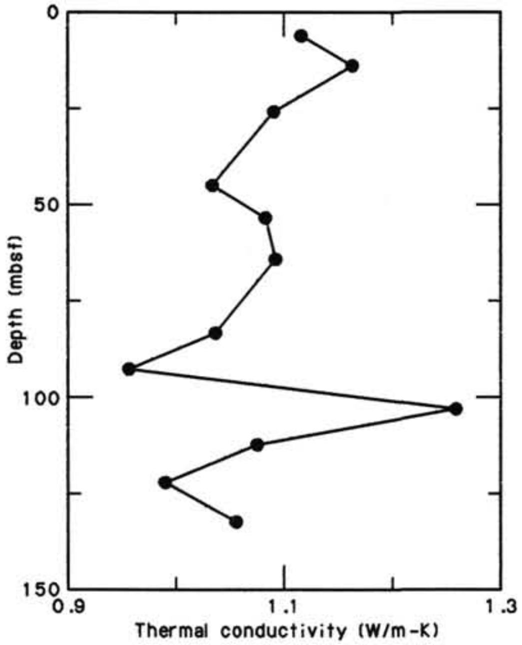

Figure 25. Thermal conductivity profile for Site 693.

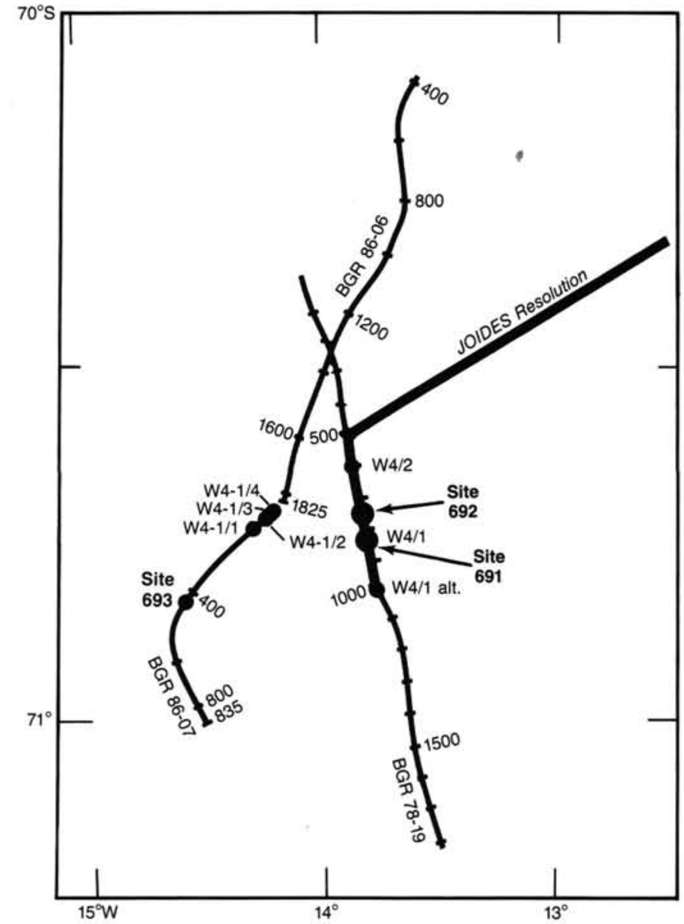

Figure 26. Track of site survey data and *JOIDES Resolution's* track approaching Site 693. The *JOIDES Resolution* track is indirect to provide a cross-tie between BGR86-07 and BGR78-19 and to avoid ice.

The sonic log shows a gradual velocity increase between 250 and 260 mbsf, with a narrow spike at 263 mbsf. The gamma ray log also changes, probably reflecting the change in biogenic silica. These changes are not correlated completely and in detail with the sediments to either side of the hiatus, because of poor recovery. However, they are assumed to be associated with it and to cause the related acoustic reflection.

By 400 mbsf, where the Oligocene/?Albian hiatus occurs, the logs are harder to interpret with confidence, since the section at that depth shows features (slumping, an erosion surface) which may not be at the same depth in each hole, and since Hole 693B, which was not logged, had much better recovery and less disturbance than 693A, which was. However, the logs show a major velocity increase at 410 mbsf, corresponding not to the hiatus but to the top of the Albian-Santonian to late Aptian claystones, 10 m beneath. Sonic velocities are low but variable in the overlying 30 m (presumably in part because of the slump). The gamma ray log changes markedly at 400 mbsf, reflecting probably the high silica content of the Cretaceous diatomite.

The reflection profiles show features corresponding to the two events described, and no other major reflectors in the section drilled.

The middle Miocene Hiatus

BGR86-07 approximates a strike section, so shows only subtle effects. Nevertheless, the complex, strong reflector at and below 330 ms sub-bottom, correlated with the 262 mbsf middle Miocene hiatus, appears noticeably rougher than the overlying reflectors, which also lie unconformably upon it (at greater distances from the site than are shown in Fig. 2). The *JOIDES Resolution* profile in Figure 27 runs approximately downdip and shows the unconformable nature of this reflector more clearly: the late Miocene section directly overlying it is 50 ms (about 40 m) thinner about 12 km upslope from the site. Late Miocene reflectors onlap the unconformity, suggesting (in this environment) an element of contour-current control over deposition. The overlying Pliocene section, in contrast, initially thickens upslope.

Farther away from the site downslope, the Neogene and Oligocene section thins to less than 100 ms: the Oligocene and Miocene section probably pinches out altogether before the scarp of the outer basement high is reached. There are indications of downlap onto the unconformity, which could again (in this environment) result from contour-current control (although seis-

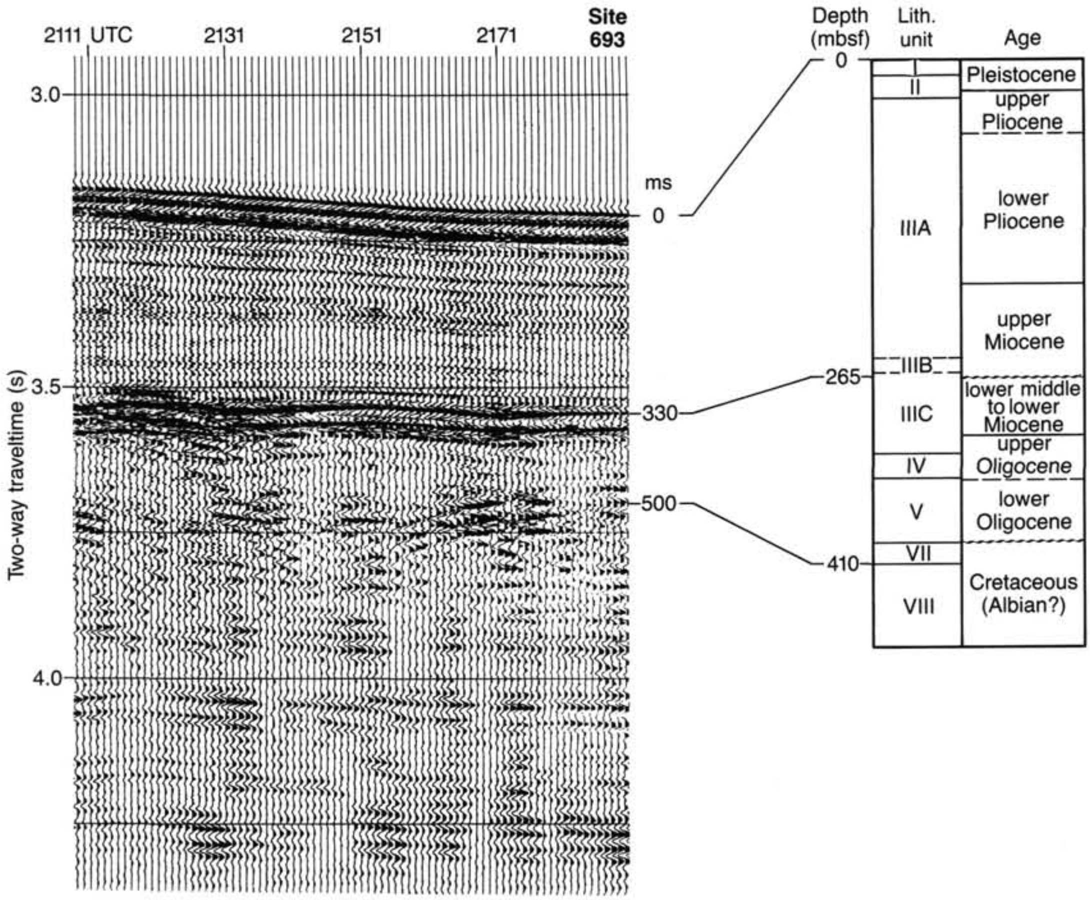

Figure 27. Reflection profile on *JOIDES Resolution's* approach to Site 694, showing identified major reflectors of Table 9.

mic coverage around the site is sparse). These suggestions of current control of deposition are compatible with the prominence of the hemipelagic component in the upper Miocene sediments. Upslope, away from the site, upper Miocene and younger sediments are missing, apparently eroded at a 200-m deep trough in the seabed (the upper Wegener Canyon?) close to the intersection with BGR78-019 (Fig. 2). Along strike (profile BGR86-07), the upper Miocene and younger section is truncated at the edge of Wegener Canyon to the northeast and thins considerably to the southwest. Thus the post-middle Miocene section appears confined to the main undissected slope of the margin, and does not attain any thickness where the seabed slopes more steeply (as on the canyon flanks at Site 692?).

The Lower Cretaceous-lower Oligocene Hiatus

This hiatus, as encountered at Site 693, does not correspond to a marked acoustic impedance contrast on the Hole 693A logs: the main impedance contrast lies deeper, by about 10 m. This marked contrast, at the top of the Albian claystones of Unit VII, coincides with a strong but irregular reflector at 500 ms on the BGR86-07 strike section (Fig. 2). On the single-channel water-gun profile of Figure 27 the short-wavelength relief on this 500-ms reflector is even greater and it is difficult to trace over any distance. We suggest that the discontinuous nature of this reflector is most probably caused by its intersection with the erosion surface of the Lower Cretaceous-lower Oligocene hiatus found 10 m higher in the section at Site 693, and that therefore, wherever it has this rough discontinuous character, the reflector can be identified with the hiatus. Where sediments above the hiatus are thinner than at Site 693, the hiatus itself becomes a strong reflector, making its correlation over long distances more certain and direct. There may be areas, however, where the Lower Cretaceous/Oligocene hiatus, essentially the most important paleoceanographic marker on the margin, is difficult to follow because of the lack of impedance contrast across it.

Near Site 693 (Fig. 27) the reflector appears to show 50–100 ms of relief, with the overlying sediments in places draped and in places ponded above it. Thus the slump or slumps of lower Oligocene sediments (most or much of Cores 113-693B-14X to 113-693B-19X) may have been controlled by this topography and may thus have moved only a short distance, not long after their original deposition. Support for this suggestion comes from the relative smoothness of the overlying reflectors, laid down upon a much more subdued topography than that of the 500-ms reflector.

Upslope on the *JOIDES Resolution* seismic profile approaching the site (east of Fig. 27), sediments above the 500-ms reflector thin until, where the profile intersects BGR78-019, the reflector lies less than 150 ms below the seabed. On BGR78-019, that depth coincides with the boundary between sequences WS-1 and WS-2 (Hinz and Krause, 1982). Again, on profile BGR86-07, the reflector (hiatus) appears equivalent to unconformity U3 (K. Hinz, pers. comm., 1986). These sequence boundaries have been traced over the entire Dronning Maud Land margin by Hinz and Krause (1982) and Hinz and Block (1984) who, however, gave them a middle or late Miocene age. The WS-1/2 boundary is said to be erosional, and to have cut down in places into WS-3. This is compatible with our knowledge of the 400 mbsf hiatus/410 mbsf (500 ms) reflector package at Site 693, and suggests that its identification with the WS-1/2 boundary is correct.

It is unknown whether anywhere there is any Upper Cretaceous to Eocene section preserved. Near Site 693, there is no clear evidence that the hiatus extends much higher in the section

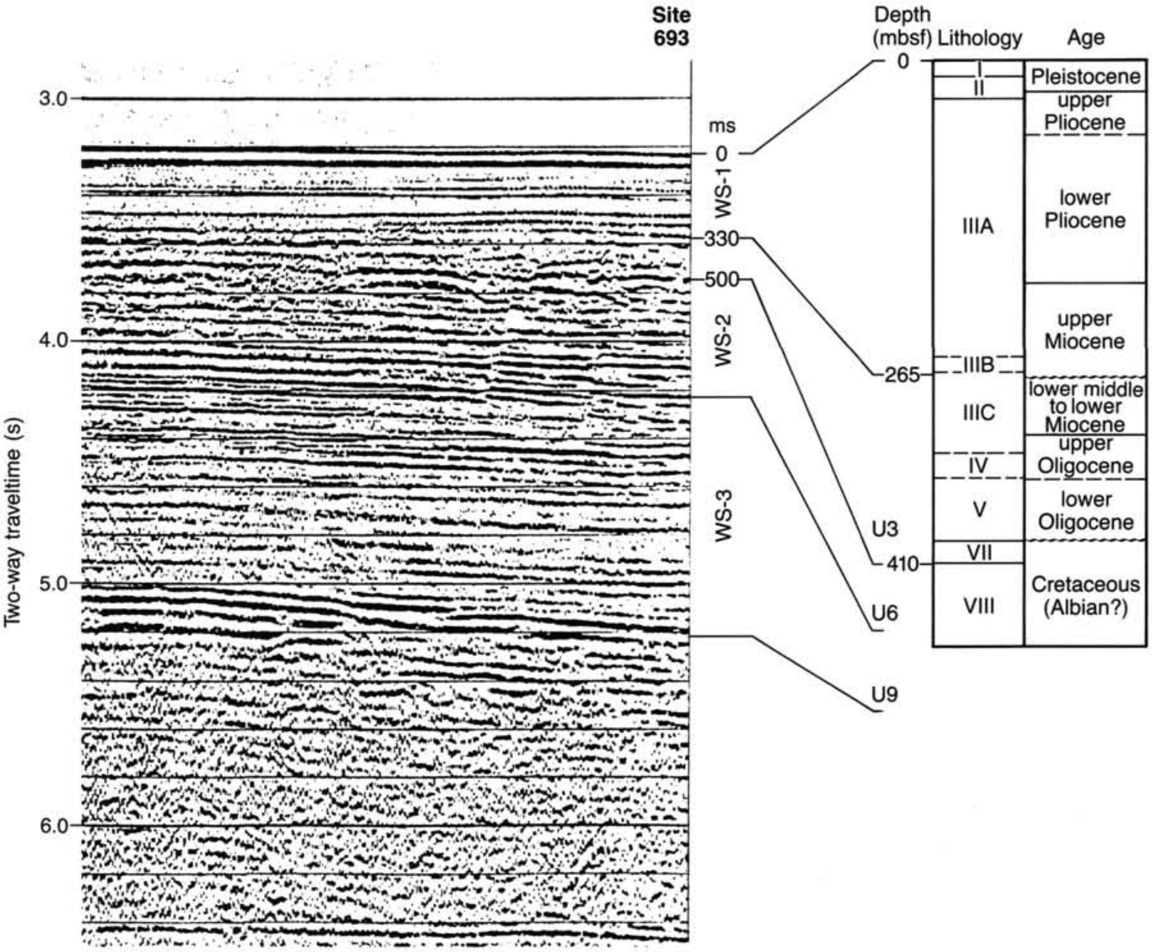

Figure 28. Profile BGR86-07, showing major reflectors identified in Table 9 and identifying unconformities of Hinz and Krause (1982) and Hinz and Block (1984).

than at this site. However, from the evidence of limited overburden pressure on the Lower Cretaceous sediments at Site 692 (see "Physical Properties" section in "Site 692" chapter, this volume), Upper Cretaceous to Eocene sedimentation rates were low, so that only a limited thickness would be expected anywhere.

Table 9. Main seismic reflectors, Site 693.

Two-way traveltime (ms)	Depth (mbsf)	Sediment age	Comments
330	264	early middle or early/ late Miocene hiatus	Complex log signal, top of strong reflector. Opaline silica drop?
WS-1			
490	400	early Oligocene/Early Cretaceous hiatus	Low impedance contrast, weak discontinuous reflector (but see 500 ms entry).
500	410	Early Cretaceous	Log velocity rise, strong rough reflector; probably U3.
WS-2			
1000 ± 100	?	?Early Cretaceous	Reflector U6.
WS-3			
1960	?	?Middle Jurassic	Weddell Sea unconformity, U9.

At greater depths than were drilled, other reflectors of regional extent may be identified. U6, now known to be of Early Cretaceous or greater age, lies 1000 ± 100 ms below the seabed, and U9, the "Weddell Sea Unconformity" above the seaward-dipping reflectors of the "Explora Wedge," of probable Middle Jurassic age, lies at 1960 ms.

BIOSTRATIGRAPHY

Introduction

At Site 693 we drilled a 483-m section consisting of 398 m of Pleistocene to lower Oligocene hemipelagic muds, and 85 m of Lower Cretaceous organic-rich shales. Two holes were drilled. At Hole 693A (0–484 mbsf) we took 51 Pleistocene to Lower Cretaceous rotary cores. Recovery was excellent in the Pleistocene and Pliocene (Cores 113-693A-1R to 113-693A-20R) but deteriorated below this level. Hole 693B was drilled with the XCB to improve recovery of the lower part of the section and to obtain sediment less disturbed than that recovered by rotary coring. After washing down to 233.8 mbsf (lower upper Miocene) and taking a wash core (113-693B-1W), we took 16 XCB and 2 APC cores (113-693B-6H and 113-693B-7H). Hole 693B terminated at 403.1 mbsf after penetrating and recovering the boundary between Lower Cretaceous and lower Oligocene sediments at 398 mbsf (113-693B-19X-4, 69 cm). Recovery in the upper 34 m of the Hole 693B was very poor (234–267.8 m, Cores 113-693B-2X through 113-693B-5X, lower upper Miocene), but improved to over 50% in the lower Miocene to Oligocene (267.8–

403.1 m, Cores 113-693B-6H to 113-693B-19X). Biostratigraphic data indicate that there are no significant discrepancies in the depth position of stratigraphic boundaries between the two holes. The two holes are therefore combined into a single composite section for purposes of discussion.

All depths referred to in the following sections are depths below seafloor, and samples are from the core-catcher (CC) sections unless specified otherwise. Biostratigraphic boundaries are placed midway between overlying and underlying samples.

Planktonic Foraminifers

Abundant and well-preserved planktonic foraminifers were recovered in the first two cores of Hole 693A. The fauna at these levels resemble those from the Quaternary of Holes 692A and 692B, consisting predominantly of "Antarctic" morphotypes of *Neogloboquadrina pachyderma*. The Tertiary portion of Holes 693A and 693B is essentially barren of planktonic foraminifers, presumably because of a shallower carbonate compensation depth (CCD) at this location than at Sites 689 and 690. Several distinct nannofossil ooze horizons do occur, however, in Cores 113-693B-12X and 113-693B-13X within the upper Oligocene. Samples taken from these horizons contained abundant benthic foraminifers, but only very rare planktonic specimens. Samples 113-693B-12X-4, 40–42 cm, and 113-693B-13X-1, 30–32 cm, contained rare, poorly preserved *Catapsydrax unicavus* and *Globorotaloides suteri*, both dissolution-resistant forms and of little stratigraphic value. *Globorotaloides suteri* was also observed in Section 113-693B-17X, CC. Rare occurrences of *N. pachyderma* observed in core-catcher samples through the Tertiary sequence in both holes are regarded as downhole contaminants.

Cores 113-693A-44R to 113-693A-47R below the Oligocene/Cretaceous unconformity in Core 113-693B-43R appear to be barren of planktonic foraminifers. Rare internal molds of planktonic foraminifers were observed in Sections 113-693A-45R, CC, and 113-693A-46R, CC, suggesting that planktonic foraminifers were present at the time of deposition but have been removed by subsequent dissolution. Rare to few, well-preserved foraminifers occur in less-indurated intervals of Cores 113-693A-47X and 113-693A-48X. Section 113-693A-47R, CC, and Samples 113-693A-48R-2, 8–12 cm, and 113-693A-48R-3, 62–66 cm, contain low-diversity assemblages consisting of *Hedbergella delrioensis* and *Gubkinella graysonensis*. Section 113-693A-47R, CC, also contains rare *Ticinella* sp. cf. *H. madecassiana*. This latter form matches *T. madecassiana* sensu stricto in size and chamber arrangement, although the secondary apertures that characterize this genus could not be seen using normal light microscopy. Scanning electron microscopy should resolve this question. If this latter form is equivalent to *T. madecassiana* sensu stricto, its presence in Site 693 samples would reflect an age of latest Albian (*Rotalipora appenninica* Zone; Caron, 1985). An Albian age is further supported by the apparent absence of *Globigerinelloides* species that usually characterize sequences of Aptian age.

Faunas similar to those observed in Cores 113-693B-47R and 113-693B-48R have been described from DSDP Sites 545 and 547 off Central Morocco (Leckie, 1984) and have been termed "Epicontinental Faunas" by Leckie (1987) because they lack the deeper dwelling, open-ocean pelagic forms. *Gubkinella* is generally less abundant in open-ocean environments and probably had broad ecologic tolerences (eurytopic). Its common presence at Site 693 would therefore agree with benthic foraminiferal evidence (see "Benthic Foraminifers" discussion below) that suggests this site was under shallow water depth (possibly 500 m), and in a restricted environment at the time of deposition.

Benthic Foraminifers

All core-catcher samples from Holes 693A and 693B and additional samples from Cores 113-693A-36R, 113-693A-37R, 113-693B-12X, 113-693B-13X, 113-693B-14X, 113-693A-47R, and 113-693A-48R were processed and the residues examined for benthic foraminifers. Eighteen samples contained more than one species (see Table 10 for numbers of species and specimens). These samples are from sediments dated as Pleistocene (2 samples), upper to middle Miocene (1 sample), Oligocene (10 samples), and Albian to upper Aptian (4 samples); Section 113-693A-43R, CC, contains only specimens thought to be downhole contaminants. In most samples the preservation varies from excellent to poor (see below). The faunas in Pleistocene and Miocene samples suggest a depth of deposition similar to the present water depth (about 2400 m); the Oligocene samples contain a fauna indicative of a similar depth, but with specimens of shallow-water (shelf) species mixed in; the Cretaceous samples suggest deposition at water depths of about 500 m.

Table 10. Abundance and diversity of benthic foraminifers, Site 693.

Sample	Depth (mbsf)	Number of species	Number of specimens	Dominant form
693A-1R, CC	2.5	33	202	*E. exigua*
693A-2R, CC	12.2	4	6	none
693A-27R, CC	246.1	18	34	none
693B-12X-2, 114-116	328.4	22	98	*Nonionella* spp.
693A-36R-1, 6-8	330.5	34	235	*N. umbonifera*
693B-12X-4, 40-42	330.7	50	211	*Nonionella* spp.
693B-12X-6, 11-13	333.4	34	294	*N. umbonifera*
693B-13X-1, 30-32	335.8	38	298	*N. umbonifera*
693A-37R-1, 27-29	340.5	23	66	*N. umbonifera*
693B-14X-5, 24-26	351.4	8	11	none
693B-15X, CC	353.2	17	32	none
693B-16X, CC	372.3	7	13	none
693B-17X, CC	376.6	7	11	none
693A-43R, CC	397.8	2	2	none
693A-47R-2, 30-34	437.5	14	99	*Coryphostoma* sp.
693A-47R, CC	438.9	9	10	none
693A-48R-2, 30-32	447.2	7	75	*Coryphostoma* sp.
693A-48R, CC	451.1	20	76	*N. australiana*

Section 113-693A-1R, CC, contained a well-preserved low-diversity fauna similar to the one in Sections 113-692A-1R, CC, and 113-692B-1R, CC, i.e., predominantly calcareous with few specimens and species of agglutinated forms, and dominated by *Epistominella exigua* (43%). Other common species are *Nonionella iridea* (16%) and *Stainforthia complanata* (12%); *Globocassidulina subglobosa* and *Angulogerina earlandi* were present but less abundant than at Site 692. The fauna in Section 113-693A-1R, CC, is more similar to the fauna in Section 113-692A-1R, CC, than to coeval faunas at the earlier-drilled sites of Leg 113. Section 113-693A-2R, CC, contained only six specimens, three of which were *E. exigua*; this poor fauna might represent downhole contamination from the level of Section 113-693A-1R, CC.

All samples not listed in Table 10 are barren with the exception of Section 113-693A-6R, CC, (one specimen of *Cyclammina cancellata*), and samples that contained a few specimens of *Martinotiella antarctica* (Sections 113-693A-8R, CC, 113-693A-17R, CC, 113-693A-26R, CC, 113-693B-2X, CC, 113-693B-11X, CC, and 113-693B-18X, CC). These two species are agglutinated; *M. antarctica* is a common species in samples from Recent diatomaceous sediments from below 2000 m water depth in the Scotia Sea area (Echols, 1971).

Section 113-693A-27R, CC (lower upper Miocene), contained 34 specimens without dominant species. The state of preservation varies from excellent to moderate; possibly the well-preserved specimens (e.g., of *E. exigua*) represent downhole contamination from the top of the hole. It is improbable, however, that all specimens are contamination from the surface: several species (e.g., *Laticarinina pauperata, Bolivina decussata*, and *Cibicidoides trincherasensis*) do not occur in the surface sample, and the latter two species have been found in the earlier-drilled holes of Leg 113 in sediment of Miocene age or older only. The assemblage is typical for lower bathyal to abyssal depths, i.e., about the present water depth at the site.

Samples from Cores 113-693A-36R and 113-693A-37R, and depth-equivalent Cores 113-693B-12X and 113-693B-13X (325–350 mbsf, upper Oligocene) were taken from light gray layers that contain slightly more carbonate than the dark gray-green sediments in the rest of the section. The preservation of the benthic foraminifers in these samples (Table 10) varies from well-preserved to moderately preserved to badly damaged, broken, and abraded. In most samples *Nuttallides umbonifera* is the most abundant species (17%–35%), with common *Uvigerina* spp. and *Stilostomella* spp.; in two samples, *Nonionella* spp. are the most abundant (about 20%; see Table 10). *Turrilina alsatica*, a species common in the Oligocene at Sites 689 and 690, is rare in all these samples. In Sample 113-693B-12X-2, 114–116 cm specimens of a trochospiral species (*Trochoelphidiella* sp.) with complicated, pustulated ventral sutures containing a canal system are common (21%). The specimens resemble some of the specimens described by Boltovskoy et al. (1980) as *Buccella peruviana* forma *frigida* (Pl. 4, Figs. 9, 20, 21; not Figs. 14 through 19). This taxon is abundant in Recent shelf sediments in the Falkland area, where it has been reported to show great morphological variation (Heron-Allen and Earland, 1932). The species also resembles *Trochoelphidiella uniforamina*, described by Leckie and Webb (1986) from upper Oligocene-lower Miocene glaciomarine sediments at DSDP Site 270 in the Ross Sea; the environment of deposition was inferred to be shelf (less than 500 m depth). The species needs to be studied by scanning electron microscopy to determine its correct taxonomic position, but its morphology suggests that it is a neritic species, as are the two species that it closely resembles. The assemblage at Site 693, however, also contains abundant *N. umbonifera* and common *L. pauperata*, lower bathyal to abyssal species that indicate a depth of deposition similar to the present water depth, and which are absent at Site 270. The faunas in the upper Oligocene samples at Site 693 are tentatively interpreted as mixed assemblages of reworked shelf specimens and *in-situ* lower bathyal specimens. It is difficult to assess exactly which specimens are *in situ* and which are reworked, but the *in-situ* fauna is probably dominated by *N. umbonifera*, with common *Uvigerina* spp., and resembles the faunas from upper Oligocene sediments at Sites 689 and 690.

Lower Oligocene(?) Sample 113-693B-14X-5, 24–26 cm, through Section 113-693B-17X, CC, contained few specimens of abraded and poorly preserved benthic foraminifers (Table 10); there are not sufficient specimens to evaluate these faunas. In all these samples rare specimens of shallow-water (neritic) species were found (*Triloculina trigonula, Elphidium macellum*), in addition to rare Cretaceous planktonic foraminifers.

Section 113-693A-43R, CC, contained only two specimens, one *Cibicides lobatulus* and one *Vaginulina sublegumen*, both well-preserved, suggesting that they are downhole contaminants.

Samples from Cores 113-693A-47R and 113-693A-48R (Lower Cretaceous) contain rare, moderately to well-preserved benthic foraminifers. Many specimens are filled with sparry calcite but usually sutures are visible. The most common taxa (each dominant in at least one sample, see Table 10) are *Coryphostoma* sp. (Scheibnerova, 1974, p. 714, Pl. 4, Figs. 13–26) and *Neobulimina australiana*. Other species are *Gavelinella* ex. gr. *intermedia* (Gradstein, 1978; Scheibnerova, 1974), *Gavelinella* sp. A (Gradstein, 1978), *Hoeglundina chapmani, Orthokarstenia shastaensis, Gyroidinoides primitiva*, and nodosariid species, including *Lenticulina turgidula, Dentalina soluta*, and several species of *Vaginulina, Saracenaria*, and other spiral and uniserial taxa. Agglutinated species are rare (*Ammodiscus tenuissimus* and *Haplophragmoides* sp.). Similar assemblages, dominated by *Coryphostoma* sp. and *Neobulimina australiana*, have been described from middle to upper Albian sediments (from the *Prediscosphaera cretacea* Zone) at Sites 259 and 260 in the Eastern Indian Ocean (Scheibnerova, 1974), and from Albian sediments at Site 249 on the Mozambique Ridge (Simpson et al., 1974). Scheibnerova considered these faunas to be very similar to faunas from the Great Artesian Basin in Australia and postulated a similar environment of deposition, i.e., a depth of between 200 and 600 m, most probably about 500 m, in a somewhat restricted marine environment. The environment of deposition of Lower Cretaceous sediments recovered at Site 693 may have been similar, at a depth of around 500 m, and with somewhat restricted conditions, i.e., probably a low oxygen content of the bottom waters. The assemblage is clearly different from and younger than the fauna in the Lower Cretaceous sediments at Site 692; the inferred environment of deposition is similar, but might have been slightly shallower at Site 693.

The fauna at Site 693 resembles middle Albian faunas, but it is not clear whether this resemblance must be interpreted as indicative of a middle Albian age or as indicative only of similarity in environment of deposition. The presence of *G. intermedia*, however, indicates an age not greater than late Aptian or less than late Albian.

Calcareous Nannofossils

Despite the relatively shallow present-day water depth at this site (2359 m), calcareous nannofossils are present only across short intervals in the Miocene and upper Oligocene diatomaceous clays (lithostratigraphic Units III–V), as well as in the Lower Cretaceous "black shales" (lithostratigraphic Unit VII). Preservation varies considerably on a bed-by-bed basis.

Cenozoic

Sparse but well-preserved Oligocene or older nannofossils in Sample 113-693A-20R-1, 2 cm (176.3 mbsf), are considered reworked, possibly introduced into this upper Miocene–lower Pliocene sediment as a turbidite. The assemblage includes common *Chiasmolithus altus*, few *Coccolithus pelagicus*, and rare *Cyclicargolithus floridanus*.

Coccoliths are few but well-preserved in upper Miocene Core 113-693A-27R (243.9–253.6 mbsf), where an *in-situ* Antarctic monospecific assemblage is composed of *Reticulofenestra perplexa*. A lower Miocene sample (113-693B-6H-4, 56–58 cm; lithostratigraphic Unit IIIC; 274.4 mbsf) yielded an assemblage composed exclusively of common but only moderate to poorly preserved *Coccolithus pelagicus*, many specimens of which are represented only by their dissolution-resistant distal rims. Sample 113-693A-34R-2, 35 cm, contained rare *Reticulofenestra perplexa*, which are considered to be downhole contaminants.

Well-preserved upper Oligocene nannofossil assemblages strongly dominated by *Chiasmolithus altus* were recovered in both holes drilled at this site. In Hole 693A, these occur in small blebs inset within the clayey matrix of Cores 113-693A-36R and 113-693A-37R (330.5–349.9 mbsf), where recovery was low (less than 10%). Recovery was much higher in Cores 113-693B-12X and 113-693B-13X (325.8–345.1 mbsf) where clay-bearing nannofossil ooze occurs in discrete, light-colored layers between 10 and 50 cm in thickness, with an average spacing of less than 1 m, to produce a quasi-cyclical color pattern in the sediment (lithostratigraphic Unit IV; see "Lithostratigraphy" section, this chapter). The contacts beneath or above some of the beds are sharp, suggesting possible emplacement of some (but not all) of the oozes as turbidites.

In conclusion, Site 693 was drilled in 2359 m of water on the Dronning Maud Land margin, 900 km southwest of Maud Rise where Sites 689 and 690 were drilled at comparable water depths (2080 and 2914 m, respectively). On Maud Rise carbonate sediments were deposited throughout the Oligocene and most of the Miocene. The CCD, however, was considerably higher at Site 693, and only descended briefly during the Oligocene and Miocene to permit nannofossil ooze deposition at this locality.

In modern oceans, the CCD generally rises toward continental margins, therefore it should be somewhat shallower at Site 693 than at Maud Rise. The elevated CCD at Site 693, however, was probably due primarily to decreased production of calcareous nannofossils in the colder waters along the Antarctic margin, where temperatures may have dropped close to or below the life-tolerance thresholds of calcareous nannoplankton during much of the Oligocene and Miocene. These waters would have been affected by the emergence of glacial ice from ice streams draining East Antarctica and the formation of sea-ice along the margin. In addition, bottom waters produced along the continental margin would have been strongly undersaturated in calcium carbonate and would have tended to dissolve any nannofossils deposited at this site. Maud Rise, on the other hand, was probably bathed in the somewhat warmer surface currents of the Weddell Gyre impinging from the northeast or east. The most extensive deposition of nannofossils at Site 693 occurred during the latest Oligocene, which would suggest an amelioration in climate, following the cooling associated with more pronounced early and middle Oligocene glaciations (see "Lithostratigraphy" section, this chapter).

Lower Cretaceous

Cretaceous Cores 113-693A-44R through 113-693A-45R are barren of calcareous nannofossils, as are most samples from the remainder of the hole. The largest numbers of nannofossils were found in Cores 113-693A-47R and 113-693A-49R, with sparse occurrences in Core 113-693A-48R. Sample 113-693A-47R-1, 60 cm, yielded the most diverse assemblage, which included abundant *Watznaueria barnesae, Seribiscutum primitivum*, and *Acaenolithus* sp.; common *Cretarhabdus conicus, Rhagodiscus aspera, Repagulum parvidentatum* (J. Mutter, written comm., 1987), *Zygolithus diplogrammus*, and *Biscutum constans*; few *Stephanolithion laffittei* and *Corollithion rhombicum*; and rare *Lithastrinus floralis* and *Nannoconus truittii*. A single specimen of *Gartnerago* sp. cf. *confossus* is present in Sample 113-693A-48R-2, 70 cm (J. Matter, written comm., 1987). No *Eiffellithus turriseiffeli* or *Prediscosphaera cretacea* were noted.

There are several possibilities for dating this section. A comparison with the middle Cretaceous sequences cored on the Falkland Plateau at Sites 327, 330, and 511 (Wise and Wind, 1977; Wise, 1983) suggests that the assemblage could be assigned to the middle Albian *Prediscosphaera cretacea* Zone, even though the nominate species has not been observed. At Site 511, the first appearance datum (FAD) of the provincial high-latitude species, *S. primitivum*, is within this zone, and nannoconids apparently do not range far above the zone. There are a number of intervals in which *Prediscosphaera cretacea* is not present within the nominate zone (example, Hole 511, 460–471 m; Wise, 1983, Table 1C). On the other hand, the section at the present site could be slightly younger (i.e., upper Albian), if *E. turriseiffeli* has been overlooked, based on the presence of *Gartnerago* sp. cf. *confossus*, which has only been recorded from the *Eiffellithus turriseiffeli* Zone on the Falkland Plateau (Wise, 1983, Table 1C).

The fact remains, however, that neither *P. cretacea* nor *E. turriseiffeli* have been observed at Site 693, and *Seribiscutum primitivum* ranges down into the upper Aptian elsewhere in the world (Perch-Nielsen, 1985). Those observations plus the presence of *Lithastrinus floralis* would require that the section be confined to the upper Aptian–lower Albian *Rhagodiscus angustus* Zone. This is contradicted, however, by the presence of a single specimen of *Gartnerago*, a genus which has not been reported below the middle Albian (Perch-Nielsen, 1985). There may also have been ecological exclusion of the middle to upper Albian markers mentioned above in the restricted environment at this site, but this cannot be readily demonstrated. Further study will be necessary to better date this section by nannofossils.

Diatoms

Hole 693A

Sections 113-693A-1R, CC, and 113-693A-2R, CC, contain few, poorly preserved diatoms of Quaternary age (*Thalassiosira lentiginosa* Zone). Species present include *Nitzschia kerguelensis, Eucampia antarctica, Thalassiosira lentiginosa, Stellarima microtans, Thalassiothrix longissima*, and reworked *Denticulopsis hustedtii*. Additional samples taken between core catchers contain much the same flora, although some levels are barren of diatoms.

Samples from Core 113-693A-3R and the upper portion of Core 113-693A-4R (down to Section 2, 50 cm) are barren of diatoms. The three sections of Core 113-693A-4R below that level contain traces of diatoms and a few reworked species including *Denticulopsis hustedtii* and *D. dimorpha*. On the basis of stratigraphic relationships, it can be assumed that this interval is late Pliocene or lower Pleistocene.

Section 113-693A-4R, CC, contains few, poor to moderately preserved diatoms including *Coscinodiscus vulnificus, Eucampia antarctica, Rouxia antarctica, Nitzschia angulata, Actinocyclus ingens*, and *Cosmiodiscus insignis*. We also found reworked diatoms such as *Denticulopsis hustedtii, Pyxilla* sp., and *Hemiaulus ?incisus*, the latter two species originating in Paleogene deposits. This sample is placed in the *Coscinodiscus kolbei–Rhizosolenia barboi* Zone, but it could also be placed in the underlying *C. insignis* Zone.

The upper part of Core 113-693A-5R is definitely within the *C. insignis* Zone because Sections 1 to 5 contain *C. insignis* and *C. vulnificus* in the absence of *Nitzschia interfrigidaria*. This latter species occurs in Sample 113-693A-5R-6, 50 cm, and in Section 113-693A-5R, CC. In addition to these three species, Section 113-693A-5R, CC, also contains *E. antarctica, R. barboi, R. antarctica, C. kolbei*, and displaced *Denticulopsis dimorpha*. We tentatively place Section 113-693A-5R, CC, at about the lower/upper Pliocene boundary (*N. interfrigidaria* Zone).

Section 113-693A-6R, CC, contains common, moderately well preserved diatoms including *Nitzschia praeinterfrigidaria, N. interfrigidaria, N. angulata, Cosmiodiscus intersectus, Rouxia naviculoides, R. barboi*, and *Thalassiosira oestrupii*. The topmost occurrence of *N. praeinterfrigidaria* is in Sample 113-693A-6R-6, 50 cm. The interval 113-693A-6R, CC, to 113-693A-18R is placed in the lower Pliocene *N. angulata–N. reinholdii* Zone. Sections 113-693A-7R, CC, to 113-693A-9R, CC, generally contain few to common, moderately to well-preserved diatoms. Species include *N. praeinterfrigidaria, N. angulata, C. intersectus, R. barboi*, and *T. oestrupii*.

The first occurrence of *N. angulata* is placed between Sections 113-693A-12R, CC, and to 113-693A-14R, CC. Above this level, we also find *R. barboi, A. ingens, N. praeinterfrigidaria, D. hustedtii*, and persistent, though never abundant, occurrences of *Thalassiosira torokina*.

Species in the interval 113-693A-14R, CC, to 113-693A-18R, CC, include *T. torokina, A. ingens, C. intersectus, Nitzschia januaria* (possibly reworked), and rare *Denticulopsis hustedtii* and *N. praeinterfrigidaria*. Section 113-693A-17R, CC, contains rare

Cosmiodiscus insignis forma *triangula*, which, in the Falkland Plateau area, straddles the Miocene/Pliocene boundary (lower Chron C3 to lower Chron C3A) according to Ciesielski (1983).

The top of the upper Miocene–lowermost Pliocene *Denticulopsis hustedtii* Zone is placed in Section 113-693A-19R, CC. This zone extends from 113-693A-19R, CC, to approximately 113-693A-28R, CC, but it may be informally subdivided on the basis of abundance changes in *Denticulopsis dimorpha*. Between Sample 113-693A-27R-1, 50 cm, and Section 113-693A-28R, CC, *D. dimorpha* is common to abundant, whereas above Core 113-693A-27R rare to few specimens are encountered. Also, *Denticulopsis praedimorpha* is present in the lowermost part of the *D. hustedtii* Zone. Other species within the *D. hustedtii* Zone include *Actinocyclus ingens, Rhizosolenia barboi, Coscinodiscus deformans, C. endoi, Azpeitia tabularis, Nitzschia donahuensis, N. claviceps, N. januaria, Eucampia balaustium, Denticulopsis hustedtii* var. *ovata, Trinacria excavata, Stellarima microrias*, and, rather consistently, an unknown species which we assign to the genus *Neodenticulopsis*. Section 113-693A-28R, CC, also contains few *Nitzschia denticuloides* and rare *Denticulopsis lauta*, and is placed in the *D. hustedtii–D. lauta–N. denticuloides* Zones.

There is an apparent unconformity between Cores 113-693A-28R and 113-693A-29R. Section 113-693A-29R, CC, contains *Thalassiosira spinosa, Rhizosolenia barboi, Nitzschia malinterpretaria, Stephanopyxis turris*, and *Thalassionema hirosakiensis*. Such middle Miocene zonal markers as *Nitzschia grossepunctata, Coscinodiscus lewisianus*, and *D. lauta* are not present, suggesting that a large portion of the middle Miocene is missing from this site. Section 113-693A-30R, CC, can also be placed in the lower Miocene *N. malinterpretaria* Zone.

Sections 113-693A-31R, CC, through 113-693A-37R, CC, are difficult to date because of poor diatom recovery, the occurrence of reworked diatoms, and the persistent problem of downhole contamination. Consequently it is difficult to identify the Oligocene/Miocene boundary although it probably occurs somewhere between Sections 113-693A-31R, CC, and 113-693A-37R, CC, because Section 113-693A-35R, CC, contains *Rocella schraderi*, a species which has its range within the lowermost Miocene to the uppermost Oligocene *Rocella gelida* Zone. In Sections 113-693A-33R, CC, through 113-693A-37R, CC, we found Paleogene species such as *Stephanodiscus superbus, S. megalopora, S. eocaenica, Kisseleviella carina, Rocella praenitida*, and *Pseudotriceratium chenevieri*, some of which may be displaced. The persistent occurrence of Pliocene species indicates downhole contamination in Core 113-693A-34R.

Section 113-693A-38R, CC, contains common, moderately preserved diatoms which indicate an age near the boundary of the *Rocella vigilans/Rhizosolenia antarctica* Zones which is placed below the lower/upper Oligocene boundary by Fenner (1984). This age assignment is based on the co-occurrence of the nominate species and the occurrence of such lower Oligocene species as *Hemiaulus pacificus, Asteromphalus oligocaenicus*, and *Melosira architecturalis*.

Sections 113-693A-39R, CC, through 113-693A-42R, CC, can be assigned to the upper lower Oligocene *Rhizosolenia antarctica* Zone of Fenner (1984) as indicated by the co-occurrence of *Rhizosolenia antarctica, R. gravida*, and *Synedra jouseana*. We also note the rare occurrence of *Stephanopyxis superba* var. *trispinosa* in Section 113-693A-42R, CC. Section 113-693A-43R, CC, contains only rare and poorly preserved diatoms. Indeed, the occurrence of *Synedra jouseana* indicates an age in the upper part of the *R. antarctica* Zone, because the first occurrence of the species falls within this zone (Fenner, 1984). The occurrence of Pliocene species indicates downhole contamination.

A major hiatus occurs between Sections 113-693A-43R, CC, and 113-693A-44R, CC. Section 113-693A-44R, CC, contains a well-preserved Cretaceous diatom assemblage of Aptian/Albian age (based on calcareous nannoplankton) which is unlike other Cretaceous assemblages previously described from the Southern Ocean (Hajós, 1975). Some of the species found can be assigned to the genera *Cerataulina, Pterotheca, Cladogramma, Skeletonema, Stephanopyxis*, and (?)*Gladius*. A similiar assemblage also occurs in Sample 113-693A-46R-1, 89–92 cm.

Hole 693B

The uppermost Miocene through Pleistocene section was not sampled and the corer washed down to the middle upper Miocene at a depth of 233 mbsf. The first sample, designated 113-693B-1W, CC, is considered suspect because of probable contamination. In spite of these concerns, the core-catcher sample contains a normal uppermost Miocene assemblage with few to common diatoms, relatively poorly preserved, and with *Denticulopsis hustedtii* as the dominant diatom. Because of the abundance of this species and because of the associated flora, Section 113-693B-1W, CC, is placed in the *D. hustedtii* Zone.

Section 113-693B-2X, CC, can also be placed in the *D. hustedtii* Zone. In addition to the nominate taxon, other species in this sample include *Rhizosolenia barboi, Nitzschia januaria, N. claviceps, Actinocyclus ingens, Azpeitia tabularis, Stellarima microrias, Chaetoceros* resting spores, and common *D. dimorpha*. The presence of significant numbers of the latter species indicates that the core reached the lower part of the *D. hustedtii* Zone.

Sections 113-693B-3X, CC, to 113-693B-5X, CC, although achieving penetration, did not recover any sediment. Core 113-693B-6H can be placed in the lower Miocene *Nitzschia malinterpretaria* Zone. This zone extends to the upper part of Core 113-693B-7H. The first occurrence of the nominate species was found in Sample 113-693B-7H-1, 75 cm. Other species within this zone include *Thalassiosira spinosa, T. spinosa* var. *aspinosa, Synedra jouseana, Trinacria excavata, Rhizosolenia alata, Lisitzina ornata*, and *Stephanopyxis turris*.

We are unsure as to the exact interval covered by the next underlying zones, the lower Miocene *Coscinodiscus rhombicus* Zone and the lower Miocene to upper Oligocene *Bogorovia veniamini* Zone, because both nominate species occur very rarely in Hole 693B. *Coscinodiscus rhombicus*, whose last occurrence defines the top of the *C. rhombicus* Zone, occurs in Sample 113-693B-7H-3, 50 cm. The *Bogorovia veniamini* Zone, which is defined by the total range of the nominate taxon, could only be identified in Section 113-693B-11X, CC, where the nominate taxon is very rare. In the same sample we also found *Coscinodiscus endoi*, a species which is found only in the Miocene in the Falkland Plateau and the Pacific sector of the Southern Ocean (Gombos and Ciesielski, 1983; Schrader, 1976). This occurrence may suggest that the interval above Core 113-693B-12X is still Miocene in age.

Cores 113-693B-12X and 113-693B-13X contain *Hemiaulus* spp., *Triceratium chenevieri, Stephanopyxis turris, Synedra jouseana, Kisseleviella* spp., *Pyxilla reticulata*, and *Coscinodiscus rhombicus*. The co-occurrence of the latter two species may indicate an upper Oligocene age. This agrees with our findings in Hole 693A where uppermost Oligocene sediments occur in Section 113-693A-35R, CC, as shown by the presence of *Rocella schraderi*. Core 113-693A-35R can be placed stratigraphically midway between Cores 113-693B-11X and 113-693B-12X. *Rocella* species as well as other biostratigraphic markers for the upper Oligocene such as *Hemiaulus taurus* and *Triceratium groningensis* were not encountered in Hole 693B. In Section 113-693B-13X, CC, there is downhole contamination by upper Miocene species.

The sediment interval from Section 113-693B-14X, CC, to Sample 113-693B-19R-4, 68 cm, can be placed in the upper lower Oligocene *Rhizosolenia antarctica* Zone. In addition to the nominate species the diatom assemblages recovered in this interval include *Synedra jouseana, Hemiaulus polymorphus, H. incisus, Kisseleviella* spp., *Triceratium macroporum, T. chenevieri, Trinacria excavata, Stephanopyxis superba, S. turris, S. eocaenica, Asteromphalus oligocaenicus, Rouxia obesa, X. panduraeformis, Pyxilla reticulata, Thalassionema hirosakiensis*, and *Rhizosolenia gravida*. There is some suggestion in the sedimentary structures of mass slumping in the lower, post-Cretaceous, portion of Hole 693B. This may explain why the lower six cores are assigned to a relatively short diatom zone in the lower Oligocene.

A hiatus between the lower Oligocene and the Cretaceous occurs at Sample 113-693B-19R-4, 69 cm. The level of this hiatus in Hole 693A could only be estimated to be somewhere between Sections 113-693A-43R, CC, and 113-693A-44R, CC, because of poor recovery. It is visible as a clear change in sediment color in Hole 693B. A sample at 113-693B-19R-4, 68 cm, contains a poor to moderately preserved upper lower Oligocene diatom assemblage including *Stephanodiscus superbus, Asteromphalus oligocaenicus, Hemiaulus incisus, Pyxilla reticulata*, and *Synedra jouseana*. Only very rare specimens of the underlying Cretaceous diatom assemblage are admixed. A sample taken from 113-693B-19R-4, 70 cm, contains common, moderately preserved diatoms assignable to the genera *Pterotheca, Acanthodiscus, Pseudopyxilla, Skeletonema, Stephanopyxis*, and ?*Gladius*. A similar assemblage was also encountered in other samples taken below this level, although changes in species composition are obvious. The assemblage shows affinities to the one recovered from the Lower Cretaceous of Hole 693A.

Summary

Site 693 (Holes 693A and 693B) recovered a Quaternary to Lower Cretaceous sequence which is largely rich in biosiliceous components. Within the Pleistocene, diatom preservation is variable. The upper Pliocene sections are mostly barren and in the upper Miocene poor preservation was encountered. Preservation is also variable in the lower Miocene and Oligocene part of the section. Cretaceous diatoms of Aptian-Albian age show good preservation.

The diversity of the diatom assemblages recovered is in general moderate. We note sparse occurrences of displaced benthic diatom species (*Cocconeis* spp., *Grammatophora* spp.) in the lower Miocene, becoming more consistent in the Oligocene. The occurrence of benthic diatoms suggests the existence of a shallow water (less than 50-m water depth), ice-free coastal environment on the adjacent Weddell Sea coast. Thus, conditions different from the present shelf-ice-dominated coast line are indicated. A detailed study of the temporal occurrence of these benthic diatoms combined with an investigation of dropstone distribution in the same holes may give additional information about the history of continental ice distribution and the formation of shelf-ice conditions during the Tertiary.

A number of prominent unconformities were identified. Missing intervals included a section of the middle upper Miocene, the middle Miocene, and the Upper Cretaceous through lowermost Oligocene. Unconformities were also recognized in the upper Oligocene but the chronology still needs to be worked out. We found no evidence for unconformities near the Miocene/Pliocene boundary or within the upper Pliocene. Additional comments on taxonomy and biostratigraphy are given in the "Diatom" discussions in the "Biostratigraphy" sections ("Site 689" and "Site 697" chapters, this volume).

Radiolarians

At Site 693 radiolarians were recovered from all cores taken, ranging in age from Quaternary to Early Cretaceous. Preservation of radiolarians varied substantially, with common to abundant, well-preserved assemblages being recovered from the upper Miocene to Pliocene section, and from one sample in the Lower Cretaceous. Radiolarians in most of the Cretaceous section and in Oligocene to middle Miocene sediments were generally poorly preserved and, in the lower Tertiary sediments, often diluted by large numbers of centric diatoms. Sample disaggregation was usually poor at these levels, even after kerosene treatment.

Rare to few, well-preserved Cretaceous radiolarians were seen in Miocene and Oligocene Sections 113-693A-31R, CC, 113-693A-33R, CC, 113-693A-39R, CC, 113-693A-42R, CC, and 113-693B-12R, CC. The taxa appear to be identical to those seen in the Cretaceous section at the base of the holes and are presumably due to local reworking.

Hole 693A

In Hole 693A we recovered a condensed uppermost Pliocene to Quaternary section containing rare to few, well-preserved radiolarians. Sections 113-693A-1R, CC, and 113-693A-2R, CC, are dated as Pleistocene, based on the occurrence of *Antarctissa denticulata* and the absence of Pliocene species. Section 113-693A-3R, CC, contained only rare, fragmented radiolarians. One fragment of *Acanthosphaera* sp. (Hays, 1965) was seen. This species is reported by Chen (1975) to have an early Pleistocene range, and on this tenuous basis Section 113-693A-3R, CC, is dated as lower Pleistocene.

Radiolarians are few and only moderately preserved in Section 113-693A-4R, CC, but they become common to abundant and generally well-preserved beginning with Section 113-693A-5R, CC, and continuing to the base of the upper Miocene. A late Pliocene (middle Upsilon Zone) age is assigned to Cores 113-693A-4R to 113-693A-7R based on the occurrence of *Helotholus vema, Desmospyris spongiosa, Antarctissa ewingi, Antarctissa strelkovi, Eucyrtidium calvertense, Clathrocyclas bicornis*, and the absence of *Cycladophora covisiana, Prunopyle titan, Lychnocanium grande*, or Miocene forms. Sections 113-693A-8R, CC, and 113-693A-9R, CC, are assigned to the lower Upsilon Zone (lower Gauss/upper Gilbert) due to the co-occurrence of *H. vema* and *P. titan*. Cores 113-693A-10R to 113-693A-20R lie below the FAD of *H. vema* but above the last appearance datum (LAD) of *Cycladophora spongothorax*, and are therefore assigned to the Tau Zone (lower Pliocene). The last common occurrence of *L. grande* marks the upper/lower Tau Zone boundary. *Lychnocanium grande* is present, though not common, in Sections 113-693A-10R, CC, and 113-693A-12R, CC, is absent in Section 113-693A-11R, CC, and is common in Section 113-693A-13R, CC, through 113-693A-20R, CC. Cores 113-693A-10R to 113-693A-12R are tentatively assigned to the Upper Tau Zone (between a and c events of Gilbert), and Cores 113-693A-13R to 113-693A-20R to the lower Tau Zone (basal Pliocene).

Cores 113-693A-21R through 113-693A-27R are assigned to the upper Miocene to upper middle Miocene *C. spongothorax* Zone based on the common occurrence of the nominate species. *Eucyrtidium pseudoinflatum*, an indicator species for the upper portion of this zone, is common in Cores 113-693A-21R through 113-693A-25R. *E. pseudoinflatum* is rare in Section 113-693A-26R, CC, and absent below this level. *Actinomma tanyacantha* co-occurs with *C. spongothorax* in Section 113-693A-27R, CC, placing this sample in the lower portion of the *C. spongothorax* Zone. The middle *C. spongothorax* subzone is inferred to fall between Sections 113-693A-25R, CC, and 113-693A-27R, CC.

Section 113-693A-28R, CC, could not be dissaggregated sufficiently to prepare a radiolarian slide. Sections 113-693A-29R, CC, through 113-693A-32R, CC, contain poorly preserved radiolarians which could not be placed in the standard Antarctic Miocene zonation. An early middle Miocene or early Miocene age is indicated, however, by the occurrence of species such as *Prunopyle hayesi, Amphistylus angelinus, Lithomelissa stigi,* *Dendrospyris haysi, Eucyrtidium cienkowski, Sethoconus* sp. (Chen, 1975), *Stylacontarium bispiculum*, and, in Cores 113-693A-31R and 113-693A-32R, *Spongomelissa dilli*. Radiolarians from Cores 113-693A-33R through 113-693A-37R were rare to few and very poorly preserved. A Miocene or Oligocene age is indicated by the presence of *P. hayesi, Cyrtocapsella isopera*, and *Sethoconus* sp. (Chen, 1975).

Radiolarians were few and moderately preserved in Sections 113-693A-38R, CC, 113-693A-39R, CC, and 113-693B-42R, CC. An Oligocene age is indicated by the presence of *Calocyclas semipolita, Arachnocalpis* sp., *Spongomelissa* sp. (Chen, 1975), *Lithomelissa challengerae*, and *Prunopyle frakesi*. Radiolarians were so diluted by lithic fragments in Section 113-693A-40R, CC, that no useful information could be extracted from the sample. Section 113-693A-43R, CC, contained only gravel and downhole cavings and was not processed. At least a part of the lower Oligocene section is missing at Site 693, and possibly part of the lower upper Oligocene. This is indicated by the absence of radiolarian species such as *Cyclampterium* sp. cf. *milowi* and *Periphaena decora* found in the lower upper Oligocene through uppermost Eocene of Sections 113-689B-10H, CC, through 113-693B-16H, CC, and 113-690B-10H, CC, and 113-693B-11H, CC.

Cores 113-693A-44R through 113-693B-50R contain common to abundant Cretaceous radiolarians, including common *Amphipyndax, Dictyomitra, Archeodictyomitra, Pseudocrucella, Eucyrtis, Cryptamphorella, Theocapsomma*, and several other genera. *Theocorys antiqua* and *Solenotryma dacryodes* are present, giving an age range of Albian to Santonian for this assemblage (Sanfilippo and Riedel, 1985). Preservation of radiolarians in Section 113-693A-44R, CC, is exceptional for material of this age. Radiolarian preservation declines rapidly in the lower cores.

Hole 693B

At Hole 693B we redrilled the lower upper Miocene through Cretaceous portion of the stratigraphic section drilled by Hole 693A. The initial wash core was not examined for radiolarians. Section 113-693B-2R, CC, contains *C. spongothorax, D. haysi*, and *Antarctissa conradae*, but *E. pseudoinflatum* and *A. tanyacantha* are absent. Section 113-693B-2R, CC, is therefore within the middle *C. spongothorax* Zone, and stratigraphically equivalent to the single core-catcher section in Hole 693A containing this interval—113-693A-26R, CC. *Actinomma tanyacantha* and *C. spongothorax* co-occur in Section 113-693B-3R, CC, placing this sample in the lower *C. spongothorax* Zone, equivalent to Section 113-693A-27R, CC.

No sediment was recovered by Cores 113-693B-4R or 113-693B-5R. Sections 113-693B-6H, CC, through 113-693B-8X, CC, contain few to abundant, poorly preserved radiolarians and are middle or lower Miocene, based on the absence of *C. spongothorax* and the presence of *Amphistylus angelinus, D. haysi, P. hayesi*, and, in Section 113-693B-8X, CC, *Spongomelissa dilli*.

Sections 113-693B-9X, CC, through 113-693B-18X, CC, contain rare to common, poor to moderately preserved radiolarians. No definitive age markers are seen, although an Oligocene age is indicated for Sections 113-693B-10X, CC, 113-693B-12X, CC, 113-693B-14X, CC, and 113-693B-18X, CC by the presence of *Prunopyle frakesi, Eucyrtidium* sp. (Chen, 1975), *Botryostrobus* sp. cf. *joides* (Bjorklund, 1976), and several undescribed taxa previously seen in Oligocene high-latitude sediments of the Antarctic and North Atlantic.

Cretaceous radiolarians are abundant and very well-preserved in Section 113-693B-19X, CC. The assemblage appears to be identical to the one recovered in Section 113-693A-44R, CC.

Discussion

Site 693 recovered radiolarian assemblages which in some respects are similar to those encountered at Sites 689 and 690 on Maud Rise, with a well-preserved upper Miocene and Pliocene, and poorly preserved middle Oligocene through lower Miocene.

At Site 693 we recovered a Pleistocene sequence not recovered at the Maud Rise sites. The Pleistocene is very thin compared with the Pliocene and upper Miocene, due either to low rates of sedimentation or to undetected hiatuses. A dramatic reduction in biosiliceous productivity is apparent during the upper Pliocene and Pleistocene (approximately 2.5 Ma to Recent), based on the highly reduced abundances of radiolarians and diatoms during this interval.

High sedimentation rates, good preservation, and, in the Pliocene, nearly continuous recovery will make the upper Miocene to upper Pliocene of Site 693 an important sequence for stratigraphic and paleoceanographic analysis. High biosiliceous productivity during this time interval appears to have extended over a much broader latitudinal band than it does in this region today, with significant accumulations of biogenic silica being recorded from near the continent (Site 693; 70°50′S), the Maud Rise (Sites 689 and 690; 64°31′S and 65°9′S), and out to the Polar Front (DSDP Sites 513 and 514 on the Falkland Plateau; 47°35′S and 46°6′S).

No well-preserved basal Oligocene radiolarians were recovered, and dilution by large diatoms and mineral grains in the remainder of the Oligocene section of Site 693 reduces the usefulness of these cores for radiolarian work.

The Lower Cretaceous assemblage recovered at Site 693 is unique in its combination of excellent preservation, geologic age, and (for Mesozoic radiolarian localities) very-high-latitude location, and will provide important new data on the Mesozoic history of the radiolarians.

Silicoflagellates

Silicoflagellates are present in varying numbers through most of the section at Site 693 below Core 113-693A-7R and provide a number of useful datums. Core 113-693A-7R contains *Distephanus boliviensis* and *D. speculum pentagonus* and could be assigned to the lower Pliocene *D. boliviensis* Zone of Ciesielski (1975). Common *Distephanus pseudofibula* range from Sections 113-693A-12R to -15R-2 and delineate the lower Pliocene *Distephanus pseudofibula* Zone. The last appearance datum (LAD) of *Mesocena diodon* in Core 113-693A-17R marks the top of the *M. diodon* Zone, which straddles the Pliocene/Miocene boundary. The top of the subjacent *Mesocena circulus–M. diodon* Zone can probably be placed at Core 113-693A-22R (latest Miocene), which contains *M. circulus* var. *dumitrica*. Silicoflagellates are infrequent throughout the remainder of the Miocene section. The lowermost(?) Miocene Section 113-693B-9X, CC, contains a nearly complete specimen of *Corbisema inermis crenulata*, which has only been reported from the Paleocene and is presumed to have been reworked into this section.

Core 113-693B-11X (316.1–325.8 mbsf) contains *Mesocera apiculata apiculata* and *Distephanus crux darwinii;* the latter taxon has only been reported from the upper Oligocene of the Falkland Plateau and elsewhere. Upper Oligocene Cores 113-693B-12X and -13X contain *D. crux* and *Naviculopsis biapiculata.*

Lower Oligocene sediment is indicated by the presence of *Dictyocha deflandrei* in Cores 113-693A-38R to -42R (349.9–397.1 mbsf). Silicoflagellates are well preserved and include forms such as *Distephanus speculum geminum*. The lower Oligocene *Naviculopsis trispinosus* acme observed at Site 689 was not noted at Site 693, an indication that the lowermost Oligocene was not cored at this site.

The Cretaceous diatomaceous sediments from lithostratigraphic Unit VI contain no members of the diverse silicoflagellate assemblage described from the Campanian-Maestrichtian siliceous ooze at DSDP Site 275 on the Campbell Plateau (Hajós, 1975). Conspicuously absent at Site 693 are Upper Cretaceous taxa reported from Site 275 and elsewhere such as *Corbisema geometrica, Lyramula deflandrei,* and species of *Vallacerta.* This negative evidence indicates that the diatomaceous sediments recovered at Site 693 are older than Campanian.

Palynology

Hole 693A

All processed samples from Sections 113-693A-1R, CC, to 113-693A-44R, CC, are barren. Sections 113-693A-45R, CC, to 113-693A-50R, CC, yielded a mixed Lower Cretaceous palynoflora, dominated by dinoflagellate cysts or by sporomorphs.

The most abundant cysts belong to the species *Diconodinium davidii* (upper Aptian, after Morgan, 1977), and *Prolixiosphaeridium parvispinum* (Neocomian-late Aptian, Albian? after Morgan, 1980). The observed species *Odontochitina operculata* was formerly reported to range from the latest Neocomian through the Aptian in Australia and was used as index fossil for the *Odontochitina operculata* dinoflagellate zone (Morgan, 1980; Burger, 1982). The cysts *Sentusidinium pilosum, Canningia* sp. A (Aptian-Albian), and *Diconodinium cristatum* (Albian-Cenomanian) were also recognized. In Sections 113-693A-45R, CC, through 113-693B-48R, CC, cysts are well preserved, but genera are commonly difficult to determine because the cyst bodies are filled with small pyrite cubes.

The sporomorph flora are composed of typical Lower Cretaceous elements such as *Cicatricosisporites australiensis, Osmundacidites wellmanii, Cyathidites australis, Lycopodiumsporites* sp., *Gleicheniidites circinidites, Densoisporites velatus*, and *Cycadopites nitidus*. Only *Neoraistrickia truncata* seems to be of stratigraphical value, described by McLachlan and Pieterse (1978) from upper Aptian-lower Albian sediments of the Cape Basin. Pollen grains of the conifers *Podocarpus* (*Podocarpidites*, several different species) and Cheirolepidiaceae/Cupressaceae (*Corollina, Inaperturopollenites*) are the most abundant types. The floral composition corresponds fairly well with a Lower Cretaceous palynomorph assemblage reported by Harris (1976) from the Falkland Plateau.

The thermal alteration index (TAI) can be determined as 1.6–1.8 (pollen color bright yellow) and is therefore slightly higher than at Site 692.

Hole 693B

The cores of Hole 693B sampled a lower Miocene through lower Oligocene sediment series. Sections 113-693B-6H, CC, through 113-693B-17X, CC, were barren of palynomorphs and nearly completely free of organic matter (see "Organic Geochemistry" section, this chapter). Section 113-693B-18X, CC, and Samples 113-693B-19X-2, 92–97 cm, and 113-693B-19X-4, 27–32 cm, dated as middle to lower Oligocene by diatoms, yielded an allochthonous palynoflora of Mesozoic and Cenozoic components, together with few Paleozoic spores. The preservation of the palynomorphs is partly very poor, partly moderate.

Some dinoflagellate species could be identified in these lower Oligocene samples. Forma T of Goodman and Ford (1983) was reported from Oligocene strata of the Falkland Plateau (Goodman and Ford, 1983). This cyst type seems to be identical with *Batiacasphaera micropapillata*, which ranges according to Williams and Bujak (1985) from the uppermost lower Oligocene to the middle upper Oligocene. *Selenopemphix nephroides* (middle Eocene-Miocene) was also present. *Australisphaera verrucosa* was described by Davey (1978) from the Southwestern African Shelf as an Upper Cretaceous floral element (Campanian-Maestrichtian).

The sporomorph flora in these samples is composed of Paleozoic (thick-walled species of *Leiotriletes*), Mesozoic (*Deltoidospora, Gleicheniidites*, and *Ephedripites*), and lower Tertiary forms, such as *Stereisporites, Polypodiidites, Phyllocladidites mawsonii*, two species of *Nothofagidites* (*N. flemingii* and *N. lachlanae*), and *Perfotricolpites digitatus*. The floral composition seems to be similar to the flora described by Bratzeva (1983) from the Falkland Plateau.

Biostratigraphic Summary of Site 693

The biostratigraphy of Site 693 is summarized in Figure 29. Tertiary sediments from Site 693 are virtually barren of calcareous microfossils, and the biostratigraphy of this part of the section is based on diatoms, radiolarians, and silicoflagellates.

The top three cores of Hole 693A contain a condensed Pleistocene section with rare to few, poorly preserved siliceous microfossils. Cores 113-693A-2R and 113-693A-3R cannot be dated by diatoms, and Core 113-693A-3R can be only tentatively dated as Pleistocene by radiolarians. The position of the Pliocene/Pleistocene boundary is thus poorly constrained. In Figure 29, it is placed at 14 mbsf, the position of the boundary as determined by magnetostratigraphy (see "Paleomagnetism" section, this chapter).

Low abundances and poor preservation of biogenic silica continue into Cores 113-693A-4R and 113-693A-5R, which are dated by both diatoms and radiolarians as upper Pliocene. Biogenic silica abundance and preservation are much better in Cores 113-693A-6R and 113-693A-7R. The age assignment of these two cores is problematic. Diatom stratigraphy places these two cores into the lower Pliocene, in contrast to the radiolarian stratigraphy, which assigns the two cores to the upper Pliocene. The radiolarian age estimate is consistent with the magnetostratigraphic age interpretation of this interval, which places the upper/lower Pliocene boundary at about 59 mbsf. Until more detailed biostratigraphic data are available, the 59 mbsf level is chosen for the boundary between the upper and lower Pliocene.

Cores 113-693A-8R through 113-693B-20R are assigned to the lower Pliocene by both radiolarian and diatom stratigraphy. Biogenic silica is abundant and well-preserved through most of this interval, although some samples from the basal Pliocene show evidence of moderate dissolution. Sedimentation rates within the lower Pliocene at Site 693 increase in the lower part of the section, and are particularly high below 4–4.5 Ma as indicated by the long lower Tau radiolarian subzone and by secondary diatom indicators within the *Nitzschia angulata/Nitzschia reinholdii* Zone (see "Diatoms" discussion above).

The Miocene/Pliocene boundary is not well calibrated to siliceous biostratigraphies in the Antarctic, but is estimated to lie at or near the top of the radiolarian *Cycladophora spongothorax* Zone, and within the uppermost part of the diatom *Denticulopsis hustedtii* Zone. The top of the *D. hustedtii* Zone occurs between Cores 113-693A-18R and 113-693B-19R. The top of the *C. spongothorax* Zone and, by definition, the boundary between the Miocene and Pliocene, occurs in the nonrecovered interval between Sections 113-693A-20R, CC, and 113-693B-21R, CC. There is no evidence for an unconformity at or near the Miocene/Pliocene boundary, although poor recovery in Cores 113-693A-20R to 113-693B-23R will make it difficult to confirm this even with more detailed sampling.

Site 693 contains a long (77 m) upper Miocene section extending from 186 to 263 mbsf (Cores 113-693A-21R through 113-693A-28R, and Cores 113-693B-2X and 113-693B-3X). Biogenic silica is abundant and well preserved in this interval. Diatom and radiolarian stratigraphies place most of this section into the upper part of the upper Miocene (upper *D. hustedtii* and upper *C. spongothorax* Zones), with the lower part of the upper Miocene being reached only below 235 mbsf, where the middle and upper part of the lower *C. spongothorax* radiolarian subzones are seen, together with the *Denticulopsis dimorpha* informal diatom subzone.

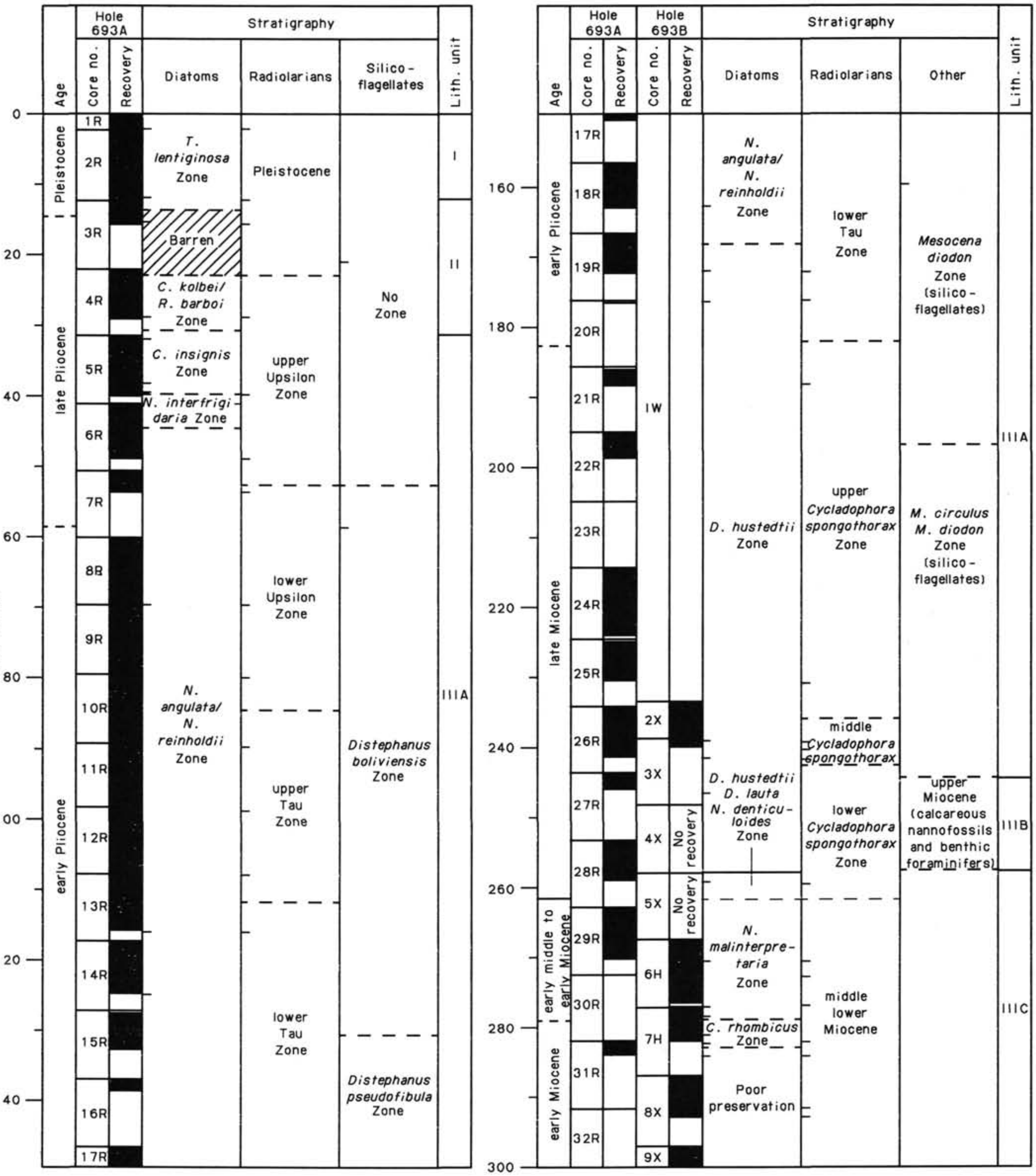

Figure 29. Biostratigraphic summary chart for Holes 693A and 693B. Core numbers and recovery (in black) are shown for both holes. Alignment of holes is by depth below seafloor. Because of the scarcity of all but siliceous microfossils at this site, separate columns are given only for the biostratigraphy of diatoms and radiolarians. All other biostratigraphic information is given in the column labeled "Other." Lithologic units are taken from "Lithostratigraphy" section (this chapter). Tick marks within each biostratigraphic column are used to show location of samples used to place biostratigraphic boundaries. Hiatuses within the section are shown by wavy lines.

A substantial hiatus occurs between Sections 113-693A-28R, CC, and 113-693A-29R, CC (263–272 mbsf), as indicated by an abrupt change from well-preserved upper Miocene diatom assemblages in Core 113-693A-28R to poorly preserved assemblages in Core 113-693A-29R assignable to the lower middle to upper lower Miocene *Nitschia malinterpretaria* Zone. Radiolarians from Core 113-693A-29R are also lower middle to lower Miocene, although no zonal assignment can be given due to poor preservation. The lower Miocene boundary between the *N. malinterpretaria* Zone and *Coscinodiscus rhombicus* Zone occurs

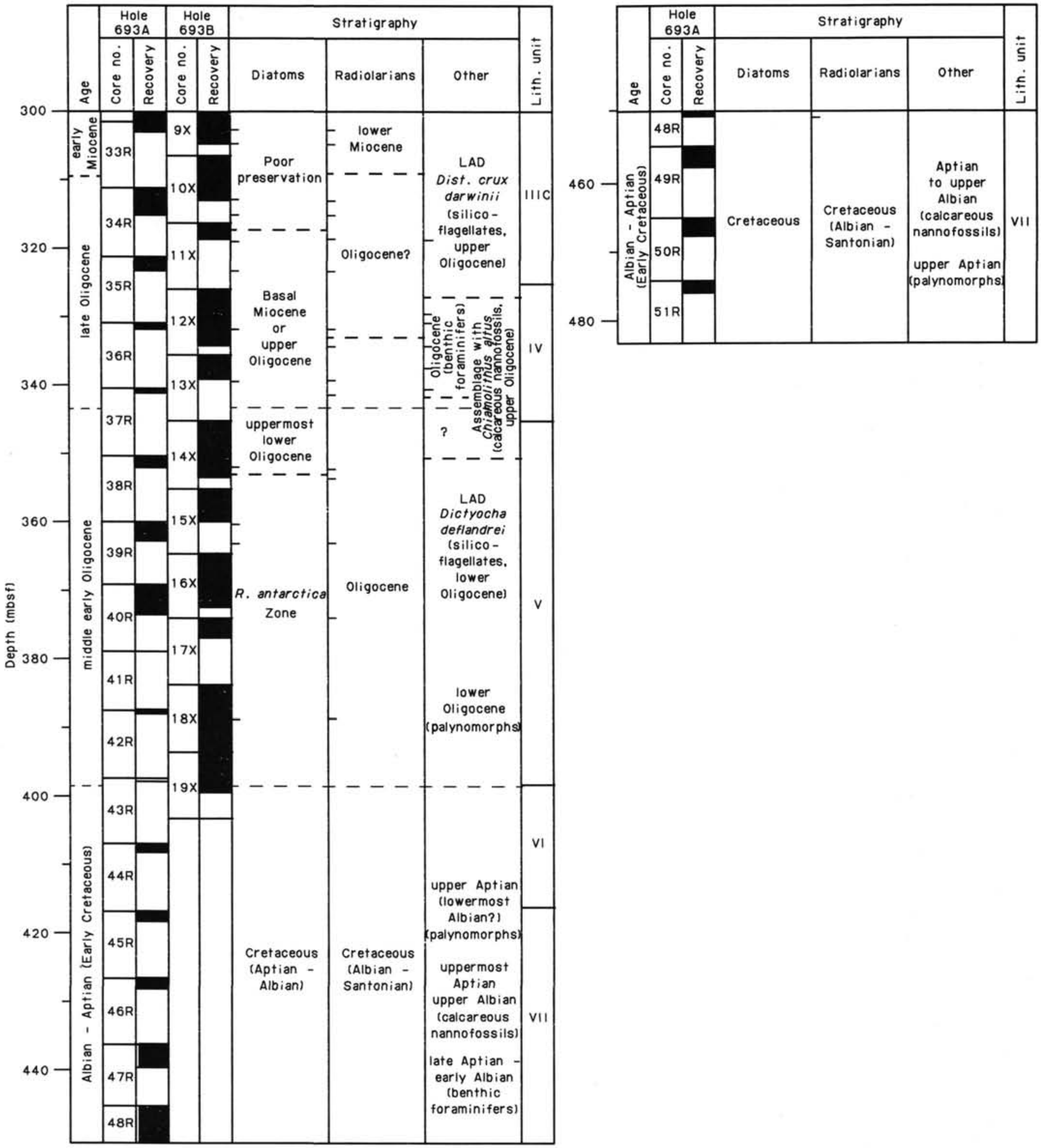

Figure 29 (continued).

at about 283 mbsf, only 10 m below the estimated hiatus, which suggests that most or all of the middle Miocene is missing in this hiatus.

The Miocene/Oligocene boundary is estimated at about 309 mbsf, although poor preservation of both diatoms and radiolarians makes the placement of this boundary difficult. The lowermost samples with unquestioned Miocene dates are radiolarians from Section 113-693B-8X, CC (293 mbsf), while the stratigraphically highest Oligocene dates are provided by radiolarians and silicoflagellates at 314 and 318 mbsf, respectively.

The interval between 309 and 345 mbsf is considered to be upper Oligocene, although biostratigraphic control in this interval is poor. Upper Oligocene dates are provided by silicoflagellates in Section 113-693B-11X, CC, and calcareous nannofossils in Section 113-693B-13X, CC. Diatoms from Section 113-693A-38R, CC, can be assigned to the uppermost lower Oligocene, and are used to place the upper/lower Oligocene boundary at 348 mbsf.

The base of the Tertiary sequence at Site 693 occurs between 345 and 398 mbsf and is assigned to the middle lower Oligocene *Rhizosolenia antarctica* diatom Zone. This zone is thought to be of relatively short duration (about 1 m.y. in the calibration scheme employed on Leg 113), and the assignment implies a high sedimentation rate for this part of the section. Lithologic data (see "Lithostratigraphy" section, this chapter) suggest that this interval has been expanded by slumping.

Organic-rich shales of Early Cretaceous (Aptian to Albian-Santonian?) age are separated from the overlying Oligocene diatomaceous muds by an erosional contact at 398 mbsf (Section 113-693B-19X-4, 69 cm). Benthic foraminifers indicate an Albian to possibly late Aptian age. An Albian age is indicated for this section by planktonic foraminifers and by calcareous nannofossils. Radiolarian age estimates of Albian to Santonian are consistent with the age provided by calcareous microfossil groups. The dinoflagellate cyst assemblage suggests a late Aptian age. Diatoms from these sediments are assignable to the Cretaceous, but no precise date can be given for the assemblage.

Paleoenvironment

In the oldest part of the section (lithologic Unit VII, Albian(?)), low oxygen concentrations in bottom waters are indicated by the benthic foraminifers, and by the high organic carbon content of the sediments (see "Organic Geochemistry" section, this chapter). Benthic foraminifers also suggest relatively shallow (about 500 m or shallower) water depths. High surface-water productivity and increased oxygen concentration of bottom waters are suggested by the diatomites and well-preserved siliceous microfossils at the top of the Cretaceous section.

The Upper Cretaceous and lower Paleogene environmental record has been removed by a major period of erosion during or prior to the late early Oligocene. Oligocene through lower Miocene sediments record low to moderate levels of biosiliceous productivity, with considerable dissolution of opal. Rates of terrigenous sedimentation were also moderate. At some time between the Aptian or Albian and Oligocene, Site 693 subsided to near its present water depth of 2500 m. Reworked Cretaceous microfossils, and microfossils transported from shallow water environments, indicate significant current transport and/or downslope movement during the Oligocene through early Miocene. The presence of benthic diatoms and neritic benthic foraminifers in this transported component, if not reworked from older deposits, indicates the existence of at least some ice-free areas along the Weddell Sea coast during the Oligocene and early Miocene.

The middle Miocene record has been lost at Site 693 in a hiatus. Upper Miocene and lower Pliocene sediments were deposited at relatively high rates (about 30 m/m.y. on average), due to increased rates of deposition of both terrigenous material and biogenic silica. Smear-slide analyses (see "Lithostratigraphy" section, this chapter) estimate the average biogenic silica content of these sediments at about 30%, and thus a sedimentation rate for biogenic silica of about 10 m/m.y. This value is very similar to the sedimentation rates for pure biosiliceous oozes in the late Miocene and early Pliocene of Maud Rise (see Sedimentation Rates" sections, "Site 689" and "Site 690" chapters, this volume). Biosiliceous productivity appears to have extended across a significantly broader latitudinal band in the late Miocene and early Pliocene in this region than it does today.

A major decrease in the rate of sedimentation of both terrigenous material and biogenic opal occurred in the late Pliocene and has continued to the present day. Decreased surface water productivity due to changing late Neogene environmental conditions can be invoked to explain the decrease in biogenic silica sedimentation rates. Decreased rates of terrigenous sedimentation are less readily explained, and may be due to any one of a number of factors, such as decreased glacial erosion on Antarctica or sediment bypassing of Site 693. Considerably more work will be needed to test such hypotheses.

PALEOMAGNETISM

Introduction

We undertook paleomagnetic measurements on samples from both holes drilled at Site 693, which is located 10 km southwest of the rim of Wegener Canyon. Hole 693A was rotary drilled to a terminal depth of 483.9 mbsf. In order to improve on the particularly poor recovery of the early Miocene and Oligocene age sediments in this hole, Hole 693B was drilled with the APC/XCB system to span a depth interval of 234 to 403 mbsf. The variability of recovery in both holes is a key factor in severely limiting our attempts to develop a high-quality Cenozoic magnetostratigraphy for this site. Drilling disturbance caused by rotary coring can also be identified as a major reason why anomalous magnetization directions often occur in semi-indurated sediments. We tried to minimize this effect by judiciously choosing apparently undisturbed material for sampling in Hole 693A. Recovery of the lithified mudstones of Cretaceous age, as at Site 692, presented a better sequence for paleomagnetic investigation.

Cenozoic Sediments

The distribution of natural remanant magnetization (NRM) inclinations for 325 samples taken from the Neogene and late Paleogene sediments of Hole 693A is shown in Figure 30. A dominant feature of this histogram is a node centered on shallow negative inclinations. This is in marked contrast to previous NRM results from Sites 689 and 690 on Maud Rise which are skewed toward steeper negative inclinations. The difference can be explained as either (1) normal overprinting during the Brunhes Chron has not been as pronounced for Hole 693A sediments as for the sediments of Maud Rise, or (2) rotary drilling has produced disturbed intervals with anomalous magnetization, despite the precautions we took in sampling. The latter may be the more likely explanation. Comprehensive magnetic cleaning should further distinguish between these possibilities.

NRM intensities encountered at Site 693 range over three orders of magnitude (0.2–215 mA/m). The lower intensities typify both the upper Miocene nannofossil oozes (e.g., Core 113-693B-28R) and the lower Miocene diatom-bearing clayey muds (e.g., Core 113-693B-9X). The close proximity of the site to East Antarctica is strongly reflected in the high intensities shown by the foraminifer-bearing silty muds of Pleistocene age that occur in the uppermost cores of Hole 693A. These intensities imply a detrital input of abundant ferromagnetic minerals.

Figure 31 shows the variation of NRM intensity and inclination for Hole 693A. For the uppermost 140 m of Hole 693A, the inferred polarity magnetozones can be satisfactorily assigned to the established geomagnetic polarity time scale. There is a provisionally acceptable fit with the chronostratigraphic interval from near the Miocene/Pliocene boundary through to the Pleistocene (Fig. 32).

Poor recovery below 140 mbsf in Hole 693A, particularly between 272 and 360 mbsf, makes meaningful correlation to the geomagnetic polarity time scale (GPTS) very difficult. A partial improvement in this situation results from the duplication of penetration over the same interval provided by Hole 693B, which gave slightly better recovery. Figure 33 gives the results of our measurements of NRM inclination and intensity for this hole.

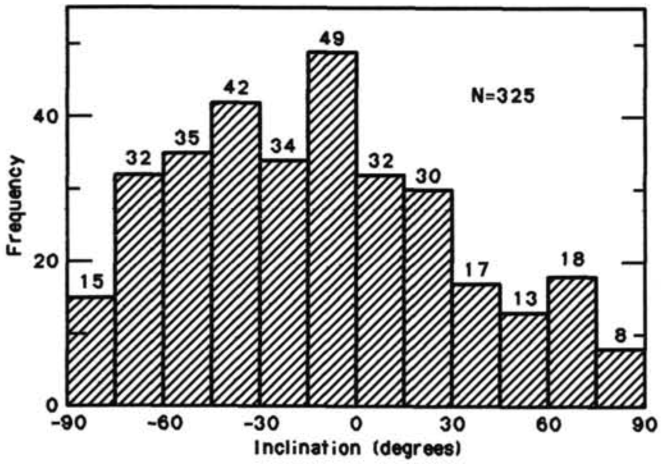

Figure 30. Frequency distribution of NRM inclination values for Hole 693A.

Dependent on refined diatom biostratigraphic assignments, it may prove feasible to determine the magnetostratigraphy of the lower Miocene and upper Oligocene sequences from our data after thorough demagnetization. A preliminary correlation to the GPTS is shown in Figure 34 for this interval. But the additional problem posed by the effects of slumping in the interval from Core 113-693B-14X downward on the inferred magnetic polarities requires further close scrutiny. Unless the slumps are of only limited extent, they could invalidate the magnetostratigraphy in this part of the sedimentary record.

Mesozoic Sediments

As at the nearby Site 692, a major unconformity occurs at Site 693, here separating the upper Paleogene sequence from the underlying Mesozoic sediments. The interval from 407 mbsf to 484 mbsf in Hole 693A comprises organic-rich mudstones of Cretaceous age. Lithologically they are broadly similar to those found at Site 692 but lack the calcareous lenses and layers of volcanic ash/pumice. Disseminated pyrite, together with occasional small pyrite nodules, is a characteristic feature of the mudstones.

Although recovery of the mudstone interval is not high, we obtained 21 samples for paleomagnetic study representing a fairly uniform sampling. All samples have a measurable NRM that is stronger in intensity than values reported previously for other Cretaceous "black shales" drilled in the South Atlantic (Falkland Plateau, Salloway, 1983) and Angola Basin (Keating and Herroro-Bervera, 1984). The presence of pyrite does not produce very low intensities in these Antarctic margin mudstones.

The lower part of Figure 31 shows the NRM intensity and inclination results for the mudstones. There is only limited change in either parameter downhole. As with Site 692, the inclinations suggest that the mudstones are normally magnetized. A stepwise alternating field demagnetization of Sample 113-693A-50R-1, 136–138 cm, shows a high magnetic stability (Fig. 35). If the other samples from this hole show similar behavior on demagnetization, it is likely that the episode of mudstone deposition occurred during Chron 34N. The rationale described previously for the interpretation of remanence results for the Lower Cretaceous mudstones of Site 692 applies equally to those of this site. That is, uneqivocal assignment of the inferred normal magnetozone to the geomagnetic polarity time scale requires biostratigraphic control.

After magnetic cleaning of the combined Cretaceous sample suite from both Site 692 and Site 693 it should be possible to determine a precise paleolatitude for the sites at the time of the organic-rich mudstone deposition.

SEDIMENTATION RATES

Biostratigraphic and Magnetostratigraphic Data

The sedimentation rate curve for Site 693 (Fig. 36) is constructed from two different sources of data. Biostratigraphic ages derived from diatoms, radiolarians, and silicoflagellates provide one source of age information for Site 693. Biostratigraphic data used to construct the age-depth relationship (Table 11) consist of selected datum levels and zonal assignments which have been correlated to the chronostratigraphic scale. The accuracy of the calibration between biostratigraphy and chronostratigraphy varies considerably for different fossil groups and time intervals. In particular, the pre-Pliocene diatom and radiolarian stratigraphies are not well calibrated chronostratigraphically.

The figure was constructed as follows: The line segment connecting unlabeled data points (solid boxes) is based on paleomagnetic data. The labeled data points with identifying numbers (Table 11) show the independently determined biostratigraphic information. The age-depth curve is shown by a dashed line based on biostratigraphic data and hiatuses indicated by wavy lines. Error boxes for paleomagnetic data represent in depth the distance between two samples of different polarities assigned to different magnetozones. From the preceding and following magnetozone boundaries, a sedimentation rate, and from this a corresponding error in the age determination, is calculated. This age error is represented by the horizontal box size.

Biostratigraphic data are of three types. First and last occurrences of species are known only to occur within a finite depth interval, although the age of the datum is generally reported without any associated error estimate. These data thus plot as vertical lines. Age ranges for individual samples by contrast have a finite age range but do not have any depth uncertainty, and plot as horizontal lines. Finally, a few FAD's and LAD's for which uncertainty estimates are available are plotted as boxes. Many samples have more than one age range estimate from different fossil groups. To make the overlap between multiple dates clear, small solid circles are used to mark the end of each datum which plots as a line. FAD's and LAD's represent, respectively, the oldest and youngest possible ages for a depth interval. Arrows indicate datums of this type, with the direction indicating the time direction which the species occurs.

Magnetostratigraphy provides a second source of age information. Magnetic polarity data were correlated with the geomagnetic polarity reversal time scale of Berggren et al. (1985) (see "Explanatory Notes" chapter, this volume, and "Paleomagnetism" section, this chapter) without recourse to biostratigraphic data. The preliminary interpretation is based on the assumptions of fairly constant sedimentation and a minimum number of hiatuses. Poor recovery (less than 50%) in some intervals makes the interpretation more difficult and open for later reinterpretation. Shore-based study including magnetic cleaning by stepwise demagnetization is required to obtain a more complete and reliable polarity record.

Sedimentation Rates and Hiatuses, Site 693

The Quaternary is marked by lower rates of deposition than much of the other section. These rates are on average less than 10 m/m.y. for the Pleistocene, based on paleomagnetic data (Fig. 37). The lower Pleistocene may be absent due to a hiatus or may be present in a condensed section. Due to the poor recovery in Core 113-693A-3R, however, the identification of the Olduvai Subchron can be in error, and a constant sedimentation rate may be provided by later reinterpretation after detailed shore-based paleomagnetic studies.

Paleomagnetic and biostratigraphic data are generally in close agreement for the remainder of the Pliocene/Pleistocene section, where a sedimentation rate of 21–46 m/m.y. (14–41 mbsf;

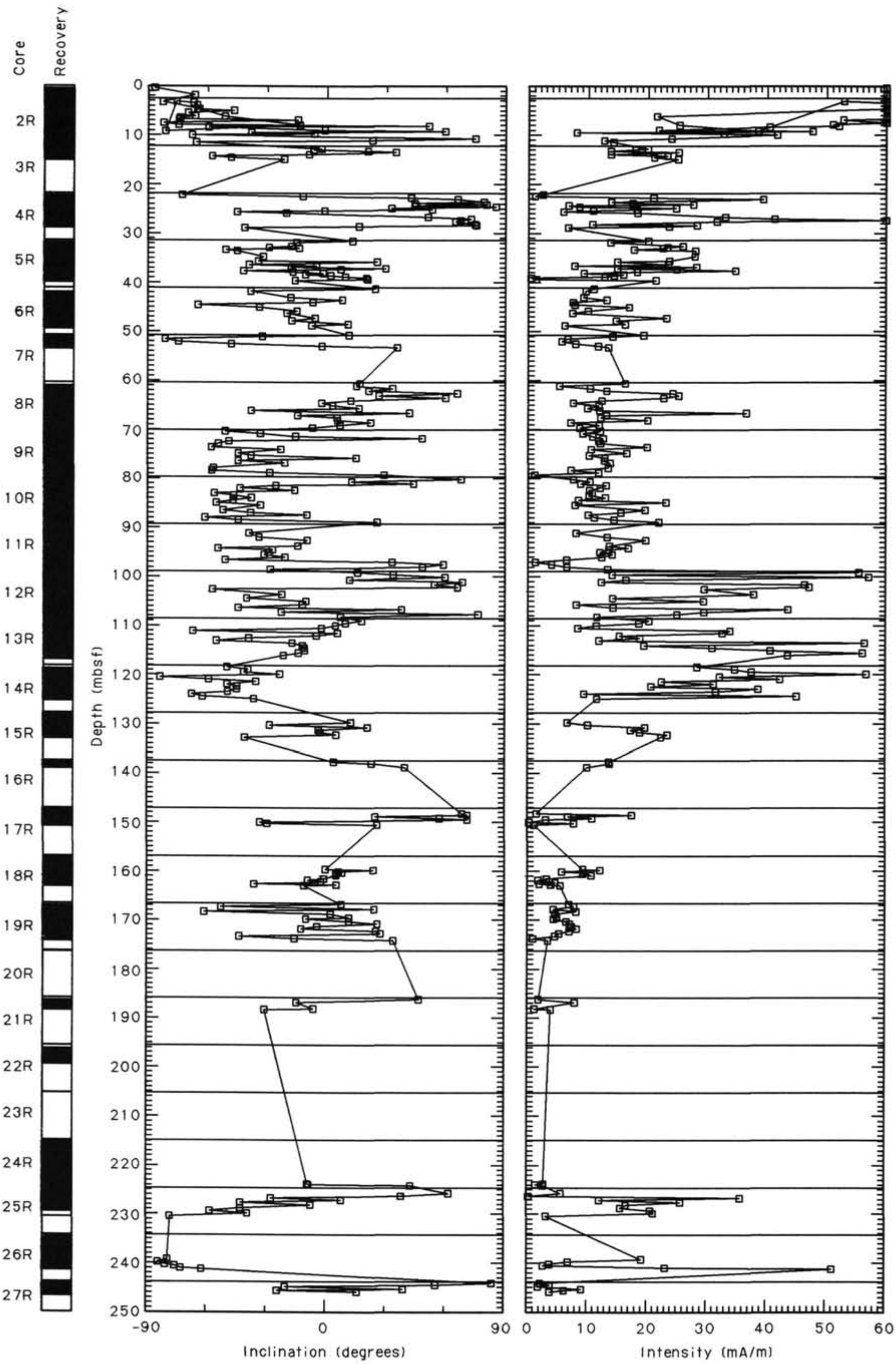

Figure 31. Downhole variation in NRM inclination and intensity for Hole 693A.

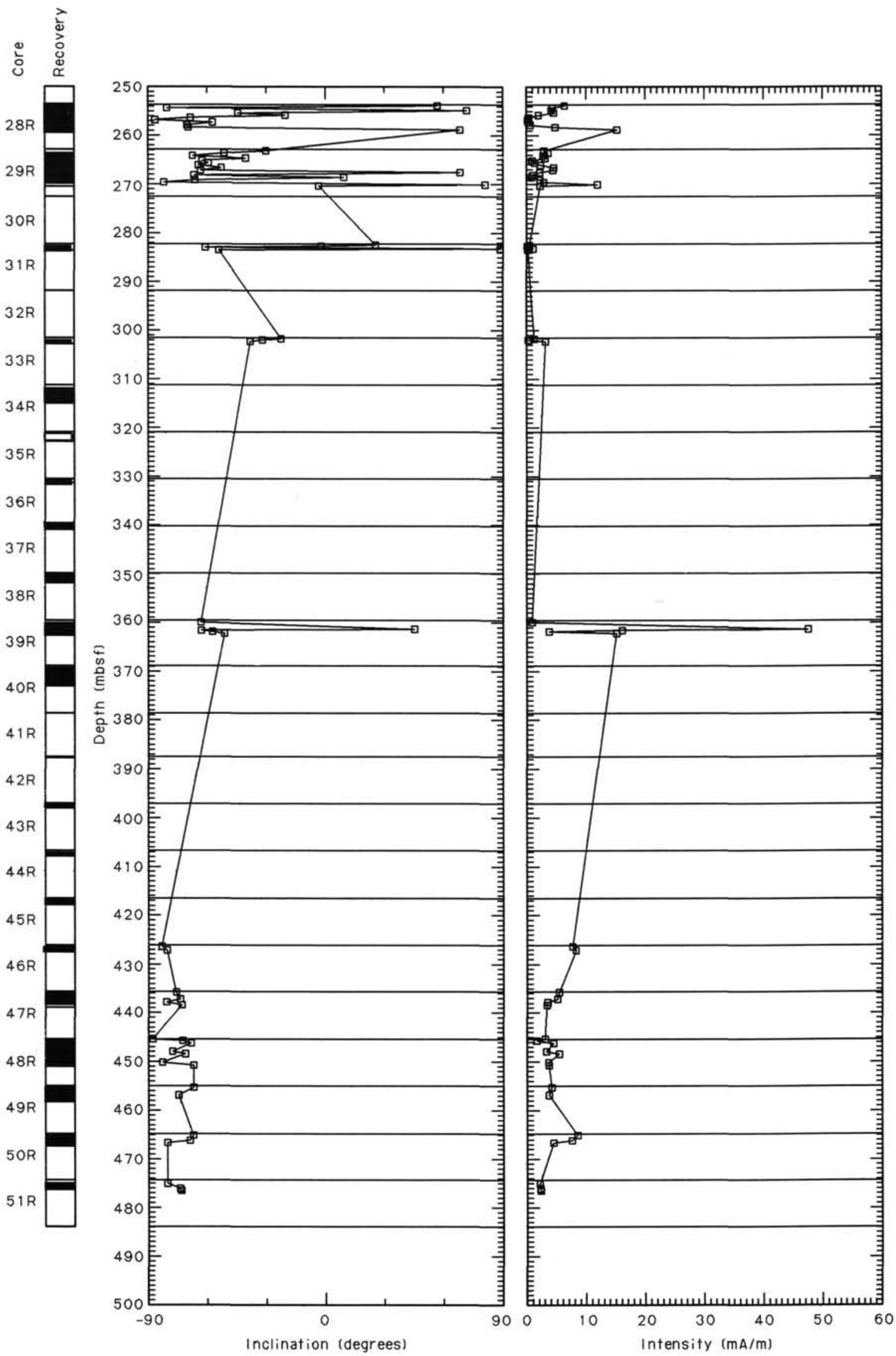

Figure 31 (continued).

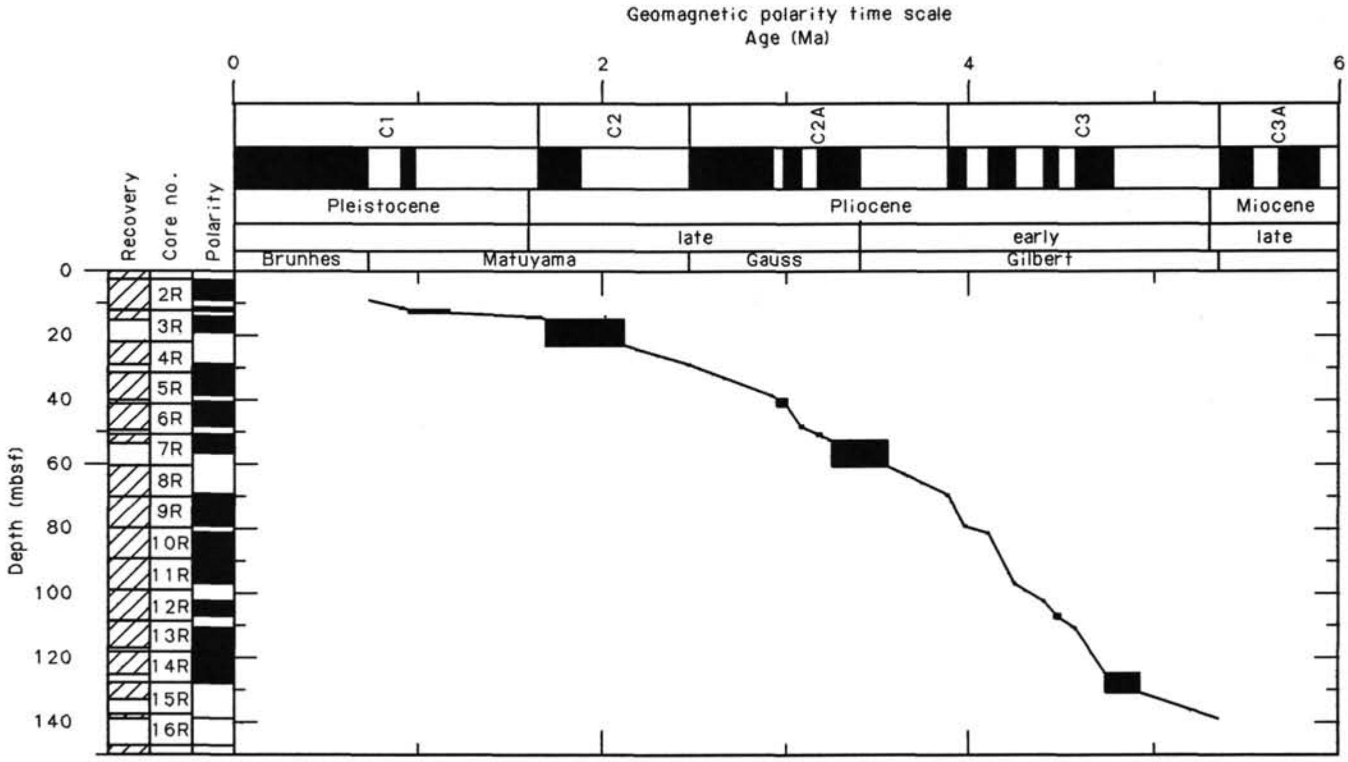

Figure 32. Assignment of the inferred magnetostratigraphy for Hole 693A to the established geomagnetic polarity time scale.

41–129 mbsf) is determined from the magnetostratigraphic assignment to the geomagnetic polarity time scale (Fig. 37). The solid portion of this curve is based on the paleomagnetic data, but it would be little changed if based strictly on biostratigraphic data points 1–3, 5, 6, 8, and 9. The exceptions to this trend are diatom zonal age determinations for the *Nitzschia interfrigidaria* (4) and *N. angulata/N. reinholdii* (7) Zones in the earliest and latest Gilbert Chron. A proper fit would require the intersection of the sedimentation rate curve with the top left and top right corners of both boxes. The discrepancy between these points and the paleomagnetic age assignment at 50 mbsf is nearly 1 m.y. This indicates a significant calibration problem for these two zonal intervals relative to the paleomagnetic time scale, and even between radiolarian and silicoflagellate age zonations. We hope that further study of ODP Leg 113 cores will resolve this problem, which at this site is particularly vexing due to the high sedimentation rate in this portion of the section.

Core recovery below 130 mbsf is generally poor, therefore only biostratigraphic data are used to define the curve through the lowest Pliocene and upper Miocene (dashed line, Fig. 36). The inferred sedimentation rate is 23 m/m.y. The Miocene section contains a hiatus at 262 m which spans about 6–7 m.y. over the lower upper and middle Miocene.

Due to poor core recovery the age of the remainder of the Miocene and Oligocene section is likewise poorly constrained by both magnetostratigraphic and biostratigrahic data (Fig. 36). A disagreement of 13–32 m between the diatom and silicoflagellate/radiolarian placements of the Miocene/Oligocene boundary may reflect, in part, a need for closer calibration of the various datums used against the paleomagnetic time scale. The magnetostratigraphic age determinations (268–282 mbsf; 326–338 mbsf) are closely tied to biostratigraphic data points 14 and 16. The long reversed sequence between 330 and 338 mbsf can be used to estimate a sedimentation rate. Assuming a continuous sedimentary sequence between 262 and 345 mbsf, this reversed magnetozone is likely to be assigned to the Chron C6CR-3, the longest reversed polarity interval in the late Oligocene. This provides a sedimentation rate of approximately 7 m/m.y. with a hiatus age of 9–15 m.y. (262 mbsf) and a correlation of the polarity sequence between 268 and 282 mbsf to the middle/lower Miocene boundary. A connecting line between these two intervals would cross the diatom placement of the boundary (data point 16, Fig. 36). Extrapolation of a mainly biostratically-constrained sedimentation rate curve (dashed line) provides a slightly greater age of about 9–16 Ma for the hiatus.

A hiatus at about 342 mbsf may separate upper Oligocene from middle lower Oligocene sediments. This possible hiatus is implied by the virtual absence of upper lower Oligocene sediments in contrast to the extensive sequence (53 m) through the diatom *Rhizosolenia antarctica* Zone (zonal box 18, Fig. 36). The sedimentation rate through this box could equal 61 m/m.y., but there is strong sedimentological evidence that much of this sequence is slumped (see "Lithostratigraphy" section, this chapter), perhaps with considerable repetition of section.

The middle lower Oligocene sediments are separated by a disconformity at 398 mbsf from a subjacent Cretaceous diatomite, directly below which is a Lower Cretaceous "black shale" sequence of Albian to Aptian(?) age. The diatomite may also be Albian. If so, the disconformity could represent a minimum of 60 m.y. duration. No sedimentation rate could be established for the relatively short Albian to Aptian section cored.

INORGANIC GEOCHEMISTRY

Introduction and Operation

Data on the chemical composition of interstitial water are presented in this section for Holes 693A and 693B. Hole 693A was drilled by rotary coring to a depth of 483.9 mbsf. Hole 693B was cored by APC and XCB from 223.8 mbsf (following washing) to 403.1 mbsf. Seventeen whole-round (10 from Hole 693A and 7 from Hole 693B, 1 of 10-cm and 16 of 5-cm thick-

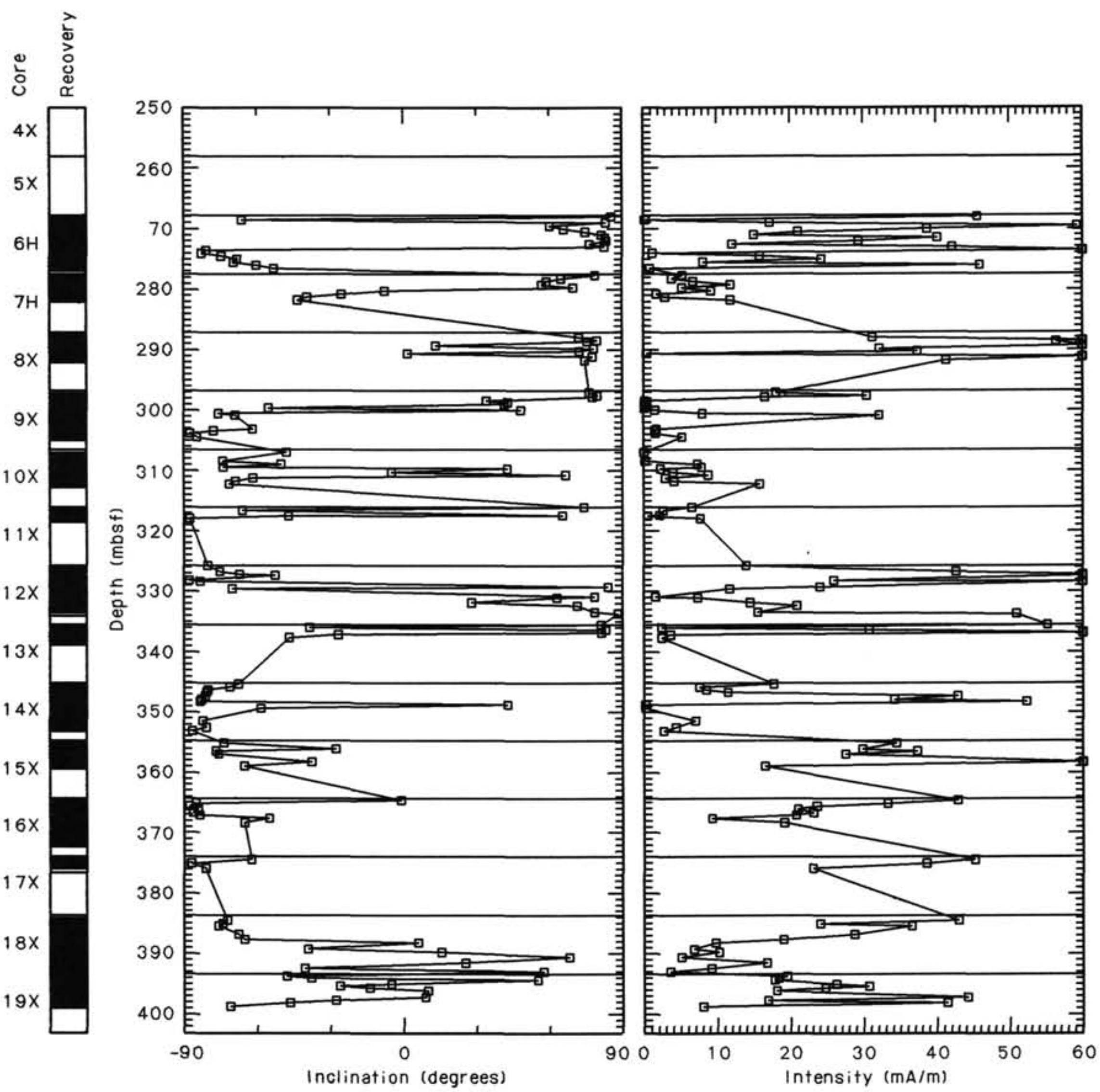

Figure 33. Downhole variation in NRM inclination and intensity for Hole 693B.

ness) sediment samples were analyzed. The samples from Hole 693B are bracketed by samples from Hole 693A, and there is a region of overlap between 227 and 258 mbsf.

Chemical analysis of water extracted from the mud used during drilling of Hole 693A was also carried out. The chemical data are summarized in Table 12 and shown graphically in Figure 38.

Evaluation of Data

For overall evaluation of the data, a charge balance was carried out. As with Sites 689 and 690 this was conducted assuming that the sodium to chloride ratio of the interstitial water is that of present-day seawater. The calculations reveal that all samples have excess negative charge. In no samples, however, does the excess charge amount to more than 1.5% of the total charge. As observed in the pelagic sediments at Maud Rise (see "Inorganic Geochemistry" sections, "Site 689" and "Site 690" chapters, this volume), the charge imbalance shows systematic variations with depth. This indicates that there may be either a systematic error in one of the analytical methods, or that the assumption of constant Na/Cl ratio is not valid. The only parameters that vary sufficiently for a systematic error to account for the observed charge imbalances are magnesium, calcium, and sulfate. Although the sulfate method is the least accurate, shipboard tests show that it does not have any associated systematic errors. The concentration of calcium was determined using a shorter version of the method of Tsunogai et al. (1968). The concentration of magnesium is determined by subtraction after the total concentration of alkaline earths have been determined by titration. An updated version of the correction procedure suggested by Gieskes and Lawrence (1976) was employed. The same methods have been used at all sites, so all data obtained during Leg 113 can be pooled and analyzed. Linear regression analysis reveals that there is no significant correlation either between excess charge and total concentration of alkaline earths or between excess charge and calcium concentration. There are also no nonlinear relations. Based on the present data a systematic variation in the Na/Cl ratio is indicated.

Hole 693A was drilled by rotary coring and an alkaline mud containing polymers and bentonite was used to clean the hole below Core 113-693A-37R. Thus the samples may have been contaminated by seawater, drilling-mud filtrate, or both. To evaluate any contamination of mud filtrate, a drilling-mud sample was separated by centrifugation and filtered through a 0.45-μm membrane filter. The results of the chemical analysis are presented in Table 12. This sample is from one batch of mud only,

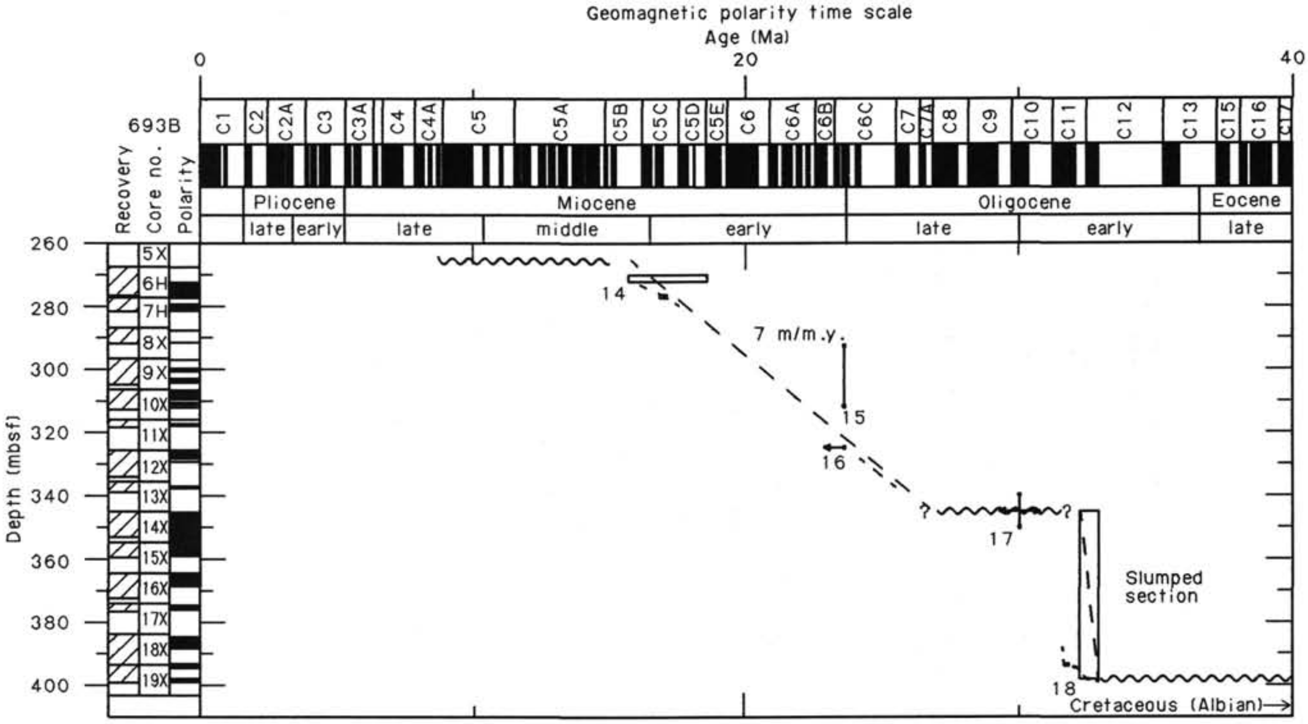

Figure 34. Preliminary correlation of the inferred polarity pattern to the geomagnetic polarity time scale using biostratigraphic data (see Table 11) as tiepoints.

and fluctuations in chemical composition from batch to batch are probably significant.

From the chloride analysis (Table 12) it is evident that Cores 113-693A-40R and 113-693A-48R are both contaminated by mud filtrate, and perhaps seawater also. From the appearance of the cores, and the mechanics of rotary coring and XCB coring, it is obvious that the former introduces more disturbance and greater risk of contaminating the samples. Thus, the very good agreement (within analytical precision for most parameters) between the two sets of data in the region of overlap (227–258 mbsf) indicates that seawater contamination is not a serious problem. This is due partly to the clay content of the sequence (low permeability and finely divided cuttings).

Based on the assumption of no significant seawater contamination and that of constant chloride concentration (see below), the amount of mud filtrate in the water extracted from Sample 113-693A-48R, 120–125 cm, is estimated to be about 10%. With this volume and the data on the composition of the mud, the data for this core were corrected. The original and corrected data are compared in Table 12 and graphed in Figure 38. In Core 113-693A-40R the degree of dilution is too small to require any corrections other than for chloride.

Chlorinity and Salinity

Chloride data are presented in Figure 38A and Table 12. Two concentration plateaus and the spurious Core 113-693A-48R result may be distinguished. The slightly elevated chloride level (average 576.2 mmol/L) from the upper sample down to 257 mbsf (113-693A-28R-3) is from samples from Hole 693A. The lower chloride level (average 563.6 mmol/L) from 257 mbsf and down is from samples from Hole 693B.

The chloride analysis on samples from Hole 693A was completed before sampling of Hole 693B commenced. The average chloride concentration for this hole corresponds to a seawater salinity of 36‰, higher than measured in any bottom-water mass around the Antarctic continent. Thus, evaporation of the samples was suspected. For samples from Hole 693B, containers with thicker walls and better seals were used. Repeating the chloride analysis from the rotary-cores when the samples from the XCB cores were analyzed revealed some small but significant differences. All samples from Hole 693A showed higher chloride concentrations when analyzed 4 days following the first analyses. During this time 2% of the water had evaporated. As the samples had been stored from 1 to 5 days prior to the first analysis, the slightly elevated chloride level in the Hole 693A samples (Fig. 38A) is probably an artifact. For all other parameters this effect is masked by the variability of the methods. Containers with thicker walls and better seals are now being used.

The average concentration of chloride in the samples from the XCB-cores corresponds to a seawater salinity of 35.1‰ (using the chlorinity/salinity relation given by Sverdrup et al., 1942). Strictly, the salinity/chlorinity relationship is valid only for waters with the same major element ratios as seawater. Except for the variations discussed above, there are no significant trends.

Salinities measured using the optical refractometer differ from those calculated from the chlorinity data by about 2‰-units. No correlation between the two is observed.

pH

The pH (Fig. 38B and Table 12) varies between 8.34 and 7.76. The only significant shift in pH occurs between 46.8 and 75.8 mbsf (Cores 113-693A-6R to 113-693A-9R) where an increase from 7.76 to 8.10 is observed. There are no changes in lithology that correlate with this shift. The average pH of 8.1 is higher than observed at Site 689 and 690.

Alkalinity, Sulfate

The alkalinity data are presented in Figure 38C. The carbonate alkalinity equals (within experimental error) the titration alkalinity, because there are are no other anions of weak acids present (mmol/L concentrations). The alkalinity varies between 2.27 meq/L at 330 mbsf (Section 113-693B-12X-3) and 3.90

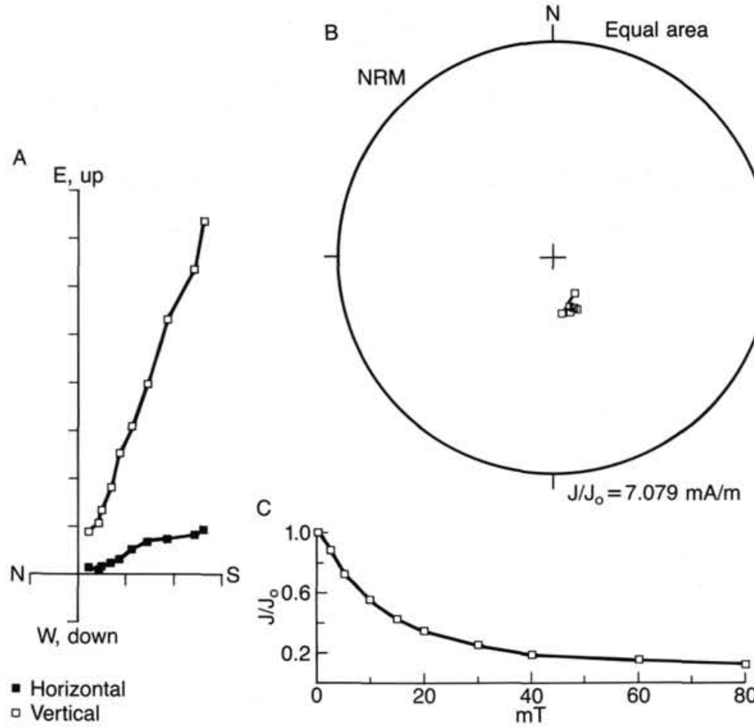

Figure 35. Alternating field demagnetization of Cretaceous mudstone Sample 113-693A-50R-1, 136 cm. A. Zijderveld orthogonal vector plot. B. Equal-area stereographic projection of resultant vector. C. Normalized intensity decay curve.

meq/L at 8.45 mbsf (Section 113-693A-2R-4). There is a slight decreasing trend with increasing depth. Assuming stoichiometric oxidation of organic carbon, the alkalinity is lower than expected from the sulfate profile. Alkalinity determination was not carried out on the mud filtrate.

The sulfate profile is presented in Figure 38D. The concentration of sulfate decreases from sea level (28.6 mmol/L) in the upper 8.45 mbsf (Core 113-693A-2R) to 16 mmol/L at 448 mbsf (Section 113-693A-48R-2). It is evident that diffusion keeps up with bacterial consumption, thus the bacterial activity is comparatively low. Without more elaborated modeling one can not tell whether the profile is a diffusion profile to a deep reaction zone or if reduction of sulfate takes place throughout.

Phosphate and Ammonia

The concentration profile for phosphate is presented in Figure 38E. The concentration of phosphate in the interstitial water decreases from about 5 μmol/L at 10 mbsf (Section 113-693A-2R-4) to 1 μmol/L at 448 mbsf in the corrected value for Sample 113-693A-48R-1, 30–35 cm. As with sulfate, the agreement with the trend established by the rest of the data set is improved by correcting for the presence of mud filtrate. The levels are low and confirm the low bacterial activity.

The concentration of ammonia is shown in Figure 38F. The concentration of ammonia increases erratically from 0.1 mmol/L at 8.45 mbsf (Section 113-693A-2R-4) to a stable level at about 0.3 mmol/L below 230 mbsf. The correction procedure is unable to account for the high concentration of ammonia in the sample from Section 113-693B-48R-2 (448.1 mbsf). This probably reflects the variability of ammonia concentration in the mud. The high concentration at 371.78 mbsf (Section 113-693A-40R-2) is considered an experimental artifact. Concentrations of ammonia are generally higher than observed at the previous Leg 113 sites.

Calcium and Magnesium

Calcium and magnesium data are presented in Figures 38G and 38H, respectively. The concentration of calcium increases steeply from seawater concentration at 8.45 mbsf (Section 113-693A-2R-4) and reaches 18 mmol/L at 161 mbsf (Section 113-693A-18R-3). Below 200 mbsf the concentration varies between 16.7 and 17.7 mmol/L.

The concentration of magnesium decreases from slightly less than seawater concentration (50.7 mmol/L) in the upper sample (Section 113-693A-2R-4) to a more or less stable level at about 37.5 mmol/L below 240 mbsf. The correction procedure is unable to bring the analytical result for magnesium from Core 113-693A-48R into accord with the trend indicated by the other data (Fig. 38H).

At this site, the relationship between the amount of calcium released and the amount of magnesium removed from the interstitial water is not a simple 1:1 relation as observed at the previous sites. Below 270 mbsf the amount of magnesium removed is about three times the increase in calcium. This difference may have been caused by precipitation of calcium carbonate, as this mechanism would also account for the low alkalinity level (see above). The amount of calcite produced would (calculated with average porosity of 50%) amount to a concentration of authigenic calcite of less than 0.1% (by volume), and thus go undetected by microscopic examination. The stable magnesium-to-calcium ratio below 140 mbsf (Fig. 38I) suggests that an equilibrium has been reached, possibly involving clays (the sequence contain 20%–40% clay-sized particles).

Potassium

In the upper 26 mbsf, concentrations of potassium are slightly higher than in sea water (Fig. 38J). Then follows a rapid decline to 7.8 mmol/L at 161 mbsf (Section 113-693A-18R-3) below which only minor fluctuations occur. The correction procedure

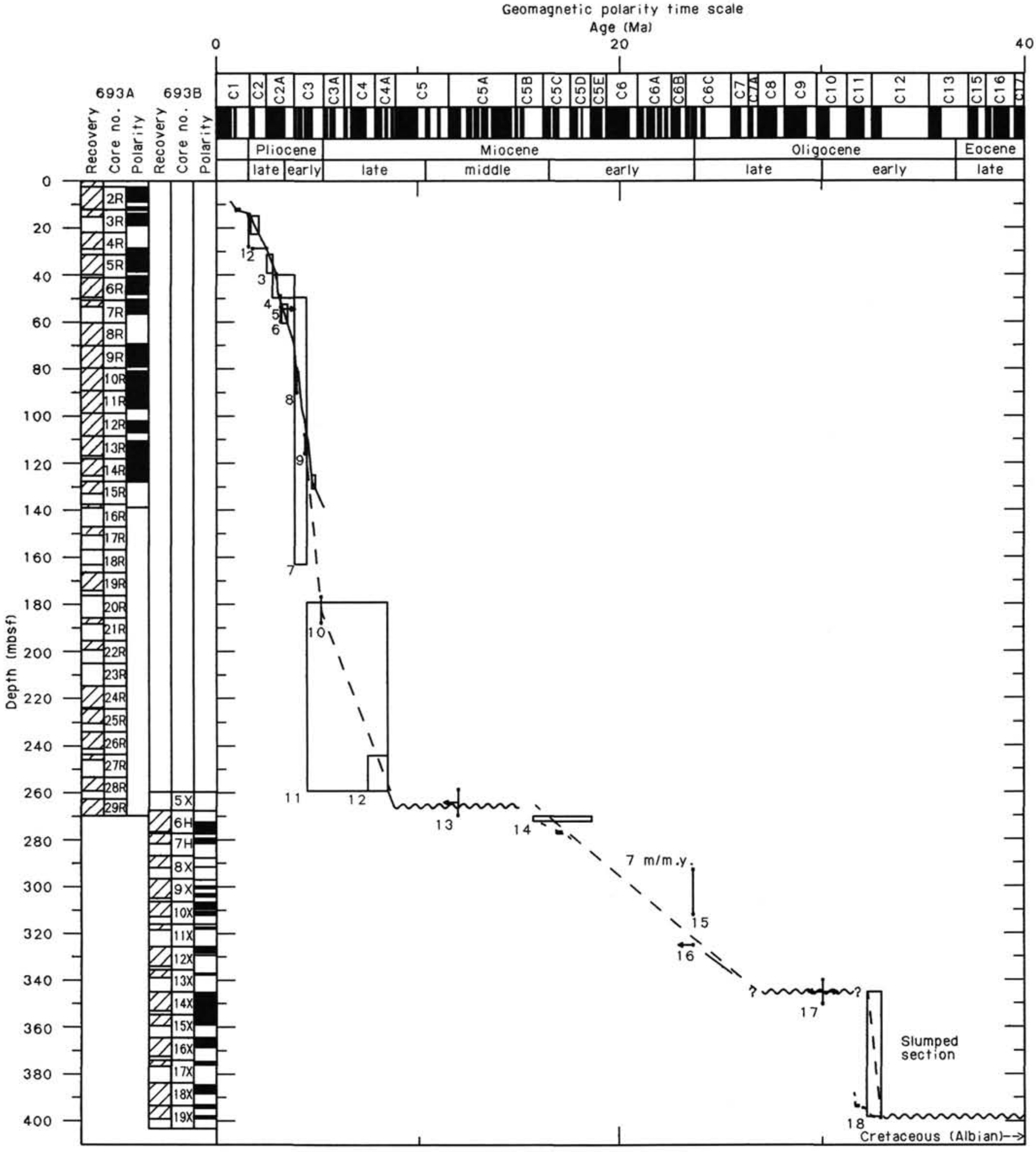

Figure 36. Age-depth interpretation of Site 693. See text for explanation.

for the sample from Core 113-693A-48R improves the agreement with the trend established by the rest of the data set. The stable level at depth may indicate that an equilibrium has been reached.

Dissolved Silica

The concentration of dissolved silica (Fig. 38K) varies between 430 μmol/L at 8.45 mbsf (Section 113-693A-2R-4) and 1370 μmol/L at 274 mbsf (Section 113-693A-6X-4). In all samples the levels fall between quartz saturation and amorphous silica saturation. The concentration of dissolved silica increases rapidly from the surface to 76 mbsf (Section 113-693A-9R-4). In this interval the major lithology changes from a clay-rich zone from the top of the section to 40 mbsf, to a diatom-bearing sequence below. Except for three samples between 274 and 330 mbsf the level of silica is constant at about 1000 μmol/L through-

Table 11. Biostratigraphic data used to construct sedimentation rate in Figures 34 and 36.

Datum number	Depth range (mbsf)	Age (Ma)	Datum or zone
1	15.0-28.0	1.6	Pleistocene/Pliocene boundary - R
2	28.9-28.9	1.8-2.5	*C. kolbei/R. barboi* Zone - D
3	31.4-39.4	2.5-2.8	*C. insignis* Zone - D
4	40.0-49.9	2.8-3.9	*N. interfrigidaria* Zone - D
5	49.0-54.0	3.2	upper/lower Upsilon Zone boundary - R
6	49.0-60.0	3.2	LAD *D. boliviensis* - S
7	49.45-163.2	3.9-4.5	*N. angulata/N. reinholdii* Zone - D
8	80.0-90.0	4.0	Upsilon/Tau Zone boundary - R
9	108.0-116.0	4.4	upper/lower Tau Zone boundary - R
10	177.0-188.0	5.2	Tau zone/*C. spongothorax* Zone boundary - R
11	179.3-259.4	4.5-8.5	*D. hustedtii* - D
12	244.4-259.4	7.5-8.5	*D. dimorpha* acme - D
13	259.0-270.0	<12	Base hiatus/*C. spongothorax* - R
	±266.0	Hiatus	Hiatus - middle Miocene
14	270.5-272.5	15.7-18.56	*N. malinterpreteria* Zone
15	293.0-312.0	23.6	Oligocene/Miocene Boundary(?)
16	325.0	<23.6	Miocene - D
17	340.0-350.0	30.0	middle/lower Oligocene boundary (D, S)
18	345.0-398.0	32.2-32.9	*R. antarctica* Zone - D
	398.0	Hiatus	Hiatus

Key to table: Depth range given for First and Last Appearance Datums (FAD's and LAD's). A single value in both depth columns indicates a sample with a zonal or assemblage age assignment. Age range given for zones, and in some instances for uncertainty in age calibration of a FAD or LAD. Letters following each datum name refer to the fossil group: S - silicoflagellates, D - diatoms, and R - radiolarians.

out the section below 76 mbsf. The correction procedure has little effect on the silica results.

ORGANIC GEOCHEMISTRY

Rock-Eval Analyses: Kerogens in Hole 693A

Subdivisions on the basis of kerogen analyses for the sediments recovered at Site 693 are shown in Table 13. Complete data are presented in Table 14. Four units are recognized.

Unit 1 (0–370 mbsf), Cenozoic, contains low concentrations of extremely variable, mature to highly mature, reworked kerogen.

Unit 2 (407–427 mbsf), Uppermost Cretaceous (Albian), is distinguished only by a slight increase in the concentration of recycled kerogen.

Unit 3 (427–465 mbsf), Cretaceous (Aptian-Albian), is of major interest, comprising 38 m (recovered) of dark grey mudstone, with occasional layers of coarse silt. The kerogens have unusual characteristics. In contrast to the older Lower Cretaceous section of Site 692, they possess almost no potential for petroleum generation, despite their dark color and substantial organic carbon content, averaging 2.56%. Unit 3 has a well-defined T_{max} of 414°C, indicating immaturity, almost identical to that observed in the Lower Cretaceous of Hole 692B, 413°C. The simultaneous occurrence of low values of T_{max}, Hydrogen Index (HI), and Oxygen Index (OI) is unusual. A feasible means of generating them might have involved syndepositional oxidation of significant quantities of planktonic kerogen precursors, along with the admixture of highly mature recycled kerogen. The latter would depress both HI and OI without obscuring the low T_{max} of the former.

Unit 4 (465–475 mbsf), Aptian-Albian, represented only in Core 113-693A-51R, appears to possess kerogen similar in origin to that in Unit 3, but the sediments are substantially leaner in organic carbon (0.96%).

Light Hydrocarbons

Relatively low levels of methane were encountered in all of the 23 analyses carried out in Hole 693A. Concentrations ranged from 0.7 to 62.8 μL of gas per liter of moist sediment. Analytical data are given in Table 15.

Ratios of methane to ethane are low, as at other sites in the Weddell Sea. Although low, no hazard to drilling is represented because only trace levels of gas are present. Bacterial methane is virtually absent. Light hydrocarbon compositional ratios are given in Table 16.

Sufficient butanes and pentanes are present in the Cenozoic section for reliable ratios to be measured between the isomers. The observations present inconsistencies. For example, the ratios of n-butane/isobutane measured in Cores 113-693A-19R and 113-693A-25R are indicative of kerogens of low maturity as they are substantially less than unity. However, Rock-Eval measurements indicate highly mature kerogens. These inconsistencies suggest that the C_{4+} hydrocarbons are not indigenous to the section. As the Cenozoic sediments contain soft sediment clasts it is possible that the anomalous hydrocarbons were transported in these allochthonous particles. Low ratios of *n*-butane/isobutane also characterize the Lower Cretaceous at Site 692. This margin has been extensively eroded and could have provided clasts with low *n*-butane/isobutane ratios.

Light Hydrocarbons in Aptian/Albian Mudstones

There are significant contrasts between the hydrocarbons of the Cretaceous sections at Sites 692 and 693, namely:

1. The *n*-butane/isobutane ratios are distinctly different, averaging 3.1 in Cores 113-693A-46R to 113-693A-51R, while at Site 692 the average is 0.77 (four analyses). As stated, low values indicate immaturity, while values substantially greater than 1.0 are found in mature sediments and petroleums. Both stratigraphic sections are immature, on several lines of evidence. For example, almost equal values of T_{max} are observed. Whelan et al. (1984) found values of the quoted ratio to vary progressively from 0.25 to 0.5 over the interval 1100–1500 m in Cretaceous "black shales" at Site 397, Canary Islands.
2. The quantities of light hydrocarbons, normalized to organic carbon, are 2.8-fold higher in the Aptian-Albian of Hole 693A than in the Lower Cretaceous of Hole 692B. The Lower Cretaceous kerogen from Hole 692B is hydrogen-rich, and represents an average organic carbon content of 8.6%, while that of the Albian from Hole 693A is hydrogen-poor, and represents only 2.6% carbon. Light hydrocarbon yields are proportional to both quantity and quality of kerogen, therefore on both counts the higher yields should occur in the Lower Cretaceous (Hole 692B).

The provenance of the apparent excess of hydrocarbons is subject only to speculation. It is possible that trace levels of petroleum are involved, possibly moving in solution in connate water. An explanation of this nature was suggested for anomalously high concentrations of toluene in the Lower Cretaceous sediments of Site 511, Falkland Plateau (Schaefer et al., 1983).

Occurrence of Gas, Core 113-693B-19X, 396–399 mbsf

Hole 693B was drilled in an attempt to sample low-recovery, highly disturbed intervals in Hole 693A. At 403.1 mbsf in Hole 693B drill-bit failure occurred. Rotation without penetration continued for some 45 min. This evidently raised the bottom-hole temperature sufficiently to pyrolyze the sediment in Section 113-693B-19X, CC, and to degrade the Delrin bushing in the barrel assembly. Both sources appeared to contribute gas (having an offensive odor) to the sediment pore space over several sections. Sufficient gas was generated to cause bulging of the end caps of Section 113-693B-19X-4. A vacutainer sample contained only 94 ppm methane. Other components resembled those of natural gas in their chromatographic behavior. However, consistent and reproducible differences in retention times from those of saturated hydrocarbons were observed, proving that the occurrence was not natural gas. Although no standards for ethene, propene, and butene are available on board, these

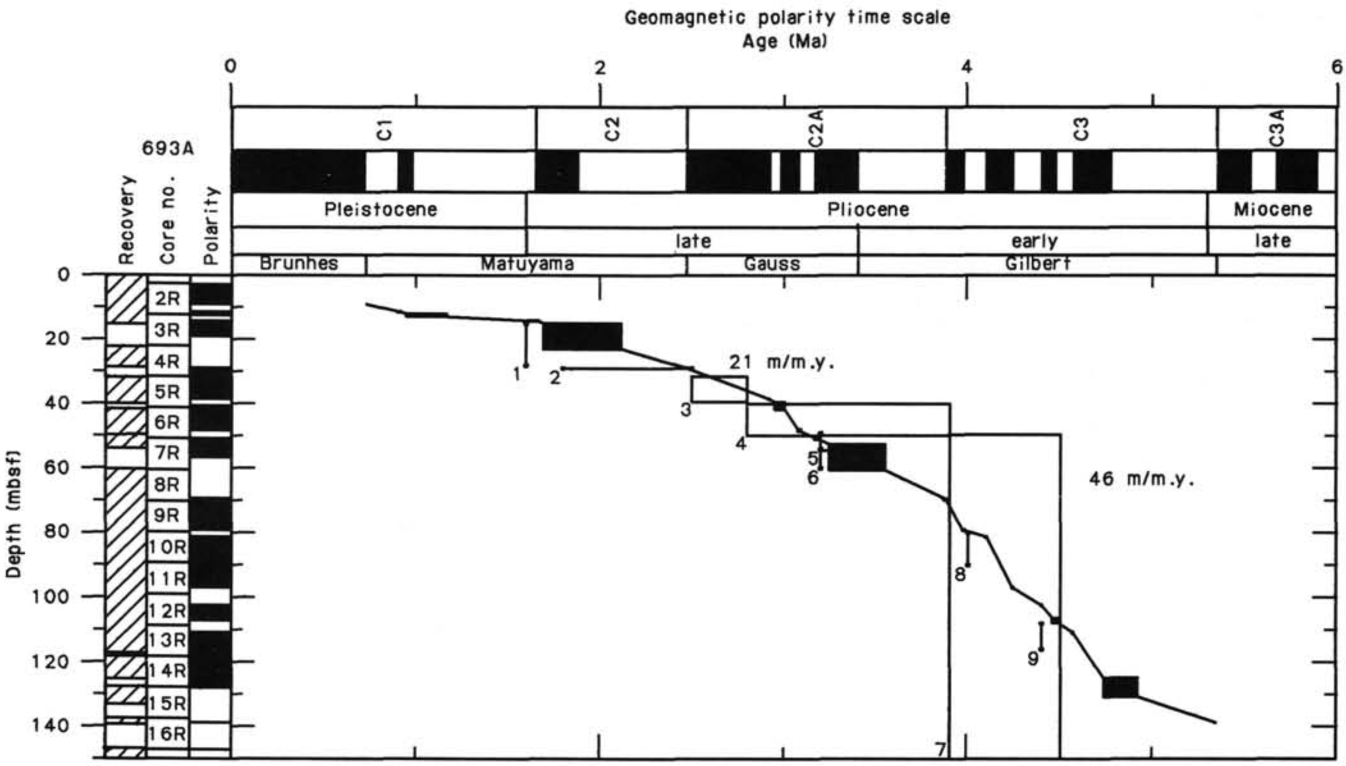

Figure 37. Enlargement of Pliocene-Quaternary portion of Figure 36 to show more clearly the different magnetostratigraphic and biostratigraphic interpretations. Age-depth curve based on magnetostratigraphic assignment is shown by a solid line connecting data points. This is close to a line that could be fitted through most of the diatom, radiolarian, and silicoflagellate data points (points 1–6, 8–9), therefore only the paleomagnetic curve is represented. However, this curve does not pass close to the intersection of boxes 4 and 7, which are based on the diatom *N. interfrigidaria* and *N. angulata/N. reinholdii* Zones. This points out a major discrepancy in the calibration of those diatom zones against the paleomagnetic time scale. Other plotting conventions explained in text.

common products of pyrolysis possibly made up the subsidiary components of the gas. Observed retention times are given in Table 17.

DOWNHOLE MEASUREMENTS

Introduction

Downhole logging at Site 693A had two primary purposes: (1) to provide a continuous record of lithologic variation, and (2) to tie core depths to seismic reflectors through the acquisition of reliable sonic velocities and calculation of a synthetic seismogram. Poor core recovery and relatively uniform gross lithology hampered sedimentological determination of lithologic variations; downhole logging has the potential of detecting subtle changes in lithology as well as placing the core in its proper stratigraphic position within the well when recovery was only partial. The wireline logs show good correlation with core data at most of the horizons. However, major changes observed in the logs at 259 and 406.5 mbsf are either not detected in the core or appear as subtle lithologic changes.

Two logging runs were planned: (1) LSS-DIL-GR-MCD and (2) LDT-CNTG-NGT-GPIT; however, only the first tool string (seismic-stratigraphy combination) was run. The focus of the first run was on velocity (LSS), approximate clay percentage (GR), porosity (DIL), and hole conditions (MCD and LSS). The tools and their function are described in "Explanatory Notes" chapter (this volume).

Operations

Logging-related operations began at 0130 local time on 4 February 1987, with lowering the bit, circulating, and pulling pipe to 108 mbsf. Because of past experience with sediment bridges (i.e., Leg 105), the sidewall entry sub was used.

At 1030 local time, the LSS combination tool was lowered at 2400 m/hr to 449 mbsf. The difference between this set-down depth and the deepest drill penetration of 484 mbsf implies the presence of a sediment bridge or caving above the hole bottom. The wireline heave compensator was then turned on and parameters were set up for the upward run. Recording of upgoing logs began at 440 mbsf at about 500 m/hr and ended approximately 10 m above seafloor. The interval through pipe and 10 m above mud line was logged for the purpose of calibrating log responses through pipe.

Initially, the sonic log was not recorded by the Schlumberger computer and after several attempts at fixing the hardware problem, the transit times (but not waveforms) were recorded from 290 mbsf to pipe (108 mbsf). The tool assembly was lowered to bottom again and the entire suite of logs was recorded from 440 to 290 mbsf to obtain a complete sonic log. Final rigdown concluded at 1845 on 4 February 1987.

Description of Measurements

The gamma ray curve provides a qualitative evaluation of clay or shale content because radioactive elements tend to concentrate in shales and clays (Borehole Research Group, 1985). The curve does not represent the percent clay in the sediment, but rather the ratio between sand and coarse silt and clay.

Sonic transit times are expressed by two curves: DT (8–10-ft spacing), and DTL (10–12-ft spacing) which has the deeper investigation depth of the two. Compressional velocities were calculated by taking the reciprocal of the sonic transit times.

Table 12. Summary of shipboard interstitial water data.

Leg, hole, core, section, interval (cm)	Depth (mbsf)	Volume (mL)	pH	Alk. (meq/L)	Sal. (g/kg)	Mg (mmol/L)	Ca (mmol/L)	Cl (mmol/l)	SO_4 (mmol/l)	PO_4 (μmol/L)	K (mmol/L)	NH_4 (mmol/L)	SiO_2 (μmol/L)	Mg/Ca
113-693A-														
2R-4, 145–150	8.45	56	7.90	3.90	34.5	50.73	10.65	577.6	28.6	4.3	11.8	0.10	433	4.76
4R-3, 120–125	26.10	60	7.83	3.56	35.0	50.42	10.59	577.5	27.7	5.1	11.8	0.17	639	4.76
6R-4, 120–125	46.80	55	7.76	3.49	35.0	46.98	14.10	579.5	27.8	4.0	11.3	0.26	803	3.33
9R-4, 120–125	75.80	62	8.10	3.75	34.5	44.77	15.37	569.9	25.1	4.4	10.1	0.09	1053	2.91
12R-4, 120–125	104.60	65	8.15	3.88	34.3	43.08	17.07	571.9	25.6	4.2	8.3	0.27	880	2.52
18R-3, 120–125	161.10	45	8.19	3.36	34.3	41.87	18.00	579.0	22.7	4.4	7.8	0.20	904	2.33
25R-2, 120–125	227.30	50	8.07	3.32	34.3	38.89	17.73	581.5	20.3	3.1	7.4	0.29	1000	2.19
113-693B-														
2X-3, 145–150	238.25	35	8.03	2.79	33.7	40.30	17.16	563.9	21.3	2.9	7.7	0.28	1100	2.35
113-693A-														
28R-3, 120–125	257.80	45	8.10	3.14	34.0	38.97	17.12	572.9	19.3	3.1	7.7	0.22	933	2.28
113-693B-														
6X-4, 145–150	273.75	25	7.98	2.99	34.0	37.43	17.42	561.0	18.6	2.3	8.0	0.36	1370	2.15
9X-3, 120–125	301.00	30	8.24	3.19	33.9	37.87	17.10	561.9	19.1	2.0	7.8	0.31	1200	2.21
12X-3, 120–125	330.00	45	7.76	2.27	33.5	37.83	16.72	562.4	17.8	2.5	7.5	0.24	1300	2.26
15X-2, 140–150	357.60	40	8.34	3.45	34.0	38.06	16.71	563.4	18.1	1.7	7.8	0.33	1035	2.27
113-693A-														
40R-2, 138–142	371.78	30	8.16	3.02	33.9	35.87	16.98	557.7	17.2	2.6	7.8	0.87	1020	2.11
113-693B-														
17X-1, 145–150	375.45	27	8.28	2.83	34.5	36.94	16.85	567.8	17.2	1.7	7.8	0.35	950	2.19
19X-2, 140–150	396.30		8.20	3.55	33.9	36.77	17.39	565.4	16.9	1.5	7.3	0.32	995	2.19
113-693A-														
48R-2, 120–125	448.10	20	8.16	2.83	32.5	27.27	16.15	519.5	16.0	1.8	6.3	0.62	394	1.69
Mud filtrate (from mud pit)			9			2.14	3.37	141.2	13.1	8.9	1.6	0.52	529	0.64
[a]48R-2, 120–125	448.10	20				30.21	17.64	563.9	16.3	1.0	6.9	0.63	378	1.71

[a]Corrected for the presence of mud filtrate.

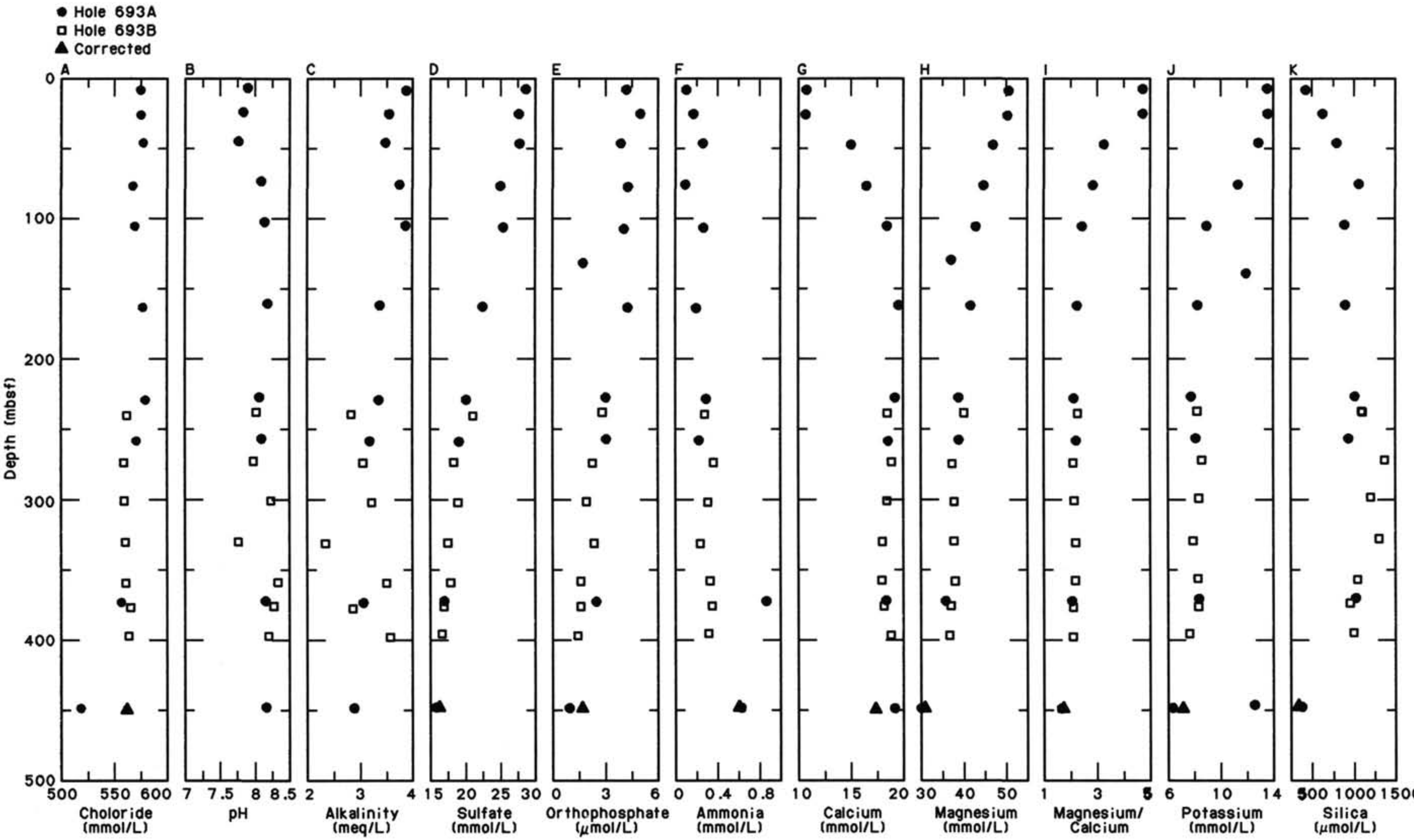

Figure 38. Concentrations vs. depth for Holes 693A and 693B. A. Chloride. B. pH. C. Alkalinity. D. Sulfate. E. Orthophosphate. F. Ammonia. G. Calcium. H. Magnesium. I. Magnesium/calcium ratio. J. Potassium. K. Silica.

Table 13. Subdivision of the drilled section on the basis of Rock-Eval data, Hole 693A.

				Average values		
Unit	Cores	Depth (mbsf)	Age	TOC (%)	Hydrogen index	T_{max}
1	1R-40R	0-370	[a]Cenozoic	0.17	[b]	551
2	44R-45R	407-427	Cretaceous	0.38	49	542
3	46R-50R	427-465	Cretaceous	2.56	100	414
4	51R	465-475	Cretaceous	1.23	75	406

[a] Base of Cenozoic approximately 397 mbsf.
[b] Values are scattered. Instrument is at limit of utility at 0.1% carbon.

Resistivity logs express the resistivity of the formation at three different depths (flushed, invaded, and virgin zone). Apparent porosities, which are calculated on the assumption that the sediments are shale-free (Doveton, 1986), were derived from the resistivity log. The porosity values are only estimates because of the fairly high clay content in Hole 693A and are used only to illustrate relative variations in porosity downhole.

Interpretation

A total of 331 m of usable open-hole logs was obtained, spanning the interval 108-439 mbsf. The caliper log indicated good hole conditions along the entire length except for the bottom 35 m. All logs were of very good quality.

Comparison of downhole logs from Hole 693A with the lithostratigraphic succession determined by the smear slides suggest certain correlations can be made. The gamma ray log shows little variation between drill pipe (108 mbsf) and 155 mbsf except for several short wavelength (< 3 m) decreases and then does not change significantly to 247 mbsf (Fig. 39). This interval corresponds to Subunit IIIA, a silty to clayey diatom-bearing mud. At 247 mbsf, a small decrease is observed on the gamma ray trace, which probably correlates with a lithologic change to a clayey nannofossil diatom ooze (Subunit IIIB) at this same depth.

The largest change in log responses in Hole 693A occurs at 259 mbsf. The gamma ray, resistivity, and sonic logs all show considerable baseline shifts, but the log responses do not appear to correlate with a major lithologic change in the core. The lithologic unit at this interval (Subunit IIIC, 258-325 mbsf) has been identified as being similar to Subunit IIIA and consists of diatom mud and silty to clayey diatom-bearing muds. The gamma ray log shows this unit to be higher in clay content and with less character variability then Subunit IIIA.

The deformed sediment sequence (Unit V) observed from 345 to 397 mbsf is identified on the logs by a downhole increase in clay content, a slight increase in resistivity, and a decrease in porosity (Fig. 22) and travel times (sonic log). The interval from 400.5 to 406.5 mbsf is marked by a sharp decrease in gamma ray, a major increase in porosity, and a decrease in velocity and resistivity. Sediment recovered at this interval from Hole 693A was identified as drilling-induced graded sand (see "Lithostratigraphy" section, this chapter) and in Hole 693B as radiolarian diatomite.

Another distinct boundary is identified on the logs at 406.5 mbsf by a moderate increase in the gamma ray response (Fig. 39) and a sharp increase in velocity (Fig. 23). No corresponding change was noted in the core from 406.5 to 416 mbsf. Below 416 mbsf, velocities decrease, averaging 1.95 km/s, but have high-amplitude, short-wavelength (< 3 m) variations that seem to correspond to changes in clay content, but have no obvious correlation with core data, possibly because of low core recovery between this depth and the end of the logged interval (440 mbsf).

A synthetic seismogram for Site 693 was generated from the sonic log using a constant density value (Fig. 40). A 25-Hz zero-phase Ricker wavelet was used in the convolution; this wavelet is approximately correct for comparison to a nearby multichannel line.

Table 14. Rock-Eval Data, Hole 693A.

Core, section interval (cm)	Depth (mbsf)	S_1 mg(HC)/g(sed) at 300°	S_2 mg(HC)/g(sed)	S_3 $mg(CO_2)/g/(sed)$	TOC (%)	HI mg(HC)/g(C)	OI $mg(CO_2/gC$	T_{max} (°C)
113-693A-								
4R-3, 120-125	26.1	0.01	0.05	0.86	0.25	20	344	594
6R-4, 120-125	46.8	0.01	0.64	0.64	0.10	640	640	585
9R-4, 120-125	75.80	0.02	0.22	1.04	0.16	137	650	547
12R-4, 120-125	104.60	0.03	0.22	1.40	0.20	110	700	560
15R-1, 146-150	129.26	0.04	0.48	0.00	0.10	480	0	463
19R-5, 32-36	172.92	0.06	0.34	1.12	0.23	148	487	590
25R-2, 117-120	227.27	0.08	0.33	1.05	0.22	150	477	584
28R-3, 120-125	257.8	0.10	0.89	0.78	0.05	(1780)	(1560)	595
40R-2, 135-138	371.75	0.03	0.07	0.20	0.19	37	105	443
44R-1, 77-77	407.47	0.06	0.64	0.00	0.32	200	0	548
45R-1, 56-58	417.06	0.05	0.20	0.00	0.43	47	0	535
46R-1, 21-23	426.31	0.20	2.06	1.10	2.11	98	52	409
46R-1, 82-84	426.92	0.11	2.68	0.42	2.48	108	17	416
47R-2, 78-80	437.98	0.18	3.63	1.28	2.64	138	48	408
47R-2, 119-120	438.39	0.07	1.84	0.37	2.04	90	18	412
48R-1, 79-80	446.19	0.09	2.23	0.67	2.07	107	32	420
48R-2, 125-129	448.15	0.16	4.42	1.93	3.22	137	60	420
48R-3, 83-84	449.23	0.11	2.17	1.83	2.51	86	73	412
48R-4, 58-61	450.48	0.13	3.74	0.85	2.70	139	31	418
48R-4, 72-74	450.62	0.15	3.05	0.87	2.37	129	37	416
49R-1, 44-45	455.44	0.14	2.91	1.03	2.97	98	35	409
49R-2, 112-114	457.62	0.08	1.98	1.27	2.60	76	49	415
50R-1, 40-42	465.20	0.10	1.98	1.27	2.05	97	62	413
50R-1, 53-55	465.33	0.10	1.88	1.56	3.15	60	50	412
50R-2, 51-53	466.81	0.08	0.96	1.14	2.99	32	38	409
51R-1, 40-42	474.70	0.05	0.46	0.54	0.82	56	66	400
51R-1, 147-150	475.70	0.04	0.79	0.13	0.94	84	14	410
51R-2, 25-26	476.05	0.36	1.64	0.71	1.94	85	37	409

Table 15. Headspace analyses of light hydrocarbons, Site 693.

Core, section interval (cm)	Depth (mbsf)	Methane	Ethane	Propane	iC_4	n-C_4	iC_5	n-C_5	iC_6	n-C_6
		(microliters (gas)/liter (sed))								
113-693A-										
2R-4, 145–150	8.45	2.14	—	1.1	—	0.2	—	—	—	—
4R-3, 120–125	26.1	5.1	0.5	1.5	—	—	—	—	—	—
6R-4, 120–125	46.80	10.90	1.6	0.9	—	—	—	—	—	—
9R-4, 120–125	75.80	10.3	2.9	1.0	0.4	0.4	—	—	—	—
12R-4, 120–125	104.6	11.4	2.7	1.2	0.5	0.2	—	—	—	—
15R-2, 146–150	130.76	4.1	0.7	0.1	0.1	—	—	—	—	
18R-3, 120–125	161.1	3.3	0.9	3.1	1.1	1.7	tr	tr	—	—
19R-4, 69–73	171.79	2.8	0.9	0.4	0.1	0.1	—	—	—	—
19R-5, 32–36	172.92	2.1	0.7	4.0	0.2	0.1	—	tr	—	—
25R-2, 117–120	227.27	11.5	3.3	1.2	1.8	0.4	—	tr	—	—
28R-3, 120–125	257.80	10.2	5.3	6.4	0.6	0.9	—	—	—	—
40R-2, 135–138	371.75	9.9	7.7	4.3	0.5	1.3	tr	tr	tr	tr
44R-1, 76–77	407.46	11.2	tr	tr	—	—	—	—	—	—
46R-1, 82–84	417.06	17.6	11.1	6.6	0.9	2.6	0.4	0.6	—	—
47R-2, 78–80	426.92	16.1	15.4	9.3	1.6	4.2	tr	0.7	tr	tr
48R-2, 125–129	437.98	17.6	13.2	7.8	0.5	1.9	0.4	0.5	0.3	0.5
48R-4, 72–74	448.15	62.8	22.5	14.3	2.2	7.1	0.6	0.9	0.4	0.9
49R-2, 112–114	449.62	16.9	16.2	9.7	1.3	3.2	0.3	0.3	—	—
50R-1, 40–42	465.20	12.5	13.1	7.2	1.2	2.9	0.6	0.7	—	—
50R-1, 53–54	465.33	20.6	20.7	10.4	1.0	3.1	0.5	0.5	tr	tr
51R-1, 40–42	474.70	9.9	6.3	3.3	0.3	1.3	0.3	0.3	—	—
51R-1, 147–150	475.79	6.0	4.9	3.1	0.2	0.7	tr	tr	—	—

SUMMARY AND CONCLUSIONS

Site 693 is located on a midslope bench on the eastern, Dronning Maud Land margin of the Weddell Sea. It lies on the main, northwest-facing slope of the bench, at 70°49.892′S, 14°34.410′W at 2359 m water depth, about 10 km southwest of the outer rim of Wegener Canyon and 30 km west of Sites 691 and 692. Site 693 had the same objectives as Sites 691 and 692, to sample the record of Late Cretaceous and Cenozoic cooling of the East Antarctic continent. The site was proposed and approved *during* the drilling of Site 692, when Lower Cretaceous sediments were recovered there at an unexpectedly shallow depth; a major revision of the regional seismic stratigraphy was required, and none of the existing alternate sites could promise a thick post-Aptian accumulation.

Site 693 was located at CDP 880 on multichannel profile BGR86-07, and tied to the main body of multichannel data using *JOIDES Resolution's* single channel water-gun profiler. The stratigraphic level reached in Hole 692B appeared to lie as deep as 900 mbsf at Site 693, giving reasonable prospects of a thick Cenozoic section.

Two holes were drilled at Site 693 in 7 days, 20 hr. Hole 693A was rotary-drilled, because we feared to encounter the concentration of cobbles and pebbles found at Sites 691 and 692. The hole penetrated to 483.9 mbsf; we recovered 213.5 m (44.1%) in 51 cores and ended drilling when a conclusive Early Cretaceous (Albian-Aptian) age for the lowest unit had been established. One logging run (gamma, resistivity, sonic, caliper) was made to 446 mbsf in Hole 693A, with the bottom of the pipe at 108 mbsf. Hole 693B was washed to 233.8 mbsf and then continuously cored (2 APC and 16 XCB cores) to 403.1 mbsf (169.3 m cored, 92.16 m, 54.5% recovered) to improve on the core quality and recovery achieved over that depth range in Hole 693A.

The section at Site 693 consists of 398 m of Pleistocene to lower Oligocene hemipelagic muds and 86 m of Lower Cretaceous claystones, mudstones, diatomite, and limestone. Seven lithostratigraphic units are recognized.

Unit I: 0.0–12.2 mbsf, middle to upper Pleistocene foraminifer-bearing clayey mud.

Unit II: 12.2–31.4 mbsf, upper Pliocene to lower Pleistocene clayey mud.

Unit III: 31.4–325.8 mbsf, upper Oligocene to upper Pliocene diatom mud and silty to clayey diatom-bearing mud, divided into three subunits, with an 11.2-m-thick upper Miocene clayey diatom nannofossil ooze separating two thicker subunits consisting of the main lithologies.

Unit IV: 325.8–345.1 mbsf, upper Oligocene alternating diatomaceous mud and ooze and minor muddy nannofossil ooze and nannofossil-bearing clayey mud.

Table 16. Comparison of light hydrocarbon compositional ratios, Holes 693A and 692B.

Core, section	Depth (mbsf)	Methane/ ethane	n-butane/ isobutane	n-pentane/ isopentane
113-693A-				
2R-4	8.45	—	—	—
4R-3	26.10	10.9	—	—
6R-4	46.8	6.8	—	—
9R-4	75.80	3.6	1.0	—
12R-4	104.6	4.2	0.4	—
15R-2	130.76	5.8	—	—
18R-3	161.10	3.7	1.5	—
19R-4	171.79	3.1	1.0	—
19R-5	172.92	3.0	0.5	—
25R-2	227.27	3.5	0.2	—
28R-3	257.8	1.9	1.5	—
40R-2	371.75	1.3	2.6	—
44R-1	407.46	—	—	—
46R-1	417.06	1.6	2.9	1.5
47R-2	426.92	1.0	2.6	—
48R-2	437.98	1.3	3.8	1.3
48R-4	448.15	2.8	3.2	1.5
49R-2	449.62	1.0	2.5	1.0
50R-1	465.20	1.0	2.4	1.2
50R-1	465.33	1.0	3.1	1.0
51R-1	474.70	1.6	4.3	1.0
51R-1	475.79	1.2	3.5	—
113-692B-				
7R-1	54.13	7.9	—	—
8R-2	60.99	7.0	1.1	—
9R-1	70.23	1.1	0.8	—
11W-1	87.0	—	0.6	—
12R-1	89.51	5.7	0.5	—

Table 17. Gas chromatographic retention times, GC1, DC200 column.

Natural gas		Unknown, Core 113-693B-19X-4	
	(min)		(min)
Methane	1.92	Methane	1.92
Ethane	2.44	Ethene?	2.56
Propane	3.25	Propene?	3.16
Isobutane	4.12	Isobutene?	4.08
n-butane	4.91	I-butene?	4.69

Unit V: 345.1-397.8 mbsf, upper lower Oligocene diatomaceous mud and silt, with subordinate muddy diatomaceous ooze, thickened and deformed by slumping.

Unit VI: 397.8-409.0 mbsf, Aptian?-Albian radiolarian diatomite.

Unit VII: 409.0-483.9 mbsf, Aptian?-Albian dark organic-rich terrigenous claystones and mudstones.

Sedimentation rates were moderate (~10 m/m.y.) in the Pleistocene and latest Pliocene, high (20-46 m/m.y.) through the Pliocene and late Miocene, and low (~7 m/m.y.) in the early Miocene and Oligocene with the exception of the slumped interval in the lower Oligocene. Cretaceous rates are unknown. A hiatus at 262 mbsf extends over about 6-7 m.y. of the lower upper and middle Miocene. A second hiatus may be present at about 343 mbsf and extend across the boundary between upper and lower Oligocene. A third hiatus at 398 mbsf covers the Upper Cretaceous, Paleocene, and Eocene and extends into the lower Oligocene, a period of about 60 m.y.

Glacial dropstones of all sizes up to the core diameter occur in Units I, II, and III. In Units I and II some are manganese-coated. They become much less common and some are weathered in Units IV and V, and they were not recovered in the Cretaceous. The sand-sized fraction changes character through the Cenozoic section: down to 190 mbsf (Pleistocene to uppermost Miocene), the sand is unsorted, from 240 to 340 mbsf (lower upper Miocene to upper Oligocene) it is mainly very fine, well-sorted sand with a coarse tail fraction, and below 340 mbsf (upper to lower Oligocene) the coarse grains form a smaller, separate group. This probably reflects a downward diminution in the importance of the ice-rafted component, particularly close to the middle Miocene hiatus but continuing to greater depth. The terrigenous component dominates the sand-sized fraction except for Unit I, and its composition is relatively unchanged downcore, except for increased brown mica and glauconite in the lower Oligocene, and prominent volcanic glass and feldspar in the Quaternary. The upper part of Unit VII contains as much as 20% glauconite.

Clay minerals also vary significantly through the sequence. Illite is the dominant clay mineral in all of the Cenozoic sediments. In the top 265 m, the less-important kaolinite, chlorite, and smectite alternate irregularly. In the underlying lower Miocene and Oligocene sediments, chlorite is rare or absent and smectite less important. In contrast, smectite occurs almost to the exclusion of all other clay minerals in the Cretaceous sediments.

The biogenic component of the sediments is almost completely siliceous, mainly diatomaceous. Siliceous microfossils are few and poorly preserved or absent in the uppermost 40 m (upper Pliocene and Quaternary), few and poorly to well-preserved between the hiatuses at 262 and 398 mbsf (Oligocene and lower Miocene), but are common to abundant and poorly to moderately well-preserved in the upper Miocene and lower Pliocene (40-265 mbsf). In this last interval, above the younger hiatus, siliceous biogenic sedimentation rates equal those on Maud Rise. Oligocene and lower Miocene diatom assemblages include ben-

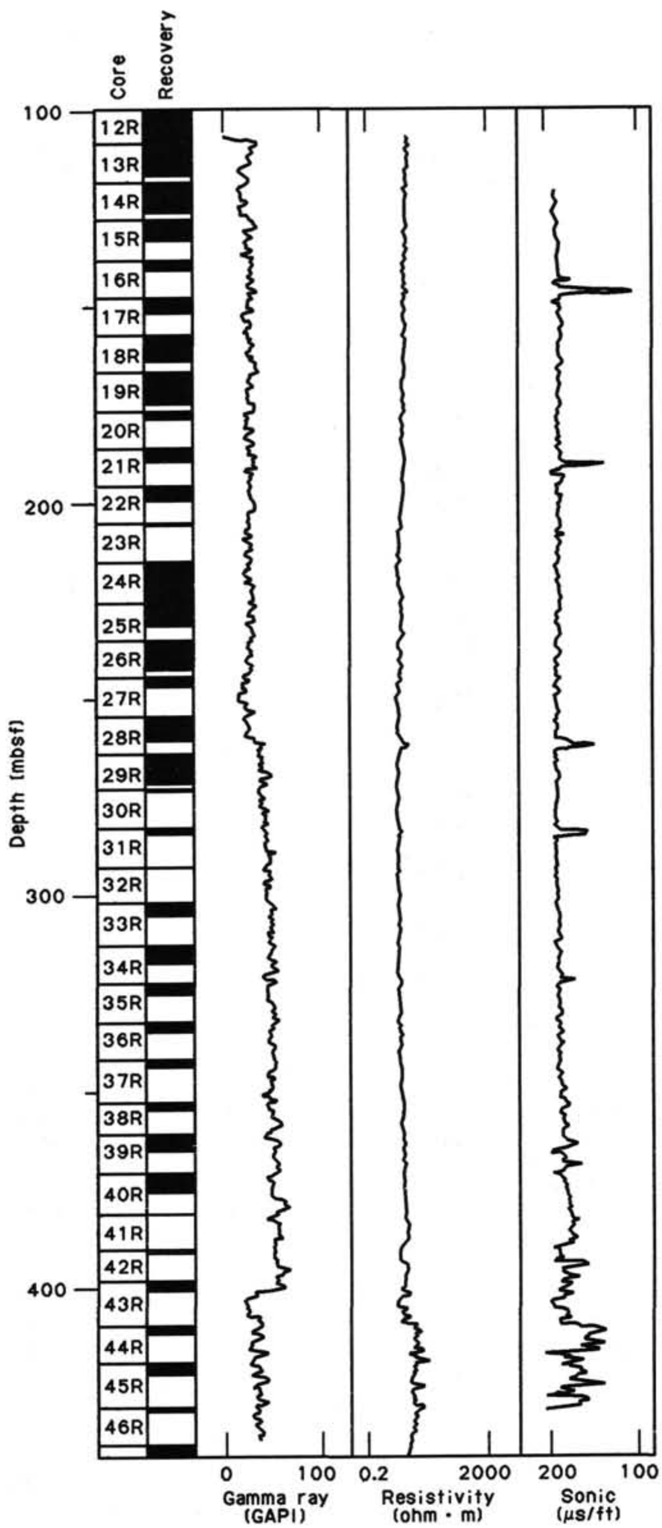

Figure 39. Gamma ray, resistivity, and sonic slowness logs for the open-hole interval at Site 693A. Core recovery (black bars) shown for comparison.

thic forms, indicating areas of shallow continental shelf lacking a permanent ice cover. Siliceous microfossils are also abundant and moderately to well-preserved in the Cretaceous sediments below 398 mbsf, and may represent some of the oldest known diatomite.

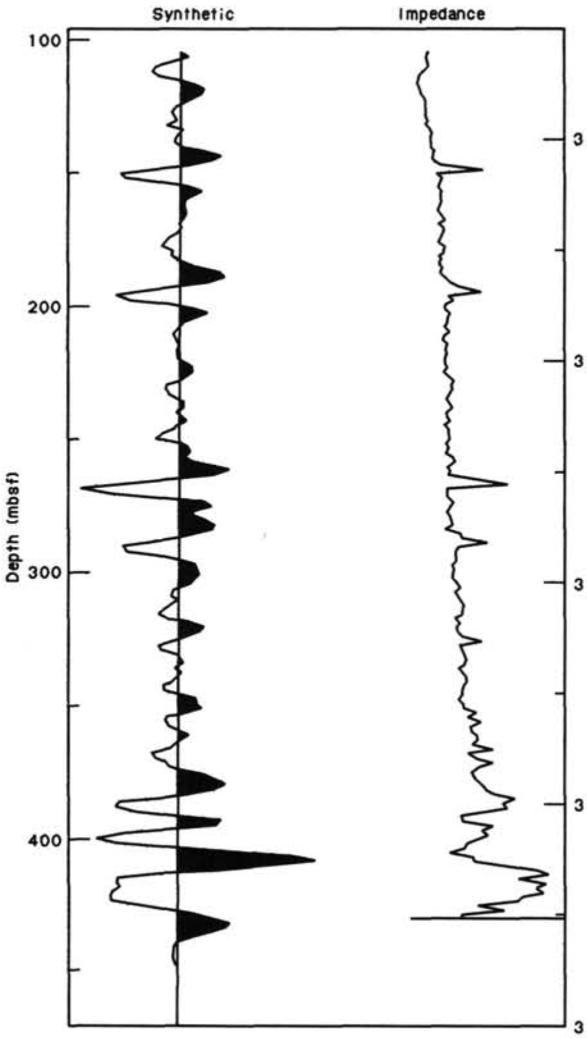

Figure 40. Synthetic seismogram for Site 693 based on a sonic log for the interval 108.8–434.9 mbsf. The synthetic seismogram is based on a *Conrad* model and an estimate of the *JOIDES Resolution* wavelet. Relative times are accurately determined from the sonic log. Absolute times are based on the assumption that the largest reflection on the synthetic seismogram corresponds to the peak observed on the seismic section in Figure 28. The scale for both the synthetic seismogram and impedance log is arbitrary.

Calcareous microfossils occur only rarely within the section. Benthic and planktonic foraminifers are found in the upper Quaternary, and the latter occur with nannofossils in one upper Miocene interval. Otherwise, Neogene sediments are virtually barren of calcareous forms. Indeed, foraminifers from the surficial sediments are useful indicators of downhole contamination. All three calcareous groups are poorly to well-preserved in thin muddy nannofossil ooze and nannofossil-bearing mud interbeds of Unit IV (upper Oligocene). The benthic foraminifers include both bathyal to abyssal and probably neritic forms, and the interbeds in this unit may be turbidites. Also, all three groups occur in two cores of the Albian-Aptian lithostratigraphic Unit VII, for which the benthic foraminifers indicate a depth of deposition of approximately 500 m. Both the planktonic and benthic foraminifers in the Albian-Aptian(?) show greater affinities with southeast Indian Ocean or Tethyan than with Falkland Plateau or Southwest Indian Ocean faunas. The dinoflagellate-dominated palynoflora of Unit VII, however, correspond well to Lower Cretaceous floras from the Falkland Plateau (Ludwig, Krashenninikov, et al., 1983).

The NRM magnetostratigraphy of the upper 140 m at Site 693 is well established. Coring disturbance and imperfect recovery affect the deeper section, but a stratigraphy for Units IV and V should emerge from post-cruise investigations. The Cretaceous sediments, like those at Site 692, appear normally magnetized and stable, and should yield an Early Cretaceous latitude for the site.

Compared with the Berriasian-Valanginian(?) sediments of Site 692, the Albian-Aptian(?) sediments at Site 693 are more oxidized, and their organic carbon content is lower. Normalized to organic carbon, the quantities of light hydrocarbons are higher at Site 693 (although still low), suggesting some hydrocarbon migration. Traces of hydrocarbons occur in the Cenozoic section also, perhaps transported in soft-sediment glacial dropstones.

The cored section and the reflection profiles were correlated using the sonic log: shipboard physical properties measurements were of little value because of the disturbed nature of the cores, particularly in the uppermost 400 m of Hole 693A. The middle Miocene hiatus at 262 mbsf and, less easily, the Albian-Aptian/Oligocene hiatus at 398 mbsf, could be identified and traced away from the site. The post-middle Miocene section is confined to the main northwest-facing slope of the midslope bench, and is nowhere much thicker than at Site 693. The basal sediments of this younger section onlap upslope from the site. Farther upslope, the younger section is missing completely where the slope is dissected (probably by a tributary of Wegener Canyon). Similarly, there is no great sediment thickness above the Albian-Aptian/Oligocene unconformity anywhere near the site; more than 90% of the sediments overlying basement on this margin appear to be Lower Cretaceous and older. On adjacent seismic profiles the Albian-Aptian/Oligocene unconformity can be correlated with the boundary between seismic sequences WS-1 and WS-2, which has been traced over the entire margin by Hinz and Krause (1982). If this identification is correct, then post-Lower Cretaceous sediments on the Dronning Maud Land margin only rarely exceed 1 km in thickness, except beneath the continental shelf.

Using these insights we can assess the history of deposition on this margin. Assuming a Middle or Late Jurassic age for basement (WS-4, the seaward-dipping reflector province beneath unconformity U9 of Hinz and Krause, 1982), long-term average sedimentation rates in the Jurassic and Early Cretaceous were 20 to 40 m/m.y. These rates are similar to those found for shorter intervals on the Falkland Plateau, which at this time was not far away. The Falkland Plateau sediments indicate conditions of intermittent anoxia, as might accompany weak circulation in a restricted basin or reflect a mid-water oxygen minimum zone in a region of high biogenic productivity. On the Falkland Plateau such sediments are Kimmeridgian (or Tithonian to Oxfordian) and Barremian to Aptian or lower Albian: it is thought that deposition on the Falkland Plateau was interrupted by uplift associated with the initial opening of the South Atlantic in the Earliest Cretaceous.

There are differences in composition between sediments from the Falkland Plateau and the equivalent strata at Sites 692 and 693. There is no volcanogenic component in the Lower Cretaceous sediments of the Falkland Plateau and a lesser terrigenous component; the Aptian-Albian sediments on the Falkland Plateau have calcareous rather than mainly siliceous microfossils. Nevertheless, similar intermittently anoxic or weakly aerobic conditions, from whatever cause, governed the deposition of the Berriasian-Valanginian(?) sediments at Site 692 and (to a lesser extent) the Albian-Aptian sediments at Site 693. The Dronning Maud Land margin was more remote from the influence of South Atlantic opening, so deposition may have been more continuous than on the Falkland Plateau (although the volcanic component at Site 692 shows some local tectonism and there is a prominent angular unconformity deeper in the section on line BGR78-019). It seems at least possible, if not probable, that the entire Lower Cretaceous and Upper Jurassic section beneath Sites 692 and 693 was deposited under similar, intermittently anoxic conditions.

During the Albian-Aptian, conditions in the region began to change. Unit VII does not contain the ash laminae and calcareous lenses of the Lower Cretaceous sediments of Site 692, and the organic material is more oxygenated. Unit VII represents a more restricted environment than Albian-Aptian sediments on the Falkland Plateau, and the different faunal affinities of the foraminifers suggest that the two localities were by then separated in some way (by land or deep water). The Cretaceous sediments at Site 693, however, show an upward increase in the degree of oxygenation, and in the upper part glauconite is common. The essentially different composition and floral and faunal assemblages of the overlying diatomites of Unit VI imply a change from earlier rapid deposition of dominantly terrigenous sediment to a slow, mainly pelagic or hemipelagic depositional regime.

We may only speculate about conditions on this margin between the Albian-Aptian and the early Oligocene. Using the reflection profiles, the erosional hiatus at 398 mbsf at the site can be correlated with the WS-1/2 sequence boundary of Hinz and Krause (1982), which is an erosional unconformity over most of the Dronning Maud Land margin. At the site, the unconformity has an erosional appearance, and the reflection profiles suggest there is no thick Upper Cretaceous or Paleogene sediment sequence either above or below it in the vicinity. However, it is not necessarily correct to assume that this absence is a result of the erosion that created the Albian-Aptian/Oligocene hiatus. The application of a range of relations between physical properties of sediments and their depth of burial at Site 692 (see "Physical Properties" section, "Site 692" chapter, this volume) suggests that the overburden removed from the Aptian claystones of Unit III did not exceed 250–300 m. A similar application to the Albian-Aptian sediments of Unit VII at Site 693 (W. F. Bryant, pers. comm., 1987) found no evidence of burial to greater than their present (410–480 m) depth. More regionally, there is minimal topography on the WS-1/2 sequence boundary, and near-conformity between reflectors above and below it. It seems more appropriate to think in terms of a thin, slowly deposited Upper Cretaceous and Paleogene sequence on this margin than in terms of a regime of rapid deposition to 300 m followed by erosion, repeated several times.

The deposition of 300 m over 60 Ma, the length of the Albian-Aptian/Oligocene hiatus at Site 693, gives an average sedimentation rate of 5 m/m.y. This is a typical open-ocean pelagic or hemipelagic rate, and if correct would classify this as a starved margin. Interestingly, the rate is similar to the 7 m/m.y. of lower Miocene and Oligocene deposition, which included ice-rafted material. Thus, in terms of sediment loading on the margin, the Oligocene and lower Miocene may not have been very different from earlier periods.

This brings us to consideration of the nature and cause of the Lower Cretaceous–middle lower Oligocene hiatus. The reflection profiles show it to have been mildly erosional in most places, rather than merely nondepositional. The low and similar sedimentation rates inferred before and observed after this erosional episode would suggest in turn that the hiatus did not result from a fundamental change in the rate of sediment supply. More probably it was caused by an increase in the vigor of deep and intermediate water circulation, such as that generally associated with the Eocene-Oligocene boundary. This phenomenon has been held responsible for hiatuses in deep-sea sedimentation worldwide (North Atlantic, Miller and Tucholke, 1983; South Atlantic, Barker, Carlson, Johnson, et al., 1983; Hsü, LaBrecque, et al., 1984; Indian and South Pacific, Moore et al., 1978; Van Andel et al., 1976) and is usually associated with the formation of cold bottom waters (Benson, 1975; Savin et al., 1975; Shackleton and Kennett, 1975) in high southern latitudes. A hiatus ending in the lower Oligocene was found at Site 690, and a lowermost Oligocene episode of increased bottom current activity near Site 689 could be inferred from the reflection profiles. The hiatus at Site 693 is altogether more extensive and deeply erosional than either of these, but this may reflect the location of the site on a sloping margin, at the edge rather than toward the center of a gyre.

If the formation of sea-ice around the Antarctic margin began in the earliest Oligocene (e.g., Shackleton and Kennett, 1975), then the Oligocene and early Miocene depositional environment was probably very different from environments before, although sedimentation rates remained low. Ice-rafted debris is found in the Oligocene and lower Miocene sediments, implying some transport by ice, but less abundantly than in younger sediments. Many of the dropstones are weathered, suggesting that the superficial deposits of a pre-glacial terrain are being eroded. Benthic diatoms are also found, suggesting areas of shallow (maximum 50 m?) water depth lacking permanent shelf-ice cover upslope from Site 693 (rather than the deep ice-covered Antarctic shelf of the present day). The dominance of illite among the clay minerals in Oligocene and lower Miocene sediments reflects the dominance of physical over chemical weathering processes on the continent, as might be expected of a glaciated terrain. The common occurrence of kaolinite in Oligocene sediments, however (but not commonly in younger sediments), may result from the erosion of deeply weathered relict soils during the early stages of glaciation.

During the Oligocene and early Miocene, Site 693 (then close to its present depth) most unexpectedly remained below the CCD for all but a few brief intervals (and some of these may be illusory, the sediments concerned being possibly turbiditic). This contrasts with Maud Rise, where calcareous sediments were recovered from most of the Oligocene and lower Miocene section. The CCD may have been elevated along this margin because calcareous biogenic productivity had been reduced by lower temperatures in the upper water masses, or because intermediate waters had become more oxygen-rich. Like the absence of ice-rafted debris in coeval sediments on Maud Rise, this difference may reflect the movement of cold surface waters and ice around the southern edge of the Weddell Gyre of the time, with Maud Rise being more probably in the return path of warmer waters from the north. This contrast persists to the present day, at least in the abundance of icebergs and the extent of seasonal pack-ice cover.

The early middle Miocene is conventionally regarded as a time of renewed cooling, and of major expansion of the East Antarctic ice-sheet. The hiatus which spans the middle Miocene (about 16–9 Ma) at Site 693 may be related to this change. The diatom-rich hemipelagic sediments that overlie the hiatus show rates of deposition which increase sharply toward the lower Pliocene, reducing gradually into the upper Pliocene and Pleistocene. There is no noticeable upper Miocene hiatus but, otherwise, the siliceous biogenic sedimentation closely resembles that on Maud Rise, with an acme of preservation and abundance in the lower Pliocene. Ice-rafted detritus is common in these sediments, and the dominant clay mineral is illite, reflecting the physical nature of the erosional regime. As on Maud Rise, calcareous sediments are essentially confined to the Quaternary, and Quaternary sedimentation rates are low.

Drilling at Sites 691 and 692 placed limits on the age of Wegener Canyon. By the early late Miocene or before, the canyon had cut down to the present shoulder (Site 692), leaving behind a coarse gravel lag (the cobbles and pebbles of Unit II). Subsequently, perhaps after having breached the outer high of "Explora Wedge," a steep inner canyon formed (Site 691). The terrigenous sediments being transported down Wegener Canyon from the Antarctic shelf to the Weddell Basin bypass the main midslope bench where Site 693 is located. At most, some of the fine fraction of such turbidity flows will become entrained in the contour-following currents running southwest along the margin, and be redeposited at Site 693. The terrigenous component of the upper Miocene and Pliocene sediment deposited at Site 693 is uniform in composition and almost completely hemipelagic and ice-rafted, with steady increase in the ice-rafted component through time and much higher rates of deposition than previously. The nature and uniformity of this terrigenous component is compatible with the theory that Wegener Canyon formation began in the late middle Miocene, as the East Antarctic glaciation deepened and the supply of sediment to the margin started to increase.

It has been argued (Kennett, 1986) that the earliest phase (16–14.6 Ma, corresponding to about 15–13.5 Ma at Berggren et al.'s (1985) time scale) of renewed climatic deterioration in the middle Miocene (as indicated by ^{18}O enrichment in benthic foraminifers) resulted from a cooling of high-latitude, bottom and intermediate waters, with the later (14.6–13.2 Ma) formation of an extensive ice sheet. At Site 693, middle Miocene sediments are absent, and the reflection profiles show that the hiatus in deposition extends to younger ages upslope. This suggests a contour-current-controlled depositional regime, as does the high hemipelagic component of the upper Miocene sediments above the hiatus. Some caution is needed, however, in inferring regional changes in circulation strength in the middle Miocene, since deposition appears continuous in this interval on Maud Rise. Nevertheless, the sedimentary record at Site 693 suggests an initial, early middle Miocene invigoration of circulation, slackening only in the early late Miocene (about 10 Ma) when deposition was renewed. The record suggests that East Antarctic glaciation continued to increase through the late Miocene and Pliocene, which according to oxygen isotopic data (e.g., Kennett, 1986) were periods of comparative climatic stability. Site 693 provides no evidence for a major deglaciation of the East Antarctic continent since the middle Miocene, including the early Pliocene for which there is a high-resolution record.

The high sedimentation rate of the lower Pliocene is partly produced by an increase in the siliceous (diatom) productivity, which equals that found on Maud Rise. Higher rates of siliceous biogenic sedimentation during the early Pliocene are also seen near the Polar Front (Site 514: Ludwig, Krasheninnikov, et al., 1983), and higher rates of calcareous biogenic productivity occur in the South Pacific near the Subtropical Divergence during the same interval (Kennett, von der Borch, et al., 1986). It will be important to pursue this enigma in post-cruise investigation of Leg 113 sediments.

A further step in the intensification of Antarctic glaciation probably occurred in the late Pliocene and Quaternary (2.5 Ma to the present). Low biosiliceous productivity and poor preservation may reflect increased sea-ice extent around Site 693. The reduced rate of terrigenous sedimentation is difficult to understand, but may result from the permanent grounding of the ice shelf to the continental shelf edge along much of the East Antarctic margin to the east (upcurrent) of Site 693 (Grobe, 1986).

A principal aim of drilling at this margin was to examine the record of latest Cretaceous and Paleogene cooling of the Antarctic continent before glaciation developed. Unfortunately, despite our efforts to find a site where these sediments might exist, this important question remains unanswered. The next opportunity appears to be at Prydz Bay, on Leg 119. Partial compensation for our failure, however, comes with the discovery of Cretaceous diatomite and black shale deposits, which extends significantly our knowledge of Mesozoic environments in the Antarctic region.

REFERENCES

Barker, P. F., Carlson, R. L., Johnson, D. A., et al., 1983. *Init. Repts. DSDP*, 72: Washington (U.S. Govt. Printing Office).

Benson, R. H., 1975. The origin of the psychrosphere as recorded in changes of deep sea ostracode assemblages. *Lethaia*, 8:69–83.

Berggren, W. A., Kent, D. V., Flynn, J. J., and Van Couvering, J. A., 1985. Cenozoic geochronology. *Geol. Soc. Am. Bull.*, 96:1407–1418.

Bjorklund, K. R., 1976. Radiolaria from the Norwegian Sea, Leg 38 of the Deep Sea Drilling Project. *In* Talwani, M., Udintsev, G., et al., *Init. Repts. DSDP*, 38: Washington (U.S. Govt. Printing Office), 1101–1168.

Boltovskoy, E., Giussani, G., Watanabe, S., and Wright, R., 1980. *Atlas of benthic shelf Foraminifera of the southwest Atlantic*: The Hague (Dr. W. Junk bv Publishers).

Borehole Research Group, 1985. *Wireline Logging Manual* (1st ed.): Palisades, NY (Lamont-Doherty Geological Observatory, Columbia Univ.).

Boyce, R. E., 1976. Definitions and laboratory techniques of compressional sound velocity parameters and water content, wet-bulk density, and porosity parameters by gravimetric and gamma ray attenuation techniques. *In* Schlanger, S. O., Jackson, E. D., et al., *Init. Repts. DSDP*, 33: Washington (U.S. Govt. Printing Office), 931–935.

Bratzeva, G. M., 1983. Spores and pollen from Cenozoic sediments of the Falkland Plateau, Site 511, Deep Sea Drilling Project Leg 71. *In* Ludwig, W. J., Krasheninnikov, V. A., et al., *Init. Repts. DSDP*, 71: Washington (U.S. Govt. Printing Office), 907–932.

Bredell, J. H., 1982. The Precambrian sedimentary-volcanic sequence and associated intrusive rocks of the Ahlmannryggen, Western Dronning Maud Land: a new interpretation. *In* Craddock, C. (Ed.), *Antarct. Geosci., I.U.G.S. Ser. B*, 4:591–598.

Burger, D., 1982. A basal Cretaceous dinoflagellate suite from northeastern Australia. *Palynology*, 6:161–192.

Carlson, R. L., Gangi, A. F., and Snow, K. R., 1986. Empirical reflection travel time versus depth and velocity versus depth functions for the deep-sea sediment column. *J. Geophys. Res.*, 91:8249–8266.

Caron, M., 1985. Cretaceous planktonic foraminifera. *In* Bolli, H., et al. (Eds.), *Plankton Stratigraphy*: Cambridge (Cambridge Univ. Press), 17–86.

Chamley, H., 1979. North Atlantic clay sedimentation and paleoenvironment since the Late Jurassic. *In* Talwani, M., Hay, W., and Ryan, W.B.F., (Eds.), *Deep Drilling Results in the Atlantic Ocean: Continental Margins and Paleoenvironment*: Washington (Am. Geophys. Union), 342–360.

Chen, P. H., 1975. Antarctic radiolaria. *In* Hayes, D. E., Frakes, L. A., et al., *Init. Repts. DSDP*, 28: Washington (U.S. Govt. Printing Office), 407–474.

Ciesielski, P. F., 1975. Biostratigraphy and paleoecology of Neogene and Oligocene silicoflagellates from cores recovered during Antarctic Leg 28, Deep Sea Drilling Project. *In* Hayes, D. E., Frakes, L. A., et al., *Init. Repts. DSDP*, 28: Washington (U.S. Govt. Printing Office), 625–691.

________, 1983. The Neogene and Quaternary diatom biostratigraphy of subantarctic sediments, DSDP Leg 71. *In* Ludwig, W. J., Krasheninnikov, V. A., et al., *Init. Repts. DSDP*, 71: Washington (U.S. Govt. Printing Office), 635–665.

Dalziel, I.W.D., and Elliot, D., 1973. The Scotia Arc and the Antarctic Margin. *In* Nairn, A.E.M., and Stehli, F. G. (Eds.), *The Ocean Basins and Margins (Vol. 1, The South Atlantic)*: New York (Plenum Press), 71–126.

Davey, R. J., 1978. Marine Cretaceous palynology of Site 361, DSDP Leg. 40, off southwestern Africa. *In* Bolli, H. M., Ryan, W.B.F., et al., *Init. Repts. DSDP*, 40: Washington (U.S. Govt. Printing Office), 883–913.

Doveton, J. H., 1986. *Log Analysis of Subsurface Geology—Concepts and Computer Methods*: New York (Wiley).

Echols, R. J., 1971. Distribution of Foraminifera in sediments of the Scotia Sea area, Antarctic waters. *In* Reid, J. L., *Antarctic Oceanology*, Am. Geophys. Union Antarct. Res. Ser., 15:93–168.

Fenner, J., 1984. Eocene-Oligocene planktonic diatom stratigraphy in the low latitudes and the high southern latitudes. *Micropaleontology*, 30:319–342.

Gieskes, J. M., and Lawrence, J. R., 1976. Interstitial water studies, Leg 35. *In* Hollister, C. D., Craddock, C., et al., *Init. Repts. DSDP*, 35: Washington (U.S. Govt. Printing Office), 407–424.

Gombos, A. M., and Ciesielski, P. F., 1983. Late Eocene to early Miocene diatoms from the southwest Atlantic. *In* Ludwig, W. J., Krasheninnikov, V. A., et al., *Init. Repts. DSDP*, 71: Washington (U.S. Govt. Printing Office), 583–634.

Goodman, D. K., and Ford, L. N., Jr., 1983. Preliminary dinoflagellate biostratigraphy for the middle Eocene to lower Oligocene from the southwest Atlantic Ocean. *In* Ludwig, W. J., Krasheninnikov, V. A., et al., *Init. Repts. DSDP*, 71: Washington (U.S. Govt. Printing Office), 859–877.

Gradstein, F. M., 1978. Biostratigraphy of Lower Cretaceous Blake Nose and Blake Bahama Basin foraminifers, DSDP Leg 44, western North Atlantic Ocean. *In* Benson, W. E., Sheridan, R. E., et al., *Init. Repts. DSDP*, 44: Washington (U.S. Govt. Printing Office), 663–702.

Grikurov, G. E., 1982. Structure of Antarctica and outline of its evolution. *In* Craddock, C., (Ed.), *Antarct. Geosci., I.U.G.S. Ser. B*, 4: 791–804.

Grobe, H., 1986. Sedimentation processes on the Antarctic continental margin at Kapp Norvegia during the Late Pleistocene. *Geol. Rundschau*, 75:97–104

Hajós, M., 1975. Late Cretaceous Archaeomonadaceae, Diatomaceae and Silicoflagellatae from the south Pacific ocean, Deep Sea Drilling Project, Leg 29, Site 275. *In* Kennett, J. P., Houtz, R. E., et al., *Init. Repts. DSDP*, 29: Washington (U.S. Govt. Printing Office), 913–1009.

Harris, W. K., 1976. Palynology of Cores from Deep Sea Drilling Sites 327, 328, and 330, South Atlantic Ocean. *In* Barker, P. F., Dalziel, I.W.D., et al., *Init. Repts. DSDP*, 36: Washington (U.S. Govt. Printing Office), 761–815.

Hays, J. D., 1965. Radiolaria and late Tertiary and Quaternary history of Antarctic seas. *In* Llano, G. A. (Ed.), *Biology of the Antarctic Seas II*, Am. Geophys. Union Antarct. Res. Ser., 5:125–184.

Heron-Allen, E., and Earland, A., 1932. Foraminifera, 1. The Ice-Free Areas of the Falkland Islands and Adjacent Areas. *Disc. Repts*, 4: 291–460.

Hinz, K., and Krause, W., 1982. The continental margin of Queen Maud Land, Antarctica: seismic sequences, structural elements and geological development. *Geol. Jahrb. Reihe E*, 23:17–41.

Hinz, K., and Block, M., 1984. Results of geophysical investigations in the Weddell Sea and in the Ross Sea, Antarctica. *Exploration in New Regions*: London (Eleventh World Petroleum Congress), PD2(1):1–13.

Hsü, K. J., and LaBrecque, J. L., et al., 1984. *Init. Repts. DSDP*, 73: Washington (U.S. Govt. Printing Office).

Keating, B. H., and Herroro-Bervera, E., 1984. Magnetostratigraphy of Cretaceous and early Cenozoic sediments of Deep Sea Drilling Project Site 530, Angola Basin. *In* Hay, W. W., Sibuet, J. -C., et al., *Init. Repts. DSDP*, 75: Washington (U.S. Govt. Printing Office), 1211–1218.

Kennett, J. P., 1986. Miocene to early Pliocene oxygen and carbon isotope stratigraphy of the Southwest Pacific, DSDP Leg 90. *In* Kennett, J. P., von der Borch, C. C., et al., *Init. Repts. DSDP*, 90: Washington (U.S. Govt. Printing Office), 1383–1411.

Kennett, J. P., and Von der Borch, C., 1986. Southwest Pacific Cenozoic paleoceanography. *In* Kennett, J. P., Von der Borch, C. C., et al., *Init. Repts. DSDP*, 90: Washington (U.S. Govt. Printing office), 1493–1517.

Kennett, J. P., Von der Borch, C. C., et al., 1986. *Init. Repts. DSDP*, 90: Washington (U.S. Govt. Printing Office).

Leckie, R. M., 1984. Mid-Cretaceous planktonic foraminiferal biostratigraphy off Central Morocco, Deep Sea Drilling Project Leg 79, Sites 545 and 547. *In* Hinz, K., Winterer, E. L., et al., *Init. Repts. DSDP*, 79: Washington (U.S. Govt. Printing Office), 579–620.

________, 1987. Paleoecology of Mid-Cretaceous planktonic foraminifera: A comparison of open ocean and epicontinental sea assemblages. *Micropaleontology*, 33:164–176.

Leckie, R. M., and Webb, P.-N., 1986. Late Paleogene and early Neogene foraminifers of Deep Sea Drilling Project Site 270, Ross Sea, Antarctica. *In* Kennett, J. P., von der Borch, C. C., et al., *Init. Repts. DSDP*, 90: Washington (U.S. Govt. Printing Office), 1093–1142.

Ludwig, W. J., Krasheninnikov, V. A., et al., 1983. *Init. Repts. DSDP*, 71: Washington (U.S. Govt. Printing Office).

Martin, A. K., Goodlad, S. W., Hartnady, C.J.H., and Du Plessis, A., 1982. Cretaceous paleopositions of the Falkland Plateau relative to Southern Africa, using Mesozoic sea-floor spreading anomalies. *Geophys. J. R. Astron. Soc.*, 71:567–579.

McLachlan, I. R., and Pieterse, E., 1978. Preliminary palynological results: Site 361, Leg 40, Deep Sea Drilling Project. *In* Bolli, H. M., Ryan, W.B.F., et al., *Init. Repts. DSDP*, 40: Washington (U.S. Govt. Printing Office), 857–870.

Mercer, J. H., 1978. Glacial development and temperature trends in the Antarctic and in South America. *In* Van Zinderen Bakker, E. M., (Ed.), *Antarctic Glacial History and World Paleoenvironments*: Rotterdam (Balkema), 73–93.

Miller, K. G., and Tucholke, B. E., 1983. Development of Cenozoic abyssal circulation south of the Greenland-Scotland Ridge. *In* Bott, M., Saxov, S., Talwani, M., and Thiede, J. (Eds.), *Development of the Greenland-Scotland Ridge*: New York (Plenum Press), 549–589.

Moore, T. C., Jr., Van Andel, T. H., Sancetta, C., and Pisias, N., 1978. Cenozoic hiatuses in the pelagic sediments. *Micropaleontology*, 24: 113–138.

Morgan, R., 1977. Elucidation of the Cretaceous dinoflagellate *Diconodinium* Eisenack and Cookson, 1960, and related peridinioid species from Australia. *Palynology*, 1:123–137.

________, 1980. Palynostratigraphy of the Australian Early and Middle Cretaceous. *Mem. Geol. Surv. N. S. W. Palaeontol.*, 18.

Perch-Nielsen, K., 1985. Mesozoic calcareous nannofossils. *In* Bolli, H. M., Saunders J. B., and Perch-Nielsen, K., (Eds.), *Plankton Stratigraphy*; Cambridge (Cambridge Univ. Press), 329–426.

Robert, C., 1987. Clay mineral associations and structural evolution of the South Atlantic: Jurassic to Eocene. *Palaeogeogr., Palaeoclimatol., Palaeoecol.*, 58:87–108.

Robert, C., and Maillot, H., 1983. Paleoenvironmental significance of clay mineralogical and geochemical data, Southwest Atlantic, DSDP Legs 36 and 71. *In* Ludwig, W. J., Krasheninnikov, V., et al., *Init. Repts. DSDP*, 71: Washington (U.S. Govt. Printing Office), 317–343.

Robert, C., and Chamley, H., 1986. La kaolinite des sédiments est-atlantiques, tétmoindes climats et environments cénozoïque. *C. R. Acad. Sci. Ser.* 2, 303:1563–1568.

Robert, C., Caulet, J. P., and Maillot, H., in press. Evolution climatique et hydrologique en mer de Ross (Site DSDP 274) au Nogne, d'après les associations de Radiolaires, la minéralogie des argiles et la géochimie minérale. *C. R. Acad. Sci.*

Salloway, J. C., 1983. Paleomagnetism of sediments from Deep Sea Drilling Project, Leg 71. *In* Ludwig, W. J., Krasheninnikov, V. A., et al., *Init. Repts. DSDP*, 71: Washington (U.S. Govt. Printing Office), 1073–1091.

Sanfilippo, A., and Riedel, W. R., 1985. Cretaceous radiolaria. *In* Bolli, H. M., Saunders, J. B., and Perch-Nielsen, K. (Eds.), *Plankton Stratigraphy*: Cambridge (Cambridge Univ. Press), 573–630.

Savin, S. M., Douglas, R. G., and Stehli, F. G., 1975. Tertiary marine paleotemperatures. *Geol. Soc. Am. Bull.*, 86:1499–1510.

Schaefer, R. G., von der Dick, H., and Leythaeuser, D., 1983. C_2-C_8 hydrocarbons in sediments from Deep Sea Drilling Project Leg 71, Site 511, Falkland Plateau, South Atlantic. *In* Ludwig, W. J., Krasheninnikov, V. A., et al., *Init. Repts. DSDP*, 71, Pt. 2: Washington (U.S. Govt. Printing Office), 1033–1043.

Scheibnerova, V., 1974. Aptian-Albian benthonic foraminifera from DSDP Leg 27, Sites 259, 260 and 263, eastern Indian Ocean. *In* Veevers, J. J., Heirtzler, J. R., et al., *Init. Repts. DSDP*, 27: Washington (U.S. Govt. Printing Office), 697–742.

Schrader, H. J. 1976. Cenozoic planktonic diatom biostratigraphy of the southern Pacific Ocean. *In* Hollister, C. D., Craddock, C., et al., *Init. Repts. DSDP*, 35: Washington (U.S. Govt. Printing Office), 605–671.

Shackleton, N. J., and Kennett, J. P., 1975. Paleotemperature history of the Cenozoic and the initiation of Antarctic glaciation: oxygen and carbon isotope analyses in DSDP Sites 277, 279 and 281. *In* Kennett, J. P., Houtz, R. E., et al., *Init. Repts. DSDP*, 29: Washington (U.S. Govt. Printing Office), 801–806.

Simpson, E.S.W., Schlich, R., et al., 1974. *Init. Repts. DSDP*, 25: Washington (U.S. Govt. Printing Office), 296–300.

Sverdrup, H. U., Johnson, M. W., and Fleming, R. (Eds.), 1942. *The Oceans: Their Physics, Chemistry and General Biology*: Englewood Cliffs, N.J. (Prentice-Hall).

Tsunogai, S., Nishimura, M., and Nakaya, S., 1968. Complexometric titration of calcium in the presence of large amounts of magnesium. *Talanta*, 15:385–390.

Ugolini, F. C., and Jackson, M. L., 1982. Weathering and mineral synthesis in Antarctic soils. *In* Craddock, C. (Ed.), *Antarct. Geosci. I.U.G.S. Ser. B*, 4:1101–1108.

Van Andel, T. H., Heath, G. R., and Moore, T. C., 1976. Cenozoic history and paleoceanography of central equatorial Pacific Ocean. *Am. Geophys. Union Monogr.*, 19:218–295.

Von Herzen, R. P., and Maxwell, A. E., 1959. The measurement of thermal conductivity of deep-sea sediments by a needle probe method. *J. Geophys. Res.*, 65:1535–1541.

Whelan, J. K., Hunt, J. M., Jasper, J., and Huc, A., 1984. *Migration of C1-C8 Hydrocarbons in Marine Sediments*. Woods Hole Oceanogr. Inst. Contrib. 5634.

Williams, G. L., and Bujak, J. P., 1985. Mesozoic and Cenozoic dinoflagellates. *In* Bolli, H. M., Saunders, J. B., and Perch-Nielsen, K. (Eds.), *Plankton Stratigraphy*: Cambridge (Cambridge Univ. Press), 847–964.

Wise, S. W., 1983. Mesozoic and Cenozoic calcareous nannofossils recovered by Deep Sea Drilling Project Leg 71 in the Falkland Plateau region, southwest Atlantic Ocean. *In* Ludwig, W. J., Krasheninnikov, V. A., et al., *Init. Repts. DSDP*, 71: Washington (U.S. Govt. Printing Office), 481–550.

Wise, S. W., and Wind, F. H., 1977. Mesozoic and Cenozoic calcareous nannofossils recovered by DSDP Leg 36 drilling on the Falkland Plateau, Southwest Atlantic sector of the Southern Ocean. *In* Barker, P. F., Dalziel, I.W.D., et al., *Init. Repts. DSDP*, 36: Washington (U.S. Govt. Printing Office), 269–492.

Ms 113A-109

Summary log for Hole 693A

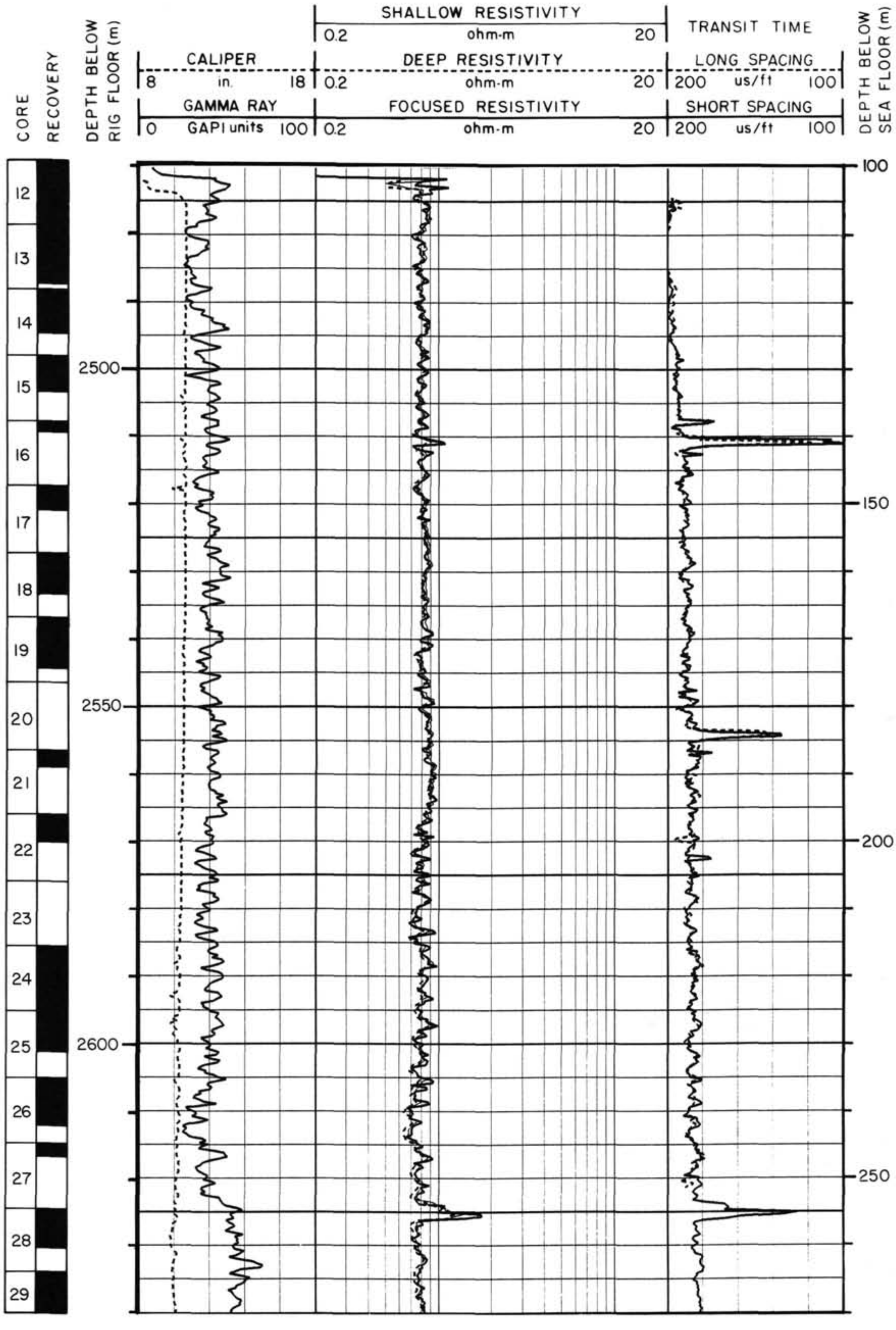

Summary log for Hole 693A (continued)

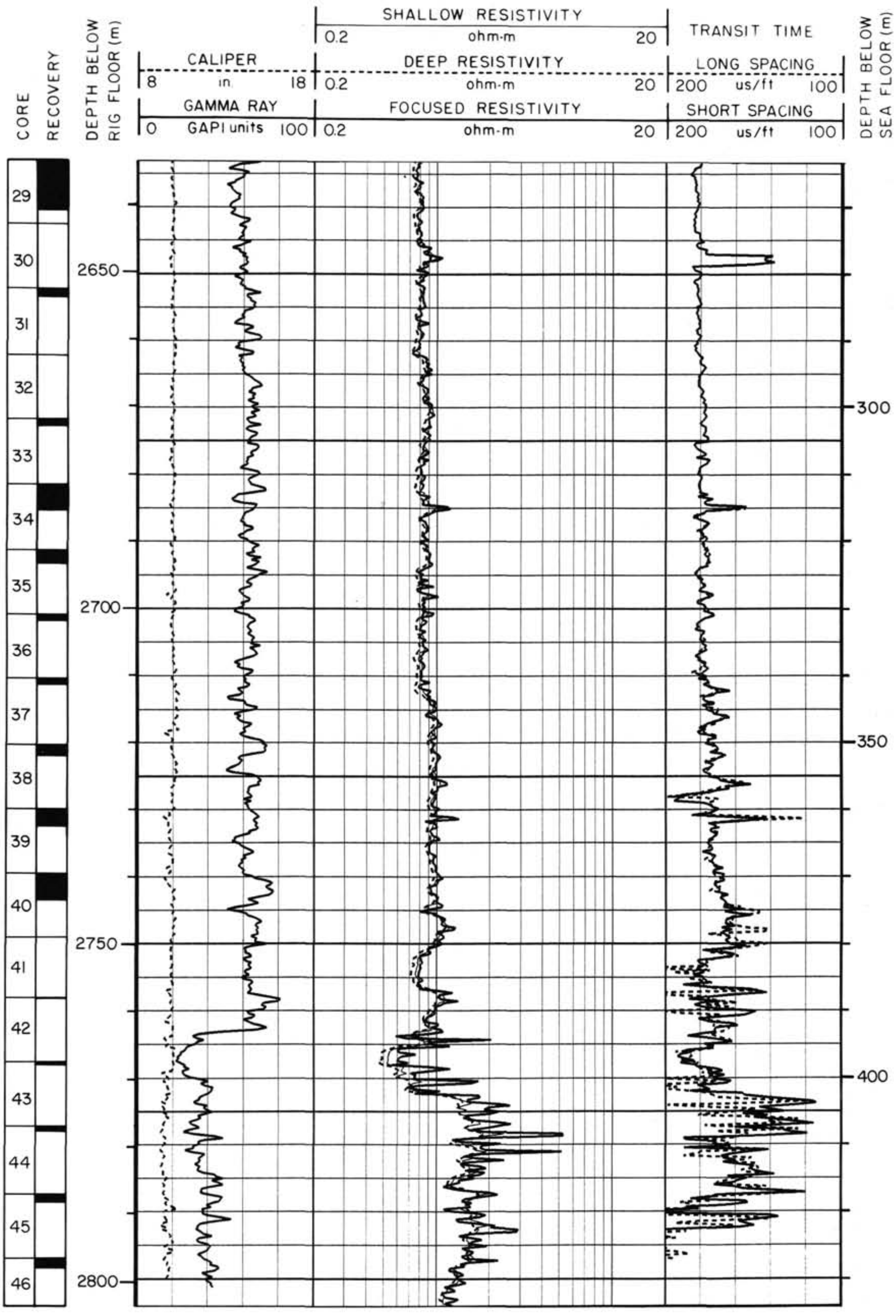

SITE 693 HOLE A CORE 1R CORED INTERVAL 2359.4-2361.9 mbsl; 0-2.5 mbsf

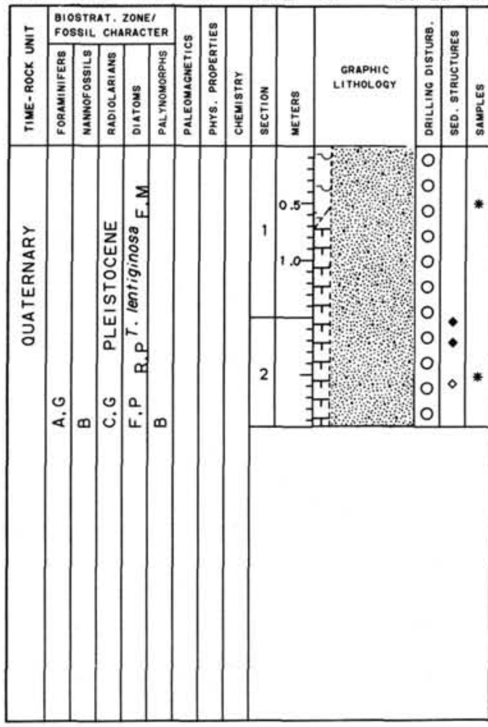

LITHOLOGIC DESCRIPTION

FORAMINIFER-BEARING SILTY MUD

Major lithology: Foraminifer-bearing silty mud, olive gray (5Y 4/2), homogenized during drilling. Coarse fraction increases downcore. It consists mainly of planktonic foraminifers, with a few metamorphic and vein quartz grains.

Minor lithology: Diatom-bearing silty mud, olive gray (5Y 4/2), homogenized during drilling from top of core, grades into major lithology in Section 1, approximately 70–80 cm.

Section 2, 7 and 30 cm: two small clasts of clayey mud, dark olive gray (5Y 3/2). Section 2, and 70 cm: one small (12 mm) subangular manganese-coated dropstone.

SMEAR SLIDE SUMMARY (%):

	1, 50 M	2, 50 D
TEXTURE:		
Sand	2	20
Silt	58	50
Clay	40	30
COMPOSITION:		
Quartz	30	45
Feldspar	8	5
Clay	40	30
Accessory minerals:		
Opaque minerals	2	5
Horneblende (+biotite, +garnet)	5	4
Glauconite	Tr	1
Foraminifers	—	10
Diatoms	15	Tr
Radiolarians	Tr	—
Sponge spicules	Tr	Tr

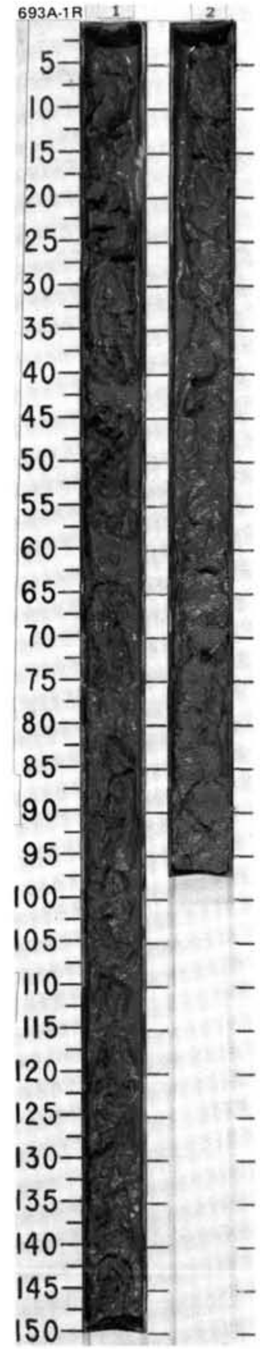

SITE 693 HOLE A CORE 2R CORED INTERVAL 2361.9-2371.6 mbsl; 2.5-12.2 mbsf

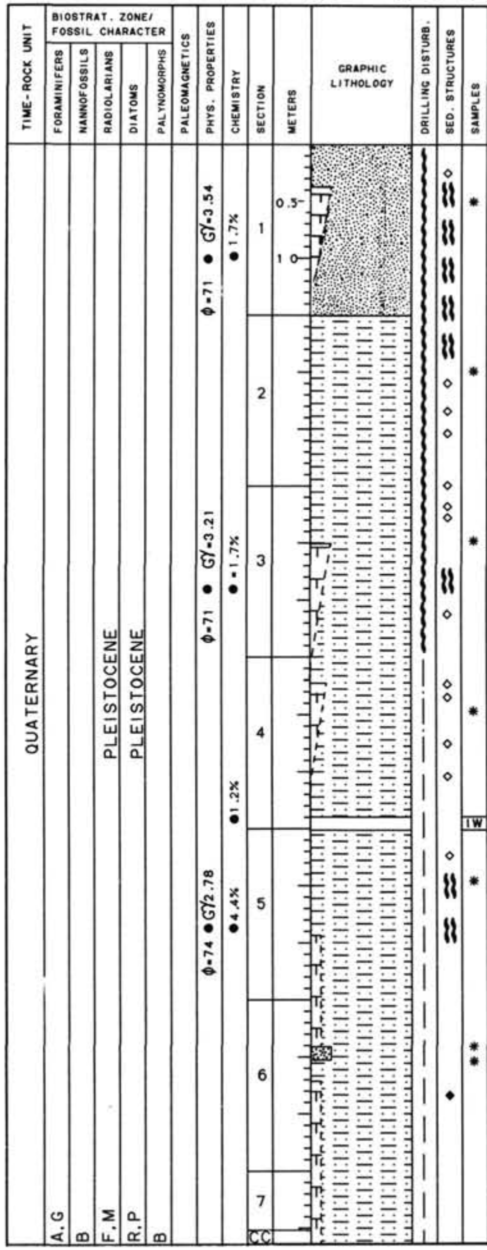

LITHOLOGIC DESCRIPTION

SILTY MUD, CLAYEY MUD, and FORAMINIFER-BEARING CLAYEY MUD

Major lithologies: Silty mud, dark grayish brown (2.5Y 4/2) to olive gray (5Y 4/2), in Section 1. Structureless mud, strong drilling disturbance, bioturbation moderate but distorted, foraminifers common, top of section, scattered sand grains throughout. Clayey mud in Sections 2, 4, and 5; dark grayish brown (2.5Y 4/2), drilling disturbance strong, bioturbation moderate but scattered, coarse fraction two-thirds planktonic foraminifers, terrigenous grains, feldspar, biotite, and garnet (metamorphic). Foraminifer-bearing clayey mud in Sections 3, 6, and 7; dark grayish brown (2.5Y 4/2), olive gray (5Y 4/2), moderate drilling disturbance, minor to no bioturbation.

Minor lithology: Silty mud, olive gray (5Y 4/2), in Section 6.

Color changes are cyclic: dark grayish brown (2.5Y 4/2) has a sharp base, then olive gray (5Y 4/2) grades down to dark grayish brown (2.5Y 4/2). The changes appear to be related to foraminifer content, hence the gradational changes in the lithologic column. Granite, basic igneous, and quartzitic dropstones are abundant throughout core. A 9-cm-long specimen occurs in working half, Section 5, 130 cm. Elsewhere dropstones occur in Section 1, 15 cm; Section 2, 60, 80, 95, and 140 cm; Section 3, 8, 22, and 80 cm; and Section 4, 20, 45, 60, 90, and 110 cm. Provenance of ice-rafted sand grains is metamorphic in Section 2 and more varied and with more angular grains in Section 7.

SMEAR SLIDE SUMMARY (%):

	1, 50 D	2, 50 D	3, 50 D	4, 50 D	5, 50 D	6, 50 D	6, 49 M
TEXTURE:							
Sand	10	20	10	5	5	10	20
Silt	50	30	40	45	35	40	70
Clay	40	50	50	50	60	50	10
COMPOSITION:							
Quartz	36	29	25	25	22	25	43
Feldspar	5	7	7	5	7	3	15
Clay	40	50	49	49	60	51	10
Accessory minerals:							
Pyroxene	—	—	—	—	—	1	3
Glauconite	—	—	Tr	—	—	—	—
Amphiboles	5	2	—	1	3	—	7
Opaque minerals	7	7	7	3	3	7	15
Heavy minerals	5	3	2	5	3	3	7
Carbonates	1	1	—	5	—	Tr	—
Foraminifers	—	1	10	7	2	10	—
Nannofossils	—	—	—	—	—	Tr	—
Diatoms	1	Tr	—	—	—	—	—
Radiolarians	—	Tr	—	—	—	—	—
Sponge spicules	Tr	—	—	—	—	—	Tr

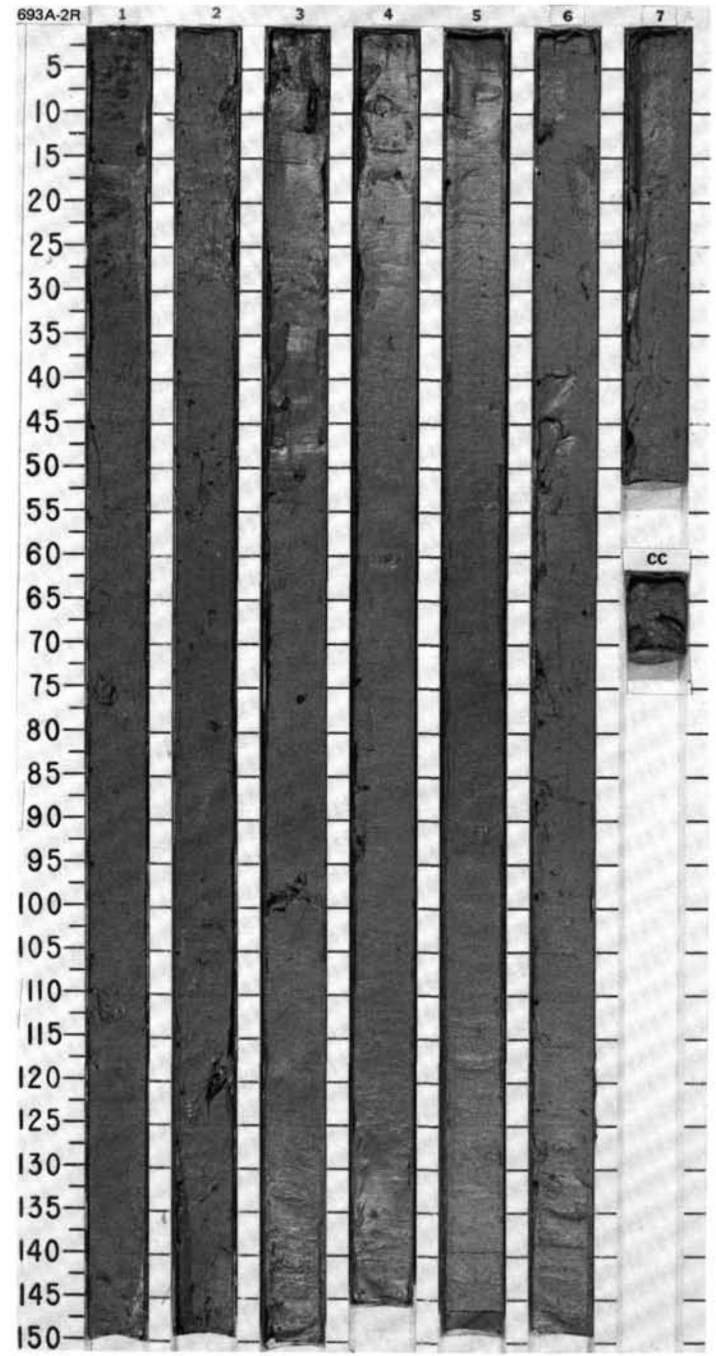

SITE 693 HOLE A CORE 3R CORED INTERVAL 2371.6-2381.3 mbsl; 12.2-21.9 mbsf

TIME-ROCK UNIT	BIOSTRAT. ZONE/ FOSSIL CHARACTER: FORAMINIFERS	NANNOFOSSILS	RADIOLARIANS	DIATOMS	PALYNOMORPHS	PALEOMAGNETICS	PHYS. PROPERTIES	CHEMISTRY	SECTION	METERS	GRAPHIC LITHOLOGY	DRILLING DISTURB.	SED. STRUCTURES	SAMPLES
QUATERNARY	B	B	R,P LOWER PLEISTOCENE (?)	R,P PLEISTOCENE (?)	B		●GY-3.33		1, 2, CC	0.5, 1.0				

LITHOLOGIC DESCRIPTION

CLAYEY MUD

Major lithology: Clayey mud, olive gray (5Y 4/2), grading down to dark grayish brown (2.5Y 4/2) at base of Section 2 and in CC. Structureless.

Color cyclicity is a continuation of that seen in 113-693A-2R, but there are no foraminifers. Scattered sand grains, and two small dropstones.

SMEAR SLIDE SUMMARY (%):

	1, 50 D	2, 50 D
TEXTURE:		
Sand	5	4
Silt	35	37
Clay	60	58
COMPOSITION:		
Quartz	25	24
Feldspar	8	8
Clay	60	58
Accessory minerals:		
Heavy minerals	—	3
Amphibole	2	3
Carbonates	2	—
Opaque minerals	3	3

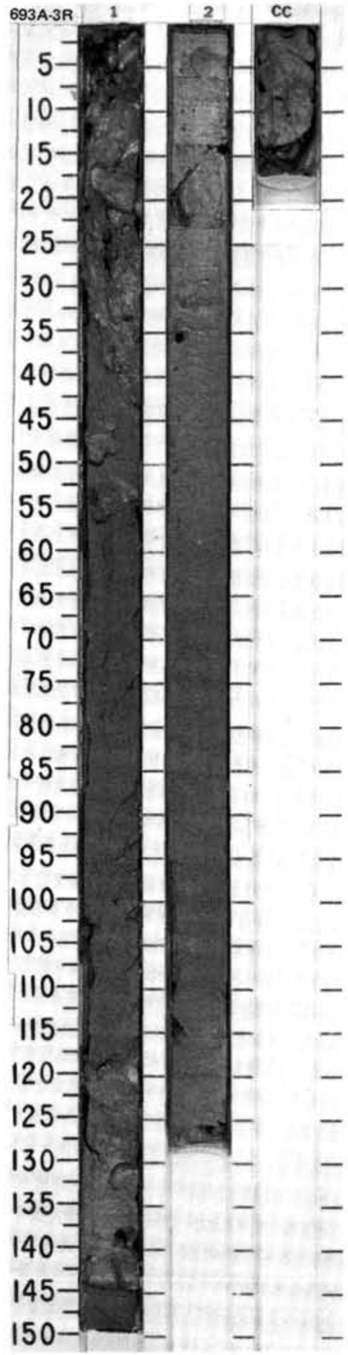

SITE 693 HOLE A CORE 4R CORED INTERVAL 2381.3-2390.8 mbsl; 21.9-31.4 mbsf

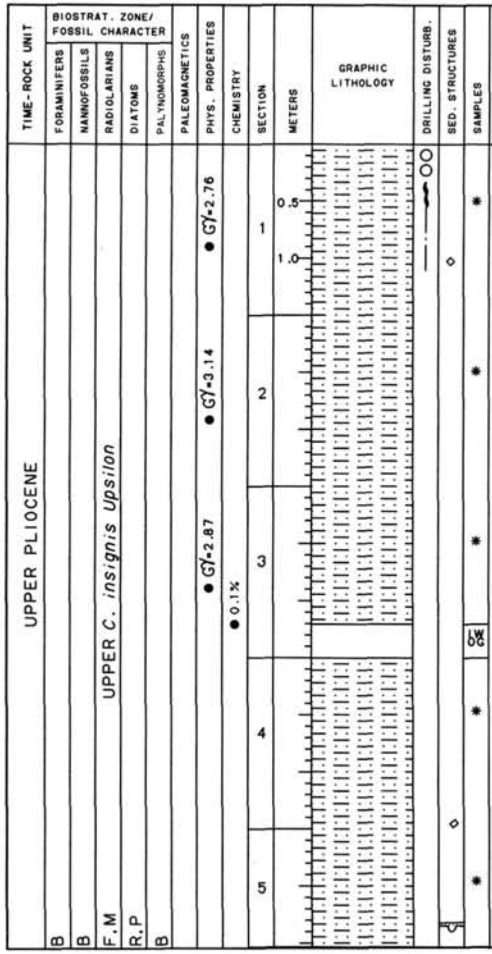

LITHOLOGIC DESCRIPTION

CLAYEY MUD

Major lithology: Clayey mud, dark greenish gray (5-6Y 4/1), gray (5Y 5/1), and olive gray (5Y 5/2). Sediment is relatively homogeneous. The color change is cyclic, with gray (5Y 5/1) at the base of Section 5, a sharp transition with a very fine-grained graded sand layer, 1 cm thick, overlain by a gradual transition from olive gray (5Y 5/2) to gray in upper Section 3.

Minor lithology: Sand in Section 5, black (5Y 2.5/2), very fine-grained, grading into silt with sharp upper and lower contacts. The sediment immediately adjacent to (above and below) the sand has a purplish color but it records as dark gray (5Y 4/1).

The top of Section 1 is soupy, with strong coring disturbance below. Dropstones in Section 1, 100-104 cm (4 cm diameter), and Section 4, 147-150 cm (3 cm diameter). Manganese and sand-sized material throughout. Based on the coarse fraction (>63 mm) from CC, sand component is about 2%.

SMEAR SLIDE SUMMARY (%):

	1, 50 D	2, 50 D	3, 50 D	4, 50 D	5, 50 D
TEXTURE:					
Sand	10	5	—	2	—
Silt	40	40	50	46	40
Clay	50	55	50	52	60
COMPOSITION:					
Quartz	26	22	26	26	20
Feldspar	—	2	Tr	—	2
Mica	1	—	2	2	2
Clay	50	55	50	52	59
Volcanic glass	12	4	4	6	3
Calcite/dolomite	—	—	—	—	2
Accessory minerals	6	9	4	2	—
Opaque minerals	5	4	4	4	3
Amphiboles	—	4	10	8	7
Diatoms	—	—	Tr	—	2

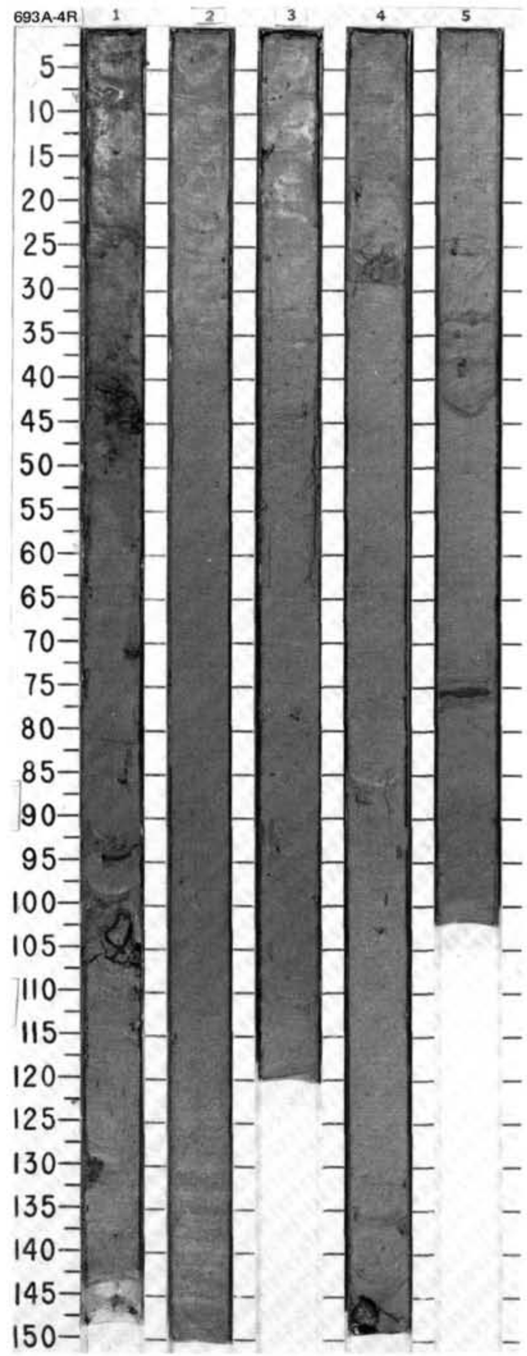

SITE 693 HOLE A CORE 5R CORED INTERVAL 2390.8-2400.5 mbsl; 31.4-41.1 mbsf

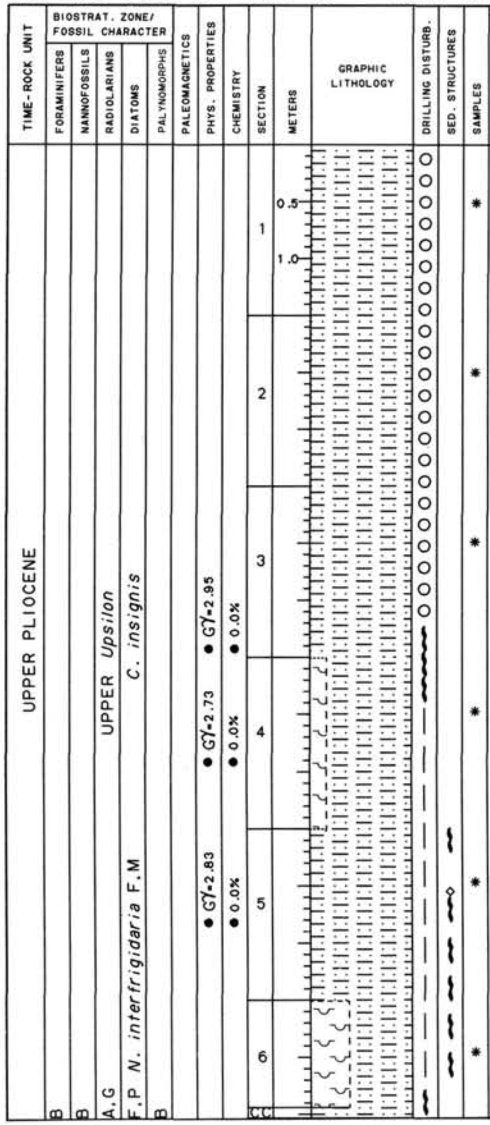

LITHOLOGIC DESCRIPTION

CLAYEY MUD, DIATOM-BEARING CLAYEY MUD, and DIATOM CLAYEY MUD

Major lithology: Clayey mud in Sections 1, 2, 3, and 5, gray (2.5Y 5/1), olive (5Y 5/3), and greenish gray (5G 5/1) soft sediment. Drilling disturbance marks all primary structures, except in Section 5 where light to moderate bioturbation is present as dark greenish (5GY 4/1) mottles. Diatom-bearing clayey mud in Section 4, upper part olive (5Y 5/3) with gray (2.5Y 5/1) and pale brown (10YR 7/4) patches smeared by drilling. At base, greenish gray slightly bioturbated. *Diatom clayey mud in Section 6, greenish gray (5G 5/1) with slightly darker* mottling. Diatoms constitute about 25% of the silt fraction. Coarse fraction dominantly angular sand with lesser amounts of feldspar and minor amounts of hornblende and mica.

Dropstone (30 × 15 mm) observed at Section 5, 43 cm.

SMEAR SLIDE SUMMARY (%):

	1, 50 D	2, 50 D	3, 50 D	4, 50 D	5, 50 D	6, 50 D
TEXTURE:						
Sand	2	5	—	2	2	2
Silt	48	45	30	48	48	60
Clay	50	50	70	50	50	38
COMPOSITION:						
Quartz	15	9	6	4	10	9
Feldspar	8	14	—	—	15	—
Mica	—	—	1	3	—	2
Clay	50	50	70	50	50	38
Volcanic glass	10	8	2	4	7	—
Calcite/dolomite	5	5	—	—	6	—
Accessory minerals	3	4	8	9	6	—
Opaque minerals	6	6	2	6	4	4
Amphiboles	—	—	4	4	—	6
Foraminifers	—	Tr	—	—	—	—
Diatoms	2	3	7	18	1	38
Radiolarians	1	1	—	2	1	2
Sponge spicules	—	Tr	—	—	—	—
Silicoflagellates	—	—	—	—	—	1

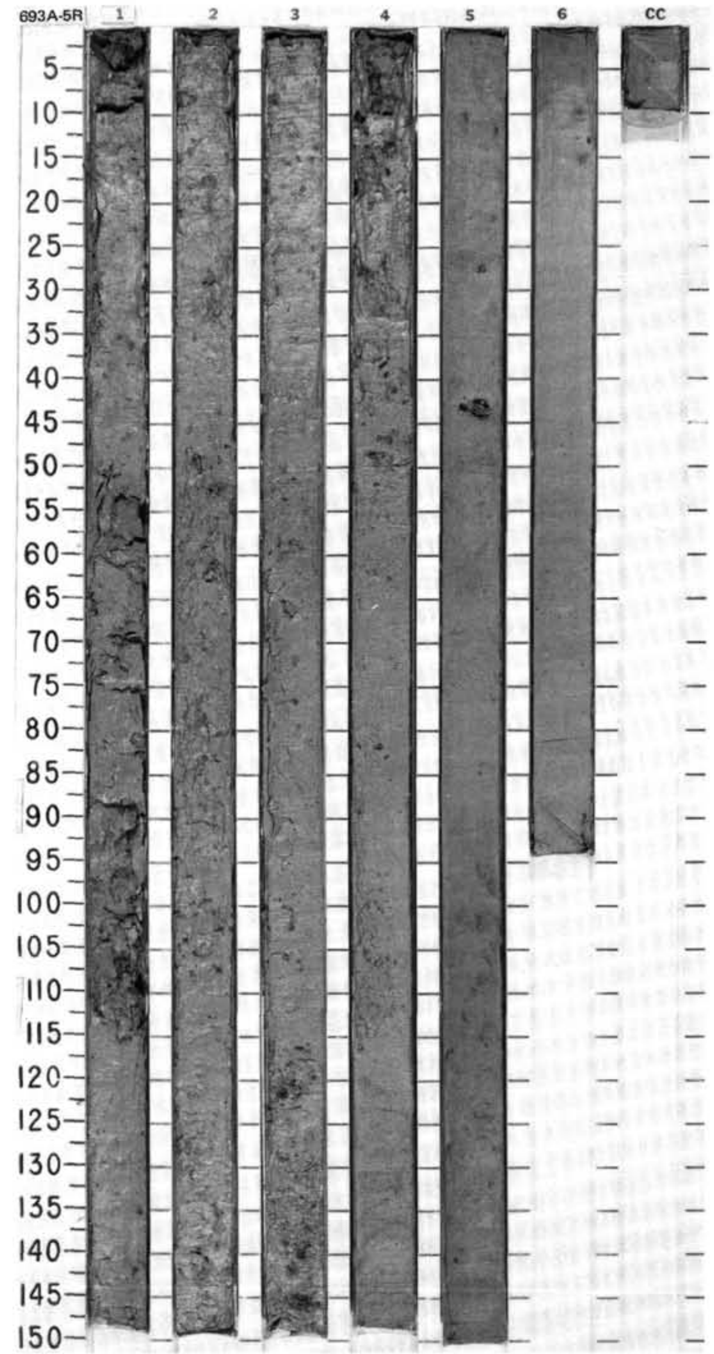

SITE 693 HOLE A CORE 6R CORED INTERVAL 2400.5-2410.2 mbsl; 41.1-50.8 mbsf

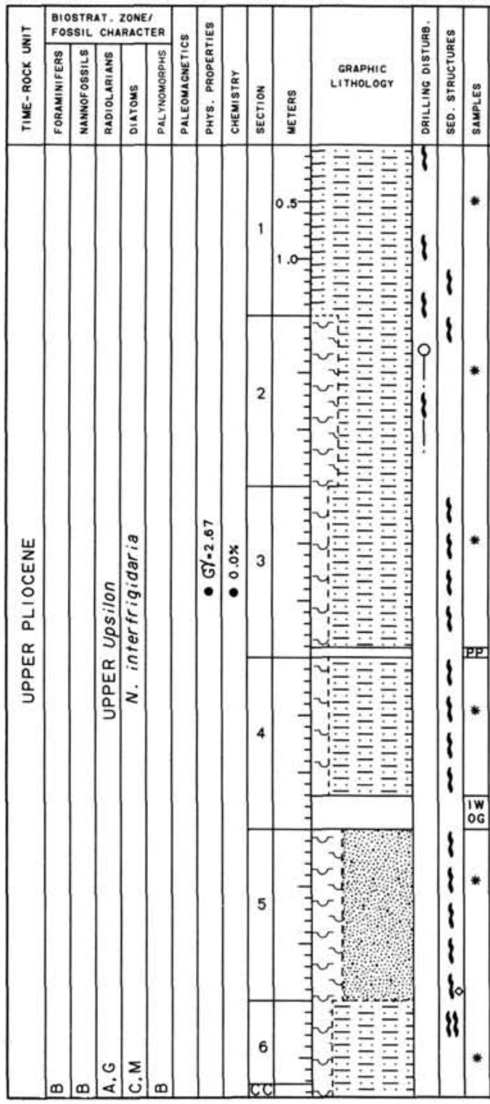

LITHOLOGIC DESCRIPTION

CLAYEY MUD, DIATOM CLAYEY MUD, DIATOM-BEARING CLAYEY MUD, and DIATOM SILTY MUD

Major lithologies: Clayey mud, greenish gray (5GY 5/1). Diatom clayey mud, greenish gray (5GY 5/1). Diatom-bearing clayey mud, greenish gray (5GY 5/1) and dark grayish green (5G 6/2). Diatom silty mud, greenish gray (5GY 5/1).

Bioturbation is absent to minor. Core shows variations in diatom percentage, without any systematic downcore change. A large (3-3.5 cm) feldspar and quartz-bearing dropstone occurs in Section 5, 125 cm. Sediment around the dropstone is slightly coarser. Additional ice-rafted material is represented by the sand-sized grains observed in the smear slides.

SMEAR SLIDE SUMMARY (%):

	1, 50 D	2, 50 D	3, 50 D	4, 50 D	5, 50 D	6, 50 D
TEXTURE:						
Sand	1	1	—	1	1	1
Silt	30	48	48	47	59	47
Clay	69	51	52	52	40	52
COMPOSITION:						
Quartz	10	15	8	9	12	10
Feldspar	3	3	5	8	8	8
Clay	69	51	52	52	40	52
Volcanic glass	4	5	7	4	5	3
Calcite/dolomite	—	2	—	—	—	1
Accessory minerals	4	3	4	3	3	2
Opaque minerals	3	2	5	5	2	4
Foraminifers	Tr	—	—	—	—	—
Diatoms	6	28	18	18	28	20
Radiolarians	1	1	1	1	2	—

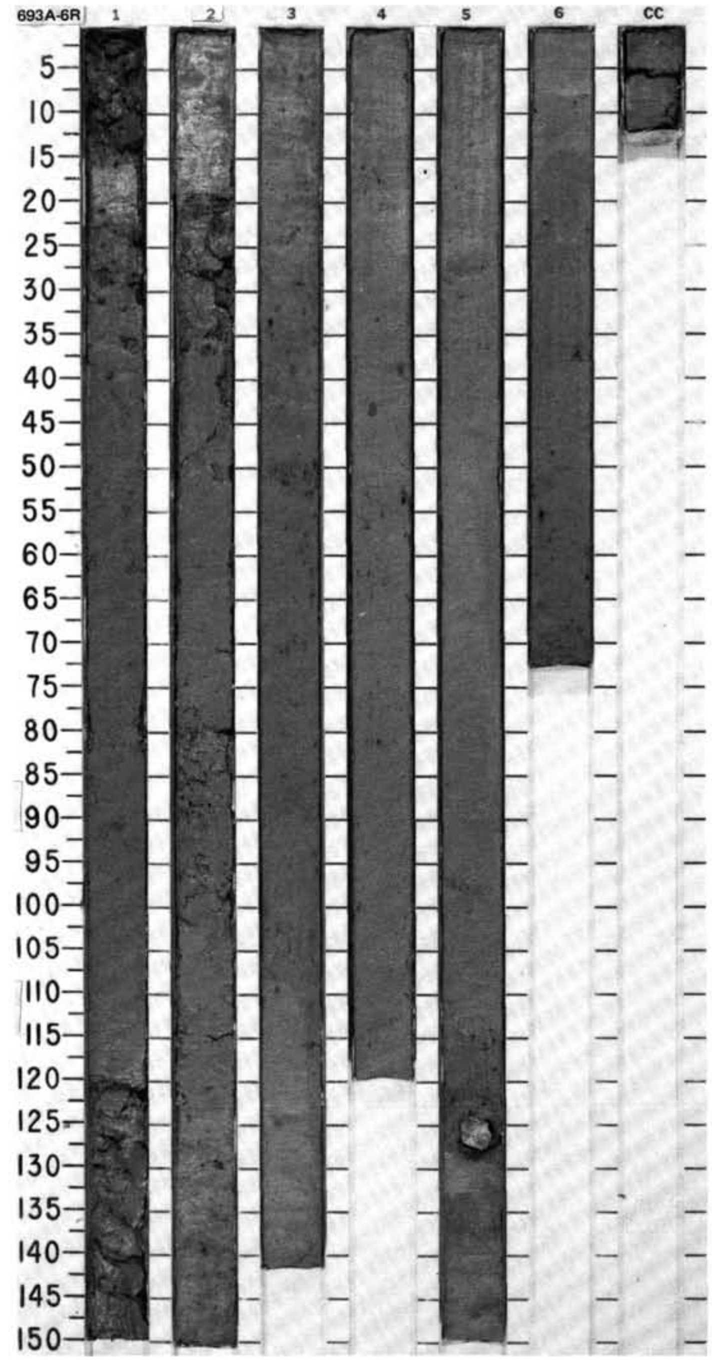

SITE 693 HOLE A CORE 7R CORED INTERVAL 2410.2-2419.8 mbsl; 50.8-60.4 mbsf

TIME-ROCK UNIT	BIOSTRAT. ZONE/ FOSSIL CHARACTER: FORAMINIFERS	NANNOFOSSILS	RADIOLARIANS	DIATOMS		PALEOMAGNETICS	PHYS. PROPERTIES	CHEMISTRY	SECTION	METERS	GRAPHIC LITHOLOGY	DRILLING DISTURB.	SED. STRUCTURES	SAMPLES
UPPER PLIOCENE	B	B	A,M UPPER *Upsilon*	F,M *N. angulata* - *N. reinholdii*	*D. boliviensis* (silicoflagellate)		● GY=2.68 ● GY=2.87	● 0.0% ● 0.0%	1 2 CC	0.5 1.0				* *

DIATOM-BEARING CLAYEY MUD and DIATOM CLAYEY MUD

Major lithologies: Diatom-bearing clayey mud and diatom clayey mud, gray (5Y 5/1) with a thin interval of dark gray (2.5Y 4/1), in Section 1, 85–105 cm.

A 2-cm-long dropstone occurs in Section 2, 15 cm.

SMEAR SLIDE SUMMARY (%):

	1, 70 D	2, 70 D
TEXTURE:		
Silt	45	48
Clay	55	52
COMPOSITION:		
Quartz	11	6
Mica	2	—
Clay	55	52
Volcanic glass	6	4
Calcite/dolomite	4	2
Accessory minerals		
Amphiboles	4	2
Opaque	6	2
Rutile	Tr	—
Diatoms	12	32
Radiolarians	—	Tr

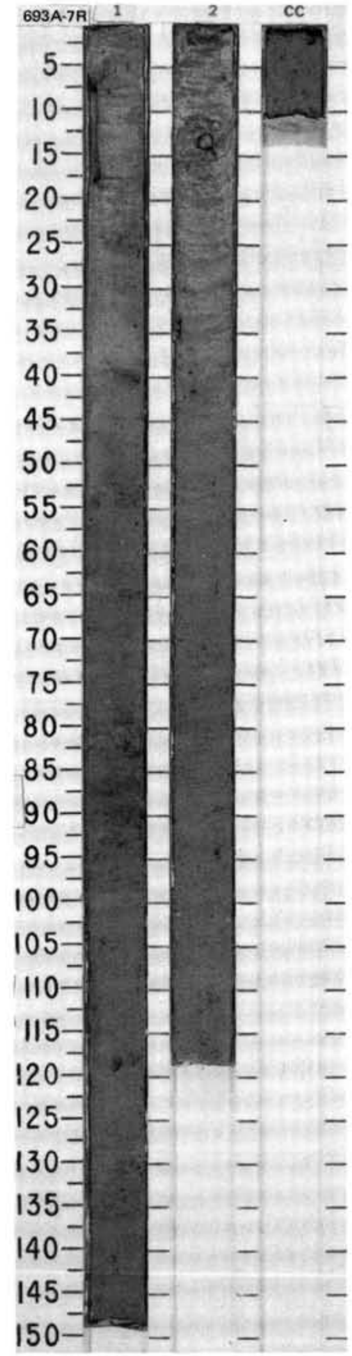

SITE 693 HOLE A CORE 8R CORED INTERVAL 2419.8-2429.5 mbsl; 60.4-70.1 mbsf

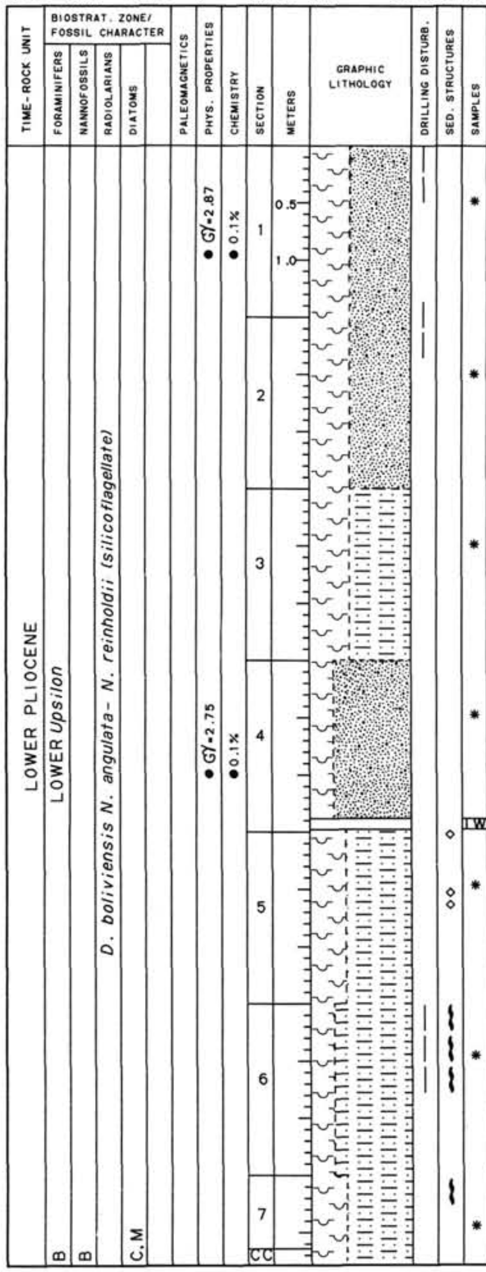

LITHOLOGIC DESCRIPTION

DIATOM SILTY MUD, DIATOM-BEARING SILTY MUD, DIATOM-BEARING CLAYEY MUD, and DIATOM CLAYEY MUD

Major lithologies: Diatom silty mud in Sections 1 and 2, diatom-bearing silty mud in Section 4, diatom-bearing clayey mud in Section 6, and diatom clayey mud in Sections 3 and 7. Gray (5Y 5/1), dark greenish gray (5GY 4/1), dark gray (2.5Y 4/1), and greenish gray (5BG 5/1) mud with gradual color transition on a scale of 100 cm.

Bioturbation is rare. Large dropstones are located at the top of Section 5. Numerous small dropstones (<2 mm) were detected along the entire core.

SMEAR SLIDE SUMMARY (%):

	1, 50 D	2, 50 D	3, 50 D	4, 50 D	5, 50 D	6, 50 D	7, 50 D
TEXTURE:							
Sand	1	1	1	—	—	—	—
Silt	89	79	64	64	52	48	48
Clay	10	20	35	36	48	52	52
COMPOSITION:							
Quartz	15	12	8	10	10	7	4
Feldspar	15	10	6	3	4	2	2
Mica	—	—	—	2	—	1	—
Clay	10	20	35	36	48	52	52
Volcanic glass	10	8	5	8	—	4	2
Calcite/dolomite	—	—	—	4	2	6	2
Accessory minerals	5	4	4	5	—	—	—
Opaque minerals	5	5	5	8	—	4	—
Amphiboles	—	—	—	2	2	4	2
Diatoms	38	40	35	22	34	20	36
Radiolarians	2	1	2	—	—	—	Tr
Sponge spicules	—	Tr	—	—	—	—	—

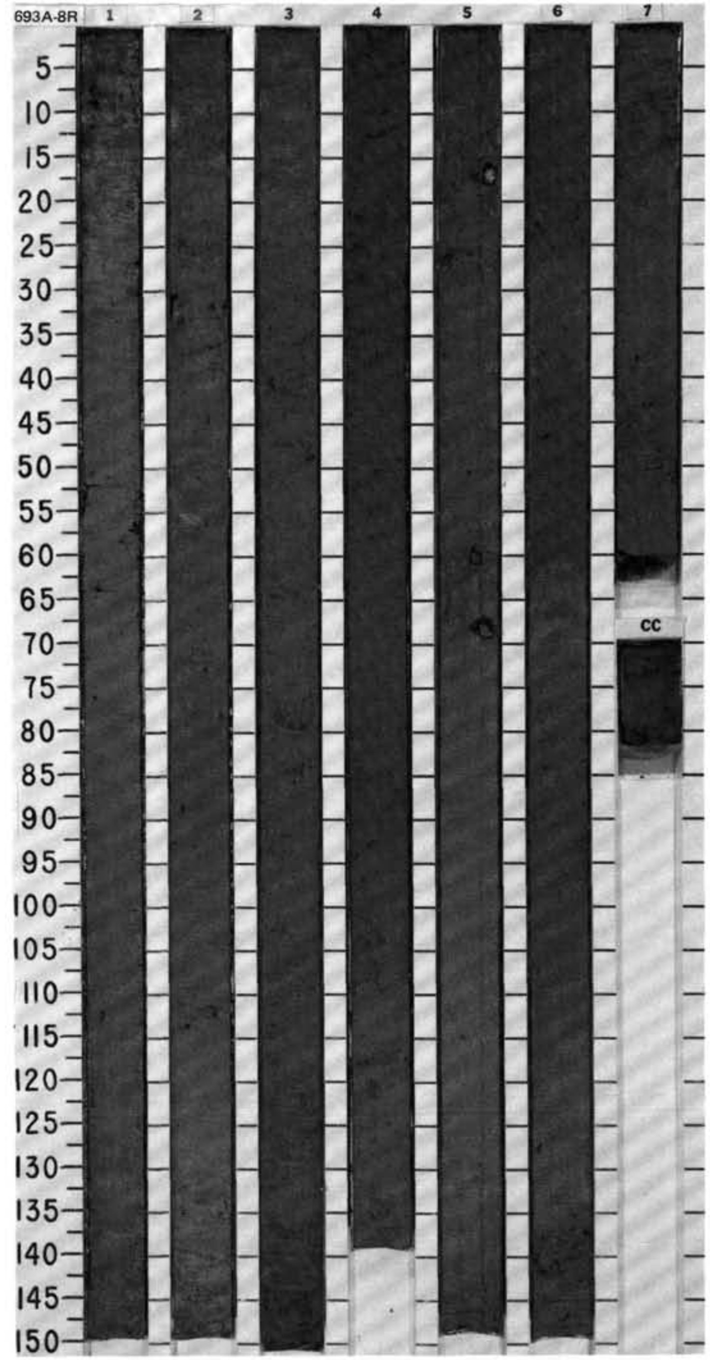

SITE 693 HOLE A CORE 9R CORED INTERVAL 2429.5-2439.1 mbsl; 70.1-79.7 mbsf

TIME-ROCK UNIT	FORAMINIFERS	NANNOFOSSILS	RADIOLARIANS	DIATOMS	PALEOMAGNETICS	PHYS. PROPERTIES	CHEMISTRY	SECTION	METERS	GRAPHIC LITHOLOGY	DRILLING DISTURB.	SED. STRUCTURES	SAMPLES
LOWER PLIOCENE	B	B	A, G LOWER *Upsilon*	C, M *N. angulata - N. reinholdii* *D. boliviensis* (silicoflagellate)			● 0.0%	1	0.5, 1.0				*
								2					*
								3					*
								4					* IW OG
								5					*
								6			◇		*
								7					*

BIOSTRAT. ZONE/ FOSSIL CHARACTER

LITHOLOGIC DESCRIPTION

DIATOM CLAYEY MUD, DIATOM SILTY MUD, and MUDDY DIATOM OOZE

Major lithologies: Diatom clayey mud in Sections 1, 2, 3, and 5; diatom silty mud in Section 4; and muddy diatom ooze in Sections 6 and 7. All dark greenish gray (5G 4/1). Primary structures obscured by drilling disturbance.

Dropstone, 2 cm long, in Section 6, 38 cm. Numerous small (<2 mm) dropstones throughout core.

SMEAR SLIDE SUMMARY (%):

	1, 50 D	2, 50 D	3, 50 D	4, 50 D	5, 50 D	6, 50 D	7, 35 M
TEXTURE:							
Silt	48	54	58	70	68	78	—
Clay	52	46	42	30	32	22	—
COMPOSITION:							
Quartz	4	4	—	4	6	2	1
Mica	—	—	—	1	—	—	—
Clay	52	46	42	30	32	22	20
Volcanic glass	2	2	5	—	4	6	4
Calcite/dolomite	—	2	2	—	—	—	—
Accessory minerals	—	—	3	12	2	6	—
Opaque minerals	4	2	2	10	2	4	1
Amphibole	2	4	2	6	12	2	2
Rutile	—	—	Tr	—	—	—	—
Diatoms	35	40	40	36	42	56	70
Radiolarians	1	Tr	2	Tr	Tr	2	2
Sponge spicules	—	—	—	—	—	—	Tr
Silicoflagellates	Tr	Tr	1	1	—	—	Tr

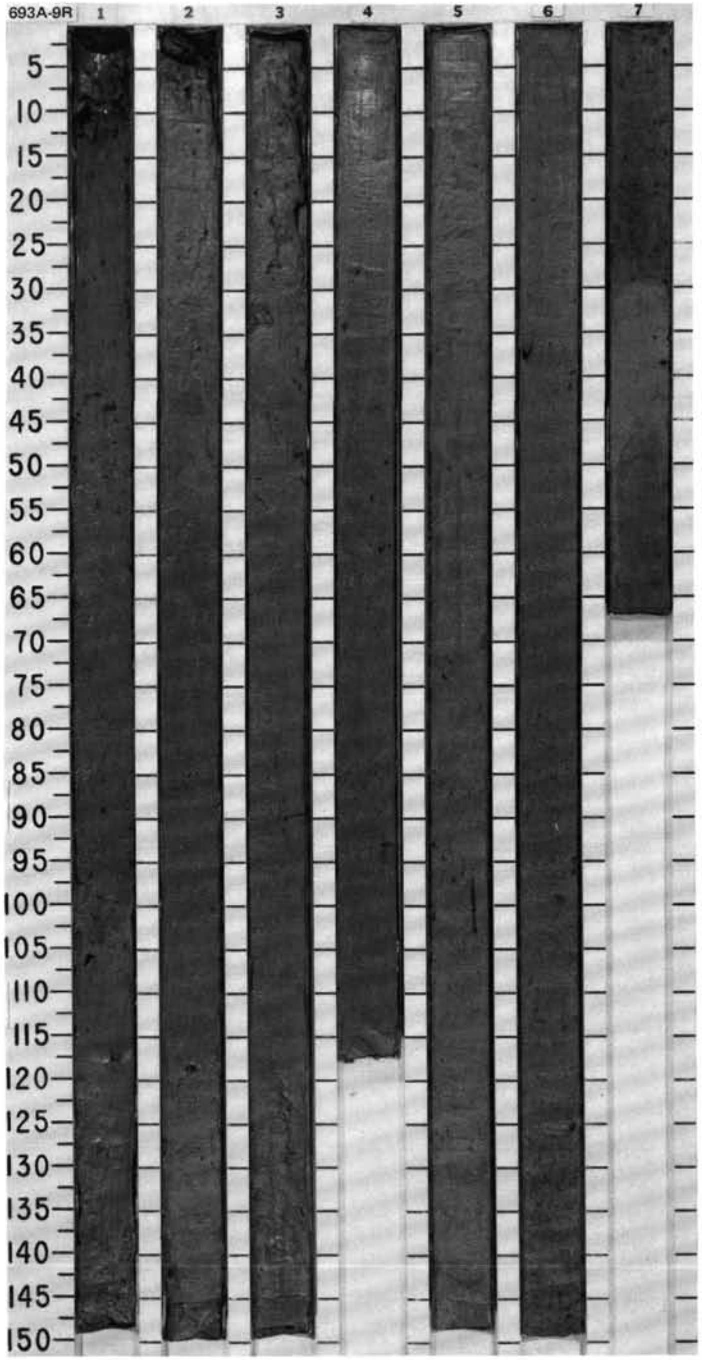

SITE 693 HOLE A CORE 10R CORED INTERVAL 2439.1-2448.7 mbsl; 79.7-89.3 mbsf

TIME-ROCK UNIT	FORAMINIFERS	NANNOFOSSILS	RADIOLARIANS	DIATOMS		PALEOMAGNETICS	PHYS. PROPERTIES	CHEMISTRY	SECTION	METERS	GRAPHIC LITHOLOGY	DRILLING DISTURB.	SED. STRUCTURES	SAMPLES
LOWER PLIOCENE	B	B	UPPER *Tau* A, G	*N. angulata - N. reinholdii* F, P	*D. boliviensis* (silicoflagellate)		●GY=2.86 ● GY=2.93	● 0.0% ● 0.0%	1, 2, 3, 4, 5, 6, 7, CC	0.5, 1.0			◇	* * * * * *

BIOSTRAT. ZONE/ FOSSIL CHARACTER

LITHOLOGIC DESCRIPTION

DIATOM CLAYEY MUD and DIATOM-BEARING CLAYEY MUD

Major lithologies: Diatom clayey mud in Sections 1, 2, 3, 4, and 6, dark greenish gray (5G 4/1). Diatom-bearing clayey mud in Section 5, dark greenish gray (5G 4/1). Primary structures destroyed by drilling.

Dropstone, 2.5 cm long, in Section 3, 100 cm. Numerous small (<2 mm) dropstones throughout core.

SMEAR SLIDE SUMMARY (%):

	1, 50 D	2, 50 D	3, 50 D	4, 50 D	5, 50 D	6, 50 D
TEXTURE:						
Sand	1	2	2	—	2	1
Silt	69	62	58	55	53	59
Clay	30	36	40	45	45	40
COMPOSITION:						
Quartz	8	8	15	5	15	11
Feldspar	5	3	—	—	—	8
Mica	—	—	3	5	—	—
Clay	30	36	40	45	45	40
Volcanic glass	5	5	—	—	—	4
Accessory minerals	3	5	8	4	10	3
Opaque minerals	3	2	3	5	10	3
Diatoms	35	40	30	35	20	30
Radiolarians	1	1	1	Tr	Tr	1
Sponge spicules	—	—	—	1	—	—
Silicoflagellates	—	—	Tr	—	Tr	—

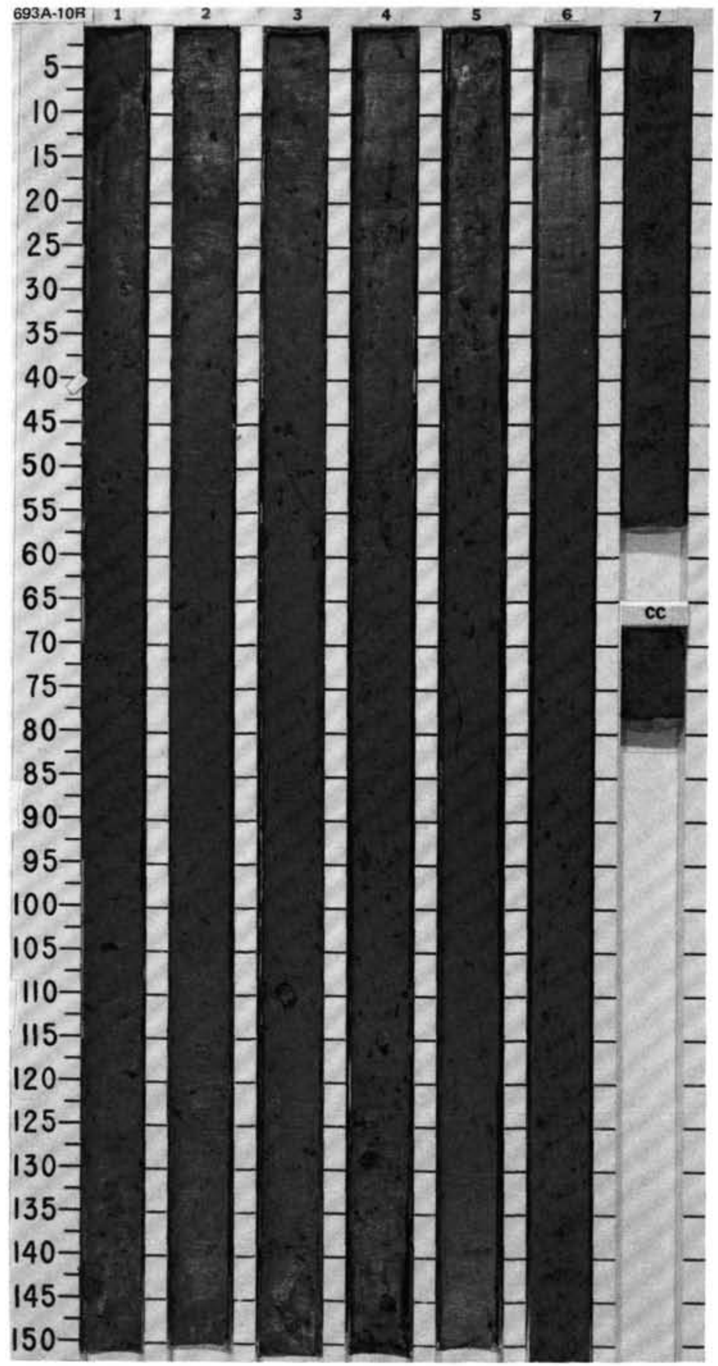

SITE 693 HOLE A CORE 11R CORED INTERVAL 2448.1-2458.3 mbsl; 89.3-98.9 mbsf

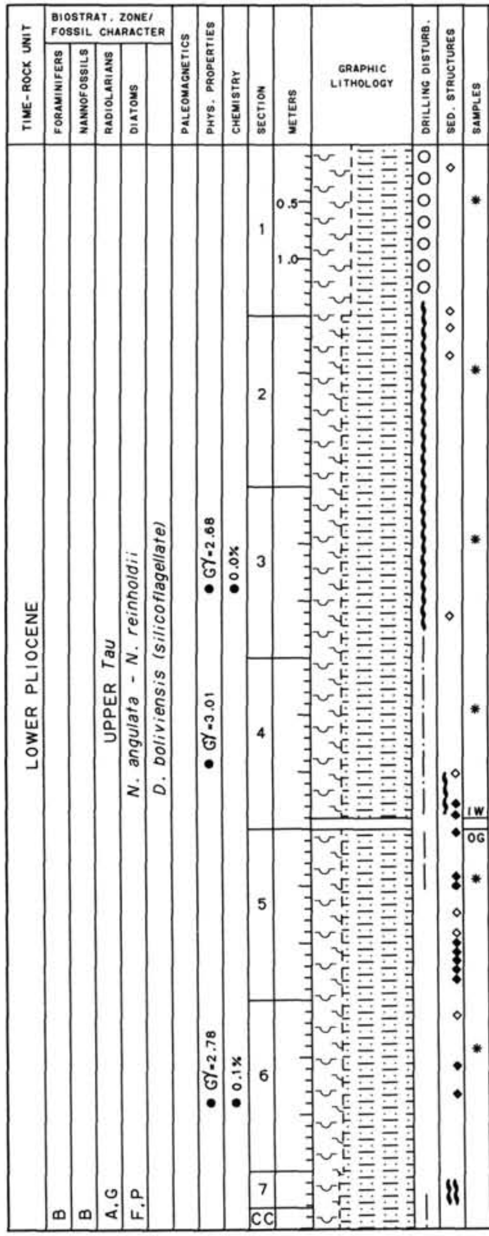

LITHOLOGIC DESCRIPTION

DIATOM CLAYEY MUD

Major lithology: Diatom clayey mud, dark greenish gray (5G 4/1 grading to 5 GY 4/1 in Sections 3 and 4), with dark greenish gray (5BG 4/1) streaks and clasts, and dark greenish gray (5G 4/1 in Section 5, 5BG 4/1 in Sections 6 and 7) with clasts of white angular sand.

Core slightly to very disturbed during drilling, and soupy in Section 1. Metamorphic dropstones occur in Section 1, 20 cm; Section 2, 5, 25, and 95 cm; Section 3, 130 cm; Section 4, 140 cm; Section 5, 75 and 90 cm; and Section 6, 20 cm. Mud clasts are present between Section 4, 100 cm, and Section 6, 85 cm. Moderately bioturbated in Section 4, 100–130 cm, and Section 7, 20–30 cm. Coarse sand fraction in Section 3 includes siliceous-*biogenic-quartz lithic fragments (igneous or metamorphic green schists?)*, feldspar, sponge spicules, glauconite, garnet, biotite, and pale gray silty mudstone.

SMEAR SLIDE SUMMARY (%):

	1, 50 D	2, 50 D	3, 50 D	4, 50 D	5, 50 D	6, 50 D
TEXTURE:						
Sand	3	7	25	15	4	7
Silt	57	52	50	55	53	43
Clay	40	41	25	30	43	50
COMPOSITION:						
Quartz	15	15	30	20	27	15
Feldspar	3	9	5	5	—	5
Mica	Tr	—	2	10	Tr	Tr
Clay	37	41	24	28	43	49
Volcanic glass	—	—	—	Tr	—	1
Accessory minerals:						
Glauconite	—	—	Tr	—	—	—
Carbonates	—	—	Tr	—	—	—
Rutile	—	—	—	—	1	—
Pyroxene	—	2	—	—	2	—
Heavy minerals	—	—	1	Tr	—	Tr
Opaque minerals	1	3	5	5	4	3
Amphiboles	1	—	—	Tr	1	Tr
Diatoms	40	29	30	30	30	25
Radiolarians	2	1	2	2	—	Tr
Sponge spicules	Tr	—	—	Tr	—	—
Silicoflagellates	1	—	1	—	1	2

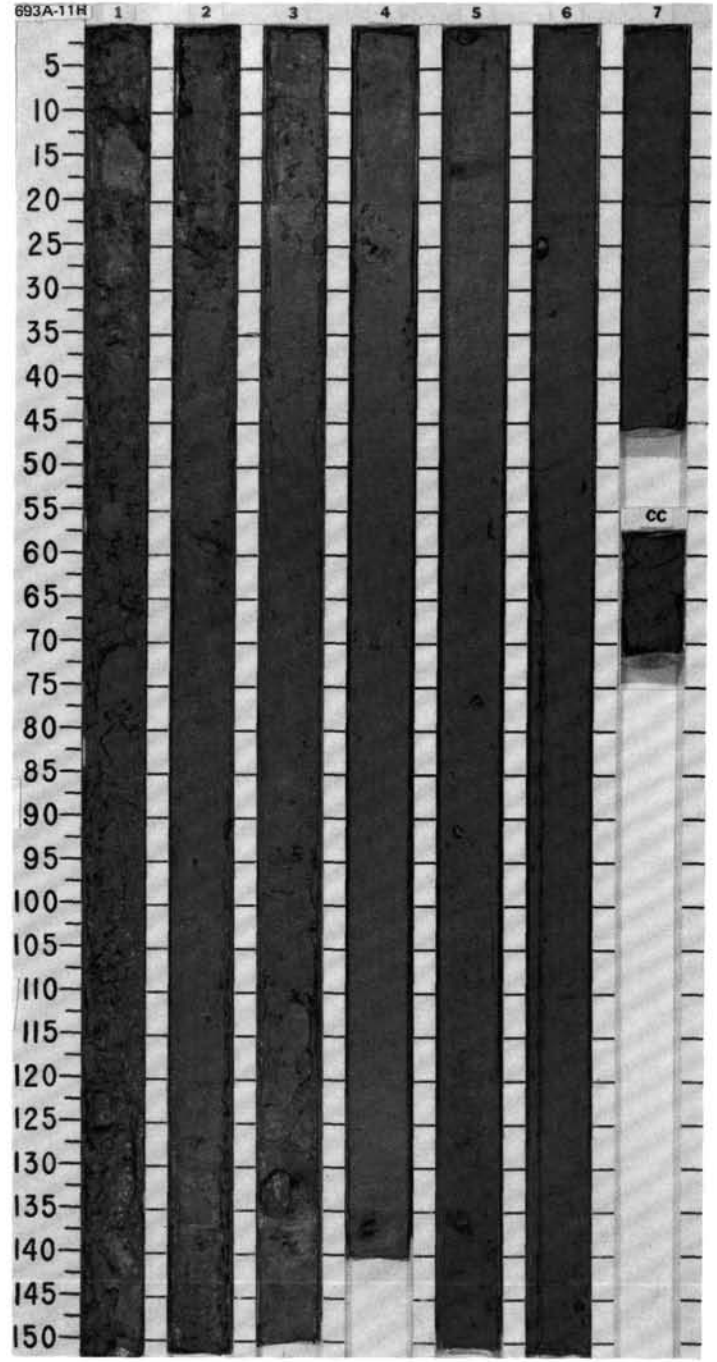

SITE 693 HOLE A CORE 12R CORED INTERVAL 2458.3-2468.0 mbsl; 98.9-108.6 mbsf

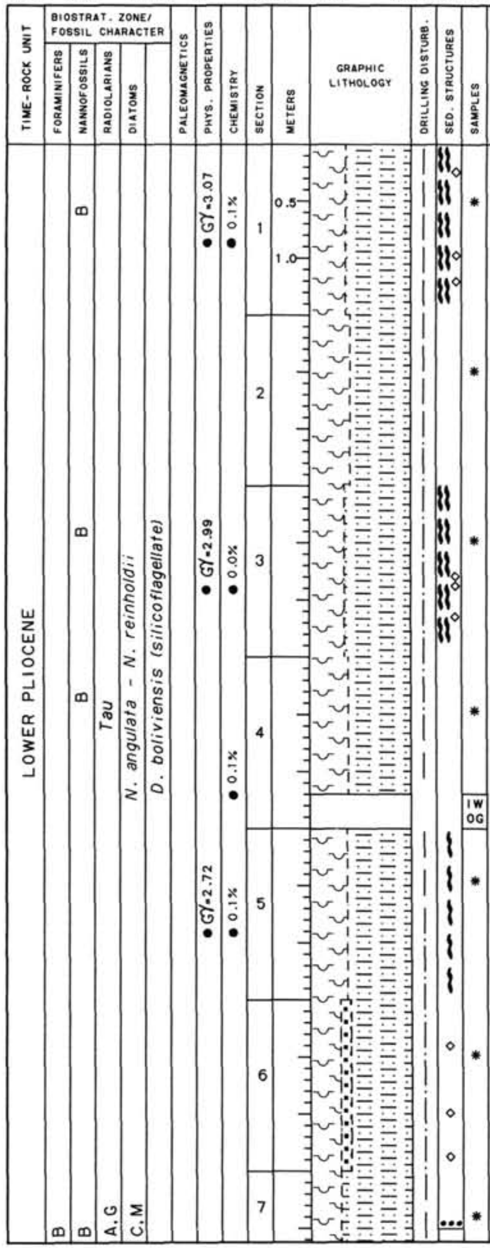

LITHOLOGIC DESCRIPTION

DIATOM CLAYEY MUD and SILICOFLAGELLATE-BEARING DIATOM CLAYEY MUD

Major lithologies: Diatom clayey mud in Sections 1 through 5 and in Section 7, dark greenish gray (5G 3/1, 4/1), with streaks of dark grayish green (5G 3/2) in Section 2. In Section 5 a greener dark greenish gray (5 4/1) in mid-section becomes lighter toward top of core. Silicoflagellate-bearing diatom clayey mud in Section 6, dark greenish gray (5GY 4/1), with faint color contrasts below 60 cm.

Coarse-grained fraction in Section 3 has many greenschists and fine-grained amphibolite fragments, diatoms, radiolarians, quartz, light gray silty mud, and other minerals (glauconite, feldspar, biotite, and ferromagnesium minerals). Dropstones throughout core: at Section 1, 20, 85, and 107 cm (acid plutonic, amphibolite, and biotite schist, respectively); Section 3, 85, 90, and 108 cm (all amphibolites); and Section 6, 45, 90, and 130 cm (amphibolites and micaceous metasediment).

SMEAR SLIDE SUMMARY (%):

	1, 50 D	2, 50 D	3, 50 D	4, 50 D	5, 50 D	6, 50 D	7, 31 M
TEXTURE:							
Sand	8	4	7	9	10	7	20
Silt	52	55	46	46	42	55	70
Clay	40	41	47	45	48	38	10
COMPOSITION:							
Quartz	11	12	8	7	5	12	50
Feldspar	5	4	3	2	1	1	10
Mica	3	Tr	1	3	5	3	—
Clay	40	41	47	45	43	38	10
Accessory minerals	—	—	2	—	—	—	—
Heavy minerals	—	—	—	—	—	—	10
Pyroxene	—	—	—	—	—	—	Tr
Glauconite	—	—	—	—	—	—	5
Rutile	1	—	Tr	Tr	—	—	—
Opaque minerals	3	2	Tr	2	3	1	10
Amphibole	2	—	—	—	—	Tr	2
Nannofossils	Tr	—	Tr	Tr	—	—	—
Diatoms	34	40	34	38	35	35	2
Radiolarians	1	1	2	Tr	1	Tr	1
Sponge spicules	—	—	—	Tr	Tr	—	—
Silicoflagellates	—	—	3	3	7	10	—

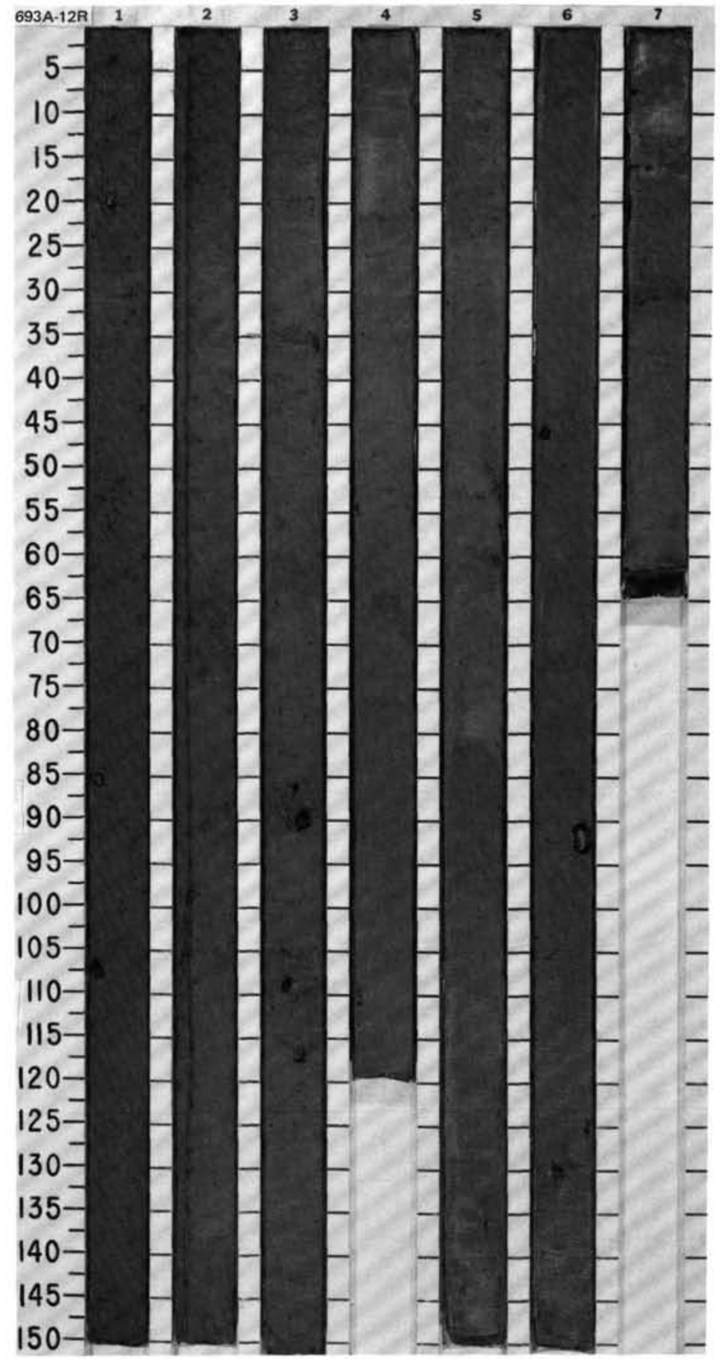

SITE 693 HOLE A CORE 13R CORED INTERVAL 2468.0-2477.6 mbsl; 108.6-118.2 mbsf

TIME-ROCK UNIT	FORAMINIFERS	NANNOFOSSILS	RADIOLARIANS	DIATOMS	PALEOMAGNETICS	PHYS. PROPERTIES	CHEMISTRY	SECTION	METERS
LOWER PLIOCENE	B	B	A, G LOWER *Tau*	F, P *N. angulata - N. reinholdii* / *D. boliviensis* (silicoflagellate)		• $\bar{G}$γ=2.67	• 0.2%	1	0.5
								2	
						• $\bar{G}$γ=2.77	• 0.2%	3	
								4	
						• $\bar{G}$γ=3.14	• 0.1%	5	
								6	
								CC	

GRAPHIC LITHOLOGY | DRILLING DISTURB. | SED. STRUCTURES | SAMPLES

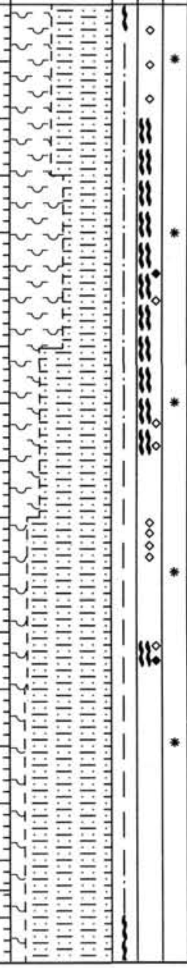

LITHOLOGIC DESCRIPTION

DIATOM CLAYEY MUD, MUDDY DIATOM OOZE, and DIATOM-BEARING SILTY MUD

Major lithologies: Diatom clayey mud in Section 1, muddy diatom ooze in Section 2, and diatom-bearing silty mud in Sections 3 through 6. Mainly dark greenish gray (5G 4/1, 5GY 4/1) and dark gray (5Y 3/1) from base of Section 4 downward.

Moderately bioturbated where slight color contrasts make burrows visible. Dropstones in Sections 1 to 4 are up to 2 cm long, and include fine-grained amphibolites, biotite schists, and a red sandstone. Scattered sand grains throughout. Coarse fraction from CC is mainly siliceous biogenic, with some pale gray siltstone; also quartz, glauconite, garnet, pyroxene, amphibole, and biotite. Tiny (<2 mm) clasts of white silty mud with very angular grains in Sections 2 and 4.

SMEAR SLIDE SUMMARY (%):

	1, 50 D	2, 50 D	3, 50 D	4, 50 D	5, 50 D
TEXTURE:					
Sand	15	—	20	10	10
Silt	40	—	50	50	45
Clay	45	25	30	40	45
COMPOSITION:					
Quartz	10	15	20	25	25
Feldspar	2	2	5	5	7
Mica	—	3	3	2	2
Clay	46	25	29	42	45
Volcanic glass	1	—	—	—	—
Accessory minerals					
Opaque minerals	3	3	7	5	5
Heavy minerals	Tr	Tr	5	2	Tr
Amphibole	Tr	—	Tr	—	—
Zeolites(?)	—	3	—	—	—
Glauconite	—	—	2	2	Tr
Foraminifers	Tr	—	—	—	—
Diatoms	30	40	20	15	15
Radiolarians	5	4	2	2	Tr
Sponge spicules	Tr	—	Tr	—	Tr
Silicoflagellates	3	5	7	Tr	1

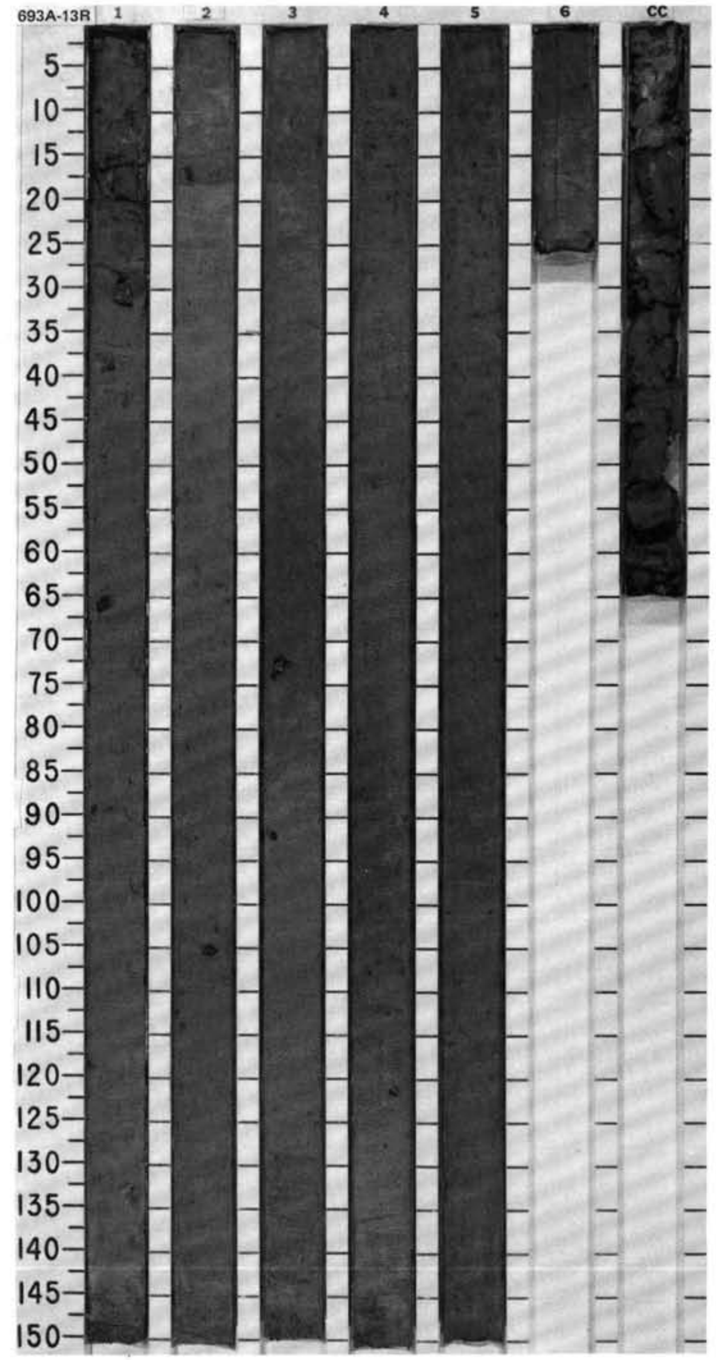

SITE 693 HOLE A CORE 14R CORED INTERVAL 2477.6-2487.2 mbsl; 118.2-127.8 mbsf

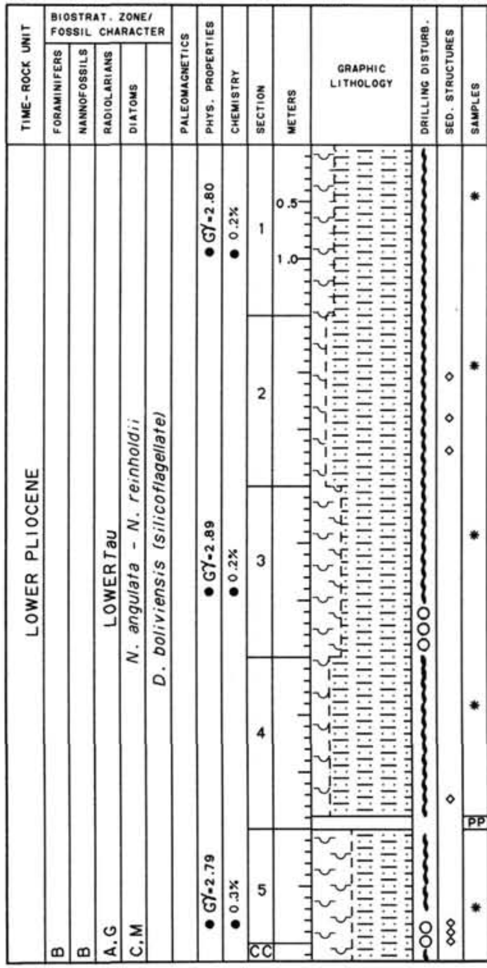

LITHOLOGIC DESCRIPTION

DIATOM-BEARING CLAYEY MUD and DIATOM CLAYEY MUD

Major lithologies: Diatom-bearing clayey mud, dark greenish gray (5GY 3/1, 4/1) approaching gray (N 4/0, 3/0), and streaks of dark greenish gray (5GY 4/1) in gray (N 4/0). Entire core badly disturbed by drilling operations and homogenized in parts; Section 1 and mid-section of Section 3 are soupy. Diatom clayey mud in Section 3 is dark greenish gray (5GY 3/1) and slightly streaky with subtle color variations.

Dropstones in Section 2, 67, 97, and 110 cm (shale and granite stones), Section 4, 125 cm (granodiorite), and Section 5, 90–100 cm (basalt and greenschist). Scattered sand grains throughout core.

SMEAR SLIDE SUMMARY (%):

	1, 50 D	2, 50 D	3, 50 D	4, 50 D	5, 70 M
TEXTURE:					
Sand	—	10	20	5	3
Silt	—	40	30	45	52
Clay	—	50	50	50	45
COMPOSITION:					
Quartz	15	20	10	15	10
Feldspar	5	5	2	5	2
Mica	1	1	—	Tr	—
Clay	41	48	51	52	45
Calcite	—	—	Tr	—	—
Accessory minerals:					
Hornblende	—	—	—	—	1
Zeolites(?)	—	—	1	—	—
Pyroxene	—	—	Tr	Tr	—
Amphibole	—	1	—	—	—
Glauconite	Tr	Tr	Tr	—	—
Heavy minerals	1	2	2	Tr	—
Opaque minerals	10	5	3	3	—
Diatoms	25	15	30	20	40
Radiolarians	2	3	1	5	1
Sponge spicules	Tr	—	—	Tr	1
Silicoflagellates	Tr	—	Tr	—	Tr

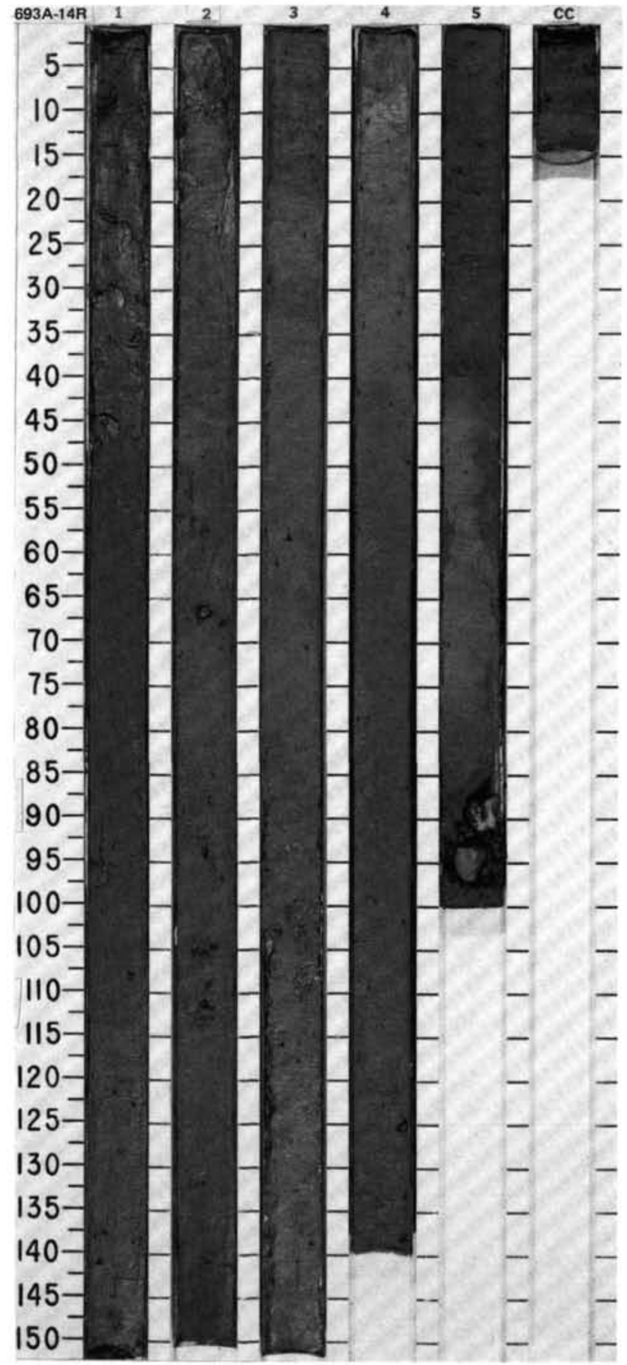

SITE 693 HOLE A CORE 15R CORED INTERVAL 2487.2-2496.9 mbsl; 127.8-137.5 mbsf

TIME-ROCK UNIT	BIOSTRAT. ZONE/ FOSSIL CHARACTER: FORAMINIFERS	NANNOFOSSILS	RADIOLARIANS	DIATOMS		PALEOMAGNETICS	PHYS. PROPERTIES	CHEMISTRY	SECTION	METERS	GRAPHIC LITHOLOGY	DRILLING DISTURB.	SED. STRUCTURES	SAMPLES
LOWER PLIOCENE	B	B	A.G LOWER N. angulata - N. reinholdii Tau	C.M N. reinholdii Zone (?)	D. pseudofibula (silicoflagellate)		• GY-2.79; • GY-2.92	• 0.2%; • 0.1%	1, 2, 3, 4	0.5, 1.0	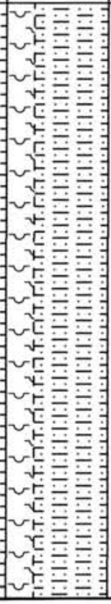			

LITHOLOGIC DESCRIPTION

DIATOM CLAYEY MUD

Major lithology: Diatom clayey mud, dark greenish gray (5G 4/1, 5BG 4/1); dark bluish gray (5B 4/1) level in Section 4.

Section 1, 0 cm, to Section 2, 40 cm, is soupy, homogenous. Section 2, 40-65 cm, and Section 4, 40-70 cm, is disturbed. Dropstones in Section 2, 16 and 72 cm; Section 3, 12 and 116 cm; and Section 4, 30, 58, and 67 cm. Scattered sand grains throughout.

SMEAR SLIDE SUMMARY (%):

	1, 50 D	2, 50 D	3, 50 D	4, 60 D
TEXTURE:				
Sand	3	6	2	6
Silt	56	47	54	42
Clay	41	47	44	52
COMPOSITION:				
Quartz	14	14	11	9
Feldspar	2	2	3	2
Mica	—	Tr	—	—
Clay	41	47	44	52
Accessory minerals:				
Rutile	Tr	—	—	—
Opaque minerals	7	3	2	2
Amphibole	—	—	1	—
Diatoms	33	30	36	31
Radiolarians	1	3	2	2
Sponge spicules	Tr	Tr	Tr	Tr
Silicoflagellates	2	1	1	2

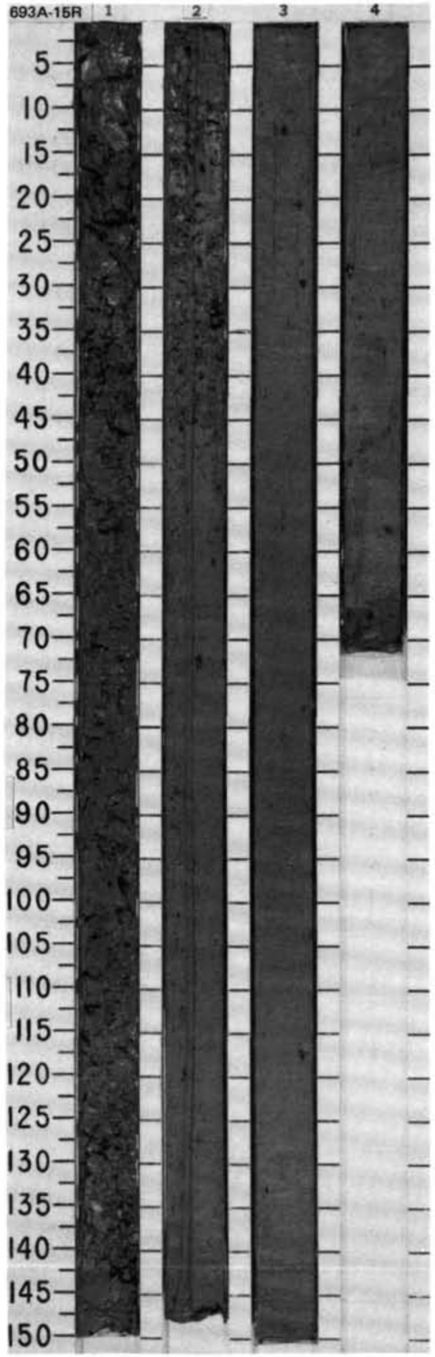

SITE 693 HOLE A CORE 16R CORED INTERVAL 2496.9-2506.6 mbsl; 137.5-147.2 mbsf

TIME-ROCK UNIT	FORAMINIFERS	NANNOFOSSILS	RADIOLARIANS	DIATOMS		PALEOMAGNETICS	PHYS. PROPERTIES	CHEMISTRY	SECTION	METERS	GRAPHIC LITHOLOGY	DRILLING DISTURB.	SED. STRUCTURES	SAMPLES
LOWER PLIOCENE	B	B	A,M LOWER Tau	C,M N. angul - N. reinh	D. pseudofibulas (silicoflagellate)		● GY=2.61	● 0.2%	1	0.5, 1.0				* *

BIOSTRAT. ZONE/FOSSIL CHARACTER

LITHOLOGIC DESCRIPTION

DIATOM CLAYEY MUD

Major lithology: Diatom clayey mud, dark greenish gray (5G 3/1, 4/1) and dark gray (5G 4.5/1); top half of section disturbed.

Minor lithology: Diatom silty mud, dark greenish gray (5G 4/1) and very dark gray (N 3/0), with many dropstones.

Dropstones at Section 1, 0, and 20 cm, and between 118 and 131 cm. Dropstones are granodiorite, gneiss, and quartzite. Scattered sand grains throughout.

SMEAR SLIDE SUMMARY (%):

	1, 50 D	1, 120 D
TEXTURE:		
Sand	7	10
Silt	48	60
Clay	45	30
COMPOSITION:		
Quartz	15	20
Feldspar	2	3
Mica	—	Tr
Clay	46	30
Accessory minerals:		
Pyroxene	—	1
Opaques	3	3
Amphibole	Tr	—
Heavy minerals	1	Tr
Glauconite	—	Tr
Diatoms	30	40
Radiolarians	2	3
Sponge spicules	Tr	Tr
Silicoflagellates	1	—

SITE 693 HOLE A CORE 17R CORED INTERVAL 2506.6-2516.3 mbsl; 147.2-156.9 mbsf

TIME-ROCK UNIT	FORAMINIFERS	NANNOFOSSILS	RADIOLARIANS	DIATOMS	PALEOMAGNETICS	PHYS. PROPERTIES	CHEMISTRY	SECTION	METERS
LOWER PLIOCENE	B	B	A,M LOWER *Tau*	C,M *N. angulata - N. reinholdii*; *M. diodon* (silicoflagellate)		• γ=2.85	• 0.3%	1, 2, 3	0.5, 1.0

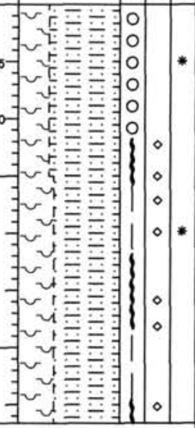

LITHOLOGIC DESCRIPTION

DIATOM CLAYEY MUD

Major lithology: Diatom clayey mud, dark greenish gray (5GY 4/1, 5G 4/1, 5BG 4/1) and dark greenish gray (5G 3/1), in 5-cm dark gray (N 3/0) layer at top of Section 1. Smeared during drilling, but sharp color boundaries remain at Section 2, 96 cm, and Section 3, 35 cm.

Scattered sand grains throughout core. Dropstones in all sections, all less than 8 mm across, include granite(?) and slate.

SMEAR SLIDE SUMMARY (%):

	1, 50 D	2, 50 D
TEXTURE:		
Sand	3	5
Silt	47	47
Clay	50	48
COMPOSITION:		
Quartz	12	12
Feldspar	3	3
Mica	Tr	Tr
Clay	50	48
Accessory minerals:		
Opaque minerals	3	2
Glauconite	—	1
Nannofossils	Tr	—
Diatoms	29	33
Radiolarians	3	Tr
Sponge spicules	Tr	1

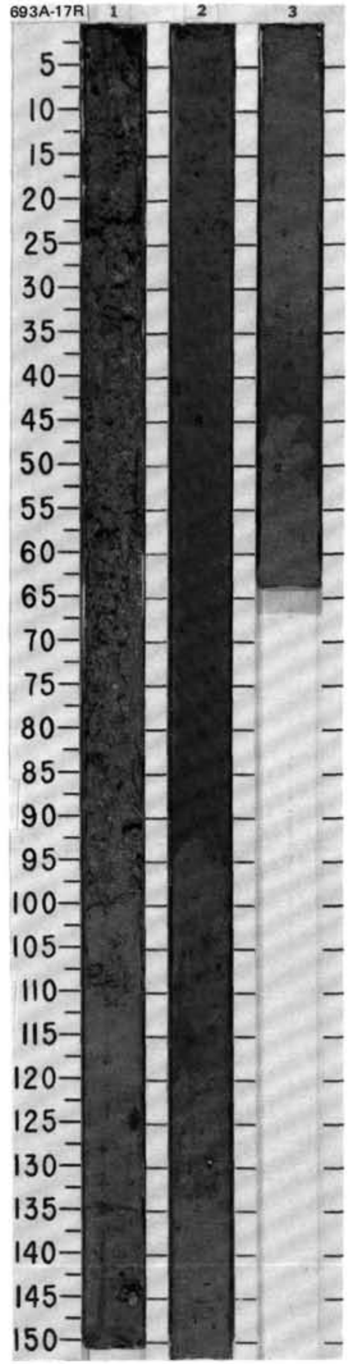

SITE 693 HOLE A CORE 18R CORED INTERVAL 2516.3-2526.0 mbsl; 156.9-166.6 mbsf

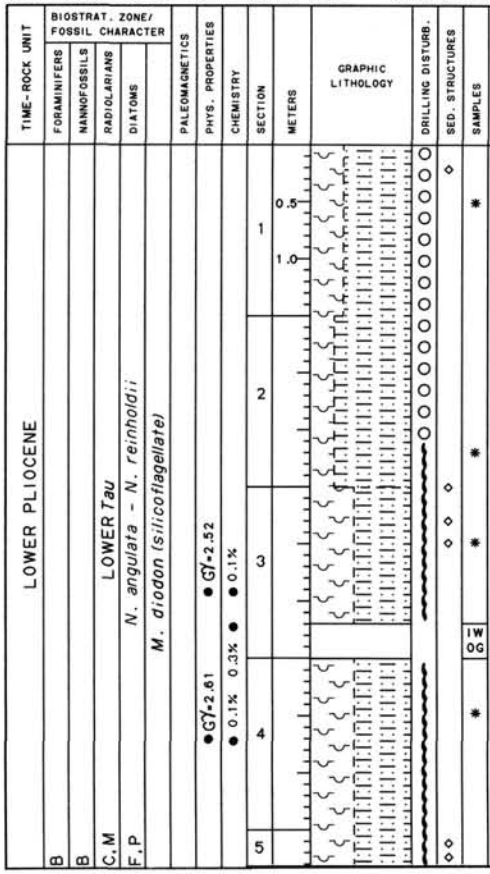

LITHOLOGIC DESCRIPTION

DIATOM CLAYEY MUD

Major lithology: Diatom clayey mud in Sections 1, 2, 4, and 5, dark greenish gray (5GY 4/1) fading into greenish gray (5G 5/1) with dark gray (5Y 4/1), vertically elongated (by drilling disturbance), mottled. All primary structures marred by drilling disturbance.

Large (50-60 mm) dropstones in top and base of core. Numerous sand-sized dropstones throughout. Numerous small (<2 mm) dropstones and larger (4-10 mm) dropstones in Section 3, 15, 45, and 50 cm.

SMEAR SLIDE SUMMARY (%):

	1, 50 D	2, 125 D	3, 50 D	4, 50 D
TEXTURE:				
Sand	—	Tr	—	—
Silt	58	58	52	56
Clay	42	42	48	44
COMPOSITION:				
Quartz	15	18	5	10
Feldspar	1	4	—	—
Mica	1	1	—	1
Clay	42	42	48	44
Calcite/dolomite	—	2	—	—
Accessory minerals	4	5	—	—
Opaque minerals	4	2	1	2
Amphibole	3	Tr	3	4
Diatoms	30	26	40	37
Radiolarians	Tr	—	2	2
Silicoflagellates	Tr	—	1	Tr

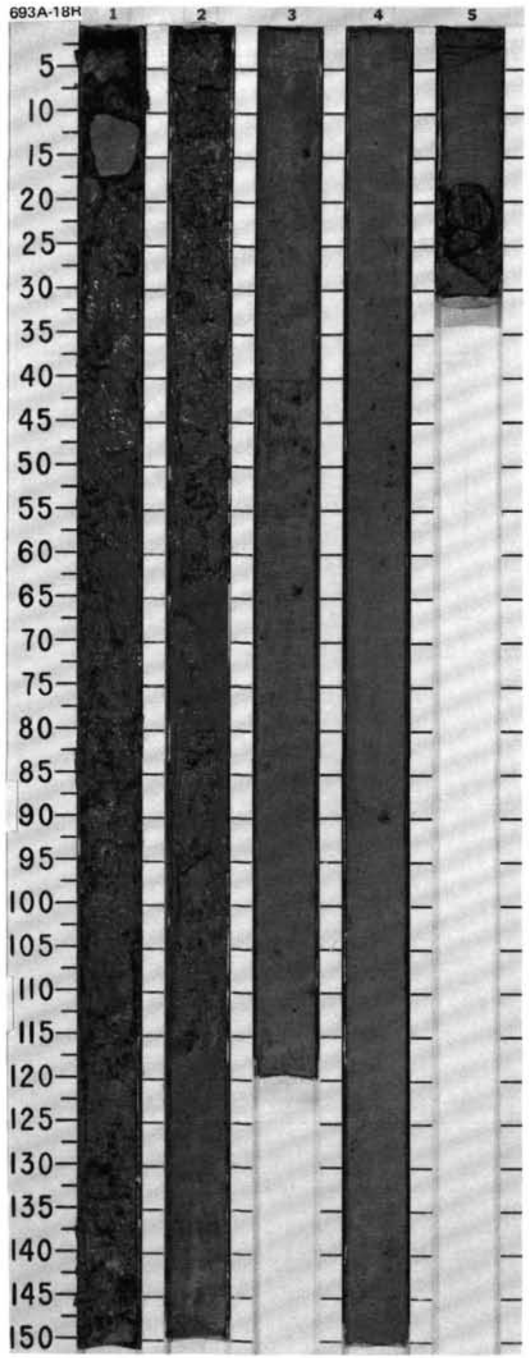

SITE 693 HOLE A CORE 19R CORED INTERVAL 2526.0-2535.7 mbsl; 166.6-176.3 mbsf

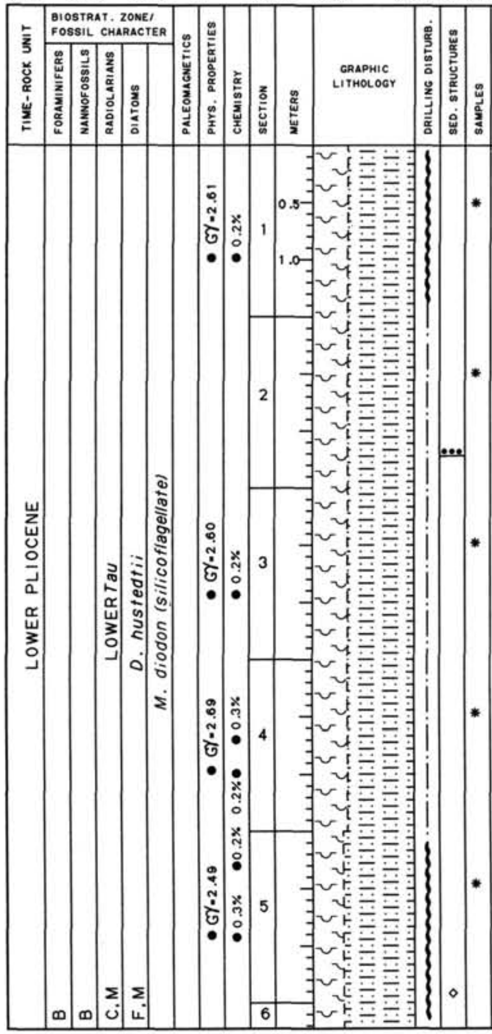

LITHOLOGIC DESCRIPTION

DIATOM CLAYEY MUD

Major lithology: Diatom clayey mud, dark greenish gray (5G 4/1), changing into greenish gray (5GY 4/1) in Section 2. Darker greenish gray (5BG 4/1) in Section 1, 0–30 cm, and dark gray (5Y 4/1) in Section 5, 40–100 cm, show disturbed (by drilling) color transitions. Drilling disturbance varies from strong *to moderate. A thin, sandy, dark gray (5Y 4/1) layer with its base at Section 2,* 127 cm, is interpreted as part of a small turbidite.

Small (mm sized) dropstones are found throughout the core; many of them are buried in the sediment. Their abundance increases in lower half of Sections 3 and 4. A 3-cm dropstone is observed in Section 5, 140 cm.

SMEAR SLIDE SUMMARY (%):

	1, 50 D	*2, 50* D	*3, 50* D	*4, 50* D	*5, 50* D
TEXTURE:					
Sand	—	3	—	1	—
Silt	64	57	56	61	60
Clay	36	40	44	38	40
COMPOSITION:					
Quartz	12	15	8	12	15
Feldspar	3	2	2	2	5
Mica	4	—	4	3	—
Clay	36	40	44	38	40
Volcanic glass	2	—	2	1	3
Accessory minerals	5	4	—	4	3
Amphiboles	1	—	1	2	—
Opaque minerals	1	2	1	1	3
Diatoms	35	35	38	37	30
Radiolarians	1	2	Tr	—	1
Silicoflagellates	Tr	—	Tr	—	—

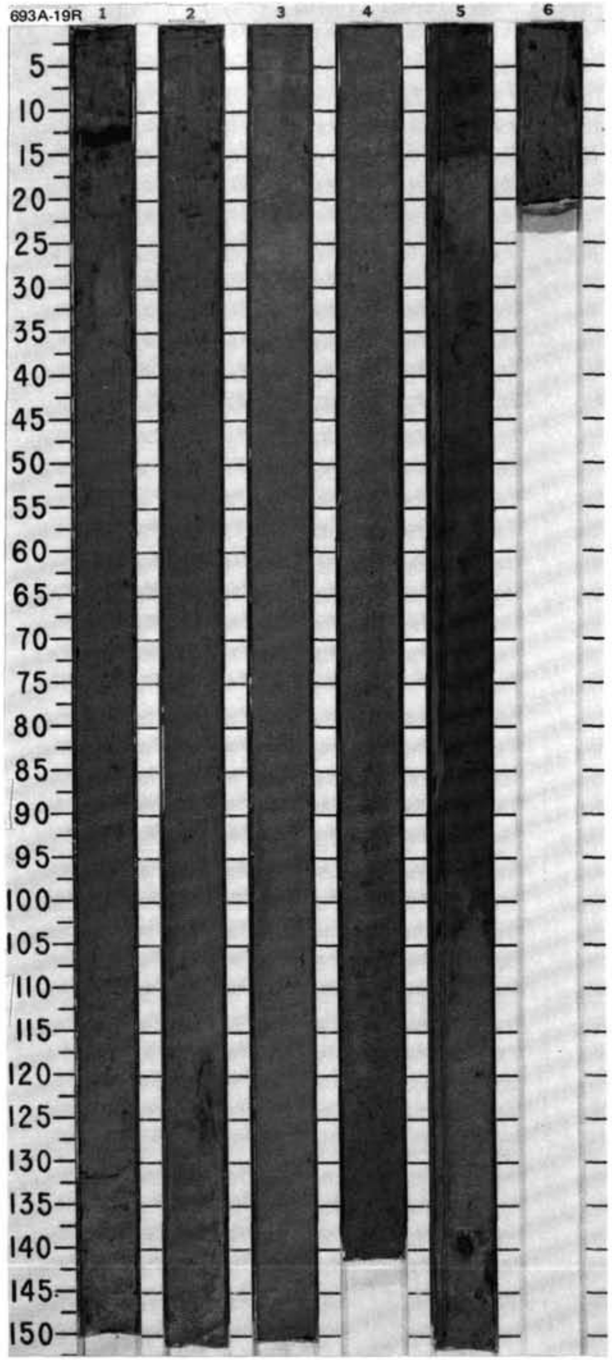

SITE 693 HOLE A CORE 20R CORED INTERVAL 2535.7-2545.3 mbsl; 176.3-185.9 mbsf

TIME-ROCK UNIT	FORAMINIFERS	NANNOFOSSILS	RADIOLARIANS	DIATOMS		PALEOMAGNETICS	PHYS. PROPERTIES	CHEMISTRY	SECTION	METERS	GRAPHIC LITHOLOGY	DRILLING DISTURB.	SED. STRUCTURES	SAMPLES
LOWER PLIOCENE	B	F, G	C, M LOWER *Tau*	C, P *D. hustedtii*	*M. diodon (silicoflagellate)*				1					*

BIOSTRAT. ZONE/FOSSIL CHARACTER

LITHOLOGIC DESCRIPTION

DROPSTONES

Major lithology: Dropstones, very dark greenish gray (5GY 3/1). Four subrounded to subangular dropstones and one lump of diatom mud.

SMEAR SLIDE SUMMARY (%):

	1, 2 M
TEXTURE:	
Sand	3
Silt	57
Clay	40
COMPOSITION:	
Quartz	14
Feldspar	3
Clay	40
Volcanic glass	2
Accessory minerals:	
Hornblende	2
Opaque minerals	2
Foraminifers	Tr
Nannofossils	1
Diatoms	35
Radiolarians	1
Sponge spicules	Tr

SITE 693 HOLE A CORE 21R CORED INTERVAL 2545.3-2555.0 mbsl; 185.9-195.6 mbsf

TIME-ROCK UNIT	FORAMINIFERS	NANNOFOSSILS	RADIOLARIANS	DIATOMS		PALEOMAGNETICS	PHYS. PROPERTIES	CHEMISTRY	SECTION	METERS	GRAPHIC LITHOLOGY	DRILLING DISTURB.	SED. STRUCTURES	SAMPLES
UPPER MIOCENE	B	B	C, M UPPER *C. spongothorax*	F, P *D. hustedtii*	*M. diodon (silicoflagellate)*		• γ=2.94	• 0.2%	1, 2	0.5, 1.0	VOID			* * *

BIOSTRAT. ZONE/FOSSIL CHARACTER

LITHOLOGIC DESCRIPTION

DIATOM CLAYEY MUD

Major lithology: Diatom clayey mud, mainly dark greenish gray (5GY 3/1) with some dark greenish gray (5GY 4/1) bands, colors swirled together during drilling, no primary structures. Only a few scattered sand grains.

Minor lithology: Sandy mud (70% very fine sand, 25% coarse silt, i.e., well-sorted) as small clasts which may be the remains of very thin beds. This forms about 10% of the sediment at the base of Section 1. Color is dark gray (5Y 3/1). Clasts are 5-15 mm across and angular.

Dropstones in Section 2: sub-rounded intermediate gneiss 7 cm long at 115 cm, and angular acid gneiss 1 cm long at 20 cm.

SMEAR SLIDE SUMMARY (%):

	1, 50 D	2, 50 D	1, 125 M
TEXTURE:			
Sand	7	7	70
Silt	46	44	25
Clay	47	49	5
COMPOSITION:			
Quartz	12	14	50
Feldspar	2	3	7
Clay	47	49	5
Accessory minerals	—	—	7
Opaque minerals	3	2	15
Amphibole/pyroxene	1	1	7
Glauconite	—	Tr	4
Epidote	—	—	5
Diatoms	35	31	Tr
Sponge spicules	—	—	Tr

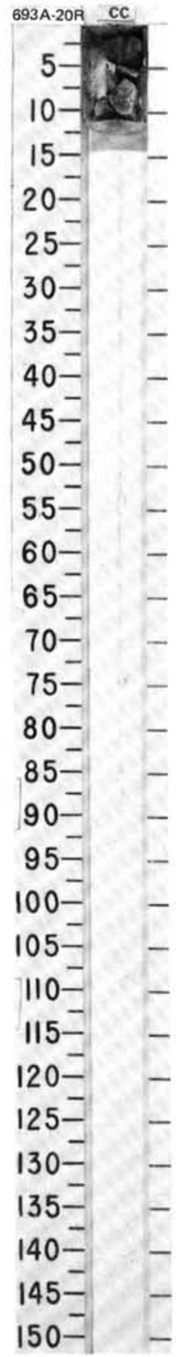

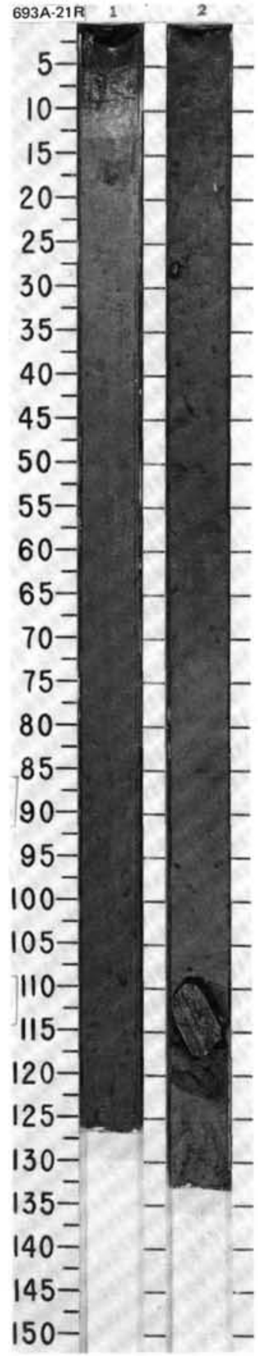

SITE 693 HOLE A CORE 22R CORED INTERVAL 2555.0-2564.1 mbsl; 195.6-205.3 mbsf

TIME-ROCK UNIT	BIOSTRAT. ZONE/FOSSIL CHARACTER: FORAMINIFERS	NANNOFOSSILS	RADIOLARIANS	DIATOMS		PALEOMAGNETICS	PHYS. PROPERTIES	CHEMISTRY	SECTION	METERS	GRAPHIC LITHOLOGY	DRILLING DISTURB.	SED. STRUCTURES	SAMPLES
UPPER MIOCENE	B	B	A,G UPPER C. spongothorax	F,M D. hustedtii	M. circulus (silicoflagellate)				1, 2, 3, CC	0.5, 1.0	VOID			* * *

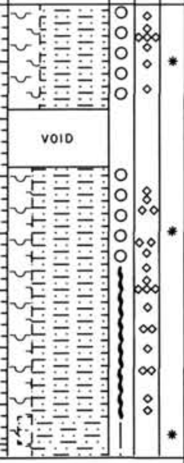

LITHOLOGIC DESCRIPTION

DIATOM CLAYEY MUD and DIATOM SILTY MUD

Major lithologies: Diatom clayey mud in Section 1, dark greenish gray (5GY 4/1). Diatom silty mud in Section 2 and Section 3, 0–68 cm, dark greenish gray (5GY 4/1).

Minor lithology: Diatom-bearing clayey mud in Section 3, 68–80 cm, very dark greenish gray (5G 3/1).

Soupy and very disturbed core. Ice-rafted detritus common throughout the core, mainly lithified dropstones, also mud clasts and pockets of sand, Section 1, 20–30 cm, and Section 3, 55 cm. Lithified dropstones include fragments of amphibolite, gneiss, quartzite, diorite, granodiorite, chlorite-garnet schist, schist, and mudstone.

SMEAR SLIDE SUMMARY (%):

	1, 50 D	2, 50 D	3, 75 M
TEXTURE:			
Sand	10	15	7
Silt	50	50	43
Clay	40	35	50
COMPOSITION:			
Quartz	15	25	20
Feldspar	5	5	5
Mica	1	—	1
Clay	40	35	49
Calcite/dolomite	—	Tr	—
Accessory minerals:			
Glauconite	Tr	1	3
Amphibole	—	Tr	—
Pyroxene	—	—	Tr
Heavy minerals	3	1	3
Opaque minerals	3	3	5
Epidote	2	2	3
Foraminifers	—	1	—
Diatoms	30	25	10
Radiolarians	1	2	Tr
Sponge spicules	Tr	Tr	1

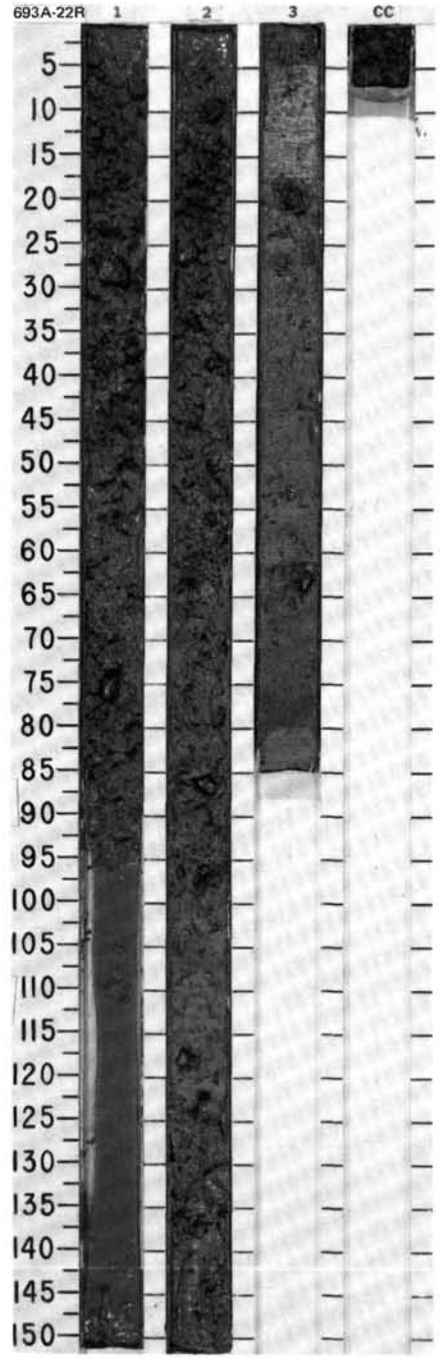

SITE 693 HOLE A CORE 23R CORED INTERVAL 2564.7-2574.3 mbsl; 205.3-214.9 mbsf

TIME-ROCK UNIT	BIOSTRAT. ZONE/ FOSSIL CHARACTER					PALEOMAGNETICS	PHYS. PROPERTIES	CHEMISTRY	SECTION	METERS	GRAPHIC LITHOLOGY	DRILLING DISTURB.	SED. STRUCTURES	SAMPLES	LITHOLOGIC DESCRIPTION
	FORAMINIFERS	NANNOFOSSILS	RADIOLARIANS	DIATOMS											
UPPER MIOCENE		B	B	*D. hustedtii* F,M					1 2	0.5 1.0					Minimal recovery, all sediment given to paleontologists.

SITE 693 HOLE A CORE 24R CORED INTERVAL 2574.3-2584.0 mbsl; 214.9-224.6 mbsf

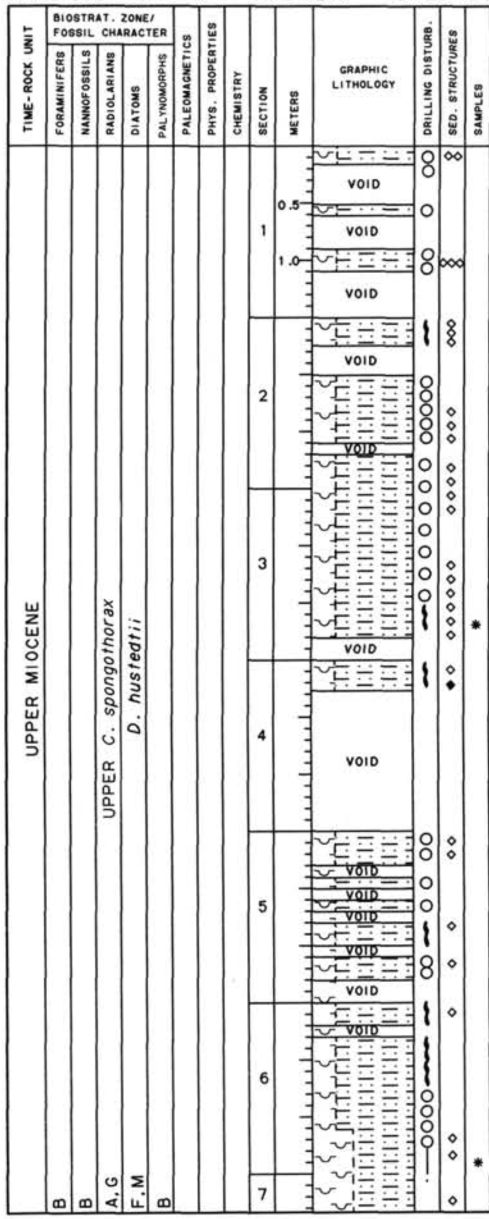

LITHOLOGIC DESCRIPTION

DIATOM-BEARING CLAYEY MUD and DIATOM SILTY MUD

Major lithologies: *Diatom-bearing clayey mud and diatom silty mud*. The two lithologies are intimately mixed by severe drilling disturbance (only coherent part is lowest half meter). Dark greenish gray (5GY 4/1) with pockets of very dark greenish gray (5G 3/1) in Sections 5 and 6; base of Section 7 is dark greenish gray (5GY 4/1).

Abundant dropstones in all sections, commonly 1-3 cm across.

SMEAR SLIDE SUMMARY (%):

	3, 120 D	6, 144 D
TEXTURE:		
Sand	3	10
Silt	52	60
Clay	45	30
COMPOSITION:		
Quartz	18	18
Feldspar	5	7
Clay	45	30
Accessory minerals:		
Hornblende	7	3
Opaque minerals	3	—
Diatoms	20	40
Radiolarians	2	2
Sponge spicules	Tr	Tr
Silicoflagellates	Tr	Tr

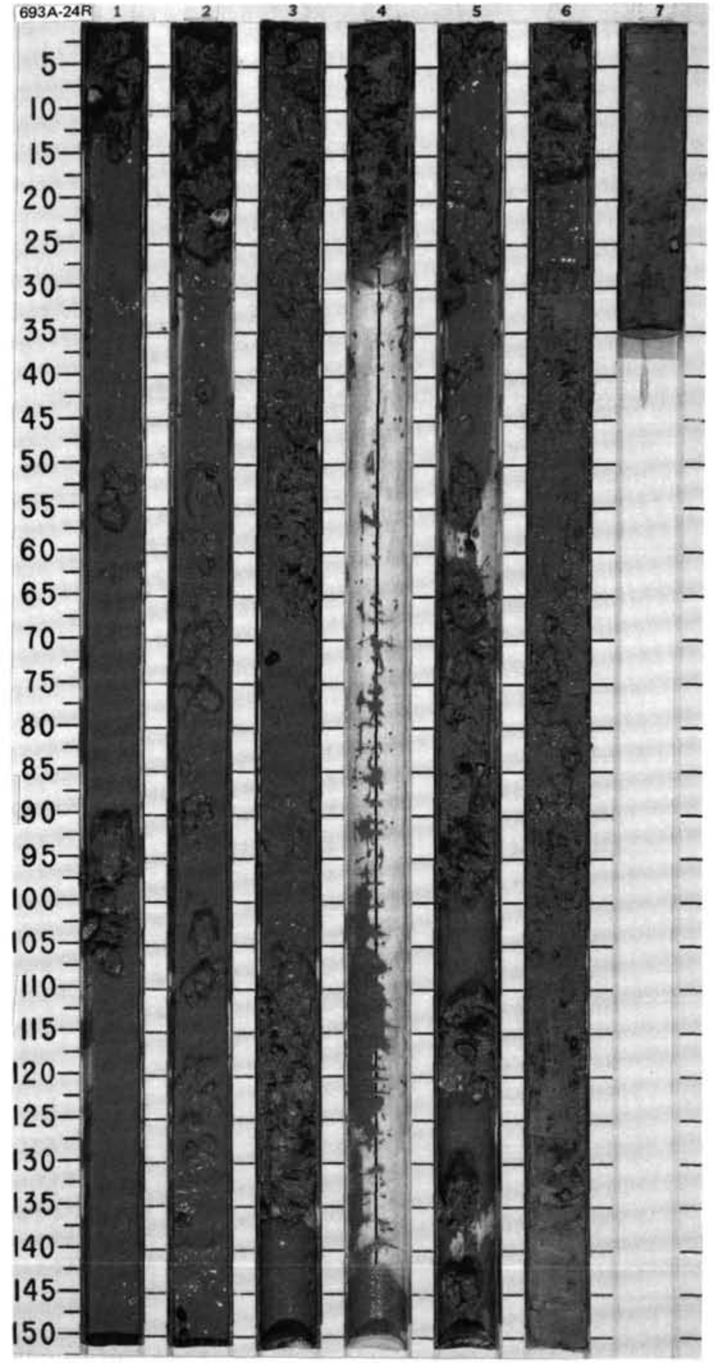

SITE 693 HOLE A CORE 25R CORED INTERVAL 2584.0-2593.7 mbsl; 224.6-234.3 mbsf

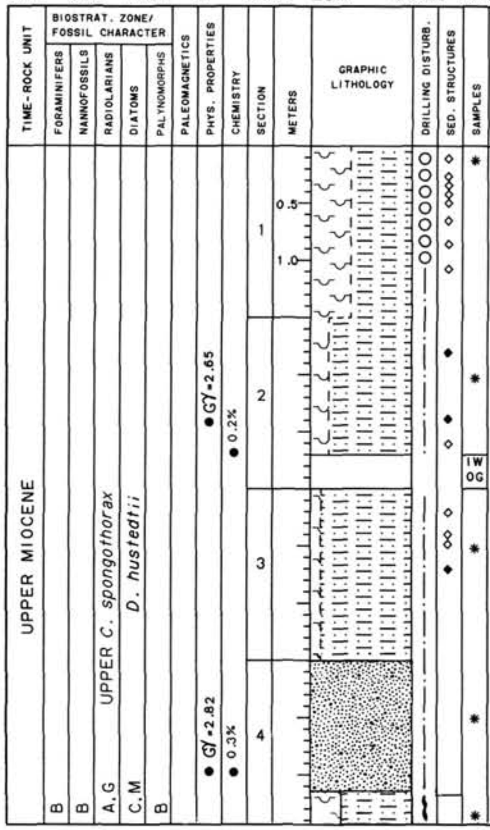

LITHOLOGIC DESCRIPTION

DIATOM CLAYEY MUD, DIATOM-BEARING CLAYEY MUD, and SILTY MUD

Major lithologies: Diatom clayey mud in Section 1, dark greenish gray (5GY 4/1); diatom-bearing clayey mud in Sections 2 and 3, dark greenish gray (5GY 4/1); and silty mud in Section 4, dark greenish gray (5G 3/1). Percentage of diatoms decreases downward from the top of the core to Section 3, about 120 cm, where silty mud sharply overlies dark greenish gray (5G 4/1) diatom mud, though contact is disturbed by drilling.

Minor lithology: Small (2-3 mm) pockets of white sand in Sections 2 and 3.

Abundant dropstones in Section 1, upper 85 cm, may have fallen downhole. The identifiable ones are metamorphic and plutonic.

SMEAR SLIDE SUMMARY (%):

	1, 10 D	2, 50 D	3, 50 D	4, 50 D	4, 142 M
TEXTURE:					
Sand	2	2	2	5	7
Silt	50	41	43	50	48
Clay	48	57	55	45	45
COMPOSITION:					
Quartz	8	19	20	30	15
Feldspar	2	5	5	10	3
Mica	—	—	1	1	Tr
Clay	48	57	57	43	47
Volcanic glass	—	—	—	—	Tr
Accessory minerals:					
Opaque minerals	2	2	3	5	1
Heavy minerals	—	2	3	4	2
Glauconite	—	1	—	—	—
Diatoms	39	14	10	7	30
Radiolarians	—	Tr	1	—	2
Sponge spicules	Tr	—	Tr	Tr	—
Silicoflagellates	1	—	—	—	—

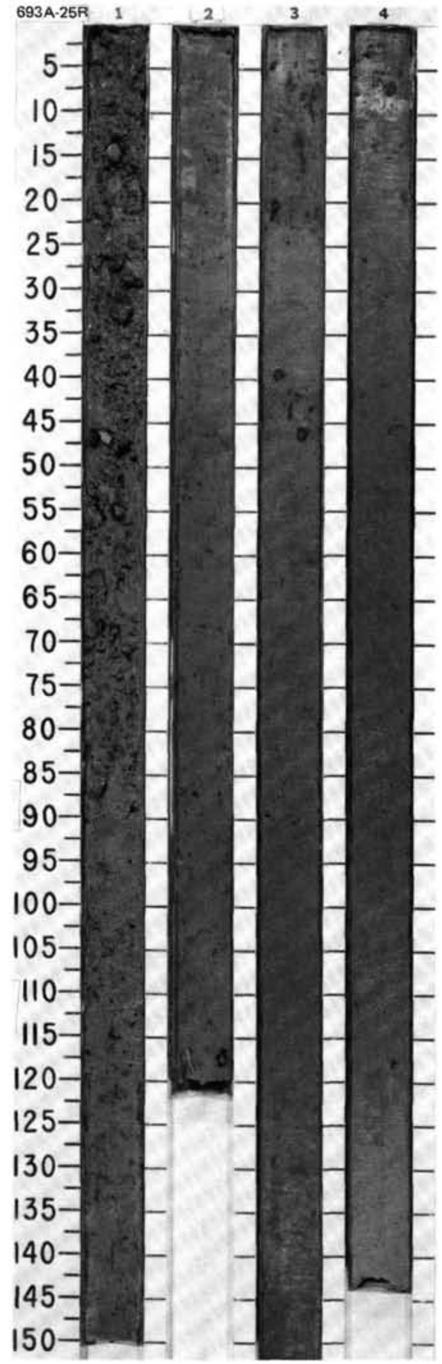

SITE 693 HOLE A CORE 26R CORED INTERVAL 2593.7-2603.3 mbsl; 234.3-243.9 mbsf

TIME-ROCK UNIT	FORAMINIFERS	NANNOFOSSILS	RADIOLARIANS	DIATOMS	PALYNOMORPHS	PALEOMAGNETICS	PHYS. PROPERTIES	CHEMISTRY	SECTION	METERS
UPPER MIOCENE	B	F,G	A,G MIDDLE C. spongothorax	C,M D. hustedtii	B		● GY=2.37 ● GY=2.79	● 0.3% ● 0.3%	1, 2, 3, 4, 5, CC	0.5, 1.0

BIOSTRAT. ZONE/ FOSSIL CHARACTER

GRAPHIC LITHOLOGY

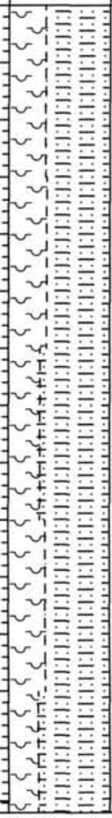

DRILLING DISTURB. · SED. STRUCTURES · SAMPLES

LITHOLOGIC DESCRIPTION

DIATOM CLAYEY MUD

Major lithology: Diatom clayey mud, greenish gray (5G 5/1) and dark greenish gray (5G 4/1), with thin layers and mottles of dark grayish brown (2.5Y 3/2), dark gray (N 4/0, 5Y 4/1), and gray (N 5/0).

First three sections are soupy and highly deformed. Sections 4 and 5 show minor disturbed layering and mottles which may, in part, be attributed to bioturbation. Colors are even, and though deformed give some hint of cyclicity. In Section 4 a faint greenish gray (5G 5/1) horizon occurs at several intervals. A 4-cm-long, slightly metamorphosed, igneous plutonic rock is present as a dropstone in Section 4, 81 cm.

SMEAR SLIDE SUMMARY (%):

	1, 90 D	2, 55 D	3, 55 D	4, 55 D	5, 50 D
TEXTURE:					
Sand	1	4	6	6	3
Silt	56	58	62	54	57
Clay	43	38	32	40	40
COMPOSITION:					
Quartz	12	12	18	10	13
Feldspar	2	1	2	5	6
Mica	1	2	—	—	—
Clay	43	48	32	40	40
Volcanic glass	Tr	1	Tr	4	6
Calcite/dolomite	—	—	1	—	—
Accessory minerals	4	2	8	5	4
Glauconite	2	4	2	—	—
Amphiboles	2	2	4	—	—
Opaque minerals	1	—	1	1	1
Diatoms	33	36	32	35	30
Radiolarians	Tr	2	Tr	—	Tr

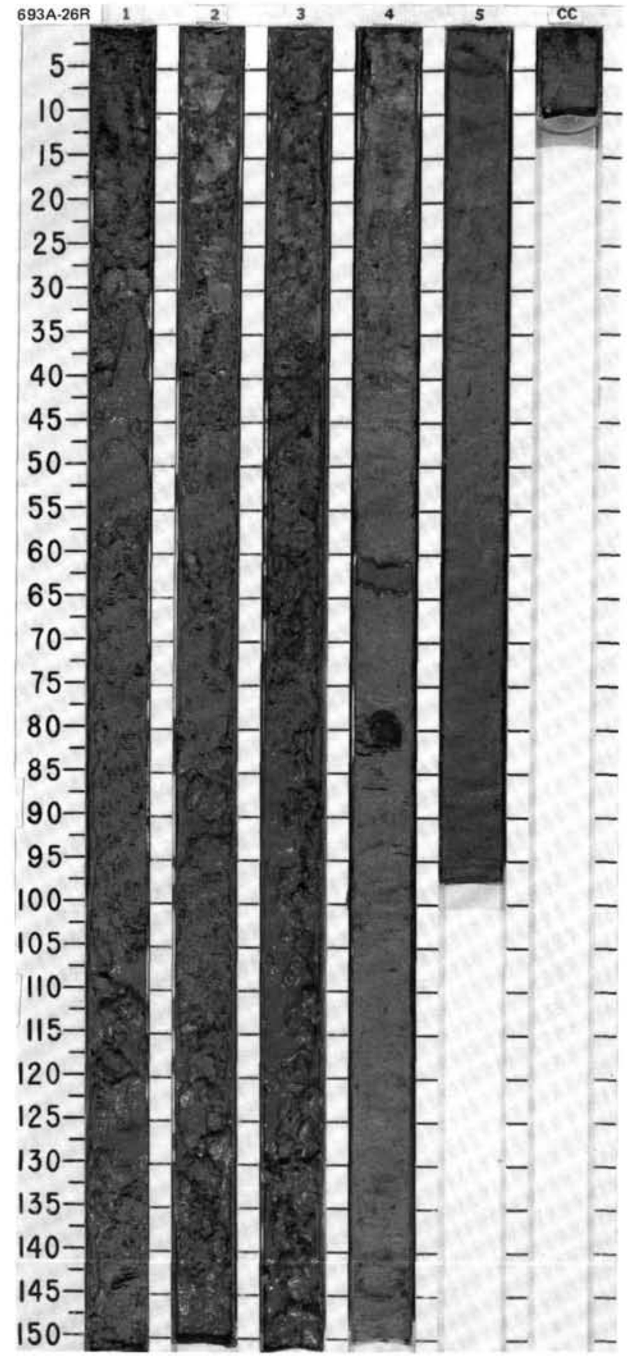

SITE 693 HOLE A CORE 27R CORED INTERVAL 2603.3-2613.0 mbsl; 243.9-253.6 mbsf

TIME-ROCK UNIT	FORAMINIFERS	NANNOFOSSILS	RADIOLARIANS	DIATOMS	PALYNOMORPHS	PALEOMAGNETICS	PHYS. PROPERTIES	CHEMISTRY	SECTION	METERS	GRAPHIC LITHOLOGY	DRILLING DISTURB.	SED. STRUCTURES	SAMPLES
UPPER MIOCENE	B	B	LOWER *C. spongothorax* C,M	*D. hustedtii* A,G	B		γ=2.46 ●	6.58% ●	1	0.5, 1.0	VOID			* *
									2					*

BIOSTRAT. ZONE/ FOSSIL CHARACTER

LITHOLOGIC DESCRIPTION

MUD-BEARING NANNOFOSSIL DIATOM OOZE and DIATOM SILTY MUD

Major lithologies: Mud-bearing nannofossil diatom ooze in Section 1, greenish gray, (5G 5/1) and (5G 6/1) alternating on a scale of about 5 cm beginning at Section 1, 40 cm. In Section 1, 15–40 cm, the lithology is partly lithified and contains *Zoophycos* burrows. Diatom silty mud in Section 2, dark greenish gray (5G 4/1), firm, moderately disturbed, containing spots of slightly greener and coarser material at Section 2, 15 cm.

Gneiss dropstones (60–40 mm) are observed in Section 1, 12 and 72 cm. Numerous small (<2 mm) dropstones throughout core. Strong to moderate disturbance.

SMEAR SLIDE SUMMARY (%):

	1, 32 M	1, 100 D	2, 50 D
TEXTURE:			
Sand	—	—	6
Silt	—	—	62
Clay	—	—	32
COMPOSITION:			
Quartz	12	6	16
Mica	—	1	—
Clay	5	33	32
Volcanic glass	—	2	—
Accessory minerals	4	—	8
Amphiboles	1	2	2
Glauconite	2	2	8
Opaques	—	—	2
Nannofossils	23	26	—
Diatoms	53	28	32
Radiolarians	—	Tr	Tr

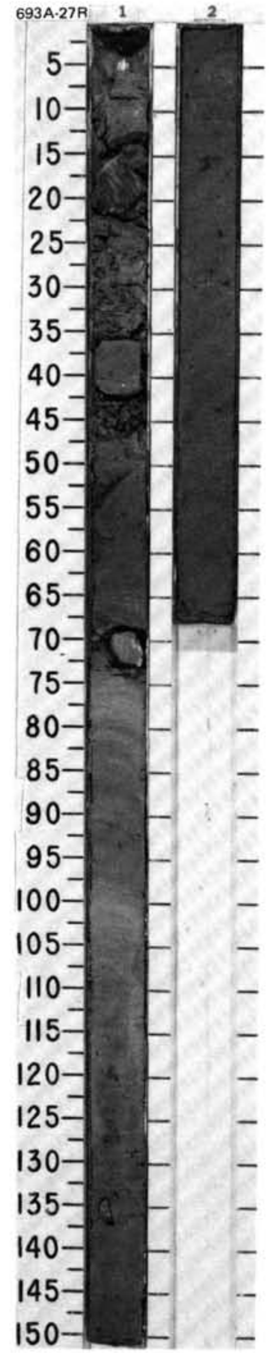

SITE 693 HOLE A CORE 28R CORED INTERVAL 2613.0-2622.3 mbsl; 253.6-262.9 mbsf

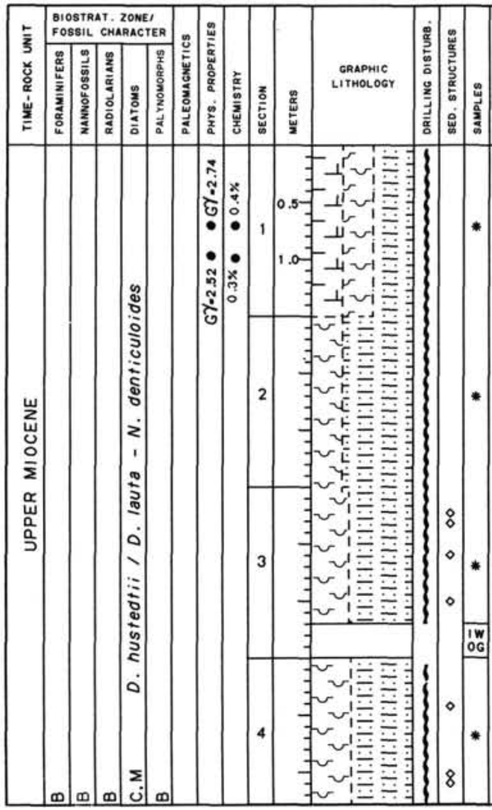

LITHOLOGIC DESCRIPTION

MUDDY DIATOM NANNOFOSSIL OOZE and DIATOM CLAYEY MUD

Major lithologies: Muddy diatom nannofossil ooze, greenish gray (5G 5/1, 6/1) with patches of light gray (N 7/0), possibly disturbed bedding. Diatom clayey mud (mudstone), greenish gray (5G 5/1) and dark greenish gray (5G 4/1). Colors show gradual transitions as well as remnants of color layering. The stiffer layers, which occur in Sections 3 and 4, are less disturbed.

Small dropstones throughout. Larger dropstones occur in Section 3, 22, 31,65, and 97 cm, and Section 4, 38–42, 102, and 106 cm. No CC.

SMEAR SLIDE SUMMARY (%):

	1, 70 D	2, 70 D	3, 70 D	4, 70 D
TEXTURE:				
Sand	—	Tr	2	6
Silt	—	70	68	64
Clay	—	30	30	30
COMPOSITION:				
Quartz	10	25	25	20
Feldspar	3	2	Tr	10
Mica	1	5	5	2
Clay	22	30	30	25
Volcanic glass	3	—	—	3
Accessory minerals	2	5	3	2
Opaque minerals	Tr	3	2	1
Nannofossils	30	—	—	—
Diatoms	29	30	35	37
Radiolarians	Tr	—	—	—

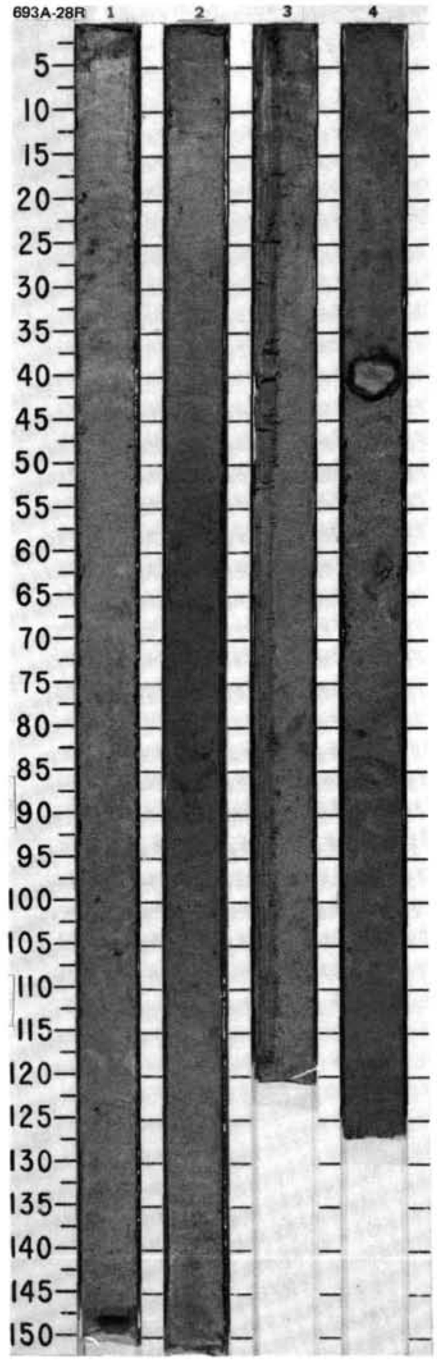

SITE 693 HOLE A CORE 29R CORED INTERVAL 2622.3-2631.9 mbsl; 262.9-272.5 mbsf

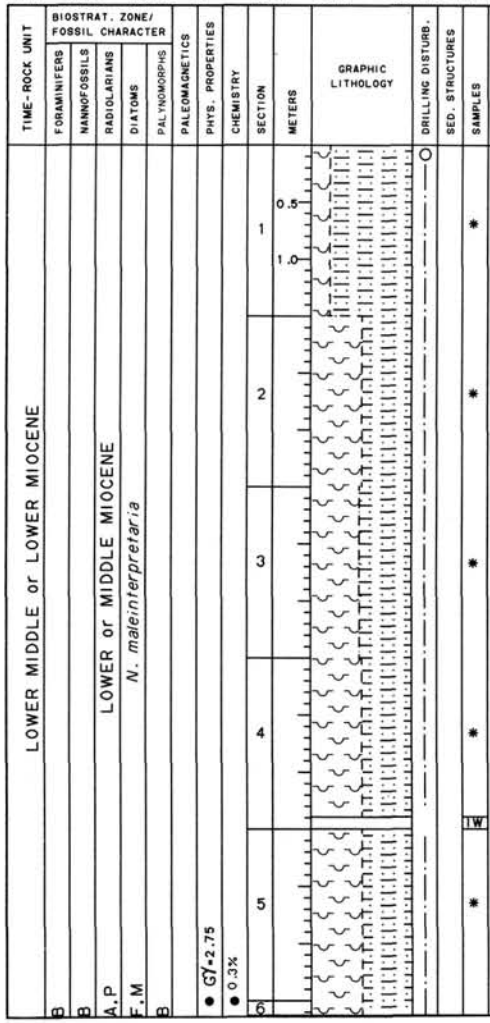

LITHOLOGIC DESCRIPTION

DIATOM MUD and DIATOM-BEARING MUD

Major lithologies: Diatom mud in Sections 2, 3, 4, and 5, greenish gray (5G 5/1), with some dark greenish gray (5G 5/1) patches fading into greenish gray (5BG 5/1) in lower Section 5. No original structures can be seen. Diatom-bearing mud in Section 1, dark greenish gray (5G 4/1), homogeneously colored.

Sediments are moderately disturbed by drilling. No bioturbation structures observed. A few millimeter-sized dropstones in Section 1. Numerous small (<2 mm) dropstones in Section 2.

SMEAR SLIDE SUMMARY (%):

	1, 70 D	2, 70 D	3, 70 D	4, 70 D	5, 70 D
TEXTURE:					
Sand	2	1	2	2	4
Silt	58	75	64	64	72
Clay	40	24	34	34	24
COMPOSITION:					
Quartz	22	18	14	15	18
Feldspar	2	4	2	2	6
Mica	4	2	1	2	2
Clay	40	24	34	32	24
Volcanic glass	2	—	—	—	—
Calcite/dolomite	—	—	—	—	1
Accessory minerals	8	3	—	—	4
Opaque	2	—	—	2	Tr
Amphibole	—	2	—	—	—
Glauconite	—	—	Tr	—	—
Diatoms	20	42	46	44	42
Radiolarians	—	4	2	3	2
Sponge spicules	—	1	1	—	1
Silicoflagellates	—	—	—	—	Tr

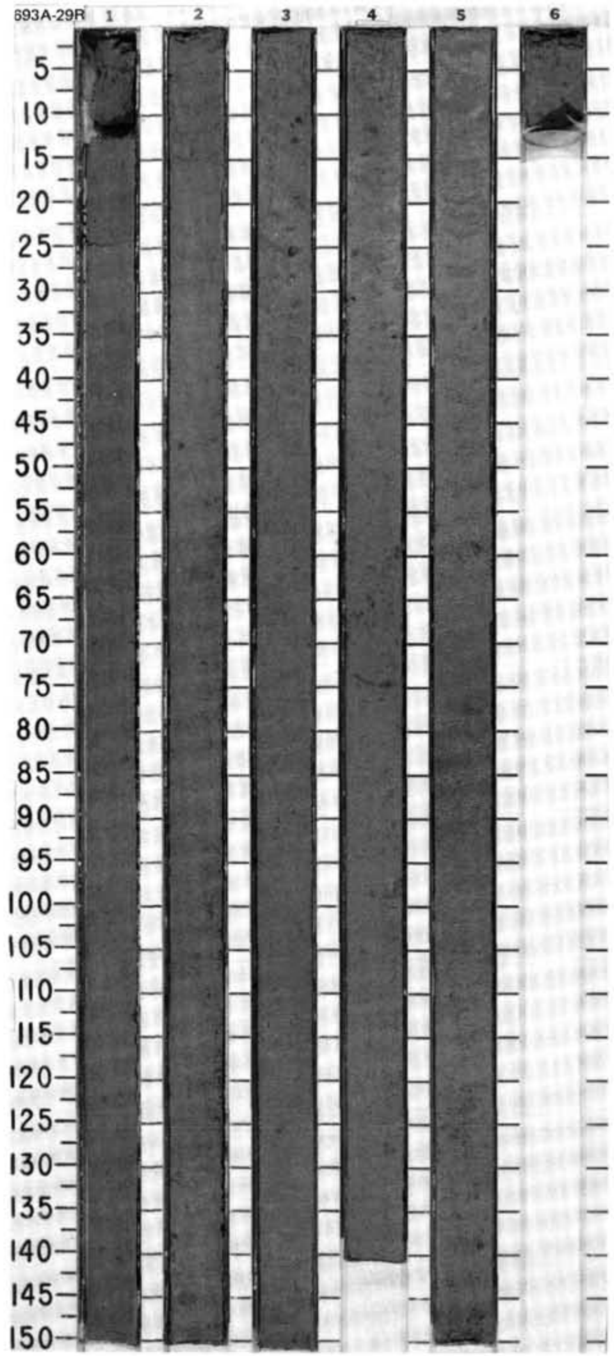

SITE 693 HOLE A CORE 30R CORED INTERVAL 2631.9-2641.6 mbsl; 272.5-282.2 mbsf

TIME-ROCK UNIT	FORAMINIFERS	NANNOFOSSILS	RADIOLARIANS	DIATOMS	PALYNOMORPHS	PALEOMAGNETICS	PHYS. PROPERTIES	CHEMISTRY	SECTION	METERS	GRAPHIC LITHOLOGY	DRILLING DISTURB.	SED. STRUCTURES	SAMPLES	LITHOLOGIC DESCRIPTION
LOWER MIDDLE or LOWER MIOCENE	B	B	LOWER or MIDDLE MIOCENE A,P	*N. maleinterpretaria* F,P	B				1 2 3	0.5 1.0					Minimal recovery. All sediment given to paleontologists.

SITE 693 HOLE A CORE 31R CORED INTERVAL 2641.6-2651.3 mbsl; 282.2-291.9 mbsf

TIME-ROCK UNIT	FORAMINIFERS	NANNOFOSSILS	RADIOLARIANS	DIATOMS	PALYNOMORPHS	PALEOMAGNETICS	PHYS. PROPERTIES	CHEMISTRY	SECTION	METERS	GRAPHIC LITHOLOGY	DRILLING DISTURB.	SED. STRUCTURES	SAMPLES	LITHOLOGIC DESCRIPTION
LOWER MIOCENE	B	B	LOWER MIDDLE or LOWER MIOCENE C,M	? F,P	B		● GY=2.72	● 0.3%	1	0.5 1.0	VOID		◇ ◇	*	see below

DIATOM BEARING MUD

Major lithology: Dark greenish gray (5G 4/1), homogeneously colored throughout. No bioturbation observed in moderately disturbed sediment.

A dropstone-rich layer containing millimeter-sized material and a few larger (about 10 mm) dropstones are observed in Section 1, between 22 and 43 cm.

SMEAR SLIDE SUMMARY (%):

	1, 70 D
TEXTURE:	
Sand	5
Silt	55
Clay	40
COMPOSITION:	
Quartz	25
Feldspar	2
Mica	4
Clay	40
Accessory minerals	5
Opaque minerals	2
Diatoms	22

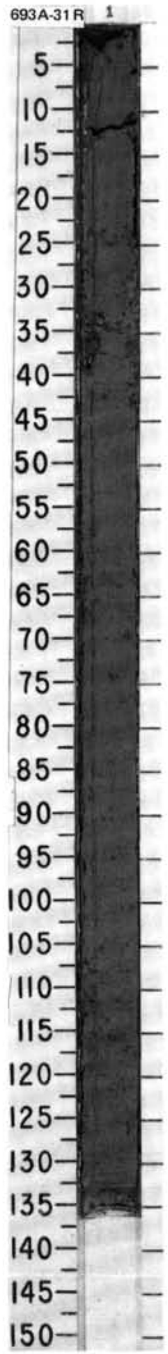

CORE 113-693A-32R NO RECOVERY

SITE 693 HOLE A CORE 33R CORED INTERVAL 2660.9-2670.6 mbsl; 301.5-311.2 mbsf

TIME-ROCK UNIT	BIOSTRAT. ZONE/ FOSSIL CHARACTER: FORAMINIFERS	NANNOFOSSILS	RADIOLARIANS	DIATOMS	PALYNOMORPHS	PALEOMAGNETICS	PHYS. PROPERTIES	CHEMISTRY	SECTION	METERS	GRAPHIC LITHOLOGY	DRILLING DISTURB.	SED. STRUCTURES	SAMPLES
?	B	B	R	UPPER OLIGOCENE (?) R,P	B		GY=2.88 ● ●	● 0.5%	1	0.5 1.0				* *

LITHOLOGIC DESCRIPTION

DIATOM-BEARING CLAYEY MUD

Major lithology: Diatom-bearing clayey mud, dark greenish gray (5GY 4/1), dark gray (N 4/0) and very dark greenish gray (5GY 3/1). Color boundaries are horizontal above Section 1, 90 cm; below this level colors are swirled together. Abundant small (<8 mm) dropstones below Section 1, 93 cm.

Minor lithology: Diatom-bearing clayey mud, dark greenish gray (5GY 4/1), occurs as lumps of firm sediment in top 12 cm; may have fallen downhole.

Coring disturbance includes a thin layer of mud containing planktonic foraminifers, washed down one side of the core. Coarse fraction, Section 1, 123-125 cm, contains about two-thirds very coarse sand, with a large amount of glauconite in the fine-medium sand size range. There is room for a disconformity.

SMEAR SLIDE SUMMARY (%):

	1, 5 M	1, 50 D
TEXTURE:		
Sand	3	2
Silt	42	38
Clay	55	60
COMPOSITION:		
Quartz	20	15
Feldspar	3	5
Mica	1	—
Clay	54	59
Accessory minerals:		
Heavy minerals	2	1
Opaque minerals	1	3
Diatoms	15	15
Radiolarians	1	Tr
Sponge spicules	3	2
Silicoflagellates	Tr	—

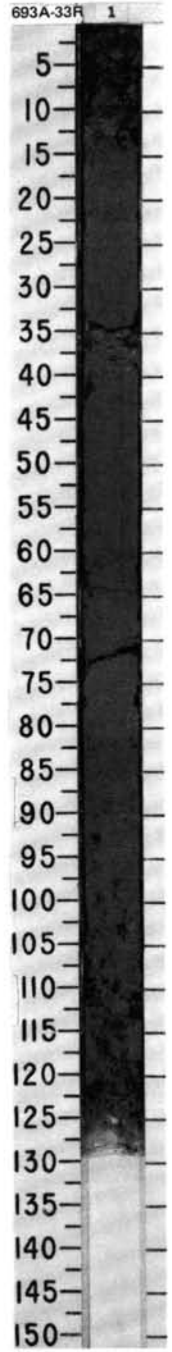

SITE 693 HOLE A CORE 34R CORED INTERVAL 2670.6-2680.3 mbsl; 311.2-320.9 mbsf

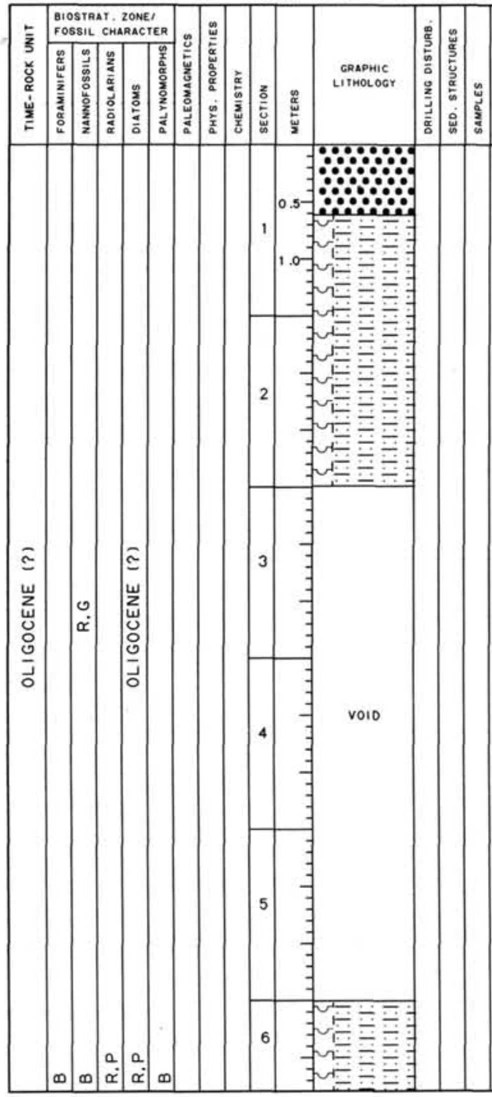

LITHOLOGIC DESCRIPTION

DIATOM-BEARING CLAYEY

Major lithology: Diatom-bearing clayey mud, dark olive gray (5Y 4/1.5) to dark gray (5Y 4/1), thoroughly disturbed and watery.

Minor lithologies: Diatom-bearing clayey mud, dark greenish gray (5GY 4/1), occurs as slightly firmer clasts within major lithology. Clasts are 1-3 cm across, sub-rounded, and form about 10% of the sediment. Gravelly mud/muddy gravel in Section 1, 0-60 cm, is dark greenish gray (5GY 4/1), homogeneous. Low-grade metasediments and vein quartz, with some feldspar, make up the granule/very coarse sand fraction; largest grains 4 mm in size. Medium and fine sand is quartz, feldspar, garnet, and hornblende, plus foraminifers; virtually no glauconite.

SMEAR SLIDE SUMMARY (%):

	1, 70 D	2, 35 D	2, 27 M
TEXTURE:			
Sand	9	5	2
Silt	38	41	29
Clay	33	54	69
COMPOSITION:			
Quartz	19	21	14
Feldspar	6	6	3
Clay	53	54	69
Accessory minerals	1	1	—
Opaque minerals	2	3	3
Foraminifers	Tr	—	—
Nannofossils	—	Tr	—
Diatoms	17	15	11
Radiolarians	1	Tr	—
Sponge spicules	1	Tr	—

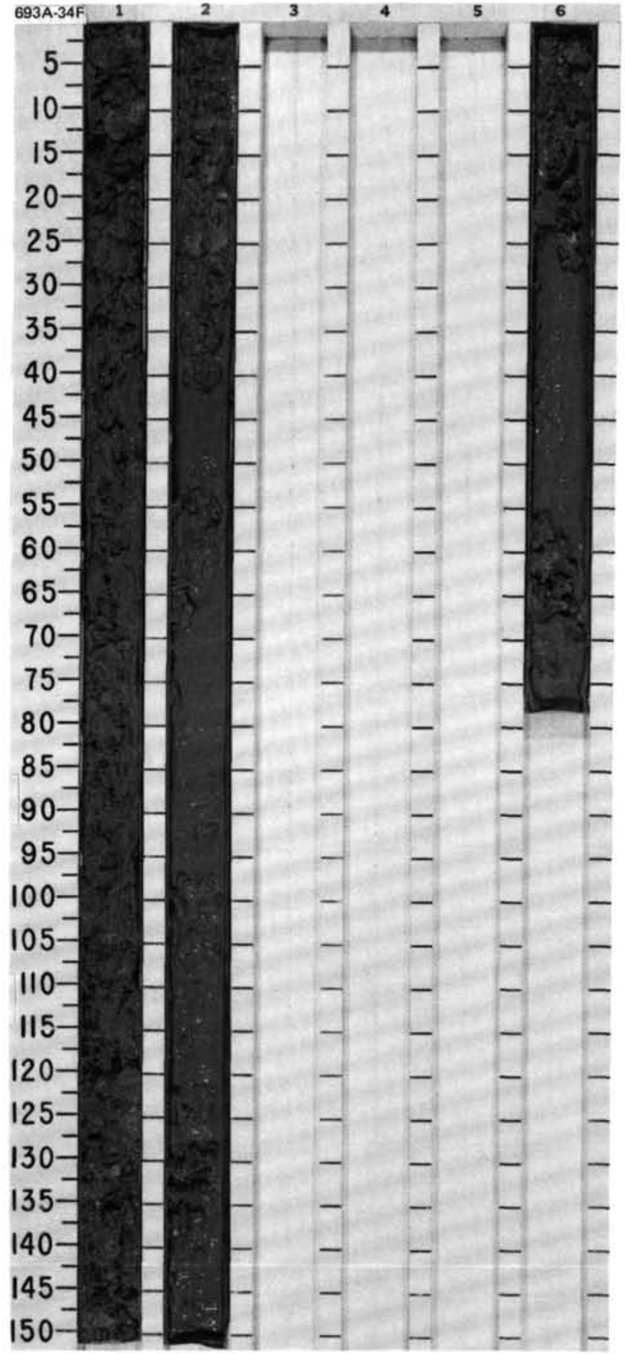

SITE 693 HOLE A CORE 35R CORED INTERVAL 2680.3-2689.9 mbsl; 320.9-330.5 mbsf

TIME-ROCK UNIT	FORAMINIFERS	NANNOFOSSILS	RADIOLARIANS	DIATOMS	PALYNOMORPHS	PALEOMAGNETICS	PHYS. PROPERTIES	CHEMISTRY	SECTION	METERS
UPPER OLIGOCENE	B	B	F, P	OLIGOCENE F, M	B		● GY=2.64	● 0.3%	1 2	0.5 1.0

LITHOLOGIC DESCRIPTION

DIATOM-BEARING CLAYEY MUD and DIATOM MUD

Major lithologies: Diatom-bearing clayey mud, dark gray (N 4/0, 5Y 4/1), with diatom mud, dark greenish gray (5GY 4/1). Clasts of these three colors have been mixed together during drilling. No primary structure preserved. The lowest 15 cm of Section 2 is predominantly dark greenish gray (5GY 4/1), with thin streaks of silt of the same color containing chlorite and hornblende. Section 1 is very disturbed and watery.

No dropstones.

SMEAR SLIDE SUMMARY (%):

	1, 12 D	1, 14 D	1, 31 D
TEXTURE:			
Sand	7	10	2
Silt	53	50	33
Clay	40	40	65
COMPOSITION:			
Quartz	20	20	15
Feldspar	3	3	Tr
Mica	Tr	Tr	2
Clay	38	39	66
Accessory minerals	1	3	1
Opaque minerals	2	7	5
Diatoms	30	25	10
Radiolarians	1	—	—
Sponge spicules	5	3	1
Silicoflagellates	Tr	—	—

SITE 693 HOLE A CORE 36R CORED INTERVAL 2689.9-2699.6 mbsl; 330.5-340.2 mbsf

TIME-ROCK UNIT	FORAMINIFERS	NANNOFOSSILS	RADIOLARIANS	DIATOMS	PALYNOMORPHS	PALEOMAGNETICS	PHYS. PROPERTIES	CHEMISTRY	SECTION	METERS
UPPER OLIGOCENE	R, G B	C, G	R, P	OLIGOCENE R, P	B		● ● GY=2.95	● 1.2%	1	0.5

LITHOLOGIC DESCRIPTION

DIATOM-BEARING CLAYEY MUD and NANNOFOSSIL OOZE

Major lithologies: Diatom-bearing clayey mud, dark greenish gray (5GY 4/1), homogenized during drilling. Nannofossil ooze, gray (5Y 5/1), in Section 1, 0-10 cm, as rounded clasts up to 3 cm across in matrix of underlying of mud.

SMEAR SLIDE SUMMARY (%):

	1, 4 M	1, 50 D
TEXTURE:		
Sand	—	2
Silt	—	43
Clay	—	55
COMPOSITION:		
Quartz	2	15
Feldspar	Tr	3
Mica	—	2
Clay	5	55
Accessory minerals:		
Hornblende	1	—
Opaque minerals	—	3
Epidote	—	1
Glauconite	—	Tr
Nannofossils	85	—
Diatoms	5	20
Radiolarians	Tr	1
Sponge spicules	2	—

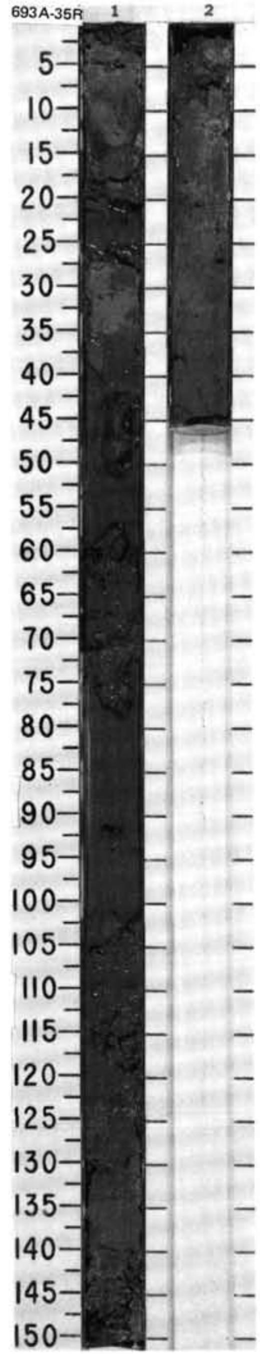

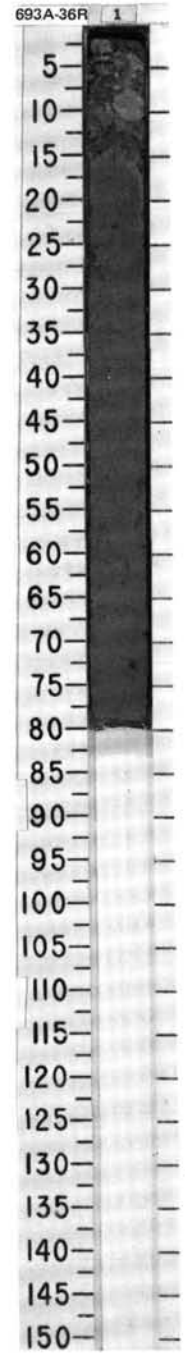

SITE 693 HOLE A CORE 37R CORED INTERVAL 2699.6-2709.3 mbsl; 340.2-349.9 mbsf

TIME-ROCK UNIT: UPPER OLIGOCENE

BIOSTRAT. ZONE/FOSSIL CHARACTER: FORAMINIFERS: R,P; B — NANNOFOSSILS: UPPER OLIGOCENE C,G; B — RADIOLARIANS: C,P — DIATOMS: OLIGOCENE F,P — PALYNOMORPHS: B

PHYS. PROPERTIES: GY=2.64 — CHEMISTRY: 0.4%

SECTION: 1 — METERS: 0.5

LITHOLOGIC DESCRIPTION

DIATOM-BEARING CLAYEY MUD

Major lithology: Diatom-bearing clayey mud, dark greenish gray (5GY 4/1) and dark gray (N 4/0).

Minor lithology: Diatom-bearing nannofossil ooze, greenish gray (5GY 5/1), as rounded clasts approximately 20-30 cm across, in matrix of dark greenish gray mud.

SMEAR SLIDE SUMMARY (%):

	1, 25 D	1, 29 M	1, 60 M
TEXTURE:			
Sand	2	—	5
Silt	38	—	40
Clay	60	—	55
COMPOSITION:			
Quartz	20	5	20
Feldspar	Tr	Tr	Tr
Mica	2	1	2
Clay	58	3	57
Volcanic glass	—	Tr	—
Accessory minerals	Tr	—	—
Opaque minerals	1	1	3
Epidote	2	3	1
Heavy minerals	—	—	Tr
Nannofossils	Tr	74	—
Diatoms	15	10	15
Radiolarians	2	2	2
Sponge spicules	—	1	—
Pollen	—	Tr	Tr

SITE 693 HOLE A CORE 38R CORED INTERVAL 2709.3-2719.0 mbsl; 349.9-359.6 mbsf

TIME-ROCK UNIT: LOWER(?) OLIGOCENE

BIOSTRAT. ZONE/FOSSIL CHARACTER: FORAMINIFERS: B — NANNOFOSSILS: B — RADIOLARIANS: OLIGOCENE F,G — DIATOMS: OLIGOCENE R,P — *D. deflandrei* (silicoflagellate)

PHYS. PROPERTIES: GY=3.01 — CHEMISTRY: 0.3%

SECTION: 1, CC — METERS: 0.5, 1.0

LITHOLOGIC DESCRIPTION

MUDDY DIATOM OOZE

Major lithology: Muddy diatom ooze, dark greenish gray (5GY 4/1), some mottling between about 55 and 85 cm in Section 1, and a thin layer of greenish gray (5G 5/1) at Section 1, 90 cm. In the CC there is a slightly fine-grained layer at 10-12 cm.

Minor lithology: Diatom mud, greenish gray (5G 5/1), some mottling and burrows.

Dropstones are common throughout the core, ranging from <mm to 4 cm in length. Large dropstones occur in Section 1 at 20 cm (1.5 cm), 27 cm (4 cm), 49 cm (3 cm), 57 cm (0.5 cm), 68 cm (0.5 cm), and 87 cm (1 cm); and in the CC, 9 cm (1.5 cm).

SMEAR SLIDE SUMMARY (%):

	1, 70 D	1, 12 M
COMPOSITION:		
Quartz	20	25
Feldspar	2	1
Mica	Tr	1
Clay	20	25
Accessory minerals	1	1
Opaque minerals	2	2
Heavy minerals	Tr	—
Glaconite	Tr	Tr
Diatoms	50	40
Radiolarians	5	3
Sponge spicules	Tr	1
Silicoflagellates	Tr	1

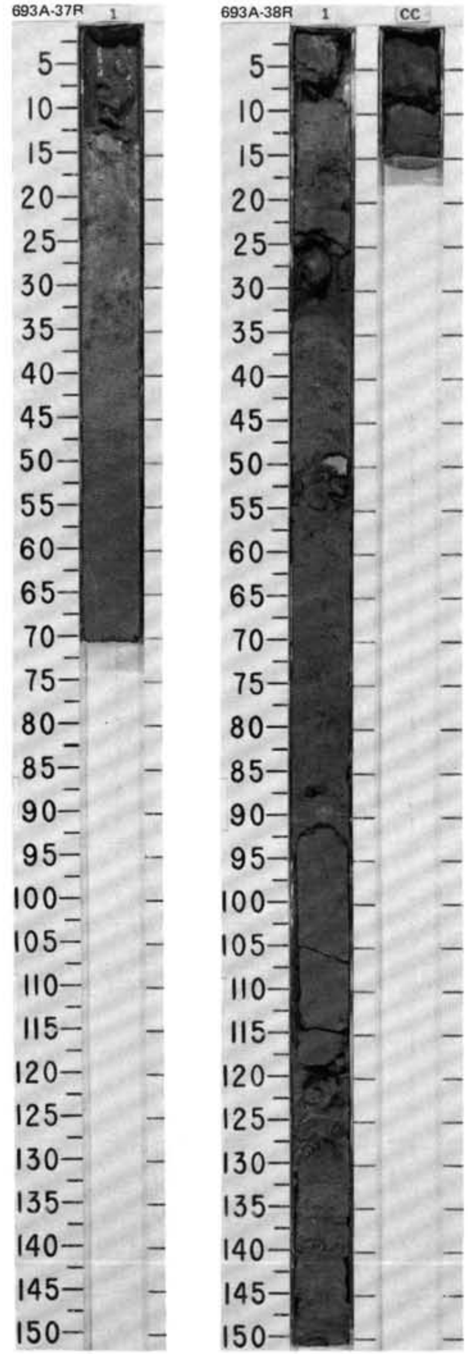

SITE 693 HOLE A CORE 39R CORED INTERVAL 2719.0-2728.3 mbsl; 359.6-368.9 mbsf

TIME-ROCK UNIT: LOWER OLIGOCENE

BIOSTRAT. ZONE/FOSSIL CHARACTER: FORAMINIFERS: B; NANNOFOSSILS: B; RADIOLARIANS: F,M, OLIGOCENE; DIATOMS: C,P, LOWER OLIGOCENE; *D. deflandrei (silicoflagellate)*

PHYS. PROPERTIES: ● GY=2.59

CHEMISTRY: ● 1.1%

SECTION: 1, 2

METERS: 0.5, 1.0

LITHOLOGIC DESCRIPTION

DIATOM MUD and DIATOM-BEARING MUD

Major lithologies: Diatom mud in Section 1, dark gray (5Y 4/1) in upper 10-40 cm and dark greenish gray (5GY 4/1) in lower 40-150 cm, with one olive brown "clay concretion" at 102-105 cm and a grayish brown mudstone at 124-128 cm. At Section 1, 25 cm, a grayish green ash layer containing 26% volcanic glass is observed. Mudstone at Section 1, 0-6 cm, contains bivalve shells. Diatom-bearing mud in Section 2, dark gray (5Y 4/1) with numerous small (1-3 mm) black-edged dropstones below 45 cm, covering about 4% of area. Large dropstone (10-15 mm) at Section 2, 59 cm. Dark brown (2.5Y 4/2) patch at Section 2, 62-71 cm. At Section 2, 96 cm, a grayish green composite stone, possibly amphibole. Slightly disturbed by drilling, no bioturbation.

SMEAR SLIDE SUMMARY (%):

	1, 50 D	2, 50 D	1, 25 M
TEXTURE:			
Sand	10	18	32
Silt	68	68	46
Clay	22	14	22
COMPOSITION:			
Quartz	14	32	20
Feldspar	7	4	4
Mica	1	2	2
Clay	22	14	20
Volcanic glass	2	—	26
Accessory minerals	2	16	—
Amphiboles	6	8	4
Glauconite	—	—	6
Diatoms	42	24	18
Sponge spicules	4	—	—

SITE 693 HOLE A CORE 40R CORED INTERVAL 2728.3-2738.0 mbsl; 368.9-378.6 mbsf

TIME-ROCK UNIT: LOWER OLIGOCENE

BIOSTRAT. ZONE/FOSSIL CHARACTER: FORAMINIFERS: B; NANNOFOSSILS: B; RADIOLARIANS: F,M; DIATOMS: C,P, LOWER OLIGOCENE; *D. deflandrei (silicoflagellate)*

SECTION: 1, 2, 3

METERS: 0.5, 1.0

SAMPLES: IW

LITHOLOGIC DESCRIPTION

DIATOM-BEARING SILTY MUD

Major lithologies: Diatom-bearing silty mud, gray (5Y 5/1) throughout, but showing a wavy, cloudy pattern of minor color changes attributed to coring disturbance.

Millimeter-sized dropstones occur throughout the core.

SMEAR SLIDE SUMMARY (%):

	1, 70 D	2, 70 D	3, 70 D
TEXTURE:			
Sand	5	6	8
Silt	70	66	60
Clay	25	28	32
COMPOSITION:			
Quartz	30	35	35
Feldspar	10	10	4
Mica	1	1	1
Clay	25	28	32
Volcanic glass	5	3	—
Accessory minerals	5	4	9
Opaque minerals	2	2	2
Hornblende	2	2	2
Diatoms	20	15	15

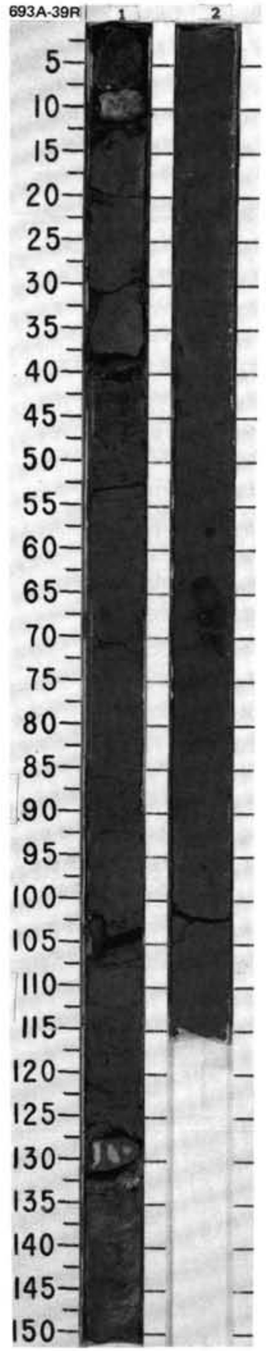

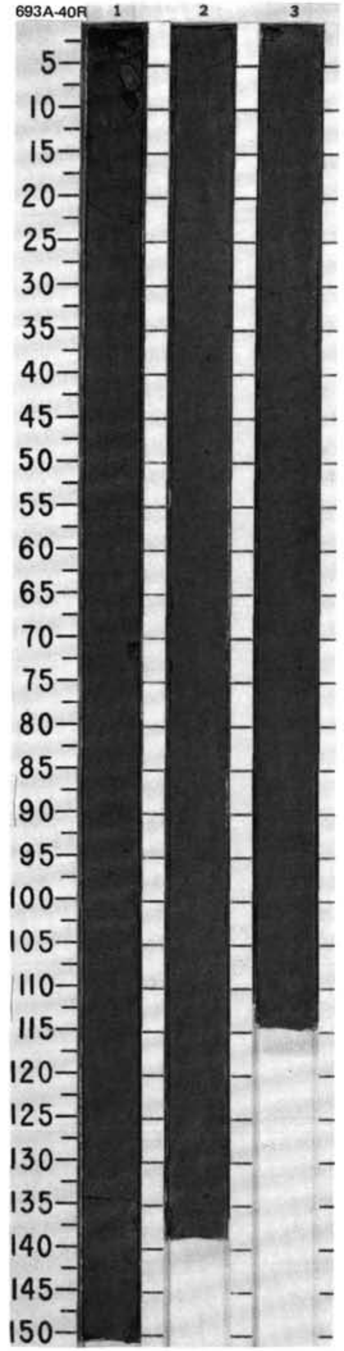

CORE 113-693A-41R NO RECOVERY

SITE 693 HOLE A CORE 42R CORED INTERVAL 2746.9-2756.5 mbsl; 387.5-397.1 mbsf

TIME-ROCK UNIT	FORAMINIFERS	NANNOFOSSILS	RADIOLARIANS	DIATOMS		PALEOMAGNETICS	PHYS. PROPERTIES	CHEMISTRY	SECTION	METERS	GRAPHIC LITHOLOGY	DRILLING DISTURB.	SED. STRUCTURES	SAMPLES	LITHOLOGIC DESCRIPTION
LOWER OLIOGCENE	B	B	F,M OLIGOCENE	F,P LOWER OLIGOCENE	D. deflandrei (silicoflagellate)				CC					*	

BIOSTRAT. ZONE/ FOSSIL CHARACTER

DIATOM-BEARING SILTY MUD

Major lithology: Diatom-bearing silty mud, dark greenish gray (5G 4/1), showing wavy cloudy patterns with dark gray (N 4/1), probably due to mini-biscuiting.

Small (mm sized) dropstones preferentially occur in the darker layers.

SMEAR SLIDE SUMMARY (%):

	CC D
TEXTURE:	
Sand	2
Silt	65
Clay	33
COMPOSITION:	
Quartz	32
Feldspar	1
Mica	2
Clay	33
Accessory minerals	7
Hornblende	4
Opaque minerals	1
Diatoms	20

SITE 693 HOLE A CORE 43R CORED INTERVAL 2756.5-2766.1 mbsl; 397.1-406.7 mbsf

TIME-ROCK UNIT	FORAMINIFERS	NANNOFOSSILS	RADIOLARIANS	DIATOMS	PALYNOMORPHS	PALEOMAGNETICS	PHYS. PROPERTIES	CHEMISTRY	SECTION	METERS	GRAPHIC LITHOLOGY	DRILLING DISTURB.	SED. STRUCTURES	SAMPLES	LITHOLOGIC DESCRIPTION
?	B	B	B	B	B				1 / CC	0.5				**	

BIOSTRAT. ZONE/ FOSSIL CHARACTER

DRILLING-INDUCED GRADED SAND

Major lithology: Sand grading from clay at top to coarse sand at base, held in core line by two large stones, one probably volcanic in origin, and the other dark gray (5Y 4/1), very fine-grained limestone. Sand is angular. Both sand and grading are attributed to coring. Pleistocene foraminifers are abundant in the topmost clay section.

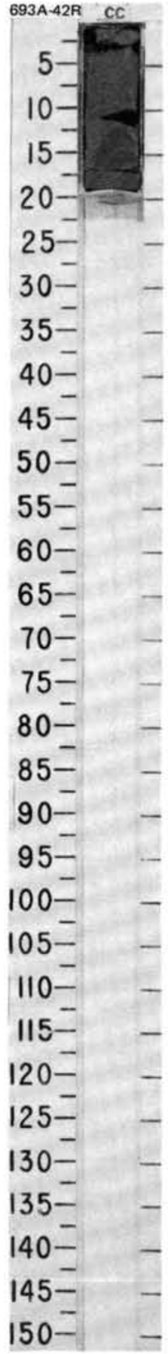

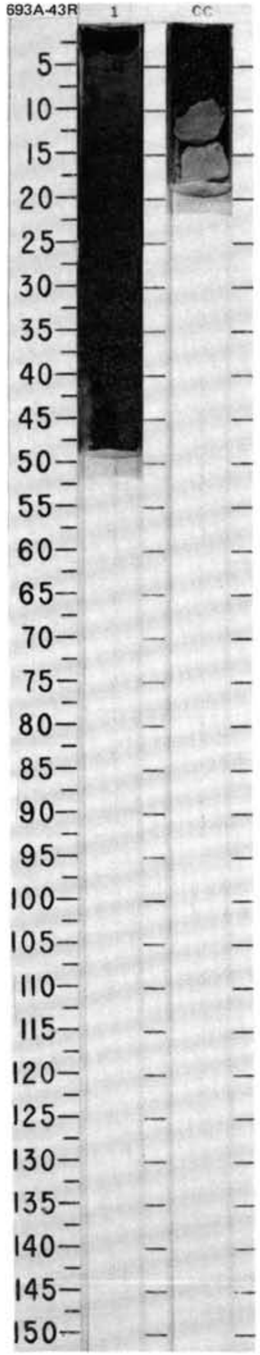

SITE 693 HOLE A CORE 44R CORED INTERVAL 2766.1-2775.9 mbsl; 406.7-416.5 mbsf

TIME-ROCK UNIT	FORAMINIFERS	NANNOFOSSILS	RADIOLARIANS	DIATOMS	PALYNOMORPHS	PALEOMAGNETICS	PHYS. PROPERTIES	CHEMISTRY	SECTION	METERS	GRAPHIC LITHOLOGY	DRILLING DISTURB.	SED. STRUCTURES	SAMPLES
ALBIAN - SANTONIAN	B	B	A,G APTIAN - SANTONIAN	F,M unzoned	B		γ=1630 ●	● 0.8%	1	0.5				**

BIOSTRAT. ZONE/ FOSSIL CHARACTER

LITHOLOGIC DESCRIPTION

CLAY-BEARING RADIOLARIAN DIATOMITE, CLAYEY RADIOLARIAN-DIATOMITE, and SILICEOUS CLAYSTONE

Major lithologies: Clay-bearing radiolarian diatomite. Clayey radiolarian diatomite, both olive gray (5Y 4/2) and dark olive gray (5Y 3/2). Siliceous claystone, dark olive gray (5Y 3/2). Moderte bioturbation, including *Planolites*, *Zoophycos*, vertical burrows, and *Chondrites*. Claystone at base is more compacted, and burrows are flattened; pseudo-lamination.

Minor lithology: Chert (as fragments) in top 5 cm, black (N 2/0), angular, up to 5 cm across.

Core is mainly drilling breccia (sludge) below 48 cm.

SMEAR SLIDE SUMMARY (%):

	1, 18 D	1, 36 M
COMPOSITION:		
Quartz	Tr	1
Clay	25	40
Accessory minerals	1	2
Diatoms	42	34
Radiolarians	30	20
Sponge spicules	2	3

SITE 693 HOLE A CORE 45R CORED INTERVAL 2775.9-2785.5 mbsl; 416.5-426.1 mbsf

TIME-ROCK UNIT	FORAMINIFERS	NANNOFOSSILS	RADIOLARIANS	DIATOMS	PALYNOMORPHS	PALEOMAGNETICS	PHYS. PROPERTIES	CHEMISTRY	SECTION	METERS	GRAPHIC LITHOLOGY	DRILLING DISTURB.	SED. STRUCTURES	SAMPLES
ALBIAN - SANTONIAN	B	B	F,P SANTONIAN	B	C,G UPPER APTIAN (LOWER ALBIAN?)			● 0.3%	1	0.5 1.0				*
									CC					

BIOSTRAT. ZONE/ FOSSIL CHARACTER

LITHOLOGIC DESCRIPTION

CLAYSTONE and CHERT

Major lithology: Claystone, very dark gray (5Y 3/1), with some thin layers (1-3 cm) of dark olive gray (5Y 3/2) and dark gray (5Y 4/1). Color boundaries, where preserved, are gradational and burrowed. Strong bioturbation (moderate in CC). Chert, occurring as angular fragments in Section 1, 25-40 cm, and as pieces up to 6 cm across in CC, 5-16 cm, dark gray (5Y 3/1). *Chondrites* burrows in CC. Quartz(?) vein at about 30 cm in Section 1.

SMEAR SLIDE SUMMARY (%):

	1, 62 D	CC, 3 M
TEXTURE:		
Silt	10	6
Clay	90	94
COMPOSITION:		
Quartz	3	2
Clay	90	94
Accessory minerals:		
Opaque minerals	3	2
Diatoms	4	2
Radiolarians	Tr	—

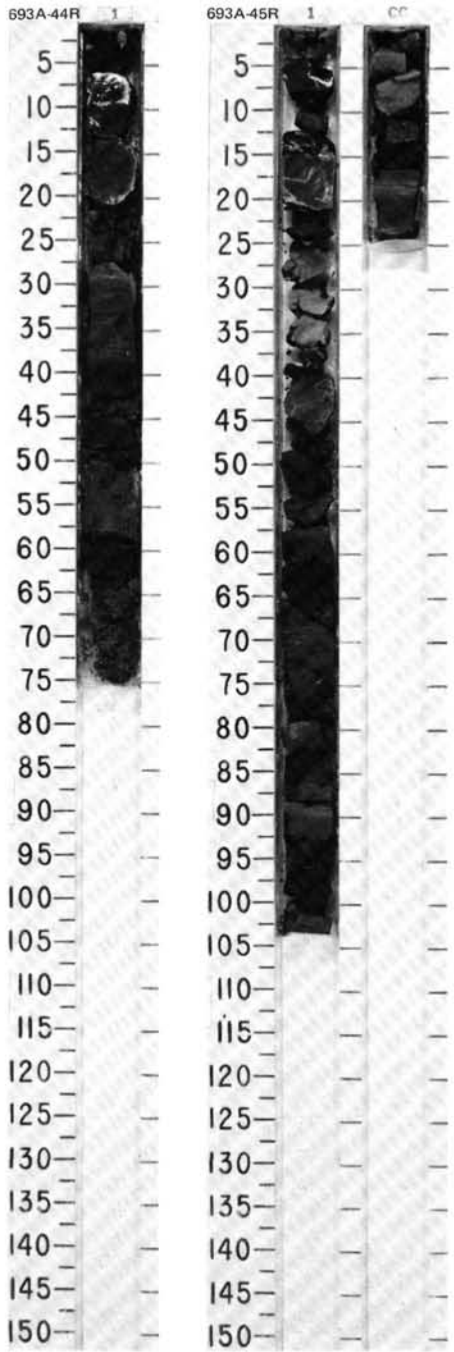

SITE 693 HOLE A CORE 46R CORED INTERVAL 2785.5-2795.1 mbsl; 426.1-435.7 mbsf

TIME-ROCK UNIT	FORAMINIFERS	NANNOFOSSILS	RADIOLARIANS	DIATOMS	PALYNOMORPHS	PALEOMAGNETICS	PHYS. PROPERTIES	CHEMISTRY	SECTION	METERS	GRAPHIC LITHOLOGY	DRILLING DISTURB.	SED. STRUCTURES	SAMPLES
ALBIAN	B	B	B	B	C, G UPPER APTIAN (LOWER ALBIAN?)			5.1% 0.8% 3.7%	1, CC	0.5, 1.0				*

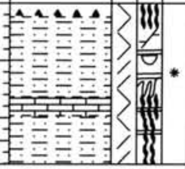

LITHOLOGIC DESCRIPTION

SILTY MUDSTONE and LIMESTONE

Major lithologies: Silty mudstone, dark greenish gray (5GY 3/1), micaceous and glauconitic. Possible slumps. Limestone, gray (5Y 5/1), sandy.

Minor lithology: Chert, black (5Y2 5/2), very hard, conchoidal fractures, granular texture.

Strong bioturbation.

SMEAR SLIDE SUMMARY (%):

	1, 60 D
TEXTURE:	
Sand	20
Silt	45
Clay	35
COMPOSITION:	
Quartz	10
Feldspar	2
Mica	10
Clay	35
Calcite/dolomite	Tr
Accessory minerals:	
Glauconite	25
Opaque minerals	15
Heavy minerals	1
Epidote	2
Nannofossils	Tr
Radiolarians	Tr

SITE 693 HOLE A CORE 47R CORED INTERVAL 2795.1-2804.8 mbsl; 435.7-445.4 mbsf

TIME-ROCK UNIT	FORAMINIFERS	NANNOFOSSILS	RADIOLARIANS	DIATOMS	PALYNOMORPHS	PALEOMAGNETICS	PHYS. PROPERTIES	CHEMISTRY	SECTION	METERS	GRAPHIC LITHOLOGY	DRILLING DISTURB.	SED. STRUCTURES	SAMPLES
UPPER ALBIAN	F, G UPPER ALBIAN	R, M UPPER APTIAN - ALBIAN	R ALBIAN - SANTONIAN	B	C, G UPPER APTIAN (LOWER ALBIAN?)	Dinocysts and Sporomorphs	φ=48 γ=1.570 γ=1.92 GY=3.02	1.0% 2.3% 3.6% 3.8%	1, 2, CC	0.5, 1.0				* *

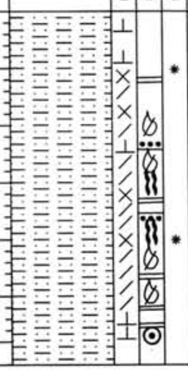

LITHOLOGIC DESCRIPTION

SILTY MUDSTONE

Major lithology: Silty mudstone, mainly dark olive gray (5Y 3/2) and black (N 2/0), in Section 1, 0-10 and 35-45 cm, and in CC; glauconitic and micaceous. Pyrite in CC; a few laminations and shell fragments.

SMEAR SLIDE SUMMARY (%):

	1, 50 D	2, 50 D
TEXTURE:		
Sand	10	7
Silt	45	48
Clay	45	45
COMPOSITION:		
Quartz	15	15
Feldspar	2	3
Mica	7	7
Clay	43	45
Volcanic glass	Tr	—
Calcite/dolomite	5	—
Accessory minerals:		
Opaque minerals	10	10
Heavy minerals	3	5
Glauconite	10	15
Foraminifers	Tr	—
Nannofossils	5	Tr

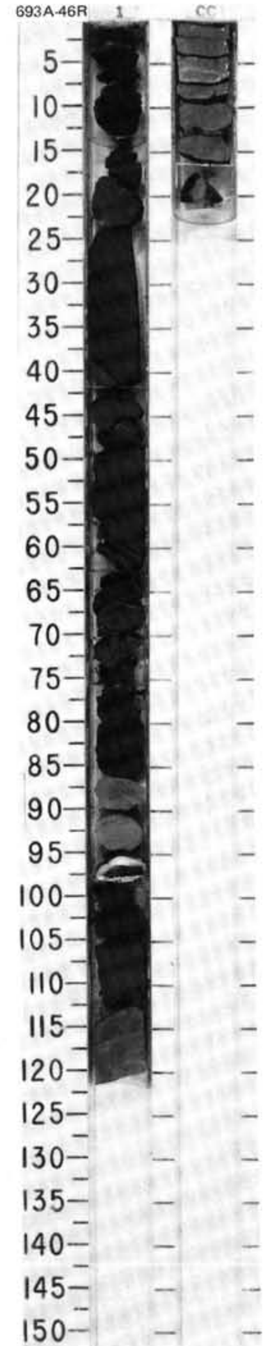

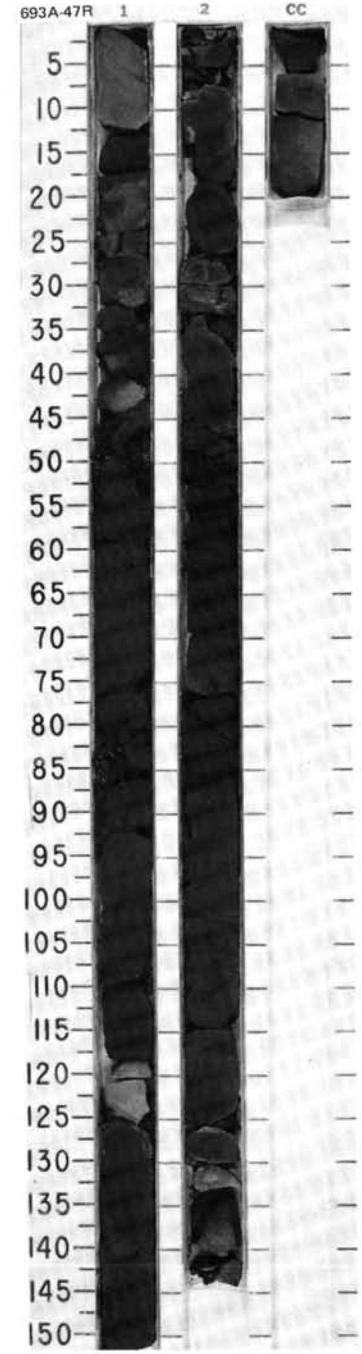

SITE 693 HOLE A CORE 48R CORED INTERVAL 2804.8-2814.4 mbsl; 445.4-455.0 mbsf

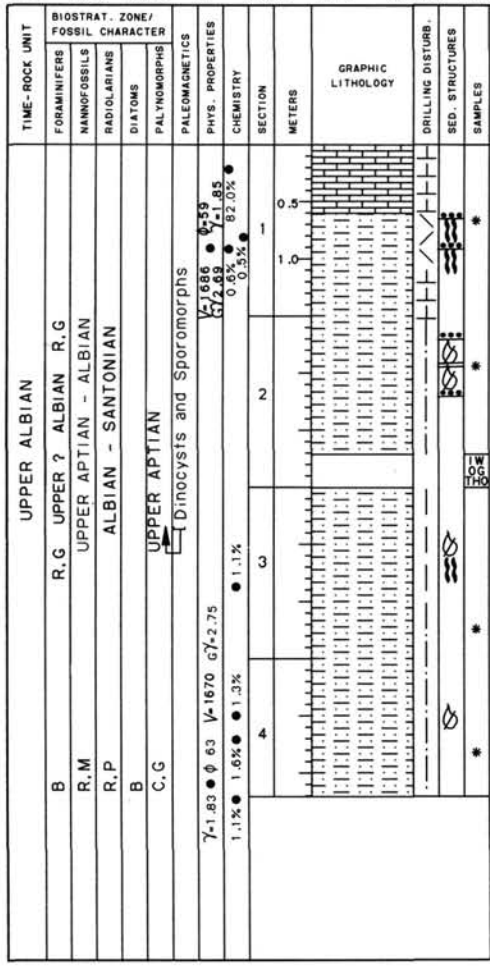

LITHOLOGIC DESCRIPTION

MUDSTONE

Major lithology: Mudstone, black (2.5Y 2/0) and dark gray (5Y 3/1). Generally structureless; laminated bedding in middle of Sections 1, 2, and 3; no laminations in Section 4. Minor to moderate bioturbation in Sections 1 and 3, possibly Section 2 as well. Two, possibly three, graded beds in Sections 1 and 2. Shell fragments almost wholly pyritized in Sections 2 and 3. Pyrite flecks scattered on all cut surfaces; laminations slightly lighter color.

Minor lithology: Limestone in Section 1, 0-40 cm, is dark gray (5Y 4/1) when wet. Bottom of last limestone biscuit has thin layer of pyrite.

SMEAR SLIDE SUMMARY (%):

	1, 68 D	2, 33 D	3, 129 D	4, 80 D
TEXTURE:				
Sand	5	3	3	1
Silt	45	42	37	34
Clay	50	55	60	65
COMPOSITION:				
Quartz	25	20	20	10
Feldspar	5	3	3	1
Mica	3	2	3	2
Clay	48	53	59	67
Volcanic glass	—	—	—	Tr
Calcite/dolomite	—	—	—	2
Accessory minerals:				
Glauconite	2	2	3	3
Heavy minerals	1	2	2	Tr
Opaque minerals	15	15	10	10
Foraminifers	—	Tr	—	—
Nannofossils	1	3	Tr	5
Calcispheres	—	Tr	—	—

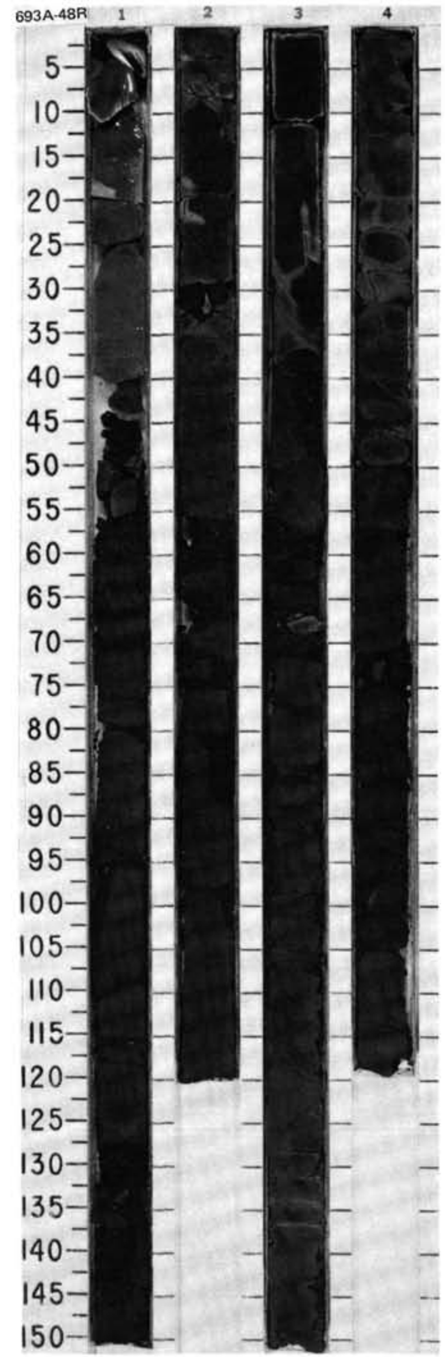

SITE 693 HOLE A CORE 49R CORED INTERVAL 2814.4-2824.2 mbsl; 455.0-464.8 mbsf

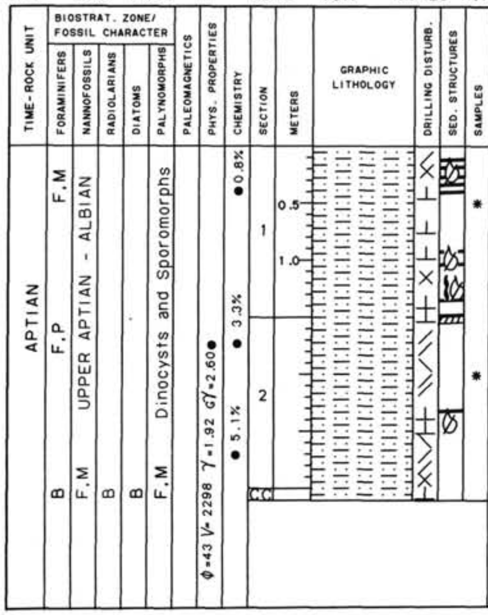

LITHOLOGIC DESCRIPTION

PYRITE-BEARING(?) CLAYEY MUDSTONE

Major lithology: Clayey mudstone, black (5Y 2.5/1), massive; shell fragments mainly in Section 1; pyrite flecks in Section 1, 118-141 cm. Dark olive gray (5Y 3/2) laminations, principally in Section 1.

SMEAR SLIDE SUMMARY (%):

	1, 53 D	2, 50 D
TEXTURE:		
Sand	1	1
Silt	34	29
Clay	65	70
COMPOSITION:		
Quartz	10	10
Feldspar	3	2
Mica	7	5
Clay	63	69
Accessory minerals:		
Glauconite	2	2
Opaque minerals	14	10
Heavy minerals	Tr	1
Nannofossils	1	1
Calcispheres	—	Tr

SITE 693 HOLE A CORE 50R CORED INTERVAL 2824.2-2833.7 mbsl; 464.8-474.3 mbsf

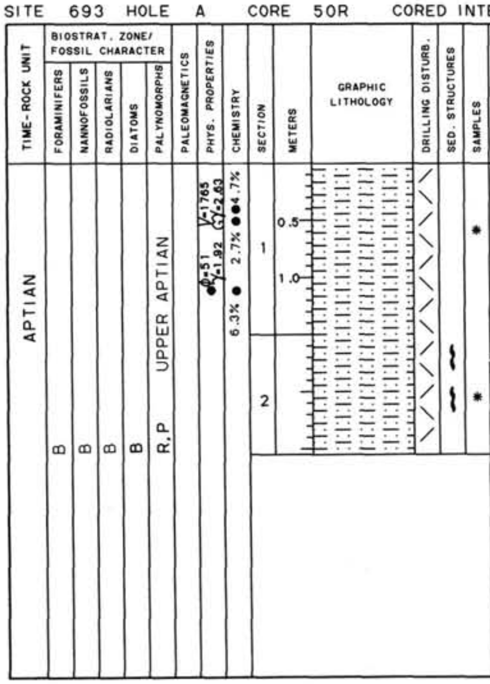

LITHOLOGIC DESCRIPTION

CLAYEY MUDSTONE

Major lithology: Clayey mudstone, very dark brown (7.5YR 2/1), showing faint, lighter laminations. Minor bioturbation occurs in Section 2. Specks of pyrite concretions as large as 1.5 cm in diameter are present in Section 1.

Minor lithology: Bluish gray (5B 5/1) layer of very altered volcanic ash, slightly bioturbated, in Section 2, 70-75 cm.

SMEAR SLIDE SUMMARY (%):

	1, 54 D	2, 54 D
TEXTURE:		
Sand	Tr	Tr
Silt	35	32
Clay	65	68
COMPOSITION:		
Quartz	8	12
Feldspar	1	2
Mica	1	3
Clay	65	66
Volcanic glass	4	3
Accessory minerals	9	6
Opaque minerals	7	2
Pyrite	3	4
Nannofossils	2	2

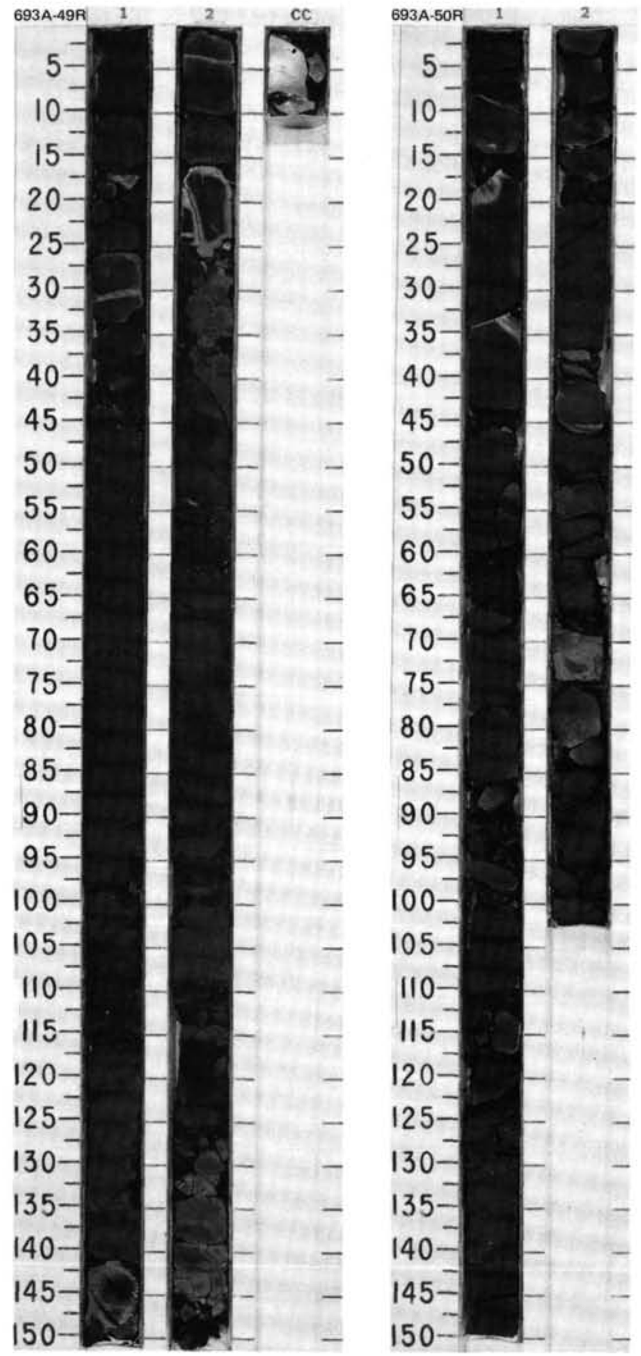

SITE 693 HOLE A CORE 51R CORED INTERVAL 2833.7-2843.3 mbsl; 474.3-483.9 mbsf

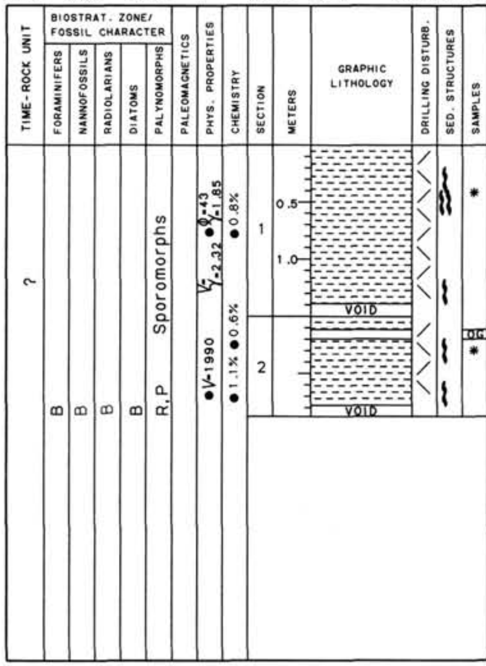

LITHOLOGIC DESCRIPTION

CLAYSTONE

Major lithology: Claystone, generally black (7.5YR 2/1) when structureless, to dark gray (2.5Y 4/1) when finely laminated. Lamination occurs when coccoliths and calcispheres are present. Pyrite concretion, 2.5 cm in diameter, occurs in Section 1, 12 cm. Bioturbation is minor, mainly of *Chondrites* type.

SMEAR SLIDE SUMMARY (%):

	1, 40 D	2, 35 D
TEXTURE:		
Silt	15	20
Clay	85	80
COMPOSITION:		
Quartz	2	3
Mica	2	4
Clay	85	80
Accessory minerals	3	4
Pyrite	8	5
Opaque minerals	—	3
Nannofossils	Tr	1

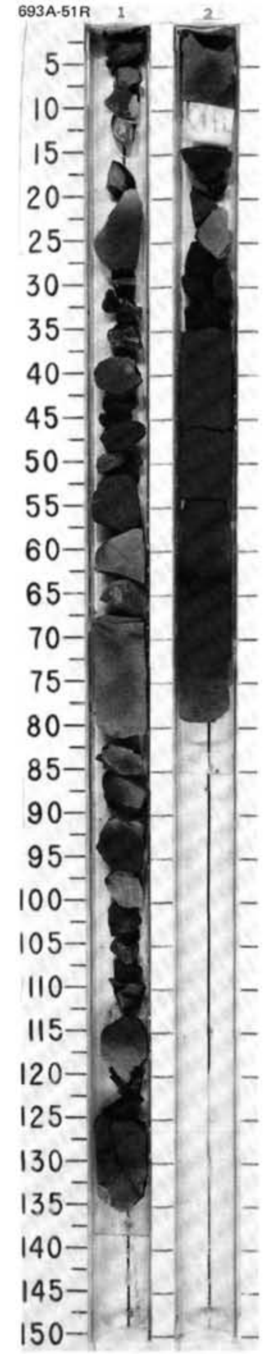

SITE 693 HOLE B CORE 1W CORED INTERVAL 2359.4-2593.2 mbsl; 0-233.8 mbsf

TIME-ROCK UNIT	BIOSTRAT. ZONE/ FOSSIL CHARACTER					PALEOMAGNETICS	PHYS. PROPERTIES	CHEMISTRY	SECTION	METERS	GRAPHIC LITHOLOGY	DRILLING DISTURB.	SED. STRUCTURES	SAMPLES	LITHOLOGIC DESCRIPTION
	FORAMINIFERS	NANNOFOSSILS	RADIOLARIANS	DIATOMS	PALYNOMORPHS										
									1	0.5 1.0					WASH CORE. Material similar to sediments recovered over same interval at Hole 693A. Sediments recovered are similar to those recovered between 0.0-234 mbsf from Hole 693A and were not described. Core not described.
									2						
									3						
									4						
									5						
									6						
									CC						

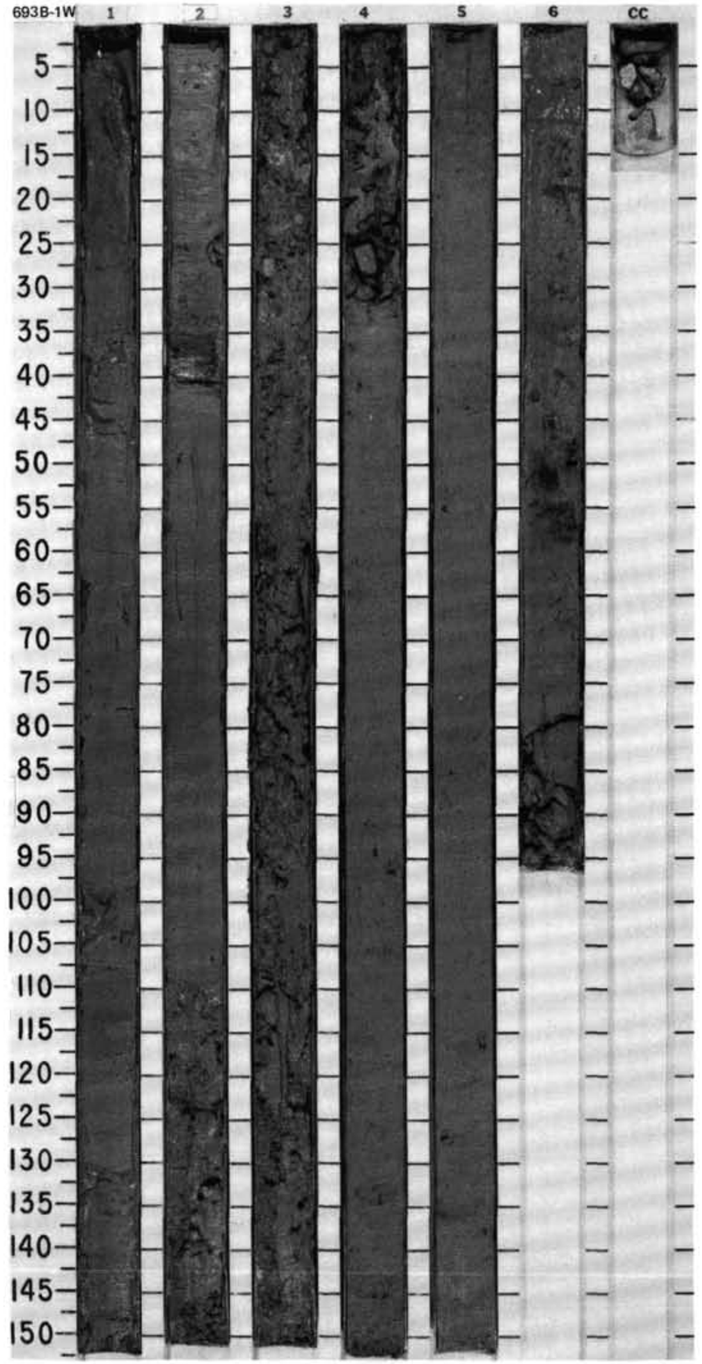

SITE 693 HOLE B CORE 2X CORED INTERVAL 2593.2-2598.2 mbsl; 233.8-238.8 mbsf

TIME-ROCK UNIT	FORAMINIFERS	NANNOFOSSILS	RADIOLARIANS	DIATOMS	PALYNOMORPHS	PALEOMAGNETICS	PHYS. PROPERTIES	CHEMISTRY	SECTION	METERS
UPPER MIOCENE		B	MIDDLE *C. spongothorax* F,M	*D. hustedtii* F,M	B		● γ=1.93 ● ϕ=67 V=1512	● 0.2%	1 2 3 4	0.5 1.0

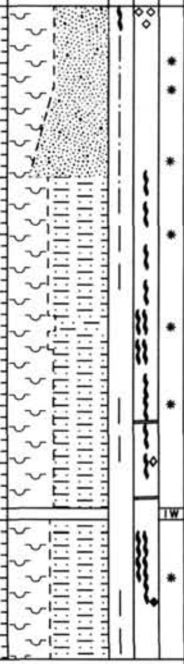

LITHOLOGIC DESCRIPTION

DIATOM CLAYEY MUD, DIATOM SILTY MUD, and DIATOM-BEARING CLAYEY MUD

Major lithologies: Diatom clayey mud and diatom silty mud, mainly greenish gray (5GY 5/1), dark greenish gray (5G 4/1, 5GY 4/1), and gray (N 4/0); color boundaries are gradational. In Section 1, diatom silty mud, greenish gray (5BG 5/1) at the top, grades down to diatom-bearing clayey mud, greenish gray (5G 6/1). Patches and laminae of dark greenish gray (5GY 4/1) diatom mud containing hornblende are common in Section 2, 0-70 cm, Section 3, 55-73 cm, and Section 4, 0-27 cm.

Minor lithologies: Muddy diatom ooze, greenish gray (5GY 5/1, 6/1), occurs as laminae at Section 3, 68 and 124 cm, and as burrow infills at Section 2, 130-136 cm. Fine sand, 2 cm clast, in Section 4, 74 cm, well-sorted; quartz, feldspar, and hornblende, with a few diatoms.

Bioturbation is present in Sections 2 through 4. It is minor to moderate and includes halo burrows and *Planolites*. Dropstones occur in Section 1, 0-6 cm (chloritized granite), and Section 3, 99 cm (black siltstone). Scattered sand grains are present throughout the core. Firmer layers 1-2 cm thick are present in all sections and result in core-splitting disturbance.

SMEAR SLIDE SUMMARY (%):

	1, 45 D	1, 70 D	1, 140 D	2, 50 D	2, 130 M	3, 50 D	4, 50 D
TEXTURE:							
Sand	10	15	2	6	2	5	2
Silt	60	65	53	53	56	64	63
Clay	30	20	45	41	42	31	35
COMPOSITION:							
Quartz	15	20	20	8	7	11	15
Feldspar	Tr	1	1	2	—	5	4
Mica	—	—	3	—	Tr	—	—
Clay	30	20	45	41	42	30	35
Volcanic glass	1	3	2	—	—	—	—
Accessory minerals	5	2	—	—	1	—	1
Rutile	—	—	—	—	Tr	—	Tr
Amphiboles	2	2	2	Tr	—	—	—
Glauconite	Tr	5	—	—	Tr	2	1
Opaques	—	Tr	1	3	—	3	2
Diatoms	45	45	25	45	50	48	42
Radiolarians	2	2	Tr	1	—	1	Tr
Sponge spicules	Tr	—	1	—	—	Tr	—
Carbonates	—	—	—	—	—	—	Tr

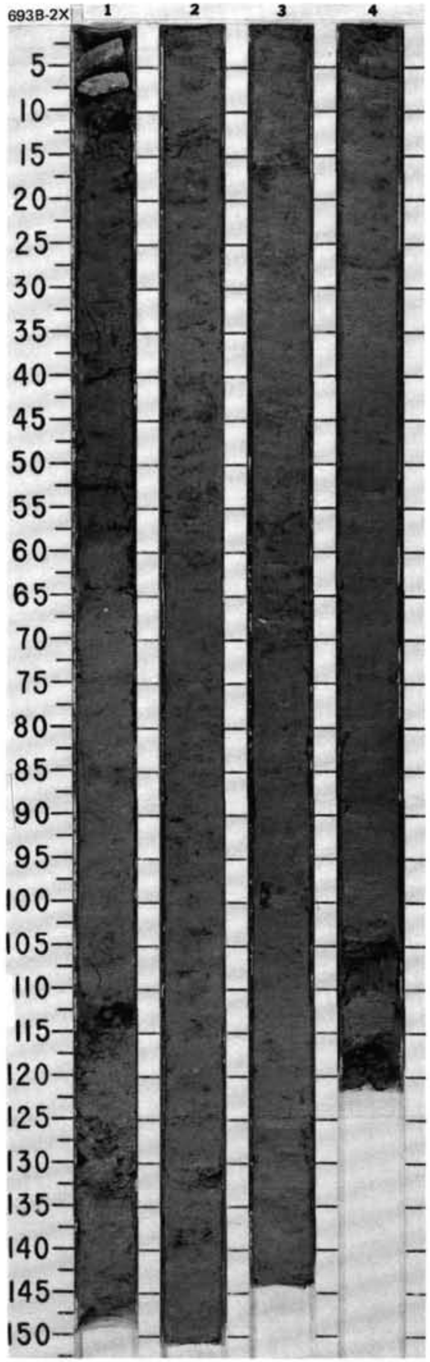

SITE 693 HOLE B CORE 3X CORED INTERVAL 2598.2-2607.8 mbsl; 238.8-248.4 mbsf

TIME-ROCK UNIT	BIOSTRAT. ZONE/ FOSSIL CHARACTER: FORAMINIFERS	NANNOFOSSILS	RADIOLARIANS	DIATOMS	PALYNOMORPHS	PALEOMAGNETICS	PHYS. PROPERTIES	CHEMISTRY	SECTION	METERS	GRAPHIC LITHOLOGY	DRILLING DISTURB.	SED. STRUCTURES	SAMPLES
UPPER MIOCENE	B	B	LOWER *C. spongothorax* A,G	*D. hustedtii* C,M	B				1, CC					*

LITHOLOGIC DESCRIPTION

DIATOM MUD

Major lithology: Diatom mud, dark greenish gray (5GY 4/1), slight bioturbation.

Dropstones include gabbro, quartzite, and diorite; 5-6 cm across.

SMEAR SLIDE SUMMARY (%):

	1, 22 D
TEXTURE:	
Silt	68
Clay	32
COMPOSITION:	
Quartz	15
Feldspar	1
Mica	2
Clay	32
Accessory minerals:	
Heavy minerals	Tr
Opaque	Tr
Epidote	Tr
Diatoms	45
Radiolarians	5

CORE 113-693B-4X NO RECOVERY

CORE 113-693B-5H NO RECOVERY

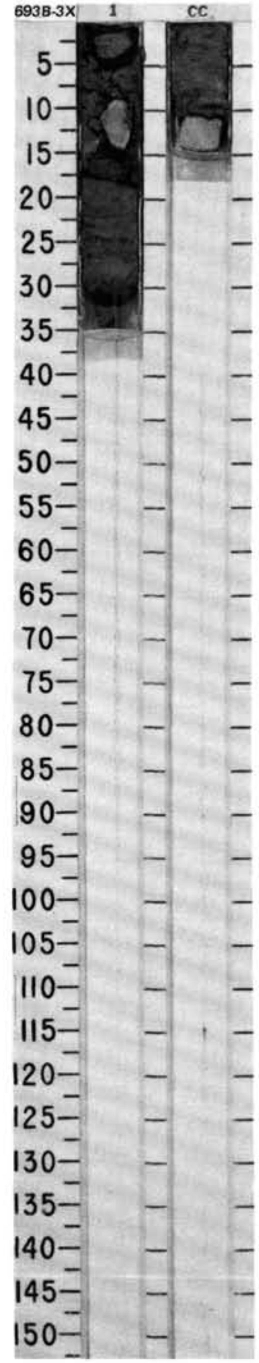

SITE 693 HOLE B CORE 6H CORED INTERVAL 2627.2-2636.9 mbsl; 267.8-277.5 mbsf

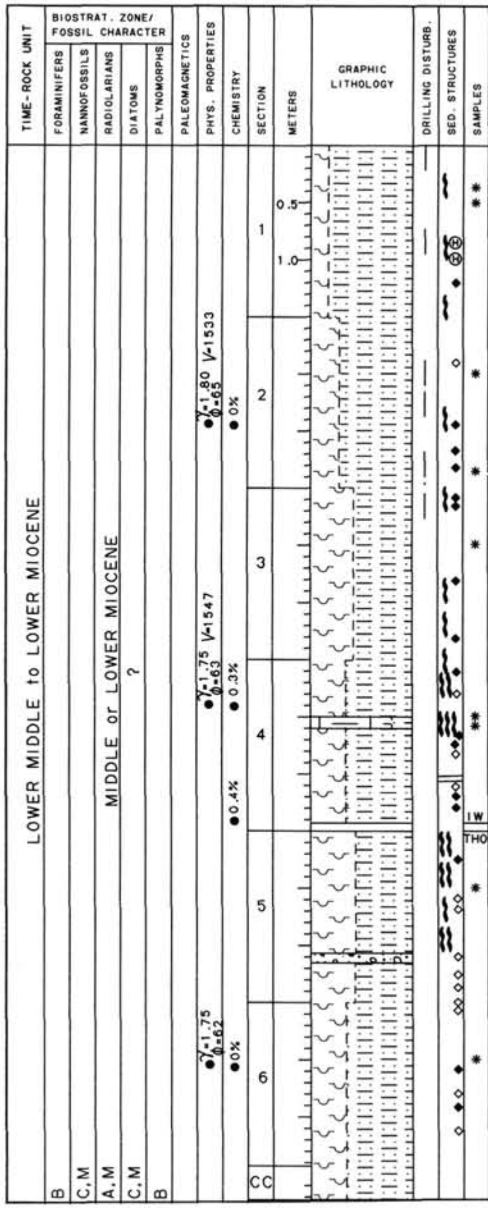

LITHOLOGIC DESCRIPTION

DIATOM-BEARING CLAYEY MUD and DIATOM CLAYEY MUD

Major lithologies: Diatom-bearing clayey mud grading down to diatom clayey mud, dark greenish gray (mainly 5BG 4/1, some 5G 4/1), and dark gray (N 4/0) in the middle of Section 3. Intervals of 5BG 4/1 have diffuse laminae of 5G 4/1 (e.g., Section 1, 47 and 116 cm, and Section 3, 6-13 cm). Sections 4 and 5 contain intervals mottled with greenish gray (5G 5/1). Large disk-shaped radiolarians on core surface from Section 3 downward. Tiny mica flakes from Section 5, 116 cm, downward.

Minor lithologies: Diatom and mud-bearing nannofossil ooze, greenish gray (5GY 6/1), in Section 4, 50-60 cm. Sand, light gray (5Y 6/1), very fine-grained, well sorted with subangular grains, occurs as tiny (1-2 mm) clasts in all sections, and as matrix to breccia unit in Section 5. Diatom mud, dark greenish gray (5GY 4/1), occurs as scattered clasts 3-10 mm across in Section 5, 88-106 cm; clasts plus sand matrix form a layer at Section 5, 106-113 cm, including one 5 cm clast of normal diatom mud. Diffuse sand/silt beds/laminae in Section 1, 66 and 117 cm, Section 3, 9-11 cm, and Section 6, 66-68 cm.

SMEAR SLIDE SUMMARY (%):

	1, 50 D	2, 50 D	2, 146 M	3, 50 D	4, 50 D	5, 50 D	6, 53 M
TEXTURE:							
Sand	2	2	80	2	2	5	—
Silt	38	43	20	63	63	65	—
Clay	60	55	—	35	35	30	—
COMPOSITION:							
Quartz	15	10	83	15	25	15	7
Feldspar	3	1	10	2	1	Tr	Tr
Mica	2	1	—	2	1	5	Tr
Clay	61	55	—	35	36	31	10
Accessory minerals:							
Pyroxene	—	—	Tr	Tr	—	—	—
Epidote	1	Tr	—	Tr	1	2	Tr
Opaque minerals	1	1	3	1	1	2	1
Heavy minerals	1	Tr	3	Tr	1	Tr	Tr
Nannofossils	—	—	—	Tr	—	—	68
Diatoms	15	30	—	40	30	40	10
Radiolarians	Tr	2	Tr	5	3	2	1
Sponge spicules	1	Tr	1	Tr	1	3	3
Silicoflagellates	—	—	—	Tr	—	—	Tr

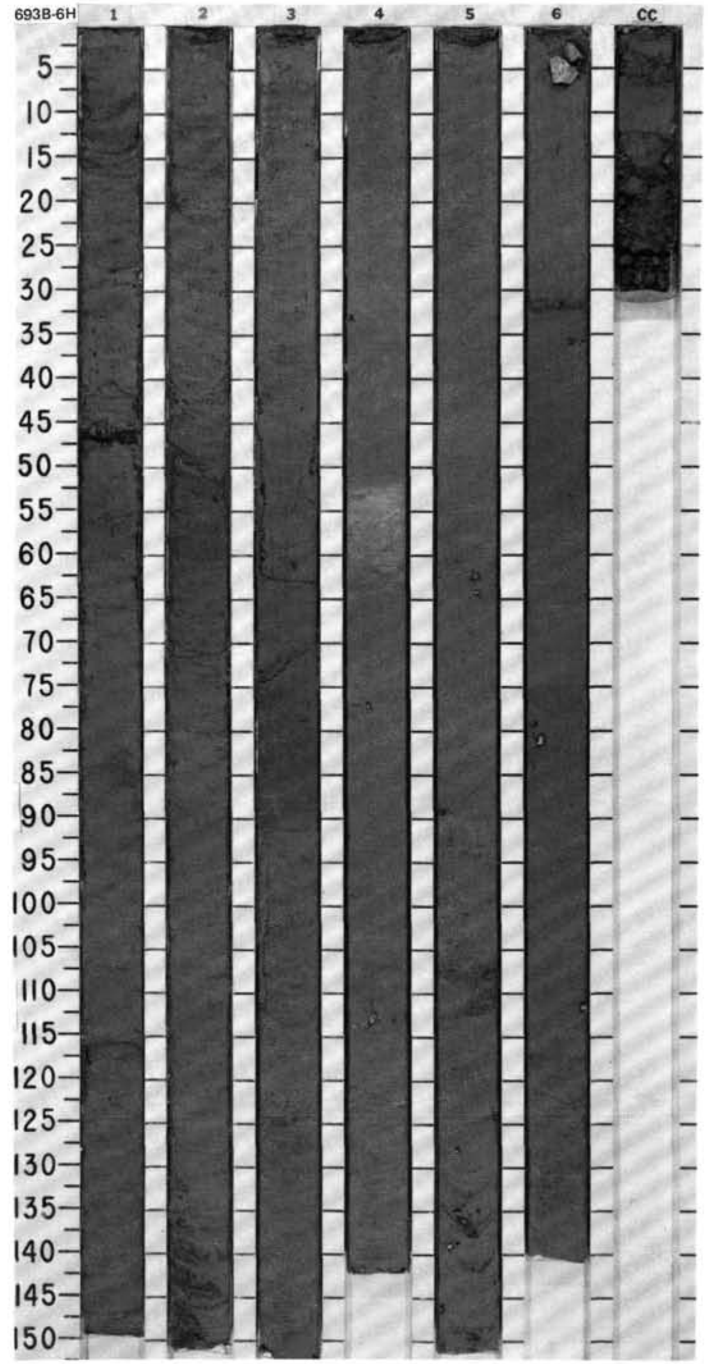

SITE 693 HOLE B CORE 7H CORED INTERVAL 2636.9-2646.5 mbsl; 277.5-287.1 mbsf

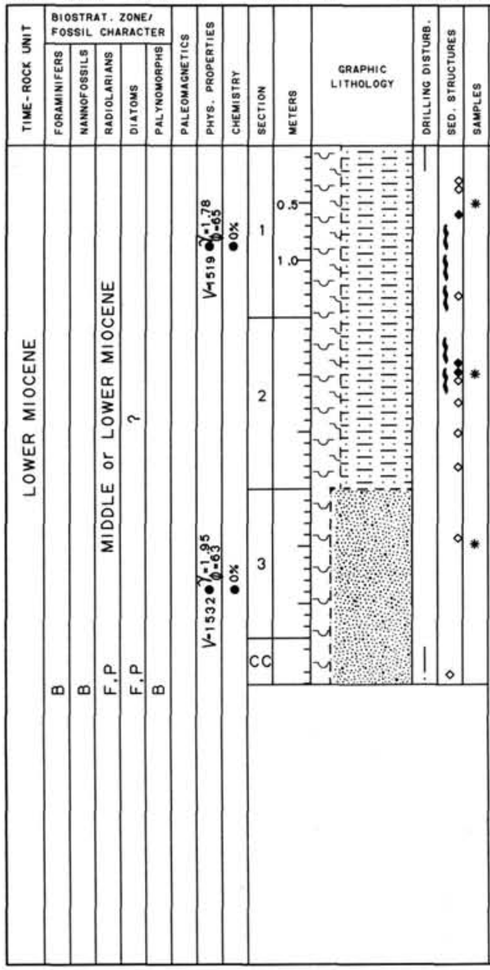

LITHOLOGIC DESCRIPTION

DIATOM CLAYEY MUD and DIATOM-BEARING SILTY MUD

Major lithologies: Diatom clayey mud, dark greenish gray (5G 4/1), faint dark gray (5Y 4/1) laminations, in Section 1, 115–150 cm. Diatom-bearing silty mud, dark greenish gray (5G 4/1), structureless, with coarse scattered sand in Section 3, 20–40 cm.

Gravel-sized lithified dropstones throughout the core; mud clasts in Section 1, 55 cm, and Section 2, 45 cm. Minor bioturbation in Section 1, 80–150 cm, and Section 2, 20–70 cm. Flecks of mica throughout the core, beginning at Section 1, 100 m.

SMEAR SLIDE SUMMARY (%):

	1, 50 D	2, 50 D	3, 50 D
TEXTURE:			
Sand	3	3	2
Silt	52	47	58
Clay	45	50	40
COMPOSITION:			
Quartz	15	10	25
Feldspar	2	1	3
Mica	2	5	3
Clay	45	51	41
Accessory minerals:			
Epidote	Tr	Tr	2
Amphibole	—	Tr	Tr
Opaque minerals	1	1	2
Heavy minerals	Tr	Tr	Tr
Glauconite	Tr	—	Tr
Diatoms	30	30	20
Radiolarians	5	2	1
Sponge spicules	—	Tr	3
Silicoflagellates	Tr	—	—

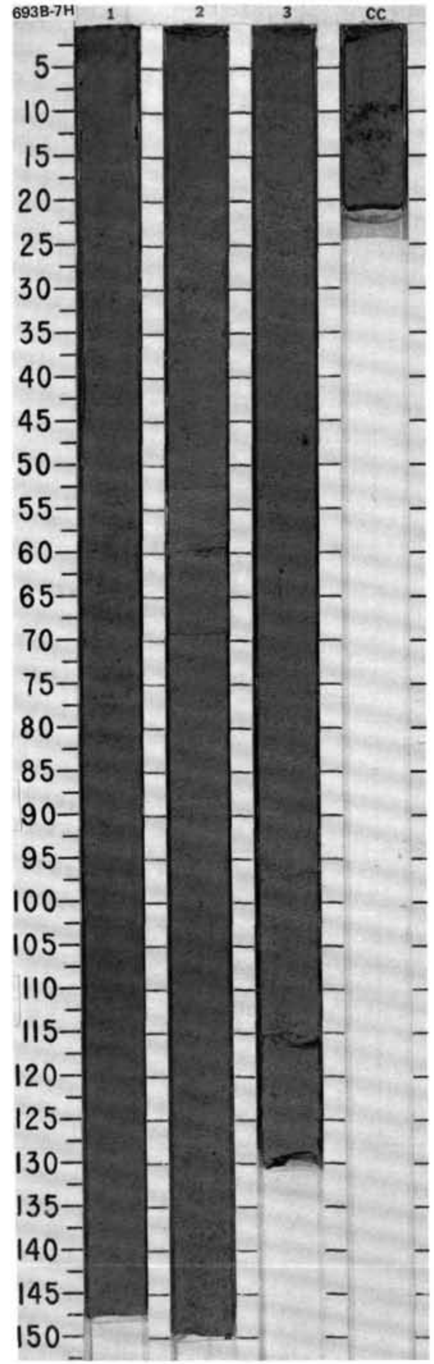

SITE 693 HOLE B CORE 8X CORED INTERVAL 2646.5-2656.2 mbsl; 287.1-296.8 mbsf

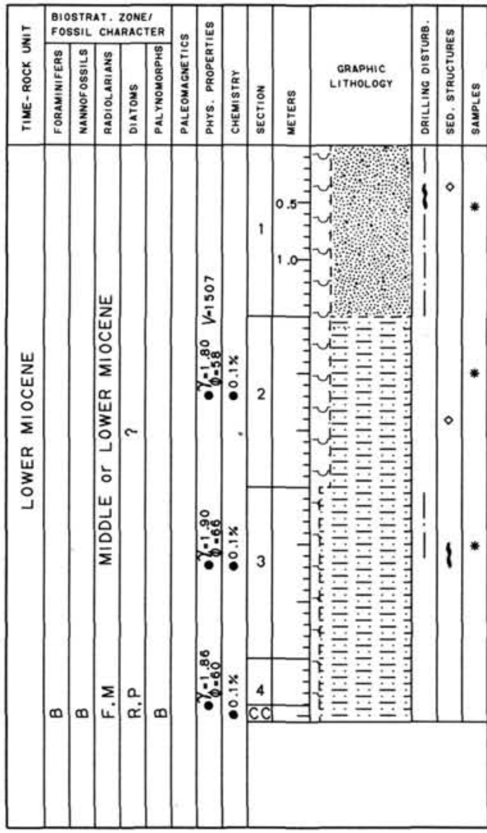

LITHOLOGIC DESCRIPTION

DIATOM-BEARING CLAYEY MUD and DIATOM-BEARING SILTY MUD

Major lithologies: Diatom-bearing clayey mud, dark greenish gray (5BG 4/1), and diatom-bearing silty mud, dark greenish gray (5BG 4/1).

Lithified dropstones, Section 1, 30 cm (50 mm long, gneiss), and Section 2 (10 mm long, gneiss). Laminae, dark greenish gray (5G 4/1), Section 3, 7-33 and 109-112 cm. Drilling and cutting biscuits are present.

SMEAR SLIDE SUMMARY (%):

	1, 50 D	2, 50 D	3, 50 D
TEXTURE:			
Sand	5	5	2
Silt	57	30	28
Clay	38	65	70
COMPOSITION:			
Quartz	25	20	10
Feldspar	2	1	Tr
Mica	5	7	5
Clay	38	66	70
Accessory minerals:			
Pyroxene	Tr	—	—
Glauconite	—	Tr	Tr
Epidote	1	2	1
Opaque minerals	2	1	1
Heavy minerals	—	1	Tr
Diatoms	25	20	10
Radiolarians	2	1	2
Sponge spicules	Tr	1	1
Silicoflagellates	Tr	Tr	—

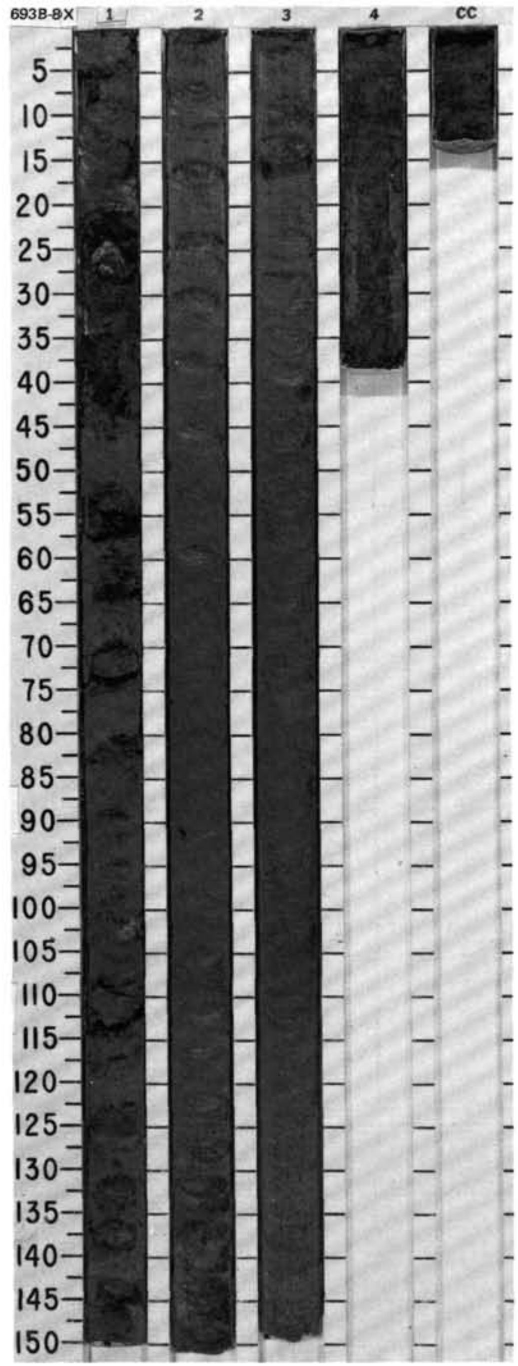

SITE 693 HOLE B CORE 9X CORED INTERVAL 2656.2-2665.9 mbsl; 296.8-306.5 mbsf

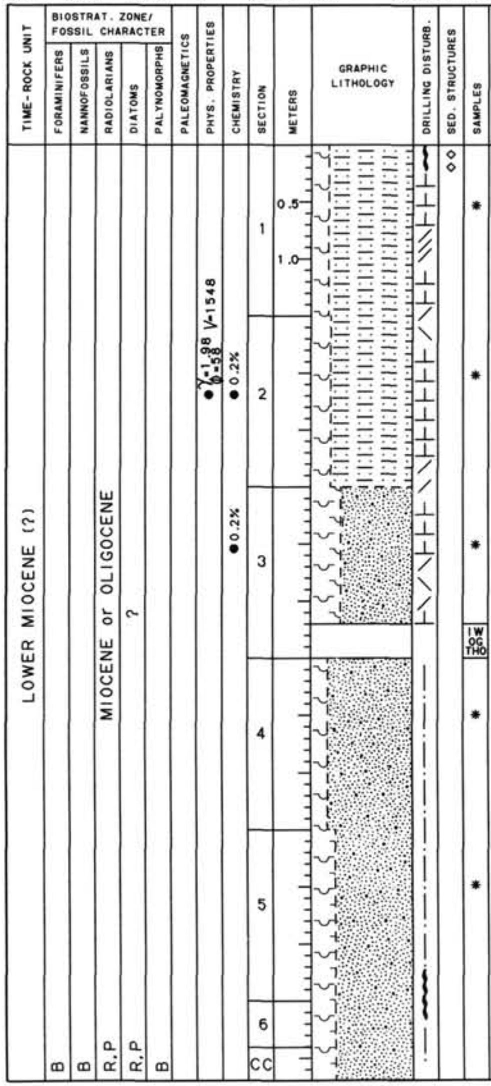

LITHOLOGIC DESCRIPTION

DIATOM-BEARING CLAYEY MUD, DIATOM SILTY MUD, and DIATOM-BEARING SILTY MUD

Major lithologies: Diatom-bearing clayey mud in Sections 1 and 2, dark greenish gray (5G 4/1) *with some black laminae (N 2/0) in Section 2. Additional* laminae, but without a distinct color change, are present in Section 1. Diatom silty mud in Sections 3, 5, and 6, dark greenish gray (5G 4/1). Diatom-bearing silty mud in Section 4, greenish gray (5G 5/1) changing to greenish gray (5B 5/1) at the base.

Drilling and cutting biscuits are present. Dropstones in Section 1, 0-8 cm, consisting of 4-cm-long chlorite schists.

SMEAR SLIDE SUMMARY (%):

	1, 50 D	2, 50 D	3, 50 D	4, 50 D	5, 50 D
TEXTURE:					
Sand	2	3	3	10	10
Silt	43	42	61	50	60
Clay	55	55	36	40	30
COMPOSITION:					
Quartz	20	15	21	30	30
Feldspar	2	3	5	—	—
Mica	2	5	4	—	2
Clay	56	54	36	40	30
Volcanic glass	—	—	—	—	1
Accessory minerals	—	—	—	14	10
Opaque minerals	1	2	3	1	1
Heavy minerals	1	Tr	—	—	—
Amphiboles	Tr	Tr	1	—	—
Diatoms	15	20	29	15	25
Radiolarians	2	1	1	—	2
Sponge spicules	1	Tr	Tr	Tr	—
Silicoflagellates	Tr	—	—	—	—

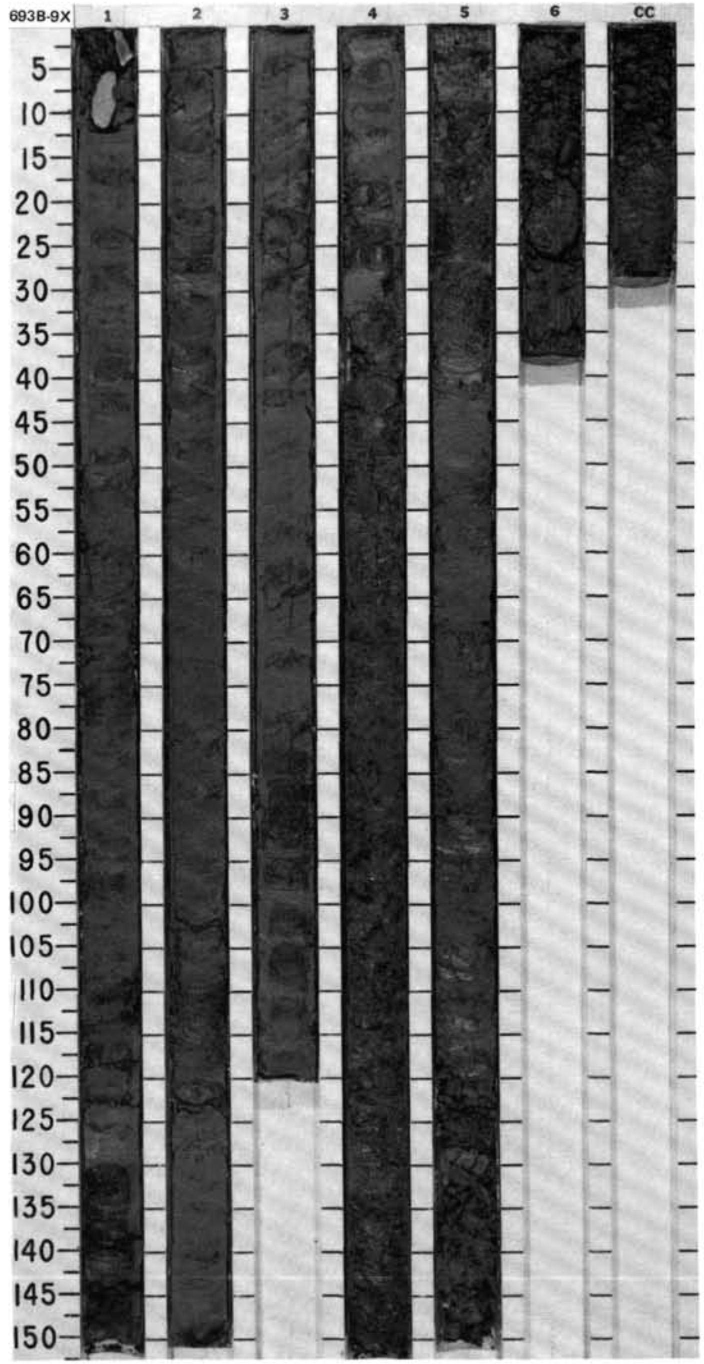

SITE 693 HOLE B CORE 10X CORED INTERVAL 2665.9-2675.5 mbsl; 306.5-316.1 mbsf

TIME-ROCK UNIT	FORAMINIFERS	NANNOFOSSILS	RADIOLARIANS	DIATOMS	PALYNOMORPHS	PALEOMAGNETICS	PHYS. PROPERTIES	CHEMISTRY	SECTION	METERS	GRAPHIC LITHOLOGY	DRILLING DISTURB.	SED. STRUCTURES	SAMPLES
UPPER OLIGOCENE (?)	B	B	OLIGOCENE (?) C,M	? F,P	B		γ=1.80 ϕ=62 V=1510; γ=1.73 ϕ=61 V=1503	0.3%; 0.2%	1, 2, 3, 4, CC	0.5, 1.0				

LITHOLOGIC DESCRIPTION

DIATOM-BEARING SILTY MUD

Major lithologies: Diatom-bearing silty mud, greenish gray (5G 5/1), moderately disturbed by biscuiting.

Minor lithologies: Sandy-gravelly mud, Section 3, between 25 and 138 cm. There are three separate coarse sand/gravel layers, smeared slightly by coring or cutting disturbance. They consist of an upper layer, 1 cm thick, which contains very coarse sand; a middle layer with fragments up to 0.5 cm, reverse graded(?); and a lower layer, 1 cm thick, with coarse grains overall the finest of the three layers. Silty mud in Section 4, 14-15 and 121-122 cm, greenish gray (5G 5/1), with some volcanic glass, so it is probably an altered volcanic ash layer.

Dropstones are rounded and common throughout. Bioturbation is present in Section 4, 46-95 cm.

SMEAR SLIDE SUMMARY (%):

	1, 60 D	2, 60 D	3, 60 D	4, 12 M	4, 60 D
TEXTURE:					
Sand	8	5	6	12	6
Silt	52	50	52	46	40
Clay	40	45	42	42	44
COMPOSITION:					
Quartz	30	30	32	32	32
Feldspar	—	2	1	Tr	Tr
Mica	—	Tr	—	2	4
Clay	40	45	42	42	44
Volcanic glass	2	—	2	4	2
Accessory minerals	7	8	4	13	8
Zeolites	Tr	Tr	Tr	—	Tr
Epidote	2	Tr	2	Tr	—
Opaque minerals	2	2	1	1	2
Diatoms	15	12	15	6	8
Radiolarians	1	1	Tr	Tr	Tr
Sponge spicules	1	Tr	1	Tr	Tr

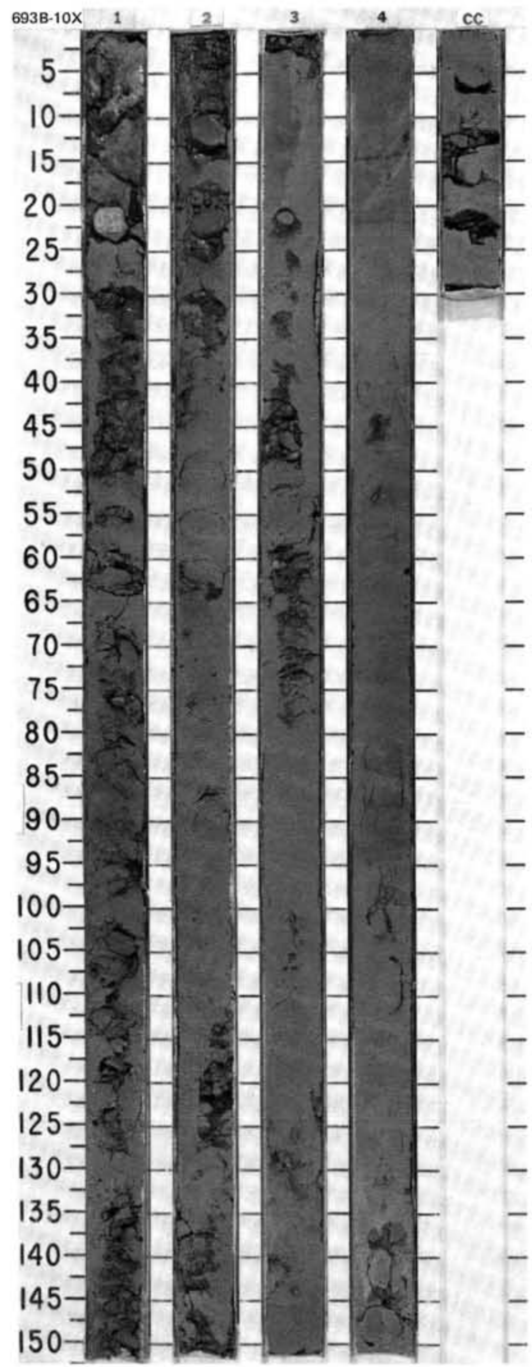

SITE 693 HOLE B CORE 11X CORED INTERVAL 2675.5-2685.2 mbsl; 316.1-325.8 mbsf

TIME-ROCK UNIT	FORAMINIFERS	NANNOFOSSILS	RADIOLARIANS	DIATOMS	PALEOMAGNETICS	PHYS. PROPERTIES	CHEMISTRY	SECTION	METERS	GRAPHIC LITHOLOGY	DRILLING DISTURB.	SED. STRUCTURES	SAMPLES
UPPER OLIGOCENE	B	B	C,M	F,M ? B. veniamini D. crux darwinii (silico)		γ=1.83 V-1584 ϕ=64 ● γ=1.83 ϕ=64 ● V-1584	●0.2%	1, 2, CC	0.5, 1.0	VOID			* * *

BIOSTRAT. ZONE/ FOSSIL CHARACTER

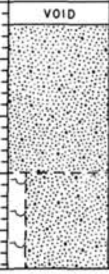

LITHOLOGIC DESCRIPTION

SILTY MUD and DIATOM-BEARING SILTY MUD

Major lithologies: Silty mud in Section 1, greenish gray (5GY 5/1), darkening toward the base of the section to dark greenish gray (5GY 4/1). Numerous grayish green (5G 4/2) laminae are present. Diatom-bearing silty mud in Section 2 and CC, dark greenish gray (5GY 4/1). Drilling biscuits are present and are slightly lighter than the surrounding sediments. In Section 2 there are some indications of bioturbation, but this may be the result of drilling disturbance.

Minor lithology: Clayey mud, grayish green (5G 4/2), as laminae found between Section 1, 114 cm, and the base in Section 2, and in the CC.

Large rounded dropstones are present in Section 1 at 22-29 cm (3 and 5 cm wide), and at 104-108.5 cm, with an adjacent smaller clast (~1 cm long). Dropstones are also present in the CC next to the void between 9 and 11 cm and at the base.

SMEAR SLIDE SUMMARY (%):

	1, 80 D	1, 114 M	2, 50 D
TEXTURE:			
Sand	6	8	8
Silt	48	40	60
Clay	46	52	32
COMPOSITION:			
Quartz	34	28	34
Feldspar	2	2	2
Mica	4	4	2
Clay	46	52	32
Volcanic glass	1	4	4
Accessory minerals	7	6	8
Rutile	—	—	Tr
Opaque minerals	—	—	2
Epidote	Tr	Tr	Tr
Zeolites	Tr	—	—
Glauconite	—	Tr	—
Diatoms	6	4	14
Radiolarians	—	—	2
Sponge spicules	—	—	Tr

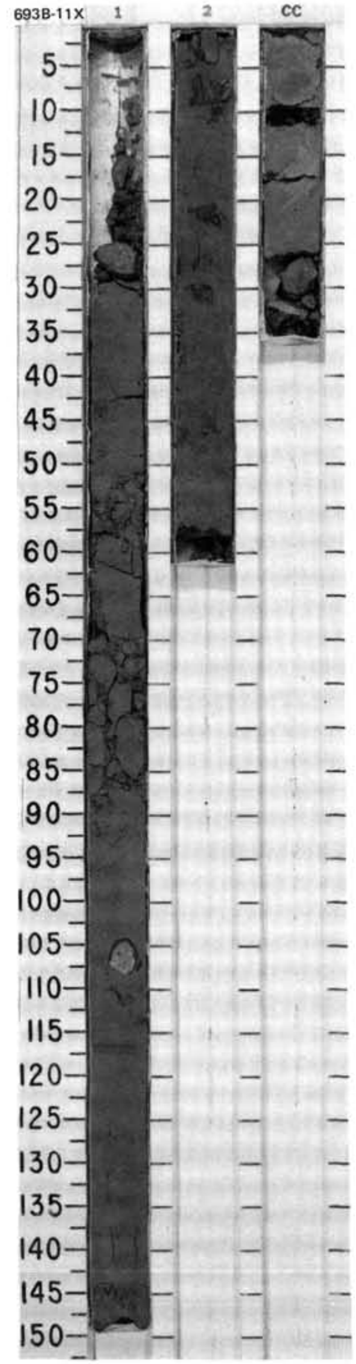

SITE 693 HOLE B CORE 12X CORED INTERVAL 2685.2-2694.9 mbsl; 325.8-335.5 mbsf

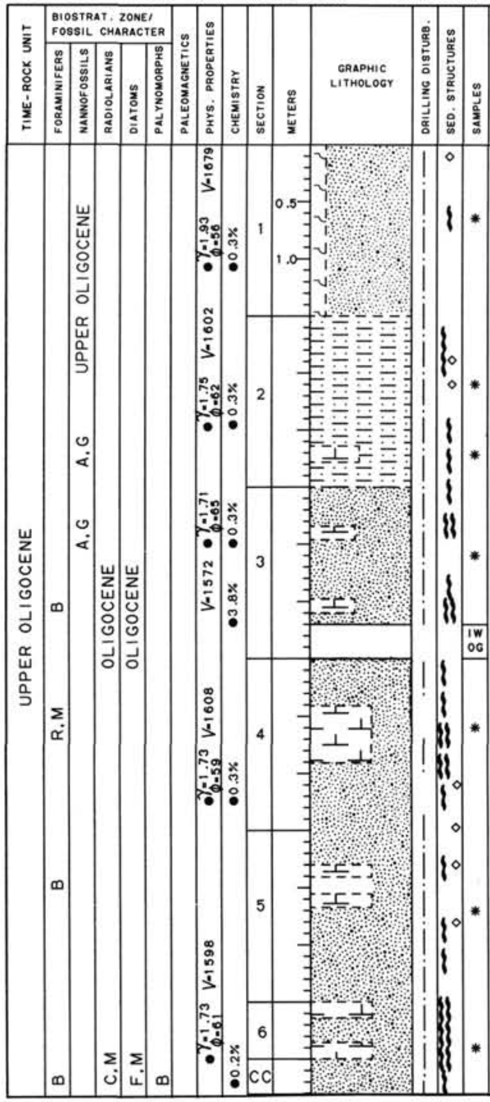

LITHOLOGIC DESCRIPTION

DIATOM-BEARING SILTY MUD, CLAYEY MUD, SILTY MUD, and MUDDY NANNOFOSSIL OOZE

Major lithologies: Diatom-bearing silty mud in Section 1, greenish gray (5G 4/1), with a sharp contact at 95 cm, between a few-cm-thick greenish gray (5G 5/1) layer and an overlying greenish gray (5G 4/1) layer. The immediately underlying darker material had a higher coarse-grained component. Other minor color changes are present and include a few thin lenses and laminae (all deformed, light gray (5Y 7/1) and dark blue gray (5B 4/1)). Clayey mud and silty mud, dark gray (N 4/1), gray (N 5/1), dark blue gray (5B 4/1), dark greenish gray (5G 4/1), and greenish gray (5GY 5/1), interbedded with muddy nannofossil ooze, greenish gray (5GY 5/1) and gray (5Y 6/1). These four lithologies vary in percentage of nannofossil component, with the lighter layers being more nannofossil-rich. Diatoms are also present in most of these lithologies.

Bioturbation is absent to moderate throughout the core and is strongest in the lighter, nannofossil-rich layers. Specific types of bioturbation include *Planolites*, *Zoophycos*, *Chondrites*, and vertical burrows. Dropstones are present throughout the core. They are more abundant in the darker layers. There are also many intervals of coarse sand (<1 mm), probably related to dropstones. Specific areas of ice-rafted detritus include: Section 2, 50-55 cm (2 cm-wide plus many sand-sized pieces), Section 4, 55, 122, and 140 cm (larger dropstones), and Section 5, 10-30 and 53-61 cm (abundant sand-sized dropstones).

SMEAR SLIDE SUMMARY (%):

	1, 60 D	2, 60 D	2, 120 M	3, 60 D	4, 60 M	5, 70 M	6, 36 M
TEXTURE:							
Sand	4	1	—	1	—	1	—
Silt	56	43	—	49	—	49	—
Clay	40	56	—	50	—	50	—
COMPOSITION:							
Quartz	27	18	15	30	10	12	11
Feldspar	6	3	6	6	—	2	—
Mica	1	2	—	—	—	—	—
Clay	40	56	18	50	20	50	13
Volcanic glass	4	8	2	1	4	5	4
Accessory minerals	4	3	5	5	5	6	5
Opaques	4	1	1	3	1	1	1
Glauconite	—	—	—	Tr	—	—	—
Nannofossils	—	—	50	Tr	58	15	60
Diatoms	12	8	—	5	2	8	6
Radiolarians	1	—	2	Tr	Tr	1	—
Sponge spicules	1	1	1	Tr	—	—	Tr

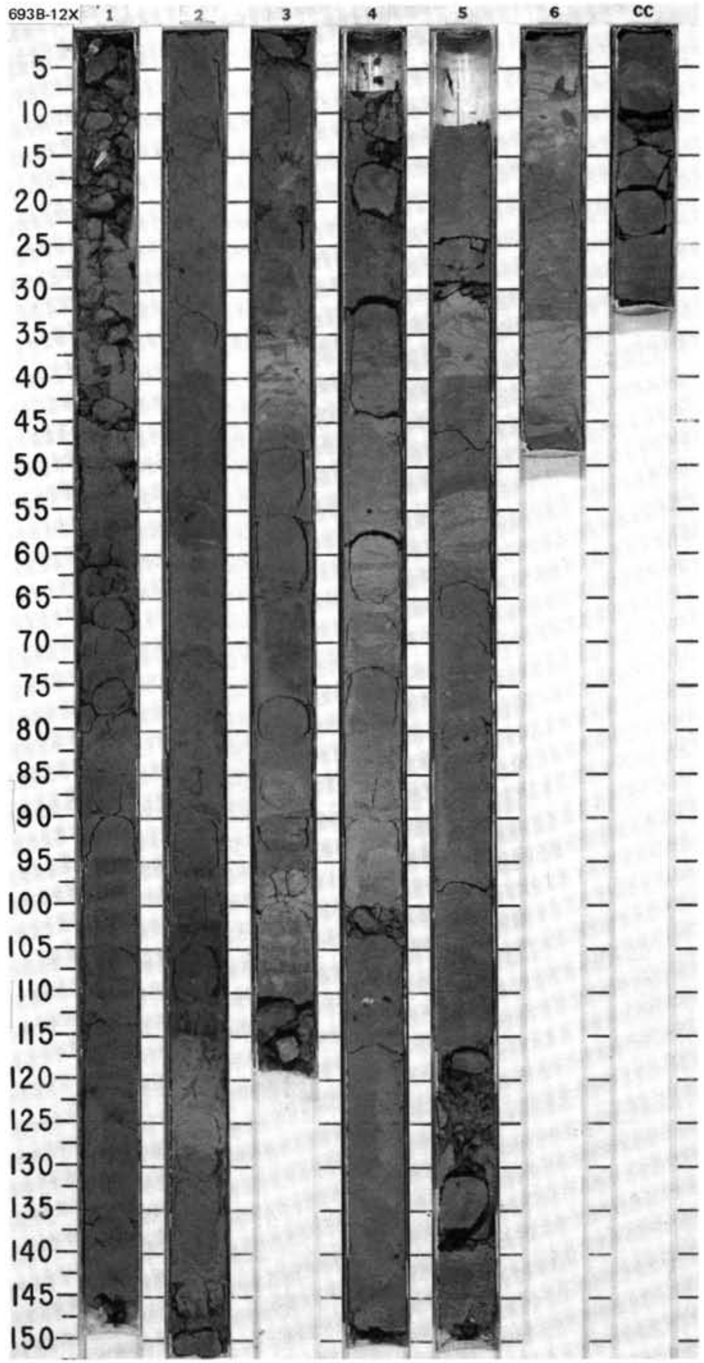

SITE 693 HOLE B CORE 13X CORED INTERVAL 2694.9-2704.5 mbsl; 335.5-345.1 mbsf

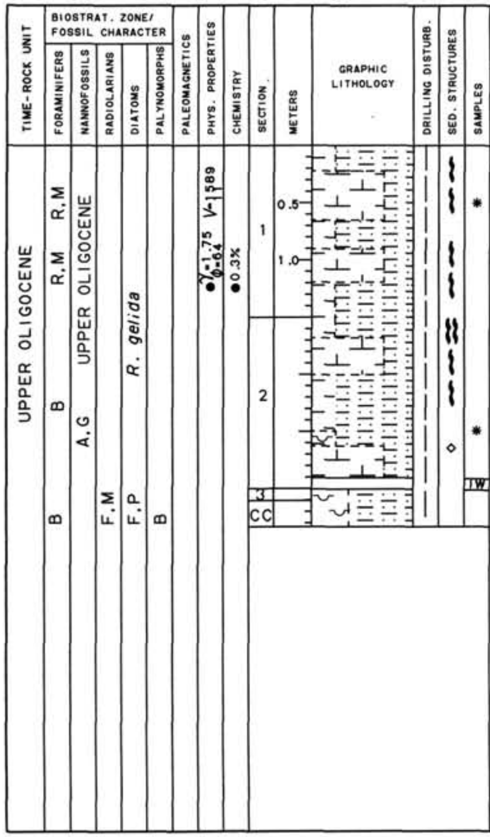

LITHOLOGIC DESCRIPTION

MUDDY NANNOFOSSIL OOZE and NANNOFOSSIL-BEARING CLAYEY MUD

Major lithologies: Muddy nannofossil ooze and nannofossil bearing clayey mud, greenish gray (5GY 5/1), gray (5Y 5/1), dark greenish gray (5G 4/1), and dark gray (N 4/1). As in 113-693B-12X, the lighter layers are nannofossil-rich and are more strongly bioturbated.

Minor lithology: Diatom-bearing clayey mud in Section 2, 100-113 cm, Section 3, and CC, dark gray (N 4/1).

A dropstone (1.5 cm long) is present at Section 2, 120 cm. Bioturbation includes *Zoophycos* (a particularly long burrow in Section 1, 10-14 cm), *Planolites*, and halo burrows.

SMEAR SLIDE SUMMARY (%):

	1, 50 D	2, 103 M
TEXTURE:		
Sand	—	1
Silt	—	30
Clay	—	69
COMPOSITION:		
Quartz	15	14
Mica	—	2
Clay	10	54
Volcanic glass	—	1
Accessory minerals	1	7
Opaque minerals	Tr	Tr
Glauconite	—	Tr
Nannofossils	65	—
Diatoms	8	22
Radiolarians	1	Tr

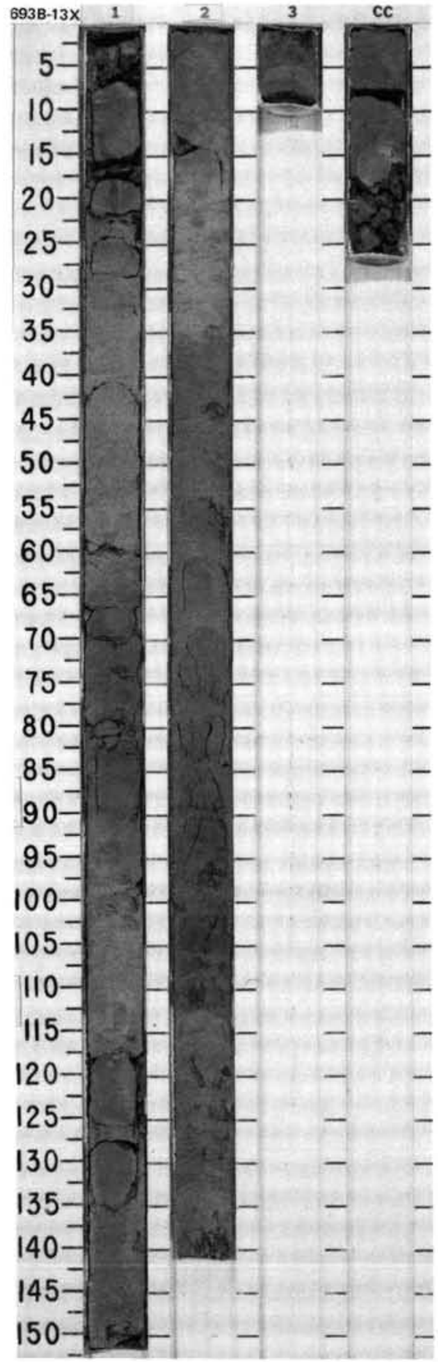

SITE 693 HOLE B CORE 14X CORED INTERVAL 2704.5-2714.1 mbsl; 345.1-354.7 mbsf

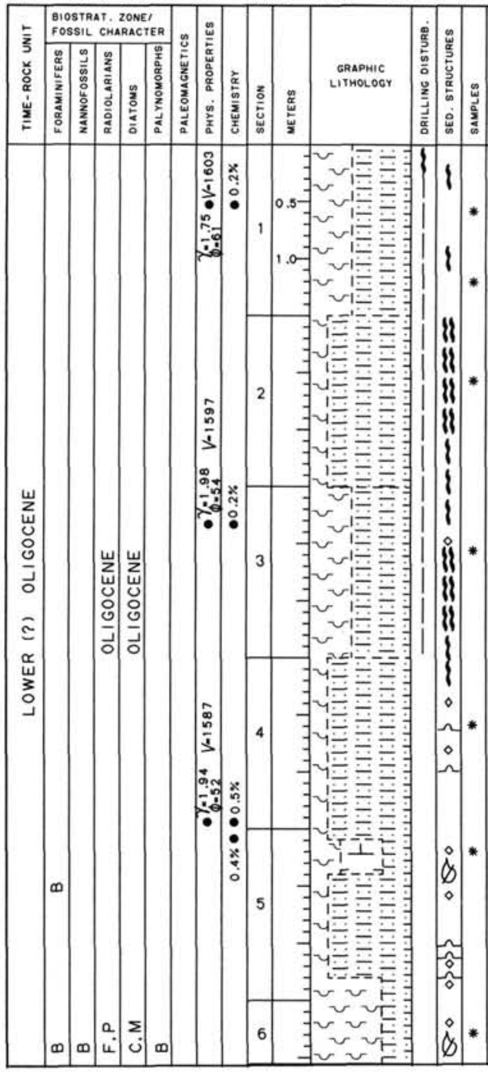

LITHOLOGIC DESCRIPTION

DIATOM SILTY MUD and DIATOM-BEARING CLAYEY MUD

Major lithologies: Diatom silty mud in Sections 1 and 3, greenish gray (5BG 5/1), dark gray (N 4/1), and different variations of greenish gray (5G 5/1, 5GY 5/1), alternating on a scale of 20–80 cm. In Section 1, 105–120 cm, a greenish gray (5G 5/1) layer (probably ash) is observed. Faint bioturbation is present. Only minor drilling disturbance. Diatom-bearing clayey mud in Sections 2, 4, and 5; alternating greenish gray (5BG 5/1) and dark gray (N 4/1) in Section 2; dark greenish gray (5GY 4/1) in Section 4.

Minor lithologies: Mud-bearing diatom nannofossil ooze in Section 5, 10–35 cm, with a sharp upper and lower boundary toward the diatom-bearing clayey mud of Section 5. Color is greenish gray (5G 6/1); no bioturbation. Muddy diatom ooze in Sections 5 and 6, olive gray (5Y 5/2), soft sediment; boundary to the diatom-bearing clayey mud in Section 5 is marked by well-developed slump structures at Section 5, 95–130 cm. In this region mm-sized dropstones are abundant. In Section 6 the lithology contains very fine (<2 mm), slightly darker laminae every 2–6 cm; bioturbation and drilling disturbance is absent.

Bioturbation varies from slight to moderate and ceases in Section 4 (*Chondrites* and *Planolites*). Dropstones are observed in Section 3, 50 cm, Section 4, 40 and 80 cm, and Section 5, 14, 60, and 120–130 cm. In Section 5, 47 cm, there are shell fragments. Also in Section 6 is a mudstone in which numerous bivalve shells are embedded.

SMEAR SLIDE SUMMARY (%):

	1, 60 D	1, 118 M	2, 60 D	3, 60 D	4, 60 D	5, 20 M	6, 25 M
TEXTURE:							
Sand	5	12	2	2	Tr	—	—
Silt	75	58	46	76	46	—	—
Clay	20	30	52	22	54	—	—
COMPOSITION:							
Quartz	24	24	16	18	18	12	12
Feldspar	—	—	Tr	Tr	—	—	Tr
Mica	1	1	—	2	1	4	4
Clay	20	30	52	22	54	8	6
Volcanic glass	2	4	—	2	2	—	2
Accessory minerals	8	9	12	11	7	6	6
Amphiboles	2	4	Tr	—	2	—	Tr
Opaque minerals	1	—	2	1	—	—	Tr
Glauconite	—	Tr	—	—	Tr	—	—
Nannofossils	—	—	—	—	—	42	—
Diatoms	40	28	18	42	16	28	70
Radiolarians	2	Tr	Tr	2	—	—	—
Sponge spicules	Tr	Tr	—	Tr	—	—	—

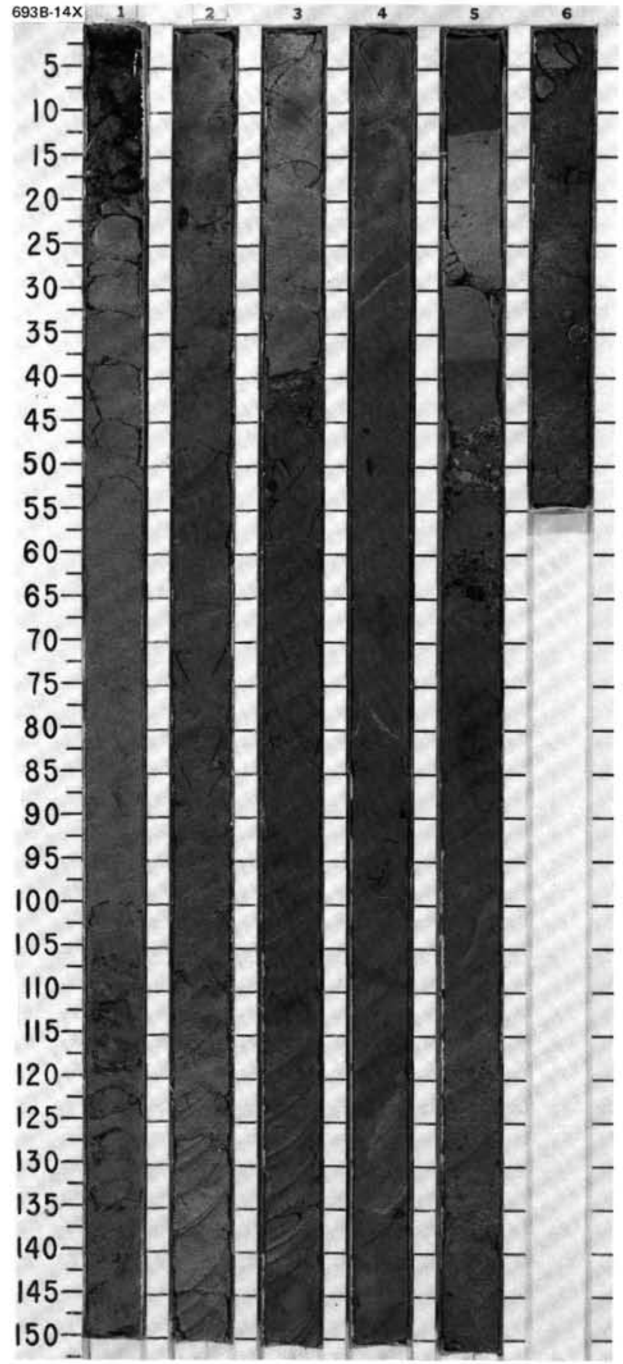

SITE 693 HOLE B CORE 15X CORED INTERVAL 2714.1-2723.8 mbsl; 354.7-364.4 mbsf

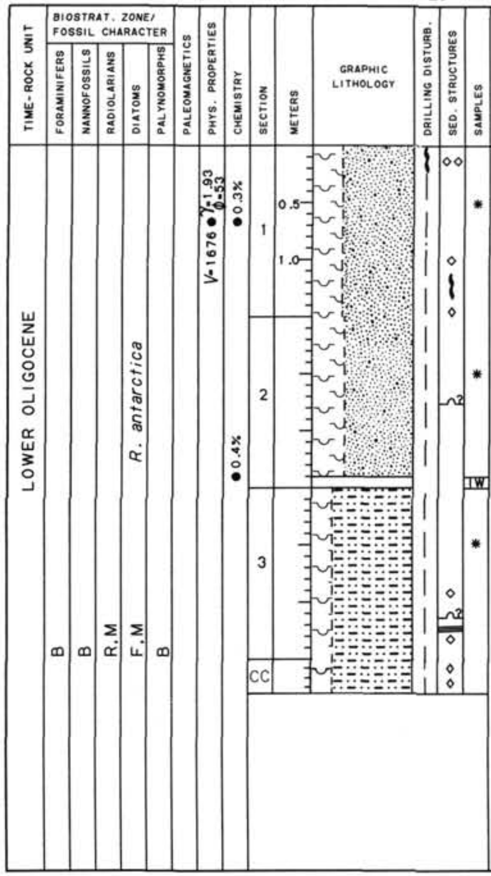

LITHOLOGIC DESCRIPTION

DIATOM SILTY MUD and DIATOM-BEARING CLAYEY MUD

Major lithologies: Diatom silty mud and diatom-bearing clayey mud, dark greenish gray (5G 4/1); sand, and a few gravel-sized dropstones throughout the core. The core may be part of a slump. In Section 2 some layers are parallel to the core liner and look "in place", i.e. not disturbed by coring. Similarly, in Section 3, some layers have non-parallel orientations.

Dropstones, two at Section 1, 15 cm (2-3 cm long), and one at Section 3, 90-95 cm (3.5 cm long). Bioturbation is present in only a few areas.

SMEAR SLIDE SUMMARY (%):

	1, 50 D	2, 50 D	3, 50 D
TEXTURE:			
Sand	12	6	4
Silt	63	64	44
Clay	24	30	52
COMPOSITION:			
Quartz	25	24	12
Feldspar	2	Tr	—
Mica	4	—	4
Clay	24	30	52
Volcanic glass	1	2	—
Accessory minerals	10	6	4
Opaque minerals	—	2	4
Amphiboles	Tr	2	Tr
Pyrite	4	—	—
Diatoms	28	32	24
Radiolarians	2	2	—

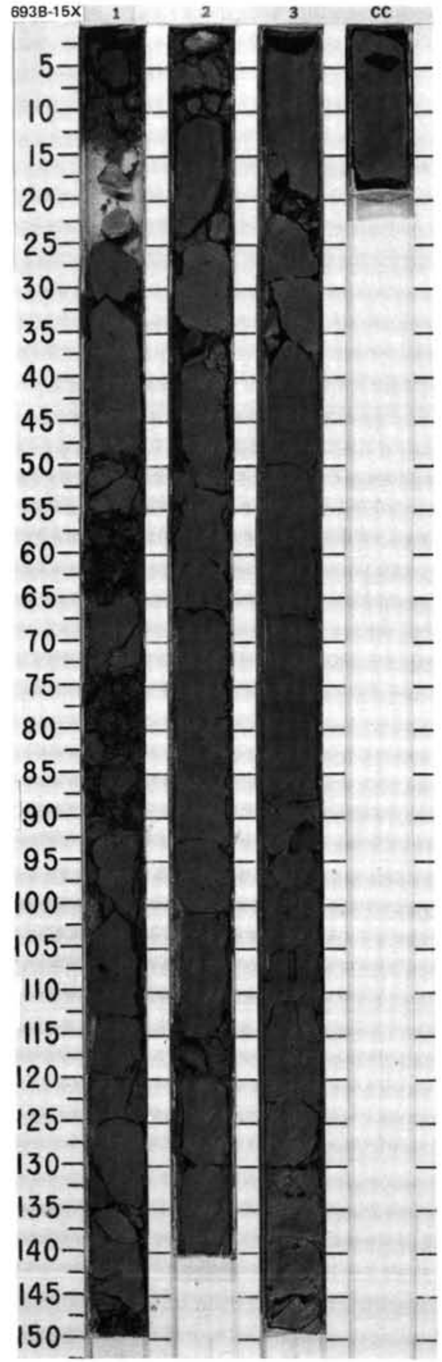

SITE 693 HOLE B CORE 16X CORED INTERVAL 2723.8-2733.4 mbsl; 364.4-374.0 mbsf

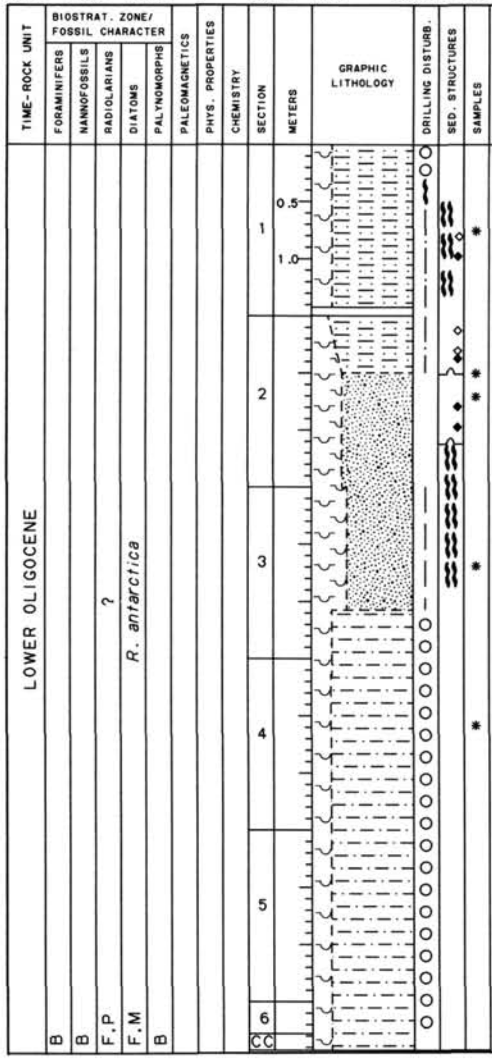

LITHOLOGIC DESCRIPTION

DIATOM-BEARING CLAYEY MUD, DIATOM SILTY MUD, and DIATOM-BEARING SANDY MUD

Major lithologies: Diatom-bearing clayey mud in Section 1 and Section 2, 0–50 cm, dark gray (5Y 4/1). Diatom silty mud in Section 2, 50–150 cm, and Section 3, 0–115 cm, dark gray (5Y 4/1). In Section 2 there are 10–50-cm-thick intervals where there are color variations between dark greenish gray (5G 4/2) and olive gray (5Y 4/2); a thin layer of dusky green (5G 3/2) occurs at Section 2, 77 cm. Mica flakes appear on surface below Section 2, 100 cm. Large clasts are also present in Section 2 between 47–59 and 98–107 cm. These may represent slumped deposits. Diatom-bearing sandy mud in Section 3, 115 cm, through CC, dark gray (5Y 4/1) core, structureless, wet, and sandy (with significant increase in coarse fraction at the base of Section 5 and in Section 6; many black, angular 2–6-mm-long clasts.

Moderate bioturbation in Sections 1, 2, and 3. Dropstones at Section 1, 72 and 86 cm. White, diatom-rich mud clasts are present in Sections 1 and 2. Flow-in in Section 1, 80 cm, downward along side; also in Section 2, down to ~45 cm.

SMEAR SLIDE SUMMARY (%):

	1, 70 D	2, 53 M	2, 70 D	3, 70 D	4, 50 D
TEXTURE:					
Sand	15	6	7	3	30
Silt	45	38	68	47	45
Clay	40	56	25	50	25
COMPOSITION:					
Quartz	30	20	25	10	30
Feldspar	3	3	3	3	5
Mica	2	1	3	Tr	2
Clay	38	56	27	50	26
Accessory minerals:					
Glauconite	—	—	—	Tr	1
Epidote	—	—	—	Tr	—
Amphibole	1	2	2	1	5
Opaque minerals	3	3	5	1	3
Heavy minerals	—	—	1	—	3
Foraminifers	—	Tr	—	—	—
Nannofossils	Tr	—	—	—	—
Diatoms	20	15	30	35	20
Radiolarians	2	Tr	2	Tr	2
Sponge spicules	1	—	2	—	3

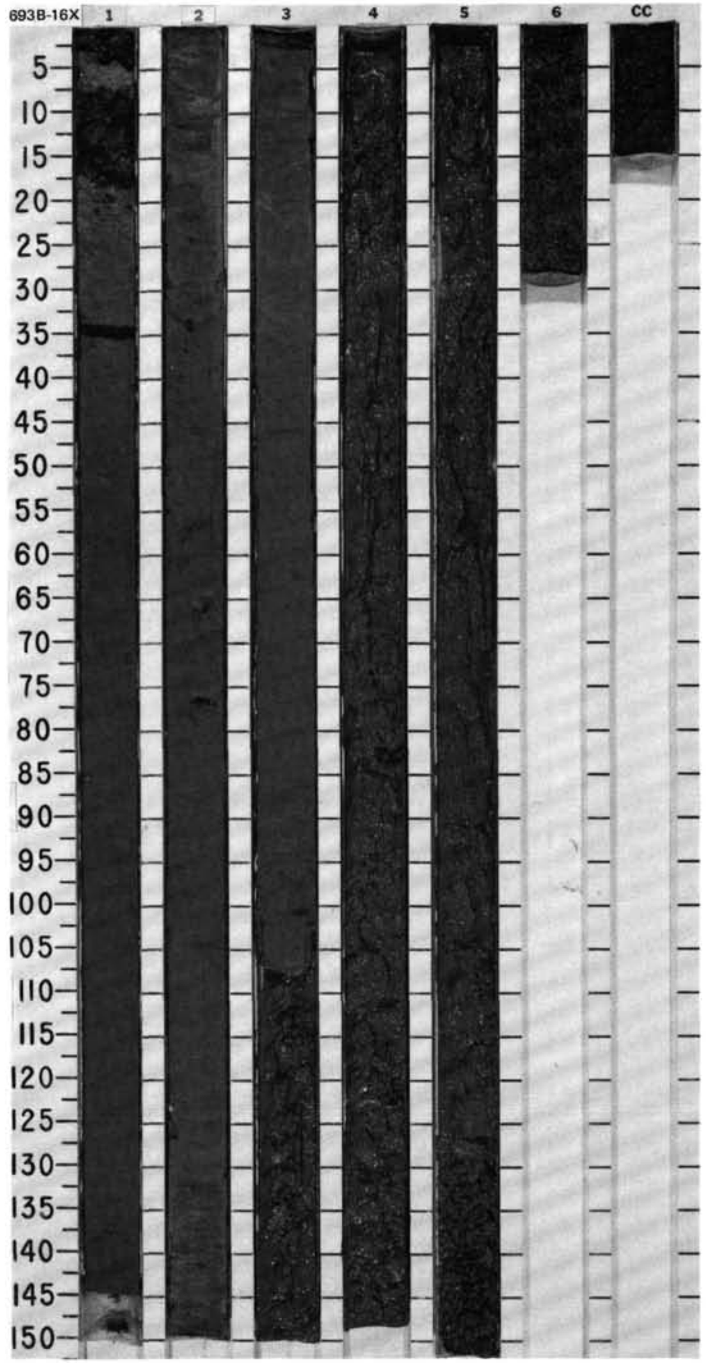

SITE 693 HOLE B CORE 17X CORED INTERVAL 2733.4-2743.1 mbsl; 374.0-383.7 mbsf

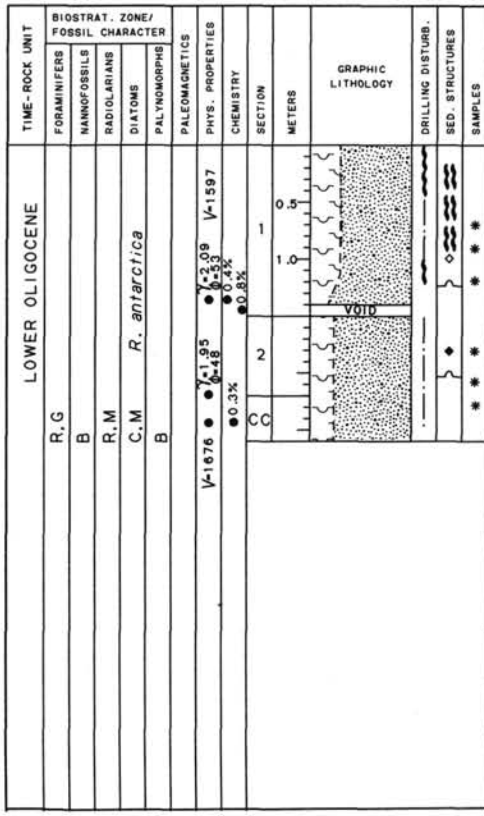

LITHOLOGIC DESCRIPTION

DIATOM SILTY MUD

Major lithology: Diatom silty mud, dark gray (5Y 4/1) to dark greenish gray (5GY 4/1). Section 1: top half moderate bioturbation, probable slump unit middle and basal section, clasts of dark greenish gray (5G 4/1), and dark gray (N 4/0). Section 2: laminae at 8, 20, 29, 38, 47, and 57 cm, between drilling biscuits, whole section may be slumped. CC: drilling breccia, micaceous, similar to base of Section 2.

Minor lithology: Clayey mud in Section 1, basal and dark greenish gray (5G 4/1), clasts are diatom-bearing.

Garnet, amphibolite dropstone at Section 1, 105 cm. Mudstone at Section 2, 18 cm.

SMEAR SLIDE SUMMARY (%):

	1, 70 D	1, 95 M	1, 133 M	2, 30 D	2, 60 M	CC, 9 D
TEXTURE:						
Sand	10	20	5	10	15	15
Silt	60	55	40	40	55	55
Clay	30	25	55	50	30	30
COMPOSITION:						
Quartz	25	30	10	15	25	30
Feldspar	2	3	2	Tr	1	5
Mica	1	3	10	2	10	—
Clay	30	23	53	50	28	30
Accessory minerals:						
Pyrite	—	—	—	Tr	—	—
Hornblende	—	—	—	—	1	—
Epidote	—	—	Tr	—	2	—
Amphibole	2	3	5	1	1	—
Opaque minerals	2	5	2	3	2	2
Heavy minerals	2	1	1	1	—	—
Glauconite	—	Tr	—	Tr	Tr	—
Nannofossils	—	—	—	—	Tr	—
Diatoms	30	30	15	25	28	25
Radiolarians	3	1	2	2	1	3
Sponge spicules	3	1	Tr	1	1	2
Silicoflagellates	—	—	—	—	Tr	—

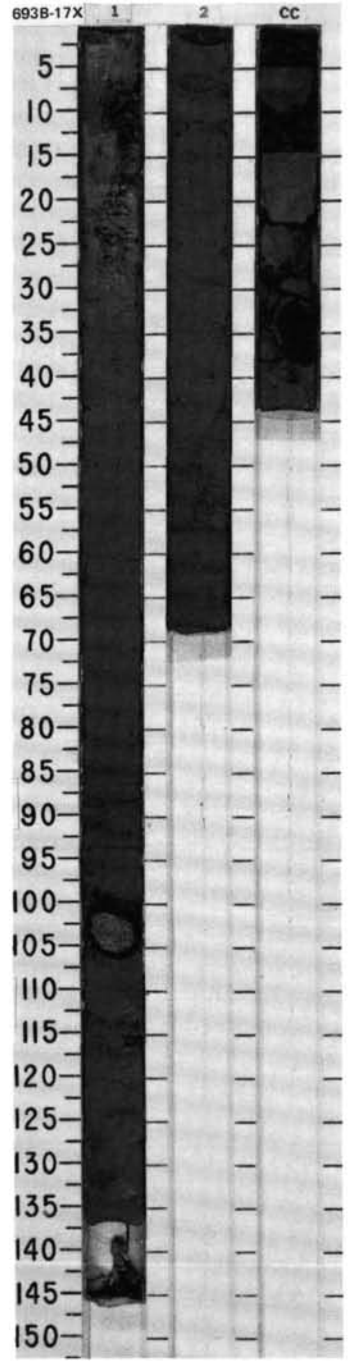

SITE 693 HOLE B CORE 18X CORED INTERVAL 2743.1-2752.8 mbsl; 383.7-393.4 mbsf

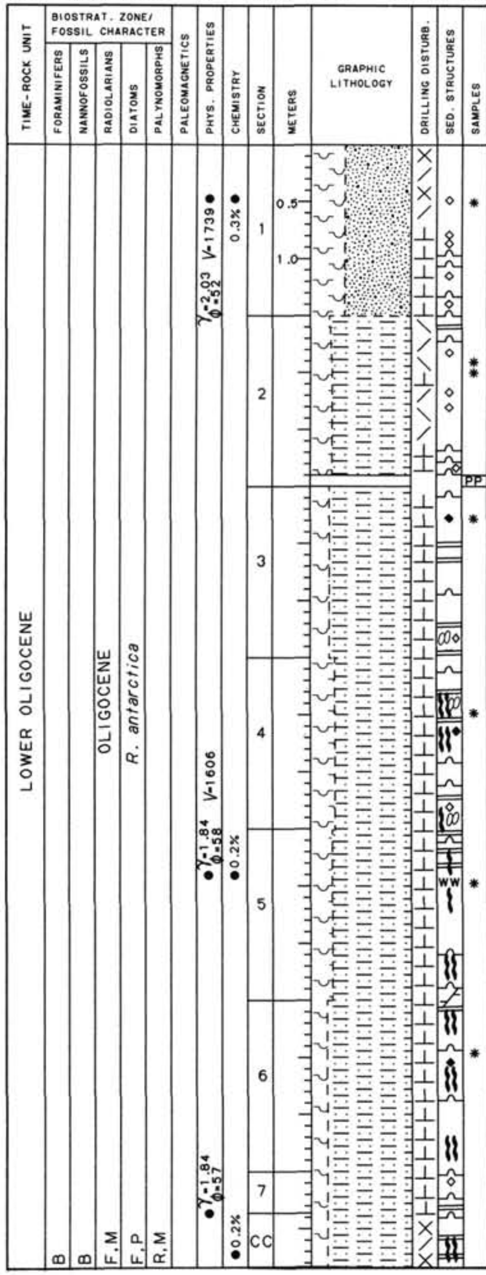

LITHOLOGIC DESCRIPTION

DIATOM SILTY MUDSTONE, DIATOM-BEARING CLAYEY MUDSTONE, and DIATOM CLAYEY MUDSTONE

Major lithologies: Diatom silty mudstone, diatom-bearing clayey mudstone, and diatom clayey mudstone, very dark gray (5Y 3/1), dark gray (5Y 4/1), and dark greenish gray (5GY 4/1). Base of Section 3, color variegated. Sections 3 and 5, laminations of greenish gray (5GY 5/1) and dark gray (N 4/0) to dark greenish gray. Entire core appears to be slumped. Drilling biscuits contain remains of slump breccia (folds and intraformational slumps) in Section 1, 80-100 cm, Section 2, 110-140 cm, Section 3, 0-10 and 85-100 cm, and intermittently in Sections 4-7. The original unslumped sequence was laminated. Laminations (predominantly lenticular, minor parallel) are disrupted by slumping. There are no obvious signs of grading or cross laminations. Tops show small-scale scours, tilled blocks, and folds up to a few centimeters across. Minor faults, with up to 2 cm displacement, are observed in Section 3.

Minor to moderate bioturbation (*Planolites*) in Section 4 and intermittently in Sections 5 and 6. Dropstones are present in Section 1, 48, 85, 104, and 150 cm; Section 2, 20, 70, and 140 cm; Section 3, 130 cm; and Section 5, 150 cm. Mudclasts are present in Section 2, 20 cm, and Section 4, 10 and 120 cm. Sand grains (some glauconite) are scattered throughout core; they are most common in Sections 1 and 2. Entire core distorted by slumping, drilling disturbance, biscuiting, and rotation of biscuits while drilling.

SMEAR SLIDE SUMMARY (%):

	1, 50 D	2, 48 D	2, 52 D	3, 16 M	4, 46 D	5, 50 D	6, 50 D
TEXTURE:							
Sand	8	5	7	4	10	3	3
Silt	65	45	41	28	50	64	47
Clay	27	50	52	68	40	33	50
COMPOSITION:							
Quartz	27	25	15	9	15	18	15
Feldspar	3	3	3	1	3	2	2
Mica	3	2	1	Tr	Tr	2	3
Clay	27	49	52	68	40	33	49
Volcanic glass	—	—	—	—	—	—	—
Accessory minerals:							
Epidote	—	—	—	—	—	Tr	—
Amphibole	1	1	1	—	Tr	—	1
Glauconite	1	—	2	5	—	4	Tr
Opaque minerals	2	3	—	1	3	2	3
Heavy minerals	—	1	2	—	—	Tr	Tr
Foraminifers	—	—	—	—	—	Tr	—
Diatoms	35	20	23	16	30	27	15
Radiolarians	1	5	1	Tr	7	2	10
Sponge spicules	Tr	1	Tr	Tr	2	—	2
Silicoflagellates	—	—	—	—	Tr	—	Tr

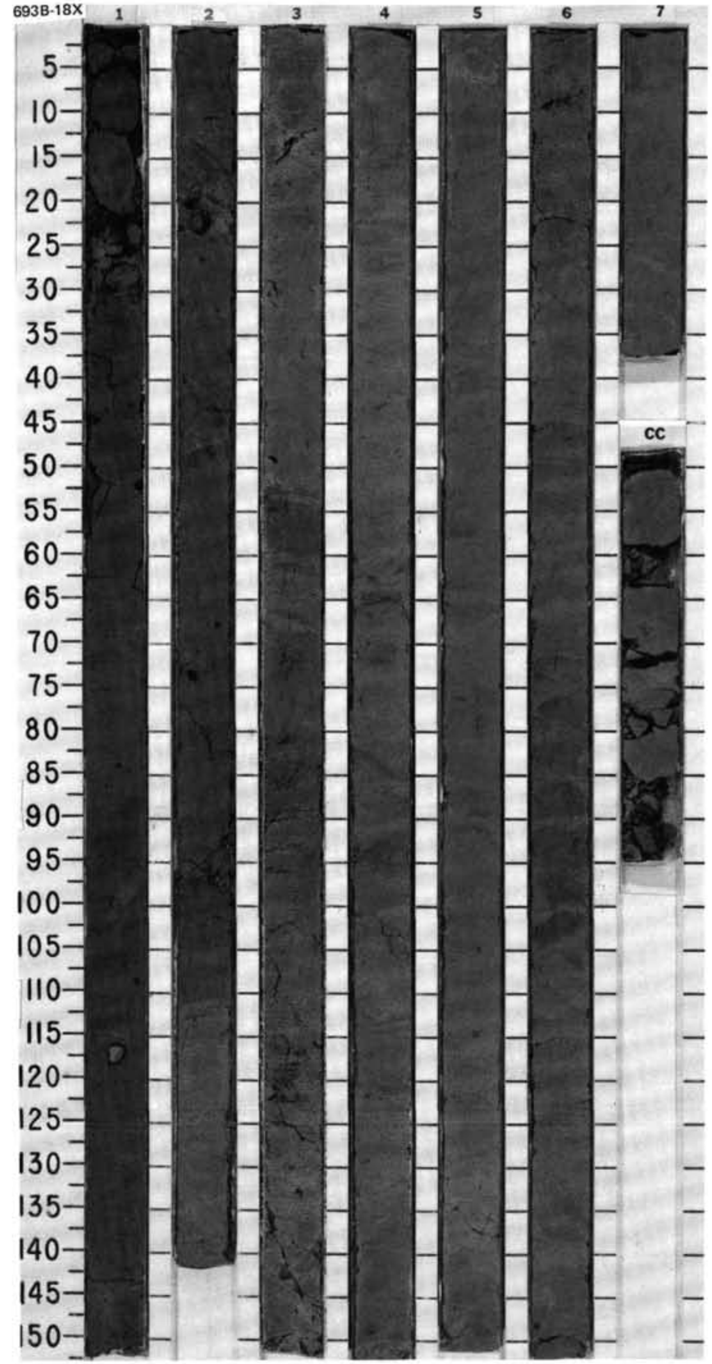

SITE 693 HOLE B CORE 19X CORED INTERVAL 2752.8-2762.5 mbsl; 393.4-403.1 mbsf

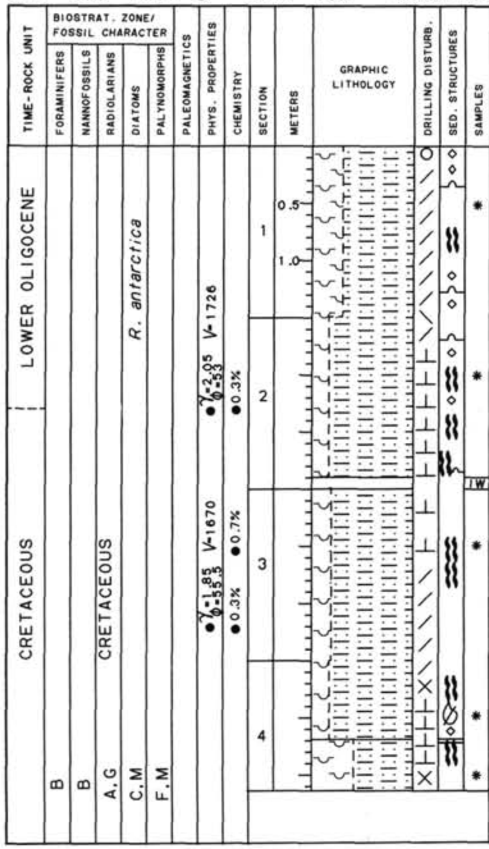

LITHOLOGIC DESCRIPTION

DIATOM-BEARING CLAYEY MUDSTONE

Major lithology: Diatom-bearing clayey mudstone, dark gray (5Y 4/1) and dark greenish gray (5GY 4/1) with some very dark gray (5Y 3/1); color boundaries tend to occur between drilling biscuits. In Sections 1 and 2 the biscuits contain parallel and wavy laminations and some moderate bioturbation; lamination dips at high angles, and Sections 1 and 2 are thought to be slumped. In Sections 3 and 4 the only structure is moderate bioturbation.

Minor lithology: Diatom claystone at Section 4, 69–111 cm, greenish gray (5GY 5/1), moderate bioturbation, noxious smell of acetylene. Top of this lithology, Section 4, 69 cm, is laminated and slightly eroded.

Ice-rafted debris includes sand and granules in Section 1, 0–33 and 109–150 cm; Section 2, 27–30 and 65–71 cm; and Section 4, 59–69 cm. The boundaries of the sandy zones are sharp. A major stratigraphic break, lower Oligocene/Cretaceous, is present in Section 2, 68–70 cm.

SMEAR SLIDE SUMMARY (%):

	1, 50 D	2, 50 D	3, 50 D	4, 50 D	4, 100 M
TEXTURE:					
Sand	5	5	5	5	—
Silt	55	40	50	45	50
Clay	40	55	45	50	50
COMPOSITION:					
Quartz	20	20	25	25	5
Feldspar	2	3	3	2	—
Mica	3	2	2	1	1
Clay	41	54	43	50	48
Accessory minerals:					
Heavy minerals	Tr	1	Tr	Tr	Tr
Opaque	3	3	2	2	1
Amphibole	1	2	5	2	—
Nannofossils	Tr	—	—	—	Tr
Diatoms	25	10	15	15	40
Radiolarians	3	3	5	3	3
Sponge spicules	2	2	Tr	Tr	2